Copper and zinc stable isotope ratios as tracers of biogeochemical processes, sources and transport of Cu and Zn in soils

Dissertation
zur Erlangung des Grades
"Doktor der Naturwissenschaften"
im Promotionsfach Geographie

Am Fachbereich Chemie, Pharmazie und Geowissenschaften
der Johannes Gutenberg-Universität Mainz

Moritz Bigalke

Geboren in Gummersbach

Mainz, 2010

Dekan:

1. Berichterstatter:

2. Berichterstatter:

3. Berichterstatter:

Tag der mündlichen Prüfung: 28.04.2010

Contents

List of tables

List of figures

List of abbreviations

BCR	=	basalt of the Columbia river (reference material)
BS	=	base saturation
C_{org}	=	organic carbon
CRM	=	certified reference material
ECEC	=	effective cation-exchange capacity
ETAAS	=	electrothermal atomic absorption spectrometer
FAAS	=	flame atomic absorption spectrometer
FAO	=	Food and Agricultural Organization
$Fe_{o/d}$	=	ratio of oxalate-extractable Fe to dithionite-extractable Fe
Fe_{tot}	=	total Fe concentrations
GSP	=	granodiorite silver plume (reference material)
HA	=	humic acid
HAS	=	high affinity sites
HR	=	high resolution
HS	=	humic substances
ICP	=	inductively-coupled plasma
IHA	=	insolubilized humic acid
LAS	=	low affinity sites
LR	=	low resolution
MC-ICPMS	=	multicollector inductively-coupled plasma mass spectrometer
MS	=	mass spectrometer
NIST	=	National Institute of Standards and Technology
NOD-P-1	=	manganese nodule (reference material)
OM	=	organic matter
RSD	=	relative standard deviation
SCL	=	silty clay loam (reference material)
SD	=	standard deviation
USGS	=	United States Geological Survey

Summary

Copper and Zn are essential micronutrients for plants, animals, and humans; however, they may also be pollutants if they occur at high concentrations in soil. Therefore, knowledge of Cu and Zn cycling in soils is required both for guaranteeing proper nutrition and to control possible risks arising from pollution.

The overall objective of my study was to test if Cu and Zn stable isotope ratios can be used to investigate into the biogeochemistry, source and transport of these metals in soils. The use of stable isotope ratios might be especially suitable to trace long-term processes occurring during soil genesis and transport of pollutants through the soil. In detail, I aimed to answer the questions, whether (1) Cu stable isotopes are fractionated during complexation with humic acid, (2) δ^{65}Cu values can be a tracer for soil genetic processes in redoximorphic soils (3) δ^{65}Cu values can help to understand soil genetic processes under oxic weathering conditions, and (4) δ^{65}Cu and δ^{66}Zn values can act as tracers of sources and transport of Cu and Zn in polluted soils.

To answer these questions, I ran adsorption experiments at different pH values in the laboratory and modelled Cu adsorption to humic acid. Furthermore, eight soils were sampled representing different redox and weathering regimes of which two were influenced by stagnic water, two by groundwater, two by oxic weathering (Cambisols), and two by podzolation. In all horizons of these soils, I determined selected basic soil properties, partitioned Cu into seven operationally defined fractions and determined Cu concentrations and Cu isotope ratios (δ^{65}Cu values). Finally, three additional soils were sampled along a deposition gradient at different distances to a Cu smelter in Slovakia and analyzed together with bedrock and waste material from the smelter for selected basic soil properties, Cu and Zn concentrations and δ^{65}Cu and δ^{66}Zn values.

My results demonstrated that (1) Copper was fractionated during adsorption on humic acid resulting in an isotope fractionation between the immobilized humic acid and the solution ($\Delta^{65}Cu_{IHA\text{-}solution}$) of 0.26 ± 0.11‰ (2SD) and that the extent of fractionation was independent of pH and involved functional groups of the humic acid. (2) Soil genesis and plant cycling causes measurable Cu isotope fractionation in hydromorphic soils. The results suggested that an increasing number of redox cycles depleted ^{63}Cu with increasing depth resulting in heavier δ^{65}Cu values. (3) Organic horizons usually had isotopically lighter Cu than mineral soils presumably because of the preferred uptake and recycling of ^{63}Cu by plants. (4) In a strongly developed Podzol, eluviation zones had lighter and illuviation zones heavier δ^{65}Cu values because of the higher stability of organo-^{65}Cu complexes compared to organo-^{63}Cu complexes. In the Cambisols and a little developed Podzol, oxic weathering caused increasingly lighter δ^{65}Cu values with increasing depth, resulting in the opposite depth trend as in redoximorphic soils, because of the preferential vertical transport of ^{63}Cu. (5) The δ^{66}Zn values were fractionated during the smelting process and isotopically light Zn was emitted allowing source identification of Zn pollution while δ^{65}Cu values were unaffected by the smelting and Cu emissions isotopically indistinguishable from soil. The δ^{65}Cu values in polluted soils became lighter down to a depth of 0.4 m indicating isotope fractionation during transport and a transport depth of 0.4 m in 60 years. δ^{66}Zn values had an opposite depth trend becoming heavier with depth because of fractionation by plant cycling, speciation changes, and mixing of native and smelter-derived Zn.

Copper showed measurable isotope fractionation of approximately 1‰ in unpolluted soils, allowing to draw conclusions on plant cycling, transport, and redox processes occurring during soil genesis and δ^{65}Cu and δ^{66}Zn values in contaminated soils allow for conclusions on sources (in my study only possible for Zn), biogeochemical behavior, and depth of dislocation of Cu and Zn pollution in soil. I conclude that stable Cu and Zn isotope ratios are a suitable novel tool to trace long-term processes in soils which are difficult to assess otherwise.

Zusammenfassung

Kupfer und Zn sind essentielle Nährelemente für Pflanzen, Tiere und Menschen, können aber in hohen Konzentrationen auch als Schadstoffe wirken. Deshalb ist das Wissen über den Cu- und Zn-Kreislauf im Boden als Lebensraum und Produktionsort für Nahrung wichtig.

Das Ziel dieser Arbeit war es zu untersuchen, ob die stabilen Isotope von Cu und Zn geeignet sind, um biogeochemische Prozesse, Quellen und Transport dieser Elemente in Böden zu untersuchen. Die Untersuchung von stabilen Cu- und Zn-Isotopen könnte besonders für die Erforschung von Langzeitprozessen hilfreich sein. Die zu beantwortenden Fragen sind: (1) Ob Cu-Isotope bei der Komplexierung mit Huminsäure fraktioniert werden, (2) ob die δ^{65}Cu-Werte im Boden Hinweise auf bodenbildende Prozesse in hydromorphen Böden liefern, (3) ob δ^{65}Cu-Werte helfen können biogeochemischen Prozesse in oxischen Böden zu verstehen und (4) ob δ^{65}Cu- und δ^{66}Zn-Werte als Tracer für Quellen und Transport von Cu und Zn in kontaminierten Böden dienen können.

Um diese Fragen zu beantworten, führte ich Adsorptionsexperimente bei verschiedenen pH-Werten durch und modellierte die Cu-Adsorption an unlösliche Huminsäure. Desweiteren wurden acht Böden, die durch verschiedene bodenbildenen Prozesse charakterisiert waren, beprobt. Jeweils zwei Böden waren durch Stauwasser und Grundwasser beeinflusst, zwei bildeten sich unter oxischen Verwitterungsbedingungen (Braunerden) und zwei durch Podsolierung. In allen Horizonten dieser Böden untersuchte ich die grundlegenden Bodeneigenschaften, die Cu Speziierung in einer sequentiellen Extraktion und δ^{65}Cu-Werte. Drei weitere Böden wurden entlang eines Depositionsgradienten in unterschiedlichen Entfernungen von einer Kupferhütte in der Slowakei zusammen mit Ausgangsgestein und Abfallprodukten der Hütte beprobt und auf ausgewählte Eigenschaften, δ^{65}Cu- und δ^{66}Zn-Werte untersucht.

Meine Ergebnisse zeigen, dass (1) Cu bei der Komplexierung durch Huminsäure fraktioniert wird ($\Delta^{65}Cu_{Huminsäure\text{-}Lösung}$ = 0.26 ± 0.11‰ (2 Standardabweichungen) und die Fraktionierung unabhängig von pH und den involvierten funktionellen Gruppen der Huminsäure war und dass (2) bodenbildende Prozesse und die Umsetzung von Cu durch Pflanzen eine messbare Isotopen-Fraktionierung verursacht. Die Ergebnisse legen nahe, dass mit steigender Zahl von Redoxwechseln im Boden die δ^{65}Cu-Werte schwerer werden. (3) Organische Horizonte zeigten meist leichtere δ^{65}Cu-Werte, was wahrscheinlich auf die Fraktionierung von Cu-Isotopen bei der Aufnahme und dem Transport von Cu in Pflanzen zurückzuführen ist. (4) In einem ausgeprägt entwickelten Podsol zeigten Cu-Abreicherungszonen leichtere und Cu-Anreicherungszonen schwerere δ^{65}Cu-Werte, was wahrscheinlich durch Fraktionierungen bei der Komplexierung und dem Transport von Cu als Organokomplex zurückzuführen ist. In einem schwach entwickelten Podsol und zwei Braunerden verursachte oxische Verwitterung einen Trend zu leichteren δ^{65}Cu-Werten mit zunehmender Tiefe, der im Gegensatz zu dem Trend in hydromorphen Böden steht. (5) Die Zn-Isotope wurden während des Schmelzprozesses fraktioniert und leichtes Zn wurde emittiert wodurch eine Quellenidentifikation möglich war. Die δ^{65}Cu-Werte in den kontaminierten Böden wurden durch die Verhüttung nicht fraktioniert. Die δ^{65}Cu-Werte tendierten bis in eine Tiefe von 0,4 m zu leichten Werten, was auf eine Fraktionierung während des Transports und eine Transporttiefe von 0,4 m in den letzten 60 Jahren hindeutet. Die δ^{66}Zn-Werte hingegen wurden mit zunehmender Tiefe schwerer, was durch Fraktionierungen durch Pflanzen, Änderung der Speziierung und Mischung mit natürlichem Zn erklärt werden konnte.

Stabile Cu-Isotope zeigen in nicht kontaminierten Böden messbare Fraktionierungen von ca. 1‰, die Rückschlüsse auf Pflanzen-induzierte Prozesse, Transport und Redoxprozesse zulassen. Die δ^{65}Cu- und δ^{66}Zn-Werte in kontaminierten Böden erlauben Rückschlüsse auf die Quellen und den Transport der Schadstoffe im Boden. Insgesamt sind stabile Cu- und Zn-Isotope dafür geeignet, Langzeitprozesse in Böden zu untersuchen, die mit anderen Methoden kaum abzuschätzen sind.

Acknowledgments

Prescribed by the regulations of the internet publisher (ArchiMed) this section had to be deleted for data protection reasons. Nevertheeless, I am still very grateful and want to acknowledge for all the support I got during my PhD time. Thanks to all the people still listed in the printed version of this thesis.

A Summarizing overview

1 Introduction

Copper and Zn are essential micronutrients but can also be pollutants at high concentrations (Alloway, 1990). Therefore, knowledge of Cu and Zn cycling in soils is required, both for guaranteeing proper nutrition and to control possible risks arising from Cu and Zn pollution.

Copper occurs in unpolluted soils in concentrations of approx. 30 $\mu g\ g^{-1}$ and varies in a range of 2-100 $\mu g\ g^{-1}$, while Zn concentrations vary between 15 and 100 $mg\ kg^{-1}$ with average concentrations of 70 $mg\ kg^{-1}$ (Alloway, 1995; Artiola, 2005). In polluted soils, Cu and Zn concentrations may reach several thousand $mg\ kg^{-1}$ (Alloway, 1995). In nonpolluted soils, Cu and Zn derive from the minerals of bedrocks and only minor contributions enter soil from the atmosphere, while in polluted soils contamination may result from direct application of Cu-containing materials like wastes and fertilizers or input from the atmosphere (Nriagu and Pacyna, 1988). Metals are emitted in gaseous or particulate form to the atmosphere and may be deposited to the surface contaminating waters and soils (Dudka and Adriano, 1997). Because of the atmospheric origin, these metals enter soils from the surface, can be transported in the soils, and finally contaminate groundwater (Alloway, 1995). Copper and Zn emissions from metal processing are the major sources of atmospheric pollution with these metals (Nriagu and Pacyna, 1988; Pacyna and Pacyna, 2002).

Transport of Cu and Zn in soil occurs in dissolved or colloidal form and causes a vertical redistribution of these metals in soil (de Jonge et al., 2004; Keller and Domergue, 1996). In soil solution, Cu and Zn mostly occur as Cu^{2+} and Zn^{2+}, but depending on pH and interacting substances also hydroxo-, (hydrogen)carbonato-, sulfato-, and organo-complexes are formed in various mixtures (Artiola, 2005; Günther and Kastenholz, 2005). Dissolved Cu and Zn species may adsorb on negatively charged surfaces of clay minerals and organic matter and may be strongly bound at the surface of oxy(hydr)oxides as outer- or inner-spheric complexes or occluded in the oxides (Alcacio et al., 2001; Artiola, 2005; Contin et al., 2007; Dube et al., 2001). Under reducing conditions, the formation of sulfides may immobilize Cu and Zn (Artiola, 2005; Günther and Kastenholz, 2005) but also mobilization is possible. Increasing pH in chemical reduction reactions may cause the release of dissolved organic matter, which

enhances metal mobility (Grybos et al., 2007). Recently, it was detected that Cu may form mobilizable elemental nanoparticles (Manceau et al., 2008; Weber et al., 2009).

Many attempts have been made to improve understanding of trace metal behavior in soil. For Cu and Zn, the most common tools to assess their fate are sequential extractions to study the binding of metals to various soil constituents (Bacon and Davidson, 2008). Other approaches to assess Cu and Zn speciation in soil include infrared and electron spin resonance spectroscopy (Senesi et al., 1986), extended X-ray absorption fine structure spectroscopy (Alcacio et al., 2001; Voegelin et al., 2005), exchange with added isotopically labeled metals (Ma et al., 2006), and voltammetry to measure dissolved species in soil solution (Luo et al., 2006; Pelfrene et al., 2008). But there are still open questions in the understanding of Cu and Zn behavior in the highly complex soil system. This is particularly true for the long-term effects of transport and redox processes in soil at time scales up to hundreds or thousands of years, which are experimentally not directly accessible. Investigation of stable isotope ratios, which integrate the effects of such long-term processes, might therefore be a useful tool to further the understanding of the biogeochemical cycling of Cu and Zn in the environment.

The δ^{65}Cu values of some common bedrocks and biogeochemical processes which occur in the soil were already reported in the literature. Common rocks like granites (-0.46 to 1.51‰; Li et al., 2009), basalts (-0.02 to 0.07‰; Archer and Vance, 2004; Li et al., 2009) and loess (-0.02 to 0.03‰; Li et al., 2009) cluster around 0‰. Thus, these parent materials for soil formation seem to show limited variations in Cu isotope ratios. In contrast, large variations occur in ores and minerals with δ^{65}Cu values of -3.44 to 7.74‰ (Asael et al., 2007; Gale et al., 1999; Marechal et al., 1999). However, the number of analyses of common parent materials for soil development is still limited and the above mentioned ranges of δ^{65}Cu values may therefore not be representative for the entire range in nature.

Results of laboratory experiments demonstrated that Cu sorption on Fe and Al oxy(hydr)oxides causes fractionation between the solid and solution phases of $\Delta^{65}Cu_{(oxy(hydr)oxide\text{-}solution)}$ from 0.34 to 1.26‰ (Balistrieri et al., 2008; Clayton et al., 2005; Pokrovsky et al., 2008). Binding on bacteria surfaces causes fractionations of $\Delta^{65}Cu_{(bacteria\text{-}solution)}$ between -1.8 and 0.6‰ depending on pH, bacterium species, and

environmental conditions (Borrok et al., 2008; Pokrovsky et al., 2008). In metal precipitates on bacteria surfaces, $\delta^{65}Cu$ was enriched by up to 3‰ compared to the aqueous medium (Mathur et al., 2005). The most pronounced isotope fractionation was observed during reduction of Cu^{2+} to Cu^{+} ($\Delta^{65}Cu_{(CuI-CuII)}$ = -4.1 to -2.8‰; Ehrlich et al., 2004; Zhu et al., 2002) or oxidation of reduced Cu^{+} minerals to Cu^{2+} ($\Delta^{65}Cu_{(CuII-CuI)}$ = 0.94 to 3‰; Asael et al., 2005; Mathur et al., 2005). Plants fractionate Cu isotopes during internal translocation ($\Delta^{65}Cu_{(root-shoot)}$ = 0.41; Jouvin et al., 2008), which may influence the Cu isotope composition of organic surface horizons of soils.

Zinc adsorption on oxy(hydr)oxides causes Zn isotope fractionations of $\Delta^{66}Zn_{solid-solution}$ from -0.2 to 0.6‰ depending on the mineral and pH (Balistrieri et al., 2008; Pokrovsky et al., 2005) and complexation by purified humic acid causes fractionation of ($\Delta^{66}Zn_{PHA-solution}$ of 0.24‰) only at pH > 6 (Jouvin et al., 2009). In laboratory experiments, Zn isotope fractionations between roots and shoots or leaves of different plant species with the shoots and leaves being enriched in light isotopes compared to the roots were shown (Moynier et al., 2009; Weiss et al., 2005). In a tropical watershed, tree leaves were enriched in the light ^{64}Zn isotope ($\delta^{66}Zn$ = -0.5‰) compared to roots (0.5‰), and shoots (0.4‰). Furthermore, organic horizons were heavier (0.1‰) than leaves (Viers et al., 2007), which is probably attributable to nutrient uptake from the litter layer. Electroplating experiments with Zn revealed voltage-dependent isotope fractionation due to reduction of Zn with reduced Zn being up to -1.88‰ lighter compared to the starting solution (Kavner et al., 2008).

A recent review suggested Cd, Cu, and Zn isotopes as new tools to trace the sources of metals in the environment (Weiss et al., 2008). It is known that Cu does not fractionate during the smelting process, probably because of its high boiling point and therefore smelting products reflect more the mineralogical differences of the processed ores (Gale et al., 1999; Mattielli et al., 2006). Because Cu ores and minerals show a wide range of isotope fractionation with $\delta^{65}Cu$ of -3.44 to 7.74‰ (Asael et al., 2006; Gale et al., 1999; Marechal et al., 1999), it seems likely, that the $\delta^{65}Cu$ values of smelter emissions are different from those of the unpolluted soil to which the smelter-derived Cu is deposited.

In previous work, Zn isotope ratios were already successfully used to distinguish anthropogenic from native metal sources (Cloquet et al., 2006; Sivry et al., 2008; Sonke

et al., 2008). Because of its low boiling point, evaporation of Zn occurs during smelting leaving the vapor phase enriched in light isotopes, while the residues of the smelting process are enriched in heavy isotopes (Mattielli et al., 2009). Because of the isotope fractionation in the vapor phase, Zn emitted to the atmosphere is isotopically light and different from natural sources (Mattielli et al., 2009), while Zn from waste dumps polluting rivers is isotopically heavy and can be distinguished from native Zn in sediment cores (Sivry et al., 2008). The isotope composition of Zn pollution around a metal smelter also depends on distance from the smelter. Near the smelter, heavy Zn blown from waste dumps and ores contaminates the surrounding in addition to Zn deposited from the atmosphere, while at greater distances only the light Zn resulting from Zn evaporation is deposited (Mattielli et al., 2009). As smelter-emitted Cu and Zn enter soils from the surface a separation of anthropogenic from native Cu and Zn with the help of the natural abundance of stable metal isotopes might help to better understand transport of these metals in the soil. This approach was already successfully used for the radiogenic Pb isotope system with, however, much larger differences in isotope signatures of anthropogenically redistributed and native Pb (Erel, 1998; Erel et al., 1997).

1.1 Objectives

In my thesis, I addressed the following research questions:

(1) Are Cu stable isotopes fractionated during complexation with humic acid and does Cu binding to different functional groups at different pH influence the extent of fractionation **(Section B)**?

(2) Can the knowledge of the $\delta^{65}Cu$ values improve the understanding of biogeochemical processes of Cu during soil genesis in hydromorphic soils **(Section C)**?

(3) Can the knowledge of the $\delta^{65}Cu$ values help to understand biogeochemical and soil genetic processes in soils developed under oxic weathering conditions **(Section D)**?

(4) Can $\delta^{65}Cu$ and $\delta^{66}Zn$ be used as tracers for source and transport of Cu and Zn in soils polluted by the emissions of a Cu smelter **(Section E)**?

2 Materials and methods

2.1 Adsorption experiment

Aldrich humic acid was insolubilized according to Seki and Suzuki (1995) by converting to its Ca salt, heating for 1 h to 330°C, grinding, and washing. The humic acid was further purified with HF:HCl (2:1) and two times HCl for 2 h at 70°C (Weber et al., 2006a). For the Cu adsorption experiments, solutions were prepared containing 0.1 M $NaNO_3$ as background electrolyte and 1.7 mg l^{-1} Cu added as $Cu(NO_3)_2$. The pH of the solutions was adjusted to values between 2 and 7 using diluted HNO_3 and NaOH solutions. A relatively broad pH range was chosen to display a wide range of natural environments and account for differences in isotope fractionation at different pH. No buffer was used to stabilize pH because of possible effects on Cu speciation and isotope fractionation. For adsorption experiments 0.2 ± 0.03 mg of insolubilized humic acid (IHA) were weighed in a 15 ml vessel and 10 ml of solution was added. Samples were shaken overhead for three days to achieve equilibrium. Then, samples were centrifuged at 4000 rpm for 45 min, 2 x 50 µl of the supernatant were removed and diluted for Cu concentration analysis and 7 ml of the supernatant were transferred to Savillex™ vessels for isotope analysis. pH was measured in the remaining solution. As solutions were not buffered, pH changes occurred during equilibration. For Cu purification, samples were evaporated to dryness and re-dissolved in 7 M HCl + 0.001% H_2O_2 and further processed as described below (**Section B**).

2.2 Study sites and sampling

Soils were sampled in Germany and Slovakia. Soils were selected according to the soil type for soil genetic studies or according to their distance from the Cu smelter in Krompachy, east Slovakia to study the suitability of Cu and Zn isotope ratios as tracer of metal sources and vertikal transport in soil. Two soils affected by stagnic water (Stagnic Luvisol/Stagnic Cambisol), two soils affected by groundwater (Gleysols), two soils which show translocation of metals and organic materials (Podzols), and two young soils which developed under oxic weathering conditions (Cambisols) were selected to study the influence of soil genesis and physico-chemical conditions on $\delta^{65}Cu$

values. The soil types were selected in order to represent the influence of changing redox conditions, metal transport, and weathering on depth distribution of δ^{65}Cu values.

Soils were classified according to the World Reference Base for Soil Resources (IUSS Working Group WRB, 2006) and soil morphology was described according to FAO (2006). All soils except the Calcari-Humic Gleysol were located in the Variscan mountain area in slope positions between 1° and 23°. The Calcari-Humic Gleysol developed from fluviatile material next to a small creek. Like many central European soils, five of the eleven study soils (Skeleti-Stagnic Luvisol, Stagnic Cambisol, Dystric Gleysol, Skeletic Cambisol and the Haplic Podzol 1) developed from periglacial cover beds consisting of up to three solifluctional layers. Depending on site conditions and vegetation, up to three organic horizons had developed and were sampled. In the mineral soils, up to six individual horizons could be distinguished and were sampled together with organic- and iron-rich spots in the Bhs horizon of the Haplic Podzol 1, bedrock, and other parent materials like loess and Laacher See tephra where parent materials were accessible. Additional technical wastes were sampled from the waste dump of the Cu smelter in Krompachy to investigate isotope fractionation of Cu and Zn during ore processing. The soils are described more in detail and basic soil parameters are given in the corresponding chapters of this thesis (**Sections C to E**). Site characteristics for the different soils are summarized in Table A1.

Table A-1. Type, location, and site characteristics of the studied soils

Soil type	Location	Altitude m above sea level	Slope	Bedrock	Age	Rainfall mm yr^{-1}	Temperature January/July °C	Vegetation
redoximorph soils								
Skeleti-Stagnic Luvisol	Germany 50° 13' N, 8° 16' E	400	6°	slate	early Devonian	700–800	0/18	beech
Stagnic Cambisol	Slovakia 49° 31' N, 19° 26'E	800	2°	sandstone with muscovite mudstone	Eocene flysch with mudstone	1000–1200	−7/16	spruce, horsetail, and moss
Calcari-Humic Gleysol	Germany 49°56' N, 8° 04' E	88	0°	fluvic materials	Pleistocene	500–600	0/18	alder, and grass
Dystric Gleysol	Slovakia 49° 22' N, 19° 37' E	630	2°	granite and sandstone	Pliocene	700–800	−7/18	spruce, blueberry, and moss
aerobically weathered soils								
Skeletic Cambisol	Germany 50°13´N 8°16´E	400	12°	slate	early Devonian	700-800	0/18	beech
Dystrsic Cambisol	Slovakia 49°23´ N 19°29´ E	1100	13°	sandstone	Eocene Flysch	1000-1200	-7/16	spruce, blueberry, and fern
Haplic Podzol 1	Germany 49°35´ N 8°50´ E	424	10°	sandstone	early Triassic	1000-1300	0/18	pine
Haplic Podzol 2	Slovakia 49°13´ N 19°45´ E	1400	23°	grano-diorite	Variscan	1200-1400	-10/8	spruce, blueberry and fern
polluted soils								
Dystric Cambisol 1.1 km	Slovakia 48°55´ N 20°54´ E	445	5°	tuffite	Permian	700	-6/17	pine, spruce, and hornbeam
Dystric Cambisol 3.8 km	Slovakia 48°55´ N 20°56´ E	455	10°	tuffite	Permian	700	-6/17	pine, spruce, and hornbeam
Stagni-Eutric Cambisol 5.3 km	Slovakia 48°55´ N 20°57´ E	380	1°	tuffite	Permian	700	-6/17	spruce, pine, and hornbeam

2.3 Sample preparation

The mineral soil, organic layer and waste samples were air-dried. The mineral soil was sieved to <2 mm. A representative sample was taken from sieved mineral soils, organic samples and grained wastes. Bedrocks and solid wastes were crushed with a hammer. To determine $\delta^{65}Cu$ and $\delta^{66}Zn$ values and total element concentrations, all samples were ground in a ball mill (**Sections C to E**).

The texture of the <2 mm sieved fine earth was determined with the "pipet method" after destruction of organic matter (OM) with H_2O_2, dispersion with $Na_6P_6O_{18} \cdot 6H_2O$ and wet sieving of sand fractions (Schlichting et al., 1995). Gravel content was determined gravimetrically or by estimation in the field (**Sections C to E**). Soil pH was measured in 0.1 mol l^{-1} $CaCl_2$ at a soil:solution ratio of 1:2.5 after equilibration for two hours with a glass electrode (**Sections C and D**) and in 0.1 mol l^{-1} KCl at the same soil:solution ratio (**Section E**). Total C, N, and S concentrations were determined by dry combustion with a CHNS analyzer (Vario EL, Elementar Analysensysteme, Hanau, Germany) (**Sections B to E**).

Carbonate concentration was determined as the difference in C concentrations of a subsample treated with 10% HCl and an untreated subsample and determined with the CHNS analyzer (**Section C**). The effective cation-exchange capacity (ECEC) was determined as the sum of the charge equivalents of Ca, K, Mg, Na, Mn, and Al extracted with 1 mol l^{-1} NH_4NO_3. Base saturation (BS) was calculated as the sum of the charge equivalents of Ca, Mg, Na and K divided by ECEC and expressed in percent (**Sections C to E**).

Copper was sequentially extracted with the method of Zeien and Brümmer (1989) to assess operationally defined Cu fractions in soil. Briefly, for the sequential extraction two g of air-dried soil were extracted with 50 ml of each:1 mol l^{-1} NH_4NO_3, 24 h (fraction 1, readily soluble and exchangeable), 1 mol l^{-1} NH_4O-acetate, pH 6.0, 24 h (fraction 2, specifically absorbed and other weakly bound species), 0.1 mol l^{-1} $NH_2OH \cdot HCl$ + 1 mol l^{-1} NH_4O-acetate, pH 6.0, 0.5 h (fraction 3, bound to Mn oxides), 0.025 mol l^{-1} NH_4EDTA, pH 4.6, 1.5 h (fraction 4, bound to OM), 0.2 mol l^{-1} NH_4-oxalate, pH 3.25, 4 h in the dark (fraction 5, bound to poorly crystalline Fe oxides), 0.1 mol l^{-1} ascorbic acid in 0.2 mol l^{-1} NH_4-oxalate, pH 3.25, 0.5 h in hot water (fraction 6 bound to crystalline Fe oxides) and 67% HNO_3 + 50% HF (3:1) (fraction 7, residual).

Fractions 1-5 were extracted at room temperature, fraction 6 was extracted at 96°C, and fraction 7 was digested at 200°C under pressure in a microwave oven. All fractions except fraction 7 were centrifuged at 2500 rpm for 15 minutes and filtered with blue ribbon filter paper (Whatman Schleicher and Schuell, Kent, England, 2µm retention) after extraction. After every extraction step except for fractions 1 and 7, the sample was rinsed once (fractions 2, 4, 5, and 6) or twice (fraction 3) with 25 ml of 1 mol l^{-1} NH_4NO_3 (fraction 2), 1 mol l^{-1} NH_4O-acetate (pH 6, fraction 3), 1 mol l^{-1} NH_4O-acetate (pH 4.6, fraction 4) and 0.25 mol l^{-1} NH_4-oxalate (pH 3.25, in the dark, fraction 5 and 6) for 10 minutes. Extracts and the rinses were combined (**Section C and D**).

Total Fe concentrations were measured in total digests with concentrated HF: concentrated HNO_3 (1:3). Fe concentrations were also measured in the fractions 5 and 6 of the sequential extraction, which are thought to represent poorly-crystalline and crystalline oxy(hydr)oxides (**Sections C and D**).

Copper and Ti concentrations of not purified samples were determined by electrothermal atomic absorption spectrometry (ETAAS, Unicam Solaar 989, Thermo Scientific, Waltham, USA) and the concentrations of Fe, Ca, K, Mg, Na, Mn, Al and Zn were measured by flame atomic absorption spectrometry (FAAS, AA 240 FS, Varian, Palo Alto, USA). Copper and Zn blanks, Ti concentrations in the purified samples, and elution profiles (Fig. 1) were measured by ETAAS or ICP-MS (HP 4500, Agilent Technologies, Santa Clara, USA). For ICP-MS analyses, samples were spiked with Rh as internal standard (**Sections B to E**).

For isotope analyses, 100 to 500 mg of ground soil were weighed in a ceramic crucible and ashed at 450°C overnight. The sample was digested in a microwave oven (MARS5Xpress, CEM Corp., Matthews, NC) at 200°C under pressure in a mixture of concentrated HF/concentrated HNO3 (1:3). For some samples from Krompachy which contained much graphite-like material, the digestion procedure was modified by taking 9 ml HNO_3 and 2 ml H_2O_2 in a first and adding 3 ml HF in a second and third run at 225°C. The acid was evaporated and redissolved several times and finally digested in 7 mol l^{-1} HCl and 0.001% H_2O_2 for purification on the anion exchange resin. The total digests were purified on a pre-cleaned AG MP-1 Biorad resin after a protocol modified from Marechal et al. (1999). After conditioning the resin with 8 ml of 7 mol l^{-1} HCl, the sample was applied in 1 ml of 7 mol l^{-1} HCl. Then, 6 ml of 7 mol l^{-1} HCl in 1-ml steps

and two times 2 ml of 7 mol l^{-1} HCl were combined to wash the sample in the resin and elute matrix elements. Twenty-eight ml of 7 mol l^{-1} HCl were used to collect the Cu fraction, 12-15 ml of 1 mol l^{-1} HCl were used to elute the Fe fraction, and finally Zn was eluted in 12 ml of a freshly prepared 0.5 mol l^{-1} HNO_3 : 0.1 mol l^{-1} HBr mixture (Fig. A-1a). Because of the low Cu to high matrix ratio, one single purification run was not sufficient to achieve good matrix separation. The Cu purification procedure was therefore repeated for each sample (Fig. A-1b). Cobalt coelutes together with Cu and can therefore not be separated from Cu. However, Co does not significantly affect Cu isotope measurements (Li et al., 2009; Petit et al., 2008).

For Zn, one single purification run was sufficient. After the purification, the sample was dried and oxidized with HNO3 and H2O2 to destroy organic compounds released from the resin and drive out any remaining HCl. Finally, the samples were redissolved in 2% HNO3 for isotope ratio measurement. Recovery was checked for every sample to rule out isotope fractionation on the resin (Marechal and Albarede, 2002). Recoveries were checked with ETAAS (Cu) and FAAS (Zn) and samples that did not show recovery of 100 ± 6% were discarded (Sections B to E).

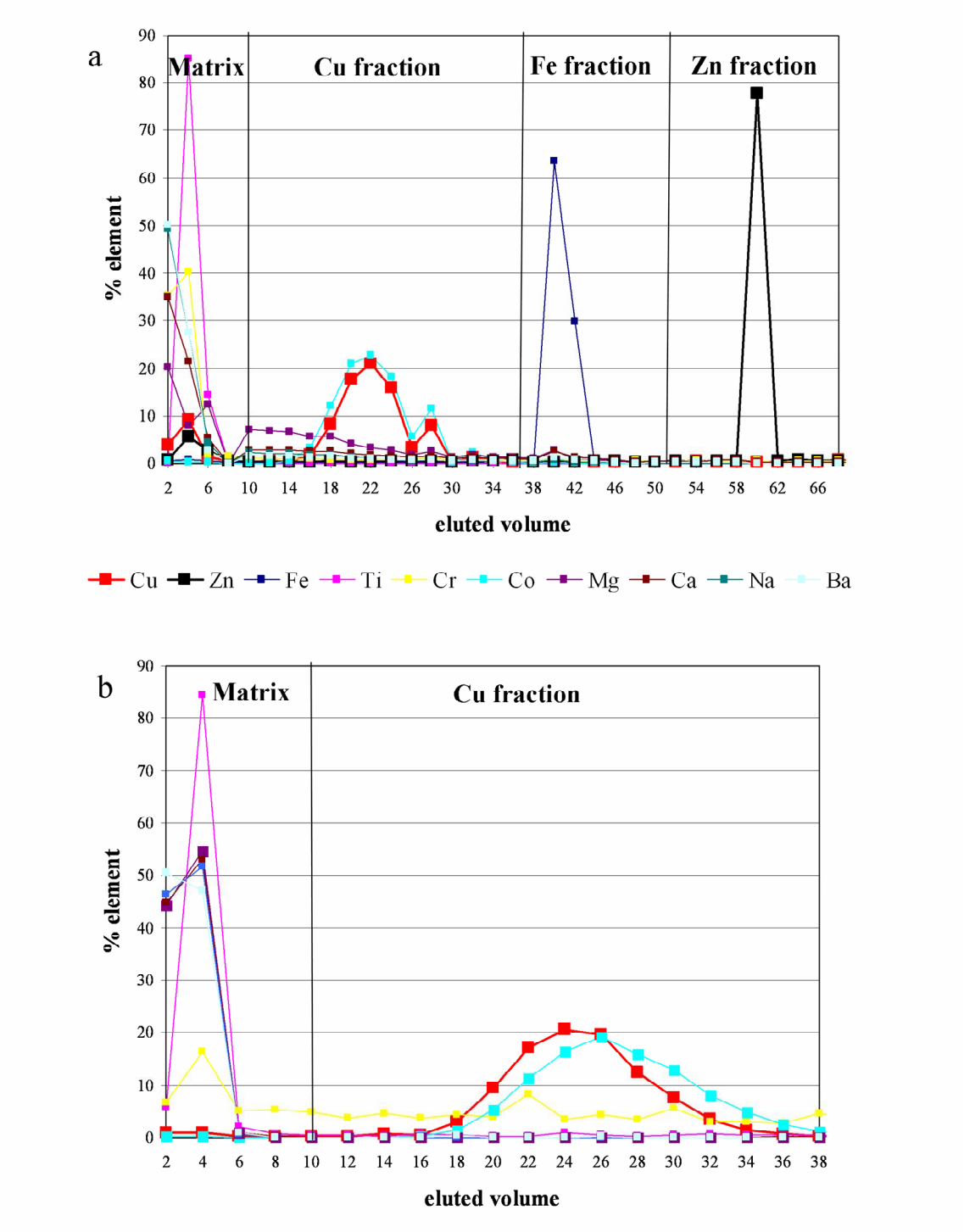

Figure A-1. (a) First and (b) second purification of a basalt sample (BCR-2). Copper and Zn and interfering elements according to Mason et al. (2004a) and Petit et al. (2008) are shown.

2.4 Copper and Zn isotope ratio measurements

Copper and Zn isotope ratios were measured with a Finnigan-Neptune (Thermo Scientific, Waltham, MA, USA) multiple collector inductively-coupled plasma mass spectrometer (MC-ICP-MS). A Ni spike (NIST 986) was used for mass bias correction of Cu (Li et al., 2009; Markl et al., 2006). Mass bias was corrected according to the certified $^{62}Ni/^{60}Ni$ ratio (0.138600) of NIST 986 added to all samples and the Cu standard prior to measurement and by applying the exponential law. After every third sample a standard (NIST 976) was analyzed as a kind of standard-sample bracketing. The $\delta^{65}Cu$ values were calculated as the deviation of the isotope ratio of the mass-bias corrected samples from the isotope ratio of the mass-bias corrected bracketing standards (Li et al., 2009). The long-term reproducibility of a Cu-ICP standard (Merck, Darmstadt, Germany) was 0.06‰ (2 SD, n = 49). Every sample was measured twice and the mean reported. All Cu isotope ratios were expressed as $\delta^{65}Cu$ values relative to NIST 976 isotope reference material according to Equation A-1 (**Sections A to D**).

$$\delta^{65}Cu[‰] = \left(\frac{\left(^{65}Cu/^{63}Cu\right)_{sample}}{\left(^{65}Cu/^{63}Cu\right)_{NIST\,976}} - 1 \right) * 1000 \qquad \text{(A-1)}$$

A Cu spike was used for mass-bias correction of Zn isotope measurements. Mass bias was corrected according to the method of Marechal et al. (1999). After every third sample, a standard (NIST 976) was analyzed as a kind of standard sample bracketing. The $\delta^{66}Zn$ values were calculated as the deviation of the isotope ratio of the mass-bias corrected samples from the isotope ratio of the mass-bias corrected bracketing standards (Li et al., 2009). The Zn isotope ratios were measured relative to the Zn isotope reference material IRMM 3702. Because Zn isotope data are usually reported relative to a Johnson Matthey (JMC) standard solution (batch 3-0749L), Zn isotope ratios measured relative to IRMM 3702 were converted by adding 0.32‰, which is the offset of the Zn isotope ratios between the two standard solutions (Cloquet et al., 2006; John et al., 2007). Thus Zn isotope ratios are presented as shown in Equation A-2.

$$\delta^{66}Zn_{JMC\,Zn}[‰] = 0.32 + \left(\frac{(^{66}Zn/^{64}Zn)_{sample}}{(^{66}Zn/^{64}Zn)_{IRMM\,3702}} - 1 \right) * 1000 \qquad \text{(A-2)}$$

Long-term reproducibility of a Zn in-house standard was 0.08 ‰ (2 SD / n = 10). Every sample was measured twice and the mean reported. Mean reproducibility of samples digested, purified, and measured in duplicate was 0.06‰ (2 SD, **Section E**).

2.5 Calculations, statistical analysis, and speciation modeling

Pearson correlation coefficients were calculated to describe relationships. The Kolmogorov-Smirnov test was used to check for normal distribution of the data sets (**Sections B to E**). To check for significant correlations or differences between means, t-tests were performed with SPSS 15 (SPSS inc., Chicago, Illinois, USA).

To assess Cu speciation at different pH during the adsorption experiment, I conducted chemical speciation calculations with the NICA-Donnan model which is one of the most common models to assess complexation of metals with humic substances. Details of the NICA-Donnan model are found in Benedetti et al. (1995) and Kinniburgh et al. (1996). The NICA-Donnan model distinguishes between low affinity sites (LAS, carboxylic groups), high affinity sites (HAS, phenolic type groups), and electrostatically bound species and is thus suitable to test if different binding sites cause distinguishable Cu isotope fractionation. The ECOSAT program which induces the NICA-Donnan model was used for speciation calculations (**Section B**).

3 Results and discussion

3.1 Copper isotope fractionation during complexation with humic acid (Section B)

To understand Cu isotope fractionation in soils, knowledge about direction and extent of isotope fractionations caused by different processes is necessary. Some fractionation mechanisms of a number of processes are known but the effect of Cu complexation by organic acids, which strongly influence bioavailability, mobility, and toxicity of Cu in soil on δ^{65}Cu values has not been studied yet. In many natural systems like soils, sediments, lakes, and river waters, organo-Cu complexes are the dominating species (Artiola, 2005; Buck et al., 2007; Hoffmann et al., 2007). The knowledge of Cu isotope fractionation during adsorption on humic acid may help to better understand Cu

isotope fractionation in natural environments and thus facilitate the use of Cu stable isotope ratios (δ^{65}Cu) as tracer of the fate of Cu in the environment. I therefore studied Cu isotope fractionation during complexation with insolubilized humic acid (IHA) with the help of adsorption experiments at pH 2-7. The Cu binding on IHA was modeled to estimate the influence of Cu binding to different functional groups on Cu isotope fractionation. The observed overall Cu isotope fractionation at equilibrium between the solution and IHA was $\Delta^{65}Cu_{IHA\text{-}solution} = 0.26 \pm 0.11$‰ (2SD). Modeled fractionations of Cu isotopes for LAS and HAS were similar with $\Delta^{65}Cu_{LAS\text{-}solution} = 0.27$ and $\Delta^{65}Cu_{HAS\text{-}solution} = 0.26$. pH did not influence Cu isotope fractionation in the applied pH range.

3.2 Stable copper isotopes: a novel tool to trace copper behavior in hydromorphic soils (Section C)

I studied the natural abundance of stable Cu isotope ratios in four soils to test whether δ^{65}Cu values can be used as a tracer for biogeochemical processes in hydromorphic soils. Two of the soils were affected by stagnic water and the other two by groundwater. I determined standard soil properties and Cu partitioning into seven fractions of a sequential extraction and Cu stable isotope ratios. Copper concentrations in the study soils were low to average (5–34 mg kg^{-1}). The variation in Cu isotope ratios was up to 0.6‰ in an individual soil. The organic layers of two of the profiles had lighter δ^{65}Cu values than the mineral soil, indicating isotope fractionation of Cu during soil–plant–soil transfer. In the mineral soil, Cu isotopes showed distinguishable variations of up to 0.45‰. The vertical distribution of the δ^{65}Cu values, which paralleled that of the poorly crystalline to crystalline Fe oxide ratios, offers the first hints that Cu isotope ratios in soils may be influenced by alternating redox conditions. I conclude that variations in δ^{65}Cu in soils are large enough to be distinguished and may be indicative of biogeochemical cycling and geochemical processes. In particular, Cu isotope ratios might be helpful to trace long-term processes such as element transport and redox conditions, which are difficult to assess otherwise.

3.3 Stable Cu isotope fractionation in soils during oxic weathering and podzolation (Section D)

In Section C, I demonstrated that Cu stable isotope ratios show fractionation by various biogeochemical processes and may trace the fate of Cu during long-term pedogenetic processes. In Section D, I assessed the effects of oxic weathering (formation of Cambisols) and podzolation on Cu isotope ratios (δ^{65}Cu). Two Cambisols and two Podzols were analyzed for Cu concentrations and forms and δ^{65}Cu values in bulk soil and selected soil fractions. Copper concentrations in the studied soils were low (1.4-27.6 mg kg^{-1}) and mainly occurred in strongly bound Fe oxide- and silicate-associated forms. Bulk δ^{65}Cu values varied between -0.57 and 0.44 ‰ in all studied horizons. The O horizons had on average significantly lighter Cu isotope ratios (-0.21‰) than the A horizons (0.13‰), which can either be explained by Cu isotope fractionation during cycling through the plants or deposition of isotopically lighter Cu from the atmosphere. I found a consistent and significant decrease in δ^{65}Cu values by up to 0.3‰ with depth as a consequence of oxic weathering without pronounced podzolation in both Cambisols and a weakly developed Podzol (Haplic Podzol 2). This is the opposite depth trend of δ^{65}Cu values to that I observed in the hydromorphic soils (Section C). In a more pronounced Podzol (Haplic Podzol 1), δ^{65}Cu values and Cu concentrations decreased from Ah to E horizons and increased again deeper in the soil. Humus-rich sections of the Bhs horizon had a heavier δ^{65}Cu value (-0.18) than oxide-rich sections (-0.35) suggesting Cu translocation between E and B horizons as organo-Cu complexes and complexation of heavy Cu as described in Section B. The different depth distributions in aerobically weathered and hydromorphic soils and the pronounced vertical differences in δ^{65}Cu values in Haplic Podzol 1 support my hypothesis that δ^{65}Cu values can be used to trace long-term pedogenetic processes.

3.4 Stable Cu and Zn isotope ratios as tracers of sources and transport of Cu and Zn in contaminated soil (Section E)

After having investigated the Cu isotope biogeochemistry in different unpolluted soils in Sections C and D, I also included Zn stable isotopes to study Cu and Zn sources and transport in soils.

Copper and Zn metals are produced in large quantities for different applications. During Cu production, high amounts of Cu and Zn are released to the environment (Pacyna and Pacyna, 2002). Therefore, the surroundings of Cu smelters are frequently metal-polluted (McMartin et al., 1999; Wilcke et al., 1999). I determined Cu and Zn concentrations and Cu and Zn stable isotope ratios (δ^{65}Cu, δ^{66}Zn) in three Cambisols at distances of 1.1, 3.8, and 5.3 km from a Slovak Cu smelter and in smelter wastes (slag, sludge, ash) to trace sources and transport of Cu and Zn in soils. Soils were heavily contaminated with concentrations up to 8087 mg kg^{-1} Cu and 2084 mg kg^{-1} Zn in the organic horizons. The δ^{65}Cu values varied little (-0.12 to 0.36‰) in soils and most wastes and therefore no source identification of Cu was possible. In soils, Cu became isotopically lighter with increasing depth down to 0.4 m, likely because of equilibrium reactions between dissolved and adsorbed Cu species during transport of smelter-derived Cu through the soil. Below 0.4 m soil depth, δ^{65}Cu values were similar in soil and unpolluted bedrock. This suggests that Cu was transported to a depth of 0.4 m during the 60 years from the start of Cu production to sampling. The δ^{66}Zn values were isotopically lighter in ash (-0.13‰) and organic horizons (-0.57 to -0.15‰) than in bedrock (-0.03‰) and slag (0.48‰) probably because of kinetic fractionation during evaporation and thus allowed separation of smelter-Zn from native Zn in soil. In particular in the organic horizons, Zn isotopes shifted to heavier δ^{66}Zn values with depth probably because of the mixing of smelter-derived Zn and native Zn in the soils and biogeochemical fractionation. Changes in speciation during dissolution of smelter dust and plant-induced fractionation mainly explain Zn fractionation. Fractionations between dissolved and adsorbed species probably only play a minor role for variations in δ^{66}Zn values in soil. My results demonstrate that δ^{65}Cu and δ^{66}Zn values in contaminated soils allow for conclusions on sources (Zn only), biogeochemical behavior, and depth of dislocation of Cu and Zn in soil.

3.5 The effects of biogeochemical processes on δ^{65}Cu and δ^{66}Zn values in soils

As shown in 3.1- 3.4, biogeochemical processes cause fractionation of stable Cu and Zn isotopes in soils. Depending on soil genesis, different processes seem to cause different directions of isotope fractionation resulting in distinguishable depth gradients

(Fig. A-2 and A-3). For Cu and Zn different processes seem to dominate isotope fractionation respectively.

As a consequence of the analysis of total digests of soil horizons, only isotope fractionations which are coupled to transport processes can be traced in soil. It was not possible to infer biogeochemical processes inside a given horizon from Cu and Zn isotope ratios, but only to identify differences among horizons. These differences were the result of the transport of fractionated Cu from one horizon to another. Furthermore, mixing of fractionated Cu and Zn which is transported from one horizon to another with native Cu and Zn of the horizon has to be considered. Zinc emitted from the Cu smelter was fractionated by evaporation during the smelting process, which allowed source identification of Zn in soil.

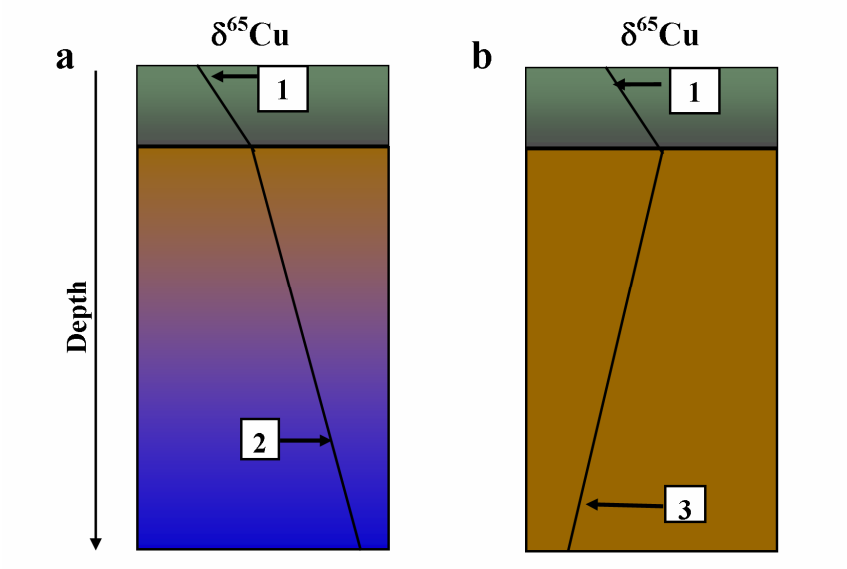

Figure A-2. Schematic depth gradients of δ^{65}Cu values in (a) hydromorphic and (b) oxic soils (except Haplic Podzol 1) and suggested biogeochemical processes causing these gradients. 1) Plant-induced fractionation, 2) redox fractionation, 3) equilibrium fractionation. Green = organic horizons, brown = mineral horizon, blue = water influenced mineral horizons.

Biogeochemical processes discussed here are characterized by transport (changes in mobility) and isotope fractionation of Cu and Zn. I suggest (1) plant-induced fractionation, (2) redox-induced fractionation and associated changes in mobility, and (3) equilibrium fractionation between mobile and immobile species as dominating processes driving Cu isotope fractionation in the soil system.

1) Plant-induced fractionation of Cu is hardly investigated but transport in plants seems to cause fractionation of $\Delta^{65}Cu_{(root\text{-}shoot)}$ = 0.41‰ (Jouvin et al., 2005). For Zn, more detailed investigations have been performed reporting Zn isotope fractionations between roots and shoots or leaves of different plant species with the shoots and leaves being enriched in light isotopes compared to the roots (Moynier et al., 2009; Weiss et al., 2005). In a tropical watershed, tree leaves were enriched in the light ^{64}Zn isotope ($\delta^{66}Zn$ = -0.5‰) compared to roots (0.5‰), and shoots (0.4‰). Furthermore, organic horizons were heavier (0.1‰) than leaves (Viers et al., 2007), which is probably attributable to nutrient uptake from the litter layer.

In the investigated soils, plant-induced fractionation can be seen from the $\delta^{65}Cu$ values of the organic horizons. These horizons mainly consist of plant material at different decomposition stages and might therefore partly reflect $\delta^{65}Cu$ values of plants. In my study six out of eight unpolluted soils show lighter $\delta^{65}Cu$ values than the underlying A horizon (Tab. C-3 and D-3). This trend to lighter $\delta^{65}Cu$ values in plant material agrees with findings in the literature (Jouvin et al., 2008; Moynier et al., 2009). In the polluted soils, this trend is overcompensated by the deposition caused by the Cu smelter and no trend to light $\delta^{65}Cu$ values in the organic layers could be seen. For $\delta^{66}Zn$ values only polluted soils were investigated and the light isotope signals of the organic horizons may only partly reflect plant-induced fractionation, while a great part of variation might be caused by emitted Zn which was fractionated during the smelting process.

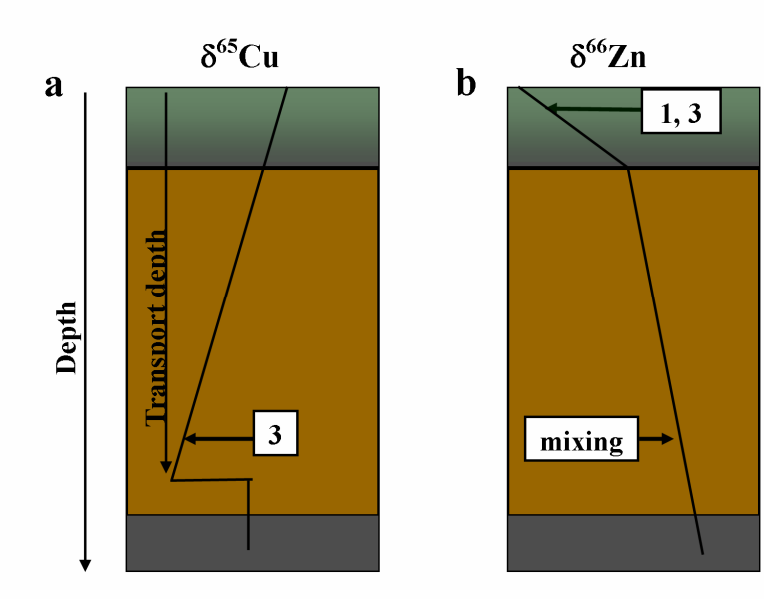

Figure A-3. Schematic depth gradients of (a) δ^{65}Cu values and (b) δ^{66}Zn values in soils polluted by a Cu smelter and suggested biogeochemical processes causing depth gradients. 1) Plant-induced fractionation, 2) redox induced fractionations are not relevant in these soils, and 3) equilibrium fractionation between mobile and immobile species. The depth gradient of δ^{66}Zn in the mineral soil is probably mainly attributable to mixing of smelter Zn and native Zn in the soil. Green = organic horizons, brown = mineral horizon, grey = bedrock.

2) Redox-induced fractionations were assumed to cause the differences in the depth distributions of δ^{65}Cu values in hydromorphic compared to soils weathered under aerobic conditions. Redox processes were only addressed for Cu isotopes but not for Zn isotopes. Redox processes are known to cause strong fractionation of Cu isotopes (Zhu et al., 2002) and strongly influence mobility of Cu in soils (Grybos et al., 2007; Weber et al., 2009). Furthermore, the stagnic of ground water in hydromorphic soils is a transport medium, which might enforce translocation of fractionated Cu. In the investigated hydromorphic soils, the trend to heavier isotope composition in water-influenced soils might point at preferential leaching of light (reduced) Cu, which would agree with findings of Weber et al. (2009) who reported enhanced mobility of reduced Cu species shortly after waterlogging. Another possibility would be the transport of heavy Cu from the not water-influenced to the water-influenced soils, but my findings from the aerobically weathered soils suggest that light Cu isotopes are preferentially translocated from not water-influenced soils.

3) Kinetic and equilibrium fractionation of Cu and Zn between different Cu and Zn species in soils might be an important process for isotope fractionation. The isotope fractionation between sorbed Cu and Cu in solution is attributable to the differences in vibrational frequencies and zero point energies of the different isotopes. The heavier isotope has lower vibrational frequencies and forms stronger molecular bonds (O´Neil 1986). Thus, at equilibrium ^{65}Cu will be enriched in the species in which Cu is more strongly bound. During weathering of minerals, the released Cu and Zn is partly incorporated into pedogenic minerals such as clay minerals or (hydr)oxides (Contin et al., 2007, Ildefonse et al., 1986, Voegelin et al., 2009) and partly bound to cation-exchange sites (Alcacio et al., 2001; Artiola, 2005). Occlusion of Cu in a mineral and binding to oxy(hydr)oxides fractionates the bound Cu towards heavier Cu isotope composition (Li et al., 2008; Pokrovsky et al., 2008). Complexation of Cu with organic substances causes isotope fractionation with the heavier isotope being adsorbed by organic compounds as described in 3.1. Consequently, Cu remaining in soil solution is isotopically lighter and can be leached or taken up by plants leaving the weathered horizons enriched in ^{65}Cu.

Zinc adsorption on oxy(hydr)oxides causes isotope fractionations with opposing directions of $\Delta^{66}Zn_{solid\text{-}solution}$ from -0.2 to 0.6‰ depending on the type of mineral and pH (Balistrieri et al., 2008; Pokrovsky et al., 2005) and complexation of Zn by humic acid causes isotope fractionations only at pH >6 (Jouvin et al., 2009). Thus, Zn isotope fractionation during weathering should be more dependent on pH and probably less pronounced than that of Cu isotopes.

The released light Cu and Zn is transported down the soil where it may interact with sorption sites, which again favor the heavy isotopes and leave the light isotopes in solution. In principle, the effect would be similar to isotope fractionation observed on ion exchange resins (Marechal and Albarede, 2002) with the difference, that in soil the heavier isotopes are preferentially adsorbed and thus light isotopes preferentially leached.

The fractionation between mobile and immobile Cu species might explain depth distribution of δ^{65}Cu values in all aerobically weathered soils (Fig. A-2 and A-3). In the Cambisols and the Haplic Podzol 2 immobile binding sites offer the stronger binding environment compared to mobile ones. Thus, light Cu is leached from the strongly

weathered surface horizons, leaving them heavier compared to the subsurface horizons which are weakly weathered and probably influenced by light Cu from the surface horizons. In the Haplic Podzol 1, mobile binding sites offer the stronger binding environment because the strongly weathered E horizon is depleted in immobile binding sites, while organic acids offer strong mobile binding sites (Section D). Thus, transported Cu is heavier leaving E horizons isotopically light and the Bhs horizon enriched in ^{65}Cu compared to the E horizon. In the polluted soils in Krompachy, Cu pollution entered the soil from the surface and was transported down the soil becoming lighter with increasing depth because immobile binding sites preferentially bind heavy Cu. This trend reaches down to a depth of 0.4 m, which is probably the maximum transport depth of Cu from the smelter in the 60 years from start of Cu production to sampling. For Zn stable isotope fractionation between mobile and immobile binding sites seem to be less important in the investigated soils, which can be derived from the finding that the depth distribution in the polluted soils showed the opposite trend to that of Cu (Section E).

A summary of Cu- and Zn-isotope variations in the different sample classes, caused by the transport of fractionated Cu and Zn in the soil is given in Table A-2.

Table A-2. Overview of mean, minimum, maximum, standard deviation and standard error of δ^{65}Cu and δ^{66}Zn value of different sample in the studied soils and smelter wastes

Sample classes	Mean	Min	Max	SD	SE	N
			δ^{65}Cu			
Organic horizons unpolluted	-0.15	-0.45	0.20	0.16	0.04	18
Water influenzed horizons	0.03	-0.12	0.33	0.13	0.04	13
Aerobically weathered horizons	-0.09	-0.57	0.44	0.22	0.05	22
Parent materials	-0.04	-0.15	0.14	0.13	0.06	4
Organic horizons polluted	0.24	0.16	0.36	0.08	0.03	9
Mineral horizons polluted	0.05	-0.12	0.18	0.10	0.03	9
Technical waste	0.59	0.05	1.81	0.75	0.33	5
			δ^{66}Zn			
Organic horizons polluted	-0.36	-0.57	-0.15	0.17	0.06	9
Mineral horizons polluted	-0.08	-0.19	-0.08	0.09	0.03	9
Technical waste	0.11	-0.46	0.11	0.42	0.17	6

3.6 Error discussion

I am aware that the presented results and interpretations based on these results include some uncertainties which may result from the uncertainties of sampling, sample preparation and measurements.

The humic acid used in the lab experiments is insolubilized by heating to allow separation of humic acid from the solution by centrifugation. However this insolubilization of the humic acid seems to significantly decrease the number of phenolic-type groups (Weber et al., 2006b). Thus, the obtained IHA was changed artificially and properties affecting Cu sorption and isotope fractionation might have been altered. However, the complexing properties of the functional groups of the IHA do not seem to be changed substantially which is illustrated by the fact that the NICA-Donnan parameters (Tab. B 2) used by Saito et al. (2004) to describe Cu binding to commercially available Aldrich humic acid also show a good match for Cu binding on IHA (Fig. B-1; **Section B**).

When interpreting the vertical distribution of δ^{65}Cu and δ^{66}Zn values in soil it must be considered that most central Euorpean soils developed from a mixture of different parent materials with variable Cu and Zn isotope signatures. Five of the 11 study soils developed from periglacial cover beds consisting of up to three solifluctional layers. To assess the influence of this soil layering, all three parent materials of the Skeleti-Stagnic Luvisol (loess, shale, and Laacher See tephra) were sampled and the δ^{65}Cu value determined. My results show that the vertical distribution of δ^{65}Cu values in soil cannot be explained by mixing of these parent materials (Tab. C-3, Fig C-5). Furthermore, layered and non-layered soils exhibited a similar vertical distribution of the δ^{65}Cu values (Fig. C-5, Fig. D-3). Thus, the assumption that variations in Cu and Zn stable isotope ratios in soil are mainly caused by transport of fractionated Cu and Zn and not by a mixture of different parent materials seem to be justified, even if exceptions might occur (**Sections C-D**).

The collected soil samples might not be representative for the studied soil horizons because of high heterogeneity of the horizon in the field or demixing of different components of the sampled horizons during preparation of subsamples for the digestion. This is hard to control as soil samples were sampled by different people, but methods used to sample Slovakian samples are described in Lobe et al. (1998) and Wilcke et al.

(1999) and are adequate for representative sampling. The samples taken by myself were collected for each macroscopically identified soil horizon from a soil pit. Organic horizons were sampled with a 0.4 x 0.4-m frame, mineral horizons with three 100-ml sampling cylinders taken from different parts of the horizon. Most subsamples for concentration and metal isotope ratio measurements were prepared by separating the sample in four aliquots from which two were mixed for grinding. This was repeated until a sufficient amount of sample was collected (**Section C-E**).

Digestion of the samples might be incomplete because of resistant soil components or of re-precipitation of minerals after digestion resulting in too low measured concentrations (Totland et al., 1992; Yokoyama et al., 1999). Incomplete extraction might also affect the measured metal stable isotope ratios. However, samples were checked visually after digestion and no solids could be detected (**Section C-E**).

Sequential extractions separate operationally defined fractions and do not offer information about the real chemical speciation of the element of interest and therefore must be interpreted carefully (Bacon and Davidson, 2008). Furthermore, it is difficult to check the quality of sequential extractions, because for many extraction schemes no certified reference materials exist. Therefore, I processed CRM 7003 three times. The precision of the sum of fractions was 13% (2 RSD), with all sums of concentrations of the seven fractions falling in the range of ±10% of the certified value. For each sample, I checked whether the concentrations of all seven fractions deviated by >20% from the concentrations measured in the total digests. If so, the results were discarded and the sample was processed once more (**Section C-D**).

Concentration measurements can be subject to various kinds of interferences, contaminations, and dilution errors. Interferences depend on the used analytical method and are different for FAAS, ETAAS, and ICP-MS. However, for concentration measurements standards were remeasured in appropriate intervals to control performance of the measurements, for ICP-MS measurements Rh was used as an internal standard and certified reference materials were measured to test for accuracy of my Cu and Zn measurements (Tab. A2). For Cu and Zn concentrations every sample was measured at least twice and several samples were independently digested and measured in replicate. Copper and Zn concentration showed a precision of ca. 10% (2 RSD). Detection limits for Cu and Zn were 0.3 µg l^{-1} (GFAAS) and 0.8 µg l^{-1} (FAAS),

respectively, and concentrations of all measured elements were in a range well above the detection limit (**Section B-E**).

Because of the small variations in the stable isotope ratios of Cu and Zn, sample preparation and the measurement of isotope ratios has to performed with maximum care to avoid erroneous results. Several problems and methods for their correction have been reported in the literature to achieve accurate high-precision results. The major challenges which have to be dealt with are (1) isotope fractionation during sample preparation (Chapman et al., 2006; Marechal and Albarede, 2002), (2) mass-bias effects (Marechal et al., 1999; Mason et al., 2004b; Petit et al., 2008), (3) spectral interferences (Mason et al., 2004a; Petit et al., 2008), and (4) contamination of the sample (Li et al., 2009; Shiel et al., 2009).

(1) Copper and Zn stable isotopes are fractionated by various processes (Cloquet et al., 2008; Zhu et al., 2002) and thus also chemical treatment during sample preparation might affect isotope ratios. Therefore, to ash samples before digestion, temperatures (450°C) were chosen that did not cause evaporations of Zn and all other steps were performed with maximum care to prevent loss of analyte and therefore possibly induce fractionation. Marechal and Albarede (2002) reported fractionation of Cu and Zn isotopes on the resin during sample purification and also overloading of the column may result in significant fractionation and cause misleading results (Chapman et al., 2006). To avoid such an artificial fractionation on the resin, recovery was checked for every sample and samples which did not show recoveries of 100±6% were rejected and reprocessed.

(2) The term “mass bias” describes the fact that the heavy isotope is preferentially transmitted in the mass spectrometer compared to the light isotope. Ionization efficiency, hydrodynamic entrainment behind the cones, space-charge effects and chromatic aberrations in the electrostatic sector are possible explanations for this phenomenon (Mason et al., 2004b; Petit et al., 2008). Mass bias can be subdivided in instrumental mass discrimination effects and matrix-dependent non-spectral mass discrimination effects (Mason et al., 2004b). Instrumental mass discrimination depends on the type of the instrument used and instrumental settings and may change with time.

One part of the instrument which can seriously influence instrumental mass bias is the sample introduction system. Sudden shifts in mass bias may occur by using desolvating nebulizers which even could not be corrected with the help of a dopant element (Archer and Vance, 2004). However, I only used wet sample introduction to avoid this problem.

Matrix-dependent non-spectral mass discrimination may occur if organic or inorganic components in the sample affect mass discrimination. Such effects were reported for example for Fe on Cu and Zn isotope measurements and organic compounds on Cd and Zn isotope measurements (Archer and Vance, 2004; Shiel et al., 2009). Cobalt, which is not separated from the Cu fraction (Fig. A1a and A1b) does not produce a significant mass bias (Li et al., 2009; Petit et al., 2008). Matrix-induced mass bias was minimized by separating matrix elements from the analyte with the help of a chromatographic purification and by heating the sample in a 1:1 mixture of HNO_3 (67%) and H_2O_2 (30%) before isotope measurement to destroy any remaining organic componds that might affect mass bias during measurement (Shiel et al., 2009).

Despite these precautions, there was still a need to correct for mass bias during the measurement. In general, there are three different approaches how to correct the mass bias. The first is the sample-standard-bracketing approach. Before and after every sample, a standard is measured and the deviation of the sample from the mean of the two standards can be expressed as $\delta^{65}Cu$ value. This approach assumes mass-bias stability between sample and standard and linear drift of mass bias with time and requires a nearly perfect purification of the sample, because non-spectral mass discrimination can not be corrected with the standard-sample-bracketing method (Mason et al., 2004b; Petit et al., 2008).

The second approach is the use of an external element dopant. The isotope ratios can be corrected according to the known isotope composition of the dopant by using the exponential law (Peel et al., 2008) or by determining the intercepts of linear regression lines of the dopant and the analyte in a ln-ln space. As the gradients of samples and standards are identical, the difference in the isotope composition can be derived from the differences of the intercepts (Marechal et al., 1999; Peel et al., 2008). Both ways of correction can be additively combined with the standard-sample-bracketing approach to get optimum results.

The third approach is the use of a double or triple spike (Galer, 1999). This approach only works for elements with four or more stable isotopes and is therefore not applicable for Cu. To correct mass bias in Zn isotope ratio measurements this approach is rarely used (Bermin et al., 2006) because it is laborious and costly.

I corrected measured Cu isotope ratios with a Ni dopant using the exponential law in combination with standard-sample-bracketing and measured Zn isotope ratios in the ln-ln space using Cu as dopant in combination with standard-sample-bracketing. The $\delta^{66}Zn$ values were corrected in a different way than Cu because I reached a slightly better precision by this method during test measurements of standards. Both approaches produce reliable corrections of mass bias with similar precision (Petit et al., 2008). Because sample to dopant ratio may affect the quality of mass-bias corrected isotope ratios (Archer and Vance, 2004; Petit et al., 2008), all samples were diluted to a defined analyte concentration for isotope measurement and spiked with a similar mass of the dopant element. Analyte to dopant ratios were chosen in a way to achieve similar beam intensities for the selected analyte and dopant isotopes.

(3) Spectral interferences occur when the analyte has the same mass to charge ratio as a matrix component or as a combination of matrix components. Besides species like e.g., $^{1}H^{1}H^{14}N^{16}O^{16}O^{16}O^{+}$ and $^{1}H^{1}H^{14}N^{16}O^{16}O^{18}O^{+}$, which are related to the HNO_3 in the sample solution, matrix-induced interferences occur ranging from simple ions (eg. $^{64}Ni^{+}$ on $^{64}Zn^{+}$) via argides ($NaAr^{+}$, $MgAr^{+}$, $AlAr^{+}$) and (hydr)oxides ($TiO^{+,}$ $TiOH^{+}$, VO^{+}, VOH^{+}, CrO^{+}, $CrOH^{+}$) to double charged species (Ba^{2+}, Ce^{2+}) on masses 63 to 70 (Mason, 2004a). To avoid matrix-related interferences, samples were chromatographically purified (Fig. A1) to separate Cu and Zn fractions from the matrix. High resolution (R = 10,000) scans on an Element 2 mass spectrometer (Thermo Scientific, Waltham, MA, USA) revealed that one single purification step was not sufficient to get clean Cu fractions of soil samples (Fig. A2a) and thus a second purification step was added (Fig. A2b). However, first measurements on the MC-ICP-MS indicated Ti interferences (Sections C and D) and therefore the extracts were measured in the high resolution mode (~10,000 M/ΔM; Weyer and Schwieters, 2003). The sample purification procedure was adjusted more carefully by rinsing eight times with altogether 10 ml of 7 mol l^{-1} HCL + 0.001% H_2O_2 after sample application to the

resin. After adjustment of the purification procedure, the mean Ti/Cu ratio was monitored in soil samples and reduced to 0.02 (n = 29) after the two column purifications. Experiments were performed with a Ti-spiked Cu standard (Tab. D3) indicating that at this Ti/Cu ratio, Ti would not significantly affect measured δ^{65}Cu values. Therefore, I returned to the low resolution mode.

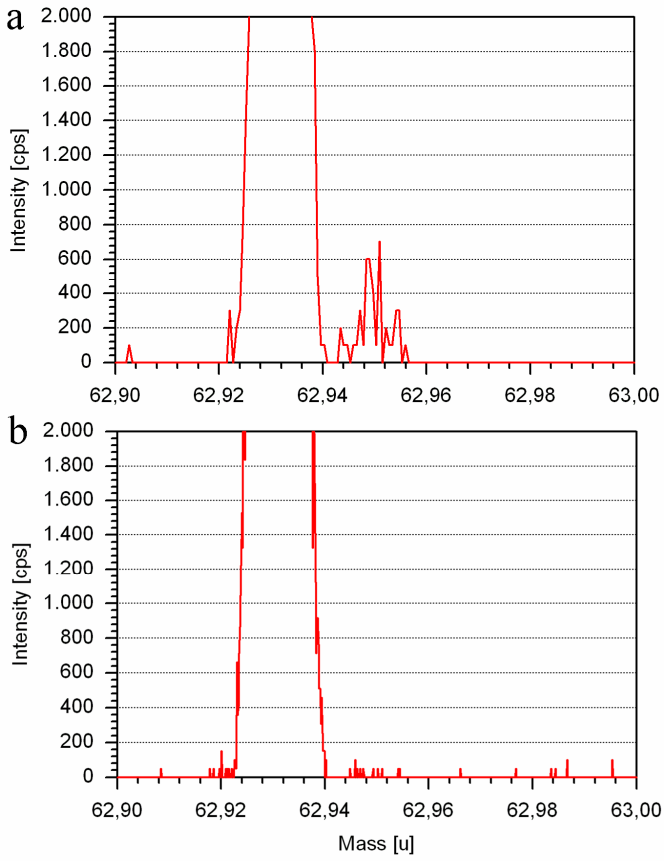

Figure A-4. High resolution scans of ^{63}Cu after (a) one and (b) two column purifications. After one purification, an interference between mass 62.94 and 62.96 can be seen which disappeared after the second purification.

(4) Contamination of the sample may affect measured stable isotope ratios. Therefore, great care was taken to avoid contamination during sample preparation by using clean air facilities and suprapur acids. Procedural blanks were prepared repeatedly reflecting the total contamination during digestion and purification. Copper blanks reached from 2.3±1.3 ng in the laboratory experiment (Section B) to 6.6±9.9 ng in Section C and probably result mainly from Cu contaminations of the resin (Shiel et al., 2009). However, the contribution of this processing-derived Cu to total Cu in the

sample was only up to 2% for few, but less than 1% for most samples. Zinc blanks were 42.5±63.5 ng and for most samples the blank accounted for <1% of the total Zn concentration in the sample. The effect of the blanks on stable isotope ratio measurements is discussed in the corresponding sections in more detail (**Sections C-E**).

For all stable isotope measurements, accuracy and precission of measurements were monitored by using in-house standards and certified reference materials. Long-term reproducibility of the in-house standards was 0.06‰ (2 SD, n = 49) for δ^{65}Cu and 0.08‰ (2SD, n = 10) for δ^{66}Zn. Currently, no environmental reference material with certified values for δ^{65}Cu and δ^{66}Zn is available. Thus, accuracy had to be checked by comparison with published values.

Reference materials were chosen in order to cover a broad range of geological materials. One soil (CRM 7003 a silty clay loam from the Czech Meteorology Institute, Brno, Czech Republic), basalt of the Columbia River (BCR-2), and granodiorite silver plume (GSP-2) reference materials from the United States Geological Survey (USGS) were selected. Furthermore, I chose a manganese nodule (NOD-P-1, USGS) because there are published δ^{65}Cu and δ^{66}Zn values available (Chapman et al., 2006) which offered the opportunity to compare the published with my own results. The δ^{65}Cu and δ^{66}Zn values of the reference materials are summarized in Table A2. The BCR-2 standard was chosen because δ^{65}Cu and δ^{66}Zn values were already published for the BCR-1 standard (which is not available anymore) and similar δ^{65}Cu and δ^{66}Zn values in BCR-1 and BCR-2 were assumed because both reference materials were prepared from the same basalt. Unfortunaly, δ^{65}Cu values of two BCR standards do not seem to be consistent. While Archer and Vance (2004) reported a δ^{65}Cu value of 0.07±0.08‰ for BCR-1, I measured 0.20±0.06‰ for BCR-2. The δ^{66}Zn values seem to be similar in both BCR standards with 0.20±0.09‰ in BCR-1 (Archer and Vance, 2004) and 0.22±0.08‰ in BCR-2 (own measurement). The reference material NOD-P-1 was measured with δ^{65}Cu 0.46±0.08‰ and δ^{66}Zn 0.78±0.09‰ (Chapman et al., 2006) which is similar to my results (Tab. A2, **Sections B-E**).

Table A-3. Copper and Zn concentrations, $\delta^{65}Cu$ and $\delta^{66}Zn$ values, and associated standard deviations.

CRM	Cu mg kg^{-1}	2SD	$\delta^{65}Cu$	2SD	n
SCL-7003[a]	27.4	2.9	0.18	0.12	6
BCR-2[b]	16.9	1.2	0.20	0.06	9
GSP-2[c]	38.0	1.1	0.30	0.13	4
NOD-P-1[d]	11386	1893	0.35	0.11	2
CRM	Zn mg kg^{-1}	2SD	$\delta^{66}Zn$	2SD	n
SCL-7003[a]	76.7	0.4	-	-	-
BCR-2[b]	140.3	5.3	0.22	0.08	5
GSP-2[c]	122.4	12.0	-	-	-
NOD-P-1[d]	1467.5	-	0.84	-	1

(a) certified values: Cu 29.1±0.8 mg kg^{-1}, Zn 81±7.6 mg kg^{-1};(b) certified values: Cu 19±2 mg kg^{-1}, Zn 127±9 mg kg^{-1}; (c) certified values: Cu 43±4 mg kg^{-1}, Zn 120±10 mg kg^{-1}; (d) certified values: Cu 11500±50 mg kg^{-1}, Zn 1600±6 mg kg^{-1}.

4 General conclusions

In the following, I answer the initially posed research questions.

(1) Are Cu stable isotopes fractionated during complexation with humic acid and does Cu binding to different functional groups at different pH influence the extent of fractionation (**Section B**)?

Copper isotopes were fractionated during complexation on humic acid ($\Delta^{65}Cu_{IHA\text{-}solution}$ = 0.26 ± 0.11‰; 2SD). The fractionation factor was similar in the pH range of 3-7. Chemical speciation modelling revealed that the size of Cu isotope fractionation on energetically different binding sites is indistinguishable.

(2) Can the knowledge of $\delta^{65}Cu$ values improve the understanding of biogeochemical processes of Cu during soil genesis in hydromorphic soils (**Section C**)?

Copper stable isotope ratios in redoximorphic soils show a trend to heavier $\delta^{65}Cu$ values with depth indicating enhanced mobility of ^{63}Cu in the redox-influenced horizons. Furthermore, plant-induced Cu isotope fractionation, i.e. fractionation during transport in plants and recycling of light Cu can be seen in the organic horizons.

(3) Can the knowledge of the δ^{65}Cu values help to understand biogeochemical and soil genetic processes in soils developed under oxic weathering condition (**Section D**)?

The δ^{65}Cu values in aerobically weathered soils seem to be driven by fractionation between mobile and immobile Cu species causing characteristic depth distributions for pronounced Podzols and Cambisols. The depth distribution allowed conclusions on Cu transport in soil during soil genesis and δ^{65}Cu values of the organic horizons indicated plant-induced fractionation. The vertical distribution of δ^{65}Cu values in the Cambisols showed increasingly lighter Cu with increasing depth which is the opposite trend compared with the hydromorphic soils.

(4) Can δ^{65}Cu and δ^{66}Zn values be used as tracers for source and transport of Cu and Zn in soils polluted by the emissions of a Cu smelter (**Section E**)?

The δ^{65}Cu and δ^{66}Zn values in contaminated soils allow for conclusions on sources, depth of metal dislocation, and biogeochemical behavior of Cu and Zn in soil. The stable isotope ratios of Zn indicated input of Zn mainly by deposition from the atmosphere originating at the Cu smelter, while stable isotope ratios of Cu indicated a transport depth of ca. 0.4 m in the mineral soil within the 60 years of operation of the Cu smelter. Copper stable isotopes seem to be fractionated by equilibrium fractionation between mobile and immobile Cu species, while variations in δ^{66}Zn values in soil seem to be mainly driven by plant-induced fractionation, changes in speciation, and mixing of native and smelter-derived Zn.

5 References

Alcacio, T. E., Hesterberg, D., Chou, J. W., Martin, J. D., Beauchemin, S., and Sayers, D. E., 2001. Molecular scale characteristics of Cu(II) bonding in goethite-humate complexes. Geochim. Cosmochim. Acta 65, 1355-1366.

Alloway, B. J., 1990. Heavy metals in soils. Blackie; Halsted Press, Glasgow, New York.

Archer, C. and Vance, D., 2004. Mass discrimination correction in multiple-collector plasma source mass spectrometry: an example using Cu and Zn isotopes. J. Anal. Atom. Spectrom. 19, 656-665.

Artiola, J. F., 2005. Speciation of copper in the environment. In: Cornelis, R. (Ed.), Handbook of elemental speciation 2 - species in the environment, food, medicine and occupational health. John Wiley & Sons, Chinchester.

Asael, D., Matthews, Butler, I., Rickard, A. D., Bar-Matthews, M., and Halicz, L., 2006. (CU)-C-65/(CU)-C-63 fractionation during copper sulphide formation from iron sulphides in aqueous solution. Geochim. Cosmochim. Acta 70, A23-A23.

Asael, D., Matthews, A., Bar-Matthews, M., and Halicz, L., 2007. Copper isotope fractionation in sedimentary copper mineralization (Tinma Valley, Israel). Chem. Geol. 243, 238-254.

Asael, D., Matthews, A., Bar-Matthews, M., Halicz, L., Ehrlich, S., and Teplyakov, N., 2005. Redox fractionation of copper isotopes in sedimentary conditions. Geochim. Cosmochim. Acta 69, A216-a216.

Bacon, J. R. and Davidson, C. M., 2008. Is there a future for sequential chemical extraction? Analyst 133, 25-46.

Balistrieri, L. S., Borrok, D. M., Wanty, R. B., and Ridley, W. I., 2008. Fractionation of Cu and Zn isotopes during adsorption onto amorphous Fe(III) oxyhydroxide: experimental mixing of acid rock drainage and ambient river water. Geochim. Cosmochim. Acta 72, 311-328.

Benedetti, M. F., Milne, C. J., Kinniburgh, D. G., Vanriemsdijk, W. H., and Koopal, L. K., 1995. Metal-ion binding to humic substances - application of the nonideal competitive adsorption model. Environ. Sci. Technol. 29, 446-457.

Bermin, J., Vance, D., Archer, C., and Statham, P. J., 2006. The determination of the isotopic composition of Cu and Zn in seawater. Chem. Geol. 226, 280-297.

Borrok, D. M., Ridley, W. I., and Wanty, R. B., 2008. Isotopic fractionation of Cu and Zn during adsorption onto bacterial surfaces. Geochim. Cosmochim. Acta 72, A99-a99.

Buck, K. N., Ross, J. R. M., Flegal, A. R., and Bruland, K. W., 2007. A review of total dissolved copper and its chemical speciation in San Francisco Bay, California. Environ. Res. 105, 5-19.

Chapman, J. B., Mason, T. F. D., Weiss, D. J., Coles, B. J., and Wilkinson, J. J., 2006. Chemical separation and isotopic variations of Cu and Zn from five geological reference materials. Geostandard Geoanal. Res. 30, 5-16.

Clayton, R. E., Hudson-Edwards, K. A., and Houghton, S. L., 2005. Isotopic effects during Cu sorption onto goethite. Geochim. Cosmochim. Acta 69, A216-a216.

Cloquet, C., Carignan, J., Lehmann, M. F., and Vanhaecke, F., 2008. Variation in the isotopic composition of zinc in the natural environment and the use of zinc isotopes in biogeosciences: a review. Anal. Bioanal. Chem. 390, 451-463.

Cloquet, C., Carignan, J., and Libourel, G., 2006. Isotopic composition of Zn and Pb atmospheric depositions in an urban/periurban area of northeastern France. Environ. Sci. Technol. 40, 6594-6600.

Contin, M., Mondini, C., Leita, L., and De Nobili, M., 2007. Enhanced soil toxic metal fixation in iron (hydr)oxides by redox cycles. Geoderma 140, 164-175.

de Jonge, L. W., Kjaergaard, C., and Moldrup, P., 2004. Colloids and colloid-facilitated transport of contaminants in soils: an introduction. Vadose Zone J. 3, 321-325.

Dube, A., Zbytniewski, R., Kowalkowski, T., Cukrowska, E., and Buszewski, B., 2001. Adsorption and migration of heavy metals in soil. Pol. J. Environ. Stud. 10, 1-10.

Dudka, S. and Adriano, D. C., 1997. Environmental impacts of metal ore mining and processing: a review. J. Environ. Qual. 26, 590-602.

Ehrlich, S., Butler, I., Halicz, L., Rickard, D., Oldroyd, A., and Matthews, A., 2004. Experimental study of the copper isotope fractionation between aqueous Cu(II) and covellite, CuS. Chem. Geol. 209, 259-269.

Erel, Y., 1998. Mechanisms and velocities of anthropogenic Pb migration in Mediterranean soils. Environ. Res. 78, 112-117.

Erel, Y., Veron, A., and Halicz, L., 1997. Tracing the transport of anthropogenic lead in the atmosphere and in soils using isotopic ratios. Geochim. Cosmochim. Acta 61, 4495-4505.

FAO, 2006. Guidlines for soil description. Food and Agriculture Organization of the United Nations, Rome.

Galer, S. J. G., 1999. Optimal double and triple spiking for high precision lead isotopic measurements. Chem. Geol. 157, 255-274.

Gale, N. H., Woodhead, A. P., Stos-Gale, Z. A., Walder, A., and Bowen, I., 1999. Natural variations detected in the isotopic composition of copper: possible applications to archaeology and geochemistry. Int. J. Mass Spectrom. 184, 1-9.

Grybos, M., Davranche, M., Gruau, G., and Petitjean, P., 2007. Is trace metal release in wetland soils controlled by organic matter mobility or Fe-oxyhydroxides reduction? J. Colloid Interf. Sci. 314, 490-501.

Günther, K. and Kastenholz, B., 2005. Speciation of zinc. In: Cornelis, R., Caruso, J., Crews, H., and Heumann, K. (Eds), Handbook of elemental speciation II - species in the environment, food, medicine and occupational health. John Wiley &Sons Ltd, Chichester.

Hoffmann, S. R., Shafer, M. M., and Armstrong, D. E., 2007. Strong colloidal and dissolved organic ligands binding copper and zinc in rivers. Environ. Sci. Technol. 41, 6996-7002.

Ildefonse, P., Manceau, A., Prost, D., and Groke, M. C. T., 1986. Hydroxy-Cu-vermiculite formed by the weathering of Fe-biotites at Salobo, Carajas, Brazil. Clay. Clay Miner. 34, 338-345.

IUSS Working Group WRB, 2006. World Soil Resource Reports No. 103. FAO, Rome.

John, S. G., Geis, R. W., Saito, M. A., and Boyle, E. A., 2007. Zinc isotope fractionation during high-affinity and low-affinity zinc transport by the marine diatom *Thalassiosira oceanica*. Limnol. Oceanogr. 52, 2710-2714.

Jouvin, D., Louvat, P., Juillot, F., Marechal, C. N., and Benedetti, M. F., 2009. Zinc isotopic fractionation: why organic matters. Environ. Sci. Technol. 43, 5747-5754.

Jouvin, D., Louvat, P., Marechal, C., and Benedetti, M. F., 2008. Fractionation of copper isotopes in plants. Geochim. Cosmochim. Acta 72, A441-A441.

Kavner, A., John, S. G., Sass, S., and Boyle, E. A., 2008. Redox-driven stable isotope fractionation in transition metals: Application to Zn electroplating. Geochim. Cosmochim. Acta 72, 1731-1741.

Keller, C. and Domergue, F. L., 1996. Soluble and particulate transfers of Cu, Cd, Al, Fe and some major elements in gravitational waters of a Podzol. Geoderma 71, 263-274.

Kinniburgh, D. G., Milne, C. J., Benedetti, M. F., Pinheiro, J. P., Filius, J., Koopal, L. K., and VanRiemsdijk, W. H., 1996. Metal ion binding by humic acid: Application of the NICA-Donnan model. Environ. Sci. Technol. 30, 1687-1698.

Li, W. Q., Jackson, S. E., Pearson, N. J., Alard, O., and Chappell, B. W., 2009. The Cu isotopic signature of granites from the Lachlan Fold Belt, SE Australia. Chem. Geol. 258, 38-49.

Lobe, I., Wilcke, W., Kobza, J., and Zech, W., 1998. Heavy metal contamination of soils in Northern Slovakia. J. Plant. Nutr. Soil. Sci. 161, 541-546.

Luo, X. S., Zhou, D. M., Liu, X. H., and Wang, Y. J., 2006. Solid/solution partitioning and speciation of heavy metals in the contaminated agricultural soils around a copper mine in eastern Nanjing city, China. J. Hazard. Mater.131, 19-27.

Ma, Y. B., Lombi, E., Nolan, A. L., and McLaughlin, M. J., 2006. Determination of labile Cu in soils and isotopic exchangeability of colloidal Cu complexes. Eur. J. Soil Sci. 57, 147-153.

Manceau, A., Nagy, K. L., Marcus, M. A., Lanson, M., Geoffroy, N., Jacquet, T., and Kirpichtchikova, T., 2008. Formation of metallic copper nanoparticles at the soil-root interface. Environ. Sci. Technol. 42, 1766-1772.

Marechal, C. and Albarede, F., 2002. Ion-exchange fractionation of copper and zinc isotopes. Geochim. Cosmochim. Acta 66, 1499-1509.

Marechal, C. N., Telouk, P., and Albarede, F., 1999. Precise analysis of copper and zinc isotopic compositions by plasma-source mass spectrometry. Chem. Geol. 156, 251-273.

Markl, G., Lahaye, Y., and Schwinn, G., 2006. Copper isotopes as monitors of redox processes in hydrothermal mineralization. Geochim. Cosmochim. Acta 70, 4215-4228.

Mason, T. F. D., Weiss, D. J., Horstwood, M., Parrish, R. R., Russell, S. S., Mullane, E., and Coles, B. J., 2004a. High-precision Cu and Zn isotope analysis by plasma source mass spectrometry - Part 1. Spectral interferences and their correction. J. Anal. Atom. Spectrom. 19, 209-217.

Mason, T. F. D., Weiss, D. J., Horstwood, M., Parrish, R. R., Russell, S. S., Mullane, E., and Coles, B. J., 2004b. High-precision Cu and Zn isotope analysis by plasma source mass spectrometry - Part 2. Correcting for mass discrimination effects. J. Anal. Atom. Spectrom. 19, 218-226.

Mathur, R., Ruiz, J., Titley, S., Liermann, L., Buss, H., and Brantley, S., 2005. Cu isotopic fractionation in the supergene environment with and without bacteria. Geochim. Cosmochim. Acta 69, 5233-5246.

Mattielli, N., Petit, J. C. J., Deboudt, K., Flament, P., Perdrix, E., Taillez, A., Rimetz-Planchon, J., and Weis, D., 2009. Zn isotope study of atmospheric emissions and dry depositions within a 5-km radius of a Pb-Zn refinery. Atmos. Environ. 43, 1265-1272.

Mattielli, N., Rimetz, J., Petit, J., Perdrix, E., Deboudt, K., Flament, P., and D. Weis, 2006. Zn-Cu isotopic study and speciation of airborne metal particles within a 5-km zone of a lead-zinc smelter. Geochim. Cosmochim. Acta 70, A 401.

McMartin, I., Henderson, P. J., and Nielsen, E., 1999. Impact of a base metal smelter on the geochemistry of soils of the Flin Flon region, Manitoba and Saskatchewan. Can. J. Earth Sci. 36, 141-160.

Moynier, F., Pichat, S., Pons, M. L., Fike, D., Balter, V., and Albarede, F., 2009. Isotopic fractionation and transport mechanisms of Zn in plants. Chem. Geol. 267, 125-130.

Nriagu, J. O. and Pacyna, J. M., 1988. Quantitative assessment of worldwide contamination of air, water and soils by trace-metals. Nature 333, 134-139.

O´Neil, J. R., Theoretical and experimental aspects of isotopic fractionation. In: Stable isotopes in high temperature geological processes, Valley, J. W.; Taylor, H. P.; J.R., O´Neil, (Eds). Mineralogical Society of America: Michigan, 1986; Vol. 16, pp 1-40.

Pacyna, J. M. and Pacyna, E. G., 2002. An assessment of global and regional emissions of trace metals to the atmosphere from anthropogenic sources worldwide. Environ. Rev. 9, 269-298.

Peel, K., Weiss, D., Chapman, J., Arnold, T., and Coles, B., 2008. A simple combined sample-standard bracketing and inter-element correction procedure for accurate mass bias correction and precise Zn and Cu isotope ratio measurements J. Anal. Atom. Spectrom. 23, 103-110.

Pelfrene, A., Gassama, N., and Grimaud, D., 2008. Dissolved Cu(II) speciation in unpolluted soil solutions of a planosolic horizon. Electroanal. 20, 841-850.

Petit, J. C. J., de Jong, J., Chou, L., and Mattielli, N., 2008. Development of Cu and Zn isotope MC-ICP-MS measurements: application to suspended particulate matter and sediments from the Scheldt estuary. Geostandard Geoanal. Res. 32, 149-166.

Pokrovsky, O. S., Viers, J., and Freydier, R., 2005. Zinc stable isotope fractionation during its adsorption on oxides and hydroxides. J. Colloid Interf. Sci. 291, 192-200.

Pokrovsky, O. S., Vim, J., Emnova, E. E., Kompantseva, E. I., and Freydier, R., 2008. Copper isotope fractionation during its interaction with soil and aquatic microorganisms and metal oxy(hydr) oxides: possible structural control. Geochim. Cosmochim. Acta 72, 1742-1757.

Saito, T., Nagasaki, S., Tanaka, S., and Koopal, L. K., 2004. Application of the NICA-Donnan model for proton, copper and uranyl binding to humic acid. Radiochim. Acta 92, 567-574.

Schlichting, E., Blume, H. P., and Stahr, K., 1995. Bodenkundliches Praktikum. Enke, Stuttgart.

Seki, H. and Suzuki, A., 1995. Adsorption of heavy-metal ions onto insolubilized humic-acid. J. Colloid Interf. Sci. 171, 490-494.

Senesi, N., Sposito, G., and Martin, J. P., 1986. Copper(Ii) and Iron(Iii) Complexation by soil humic acids - an Ir and electron-spin-resonance study. Sci. Total Environ. 55, 351-362.

Shiel, A. E., Barling, J., Orians, K. J., and Weis, D., 2009. Matrix effects on the multi-collector inductively coupled plasma mass spectrometric analysis of high-precision cadmium and zinc isotope ratios. Anal. Chim. Acta 633, 29-37.

Sivry, Y., Riotte, J., Sonke, J. E., Audry, S., Schafer, J., Viers, J., Blanc, G., Freydier, R., and Dupre, B., 2008. Zn isotopes as tracers of anthropogenic pollution from Zn-ore smelters The Riou Mort-Lot River system. Chem. Geol. 255, 295-304.

Sonke, J. E., Sivry, Y., Viers, J., Freydier, R., Dejonghe, L., Andre, L., Aggarwal, J. K., Fontan, F., and Dupre, B., 2008. Historical variations in the isotopic composition of atmospheric zinc deposition from a zinc smelter. Chem. Geol. 252, 145-157.

Totland, M., Jarvis, I., and Jarvis, K. E., 1992. An assessment of dissolution techniques for the analysis of geological samples by plasma spectrometry. Chem. Geol. 95, 35-62.

Viers, J., Oliva, P., Nonell, A., Gelabert, A., Sonke, J. E., Freydier, R., Gainville, R., and Dupre, B., 2007. Evidence of Zn isotopic fractionation in a soil-plant system of a pristine tropical watershed (Nsimi, Cameroon). Chem. Geol. 239, 124-137.

Voegelin, A., Pfister, S., Scheinost, A. C., Marcus, M. A., and Kretzschmar, R., 2005. Changes in zinc speciation in field soil after contamination with zinc oxide. Environ. Sci. Technol. 39, 6616-6623.

Weber, F. A., Voegelin, A., Kaegi, R., and Kretzschmar, R., 2009. Contaminant mobilization by metallic copper and metal sulphide colloids in flooded soil. Nature Geosci. 2, 267-271.

Weber, T., Allard, T., and Benedetti, M. F., 2006a. Iron speciation in interaction with organic matter: modelling and experimental approach. J. Geochem. Explor. 88, 166-171.

Weber, T., Allard, T., Tipping, E., and Benedetti, M. F., 2006b. Modeling iron binding to organic matter. Environ. Sci. Technol. 40, 7488-7493.

Weiss, D. J., Mason, T. F. D., Zhao, F. J., Kirk, G. J. D., Coles, B. J., and Horstwood, M. S. A., 2005. Isotopic discrimination of zinc in higher plants. New Phytol. 165, 703-710.

Weiss, D. J., Rehkämper, M., Schoenberg, R., McLaughlin, M., Kirby, J., Campbell, P. G. C., Arnold, T., Chapman, J., Peel, K., and Gioia, S., 2008. Application of nontraditional stable-isotope systems to the study of sources and fate of metals in the environment. Environ. Sci. Technol. 42, 655-664.

Weyer, S. and Schwieters, J., 2003. High-precision Fe isotope measurements with high mass resolution MC-ICPMS. Int. J. Mass Spectrom. 226, 355-368.

Wilcke, W., Guschker, C., Kobza, J., and Zech, W., 1999. Heavy metal concentrations, partitioning, and storage in Slovak forest and arable soils along a deposition gradient. J. Plant. Nutr. Soil. Sc. 162, 223-229.

Yokoyama, T., Makishima, A., and Nakamura, E., 1999. Evaluation of the coprecipitation of incompatible trace elements with fluoride during silicate rock dissolution by acid digestion. Chem. Geol. 157, 175-187.

Zeien, H. and Brümmer, G. W., 1989. Chemische Extraktion zur Bestimmung von Schwermetallbindungsformen in Böden. Mitteilu. Dtsch. Bodenkundl. Gesellsch. 59, 505-510.

Zhu, X. K., Guo, Y., Williams, R. J. P., O'Nions, R. K., Matthews, A., Belshaw, N. S., Canters, G. W., de Waal, E. C., Weser, U., Burgess, B. K., and Salvato, B., 2002. Mass fractionation processes of transition metal isotopes. Earth. Planet. Sc. Lett. 200, 47-62.

B Copper isotope fractionation during complexation with insolubilized humic acid

Moritz Bigalke[1,3], Stefan Weyer[2+], Wolfgang Wilcke[3]

[1]Johannes Gutenberg University Mainz, Earth System Science Research Center, Geographic Institute, Professorship of Soil Science/Soil Geography, Johann-Joachim-Becher-Weg 21, 55128 Mainz, Germany.

[2]University of Frankfurt, Institute of Geoscience, Altenhöferallee 1, 60438 Frankfurt am Main, Germany.

[3]Geographic Institute, University of Berne, Hallerstrasse 12, 3012 Berne, Switzerland.

[+]Current address: Institute of Geology and Mineralogy, University of Cologne, Zülpicher Str. 49b, 50674 Köln

Environmental Science & Technology, 44, 5496-5502

1 Abstract

The bioavailability, mobility, and toxicity of Cu depend on Cu speciation in solution. In natural systems like soils, sediments, lakes, and river waters, organo-Cu complexes are the dominating species. Organo-complexation of Cu may cause a fractionation of stable Cu isotopes. The knowledge of Cu isotope fractionation during sorption on humic acid may help to better understand Cu isotope fractionation in natural environments and thus facilitate the use of Cu stable isotope ratios ($\delta^{65}Cu$) as tracer of the fate of Cu in the environment. We therefore studied Cu isotope fractionation during complexation with insolubilized humic acid (IHA) as a surrogate of humic acid in soil organic matter with the help of sorption experiments at pH 2-7. We used NICA-Donnan chemical speciation modeling to describe Cu binding on IHA and to estimate the influence of Cu binding to different functional groups on Cu isotope fractionation. The observed overall Cu isotope fractionation at equilibrium between the solution and IHA was $\Delta^{65}Cu_{IHA\text{-}solution}$ = 0.26 ± 0.11‰ (2SD). Modeled fractionations of Cu isotopes for low- (LAS) and high-affinity sites (HAS) were identical with $\Delta^{65}Cu_{LAS/HAS\text{-}solution}$ = 0.27. pH did not influence Cu isotope fractionation in the investigated pH range.

2 Introduction

Bioavailability, mobility, and toxicity of Cu depend on Cu speciation in natural systems (Erickson et al., 1996; Dube et al., 2001; Kunito et al., 1999). In soils, sediments, and natural waters, at the interface between geosphere and biosphere, organo-Cu complexes are frequently the most important chemical Cu species strongly influencing the fate of Cu in the environment (Aritola et al., 2005; Buck et al., 2007; Hoffmann et al. 2007). Understanding stable isotope fractionation caused by the complexation of Cu by organic matter (OM) may help to interpret Cu isotope signatures in environmental samples and accordingly improve our knowledge about the environmental behavior of Cu.

Currently, only few published studies of Cu isotope ratios in natural biogeochemical systems are available. A first study of Cu isotope fractionation in soils pointed at the need for detailed investigation of Cu isotope fractionation during Cu complexation by organic matter as a prerequisite for appropriate interpretation of Cu isotope ratios in soil (Bigalke et al., 2010). A study of Cu speciation in natural waters demonstrated that organo-complexation of Cu influences the partitioning of stable Cu isotopes between particulate and dissolved Cu species (Vance et al., 2008). These authors observed that particle-bound Cu was isotopically lighter compared to dissolved Cu species (<0.2µm). Other studies showed that adsorption of Cu to metal oxy(hydr)oxides causes a Cu isotope fractionation expressed as difference in Cu isotope ratios (i.e., δ^{65}Cu values) between sorbent and solution, $\Delta^{65}Cu_{oxy(hydr)oxide\text{-}solution}$ of 0.34 to 1.00‰ (Clayton et al., 2005; Balistrieri et al., 2008; Pokrovsky et al., 2008). The adsorption to bacteria surfaces caused a fractionation of $\Delta^{65}Cu_{bacteria\text{-}solution}$ -1.80 to 0.60‰ (Pokrovsky et al., 2008, Borrok et al., 2008). Mathur et al. (2005) reported that bacterial cells in a supergene environment can be covered by surface precipitates with $\Delta^{65}Cu_{bacteria\text{-}solution}$ of 3.04‰.

In studies of Fe and Zn isotope fractionations during organo-metal complexation, an enrichment of the heavier isotopes in the complexed form was reported. Similarily to Cu (Vance et al., 2008), this was attributed to the stronger bonding of the heavy metal isotope in organo complexes at equilibrium (Dideriksen et al., 2008; Jouvin et al., 2009). Iron which was complexed by desferrioxamine B (DFOB) showed $\Delta^{56}Fe_{DFOB\text{-}}$

$_{inorgic\ Fe}$ of 0.60 ± 0.15‰, while Zn bound to purified humic acid (PHA) showed $\Delta^{66}Zn_{PHA\text{-}freeZn^{2+}}$ of 0.24 ± 0.06‰ at pH ≥ 6 and no significant fractionation at pH ≤ 6 (Dideriksen et al., 2008; Jouvin et al., 2009). The pH dependence of Zn isotope fractionation during binding on PHA is explained by Zn bonding to different binding sites at different pH.

Metal binding to humic acids is pH dependent and occurs at various binding sites, including carboxyl, phenolic and other hydroxyl, carbonyl, amine, amide, sulfhydryl, ester, and other reactive sites (Dube et al., 2001; Kudeyarova, 2007; Stevenson, 1982). The Cu^{2+} ion can be bound by O-, N-, P-, and S-containing functional groups in which the O, N, P, and S atoms serve as electron donors. The dominating metal-complexing functional groups are carboxyl, phenolic hydroxyl, and carbonyl groups (Stevenson, 1982). To assess Cu binding to insolubilized humic acid (IHA) at fixed ionic strength and varying pH the NICA-Donnan model can be used. The NICA-Donnan model describes metal binding to organic substances by considering site heterogeneity, non-ideality, and electrostatic interactions. The model calculates metal binding to low affinity sites (LAS; carboxylic groups), high affinity sites (HAS; phenolic type groups) and electrostatically bound species (Benedetti et al., 1995; Kinniburgh et al., 1996) and is an often used tool to describe metal binding to organic substances (OS) (Saito et al., 2004; Villaverde et al., 2009; Weber et al., 2006).

Our objectives were to determine the stable Cu isotope fractionation factor for Cu complexation by insolubilized humic acid (IHA) as a model compound for humic substances (HS) in soil organic matter at equilibrium conditions with the help of sorption experiments at different pH values and to assess the role of different binding sites for Cu isotopic fractionation using geochemical speciation modeling.

3 Materials and methods

3.1 Sorption experiments

Aldrich humic acid was insolubilized according to Seki and Suzuki (1995). For insolubilization, Aldrich humic acid was converted to its Ca salt, heated for 1 h to 330°C, ground and washed several times with hot water and 1 M HNO_3. The humic acid was further purified with HF:HCl (2:1) and two times HCl for 2 h at 70°C (Weber et al.,

2006). For the Cu Sorption experiments, solutions were prepared containing 0.1 M $NaNO_3$ as background electrolyte and ca. 1.7 mg l^{-1} Cu added as $Cu(NO_3)_2$. The Cu concentrations at the different pH steps varied by up to 9.4% (2 RSD) of the target Cu concentrations. The pH of the solutions was adjusted to pH values between 2 and 7 using diluted HNO_3 and NaOH solutions. A relatively broad pH range was chosen to display a wide range of natural environments and account for differences in isotope fractionation at different pH. No buffer was used to stabilize pH because of possible effects on Cu speciation and isotope fractionation. For Sorption experiments, 0.2 ± 0.03 mg of IHA were weighted in a 15 ml polypropylene vessel and 10 ml of solution were added. Samples were shaken overhead for three days at ambient temperature and light conditions. During this time, equilibrium was reached in the experimental setup (Fig. B-4). Then, samples were centrifuged at 4000 rpm for 45 min, 2 x 50 µl of the supernatant were removed and diluted for Cu concentration analysis by graphite furnace atomic absorption spectrometry (GFAAS) and 7 ml of the supernatant were transferred to Savillex™ vessels for isotope analysis. pH was measured in the remaining solution. Additional samples were processed to prove that no IHA was solubilized during the experiment and that Cu sorption to IHA was reversible. The dissolved organic carbon (DOC) analysis in the solution indicated no solubilization and sorption-desorption experiments indicate total reversibility of Cu sorption on IHA (Fig. B-5).

For Cu purification, samples were evaporated to dryness and re-dissolved in 7 M HCl + 0.001% H_2O_2. Samples were purified according to a method modified from Marechal et al. (1999) on 2 ml Biorad™ AG-MP1 resin to avoid interference of Na during Cu isotope measurement. After purification, samples were evaporated to dryness, treated with 200 µl of conc. HNO_3 and 200 µl of 30% H_2O_2 on a hot plate for at least 4 h to rule out the presence of organics during isotope measurements. Samples were evaporated to dryness, re-dissolved in conc. HNO_3 and evaporated again to drive out Cl resulting from the purification procedure. Finally, samples were redissolved in 2% HNO_3. Recovery for every sample was checked using GFAAS, to avoid isotope fractionation on the resin (Marechal and Albarede, 2002). Samples which did not show a recovery of 100 ± 5% were rejected and not used for isotope analysis. Additional description of chemicals used, characterization of the IHA and work conditions are given in the supporting

information. Copper blanks for the whole experiment were 2.3 ± 1.3 ng (2SD, n = 6) compared to at least 356 ng of Cu in the samples.

3.2 Speciation modeling

Chemical modeling is a common tool to obtain information about metal binding to OM. We used the NICA-Donnan model which is one of the most common models to assess complexation of metal with humic substances. Details about the NICA-Donnan model are given elsewhere (Benedetti et al, 1995; Kinniburgh et al., 1996). The NICA-Donnan model distinguishes between low affinity sites (LAS; carboxylic groups), high affinity sites (HAS; phenolic type groups) and electrostatically bound species and may thus be suitable to test if different binding sites cause distinguishable Cu isotope fractionation.

Values for NICA-Donnan parameters were taken from the literature. The maximum sorption capacities for LAS and HAS, $Q_{max1\&2}$ were taken from a study in which insolubilized Aldrich HA was used (Weber et al., 2006). The log $K_{H1\&2}$ and $n_{H1\&2}$ $p_{1\&2}$, log $K_{Cu1\&2}$, and $n_{Cu1\&2}$ were taken from a study of Cu and UO_2 binding to Aldrich HA which was not altered by insolubilization (Saito et al., 2004; Tab. B2) and showed a good fit to the experimental data (Fig. B-1). The Donnan parameter b was set to 0.630 (Saito et al., 2004). A more detailed describtion of the imput parameters can be found in the literature (Benedetti et al., 1995; Kinniburgh et al., 1996). The ECOSAT program was used for speciation calculations.

3.3 Copper isotope measurements

Copper isotope ratios were measured with a Finnigan-Neptune (ThermoFisher) multiple collector inductively-coupled plasma mass spectrometer (MC-ICP-MS) similar to the method described in Bigalke et al. (2010). All Cu isotope ratios were expressed as δ^{65}Cu values relative to NIST 976 isotope reference material according to Equation B-1.

$$\delta^{65}Cu[‰] = \left(\frac{\left({}^{65}Cu/{}^{63}Cu\right)_{sample}}{\left({}^{65}Cu/{}^{63}Cu\right)_{NIST976}} - 1 \right) * 1000 \qquad \text{(B-1)}$$

A Cu standard (Merck, Darmstadt, Germany) was used as an in-house standard to check for intra-day and long-term reproducibility of δ^{65}Cu. The long-term reproducibility of this standard was 0.06‰ (2 SD, n= 49).

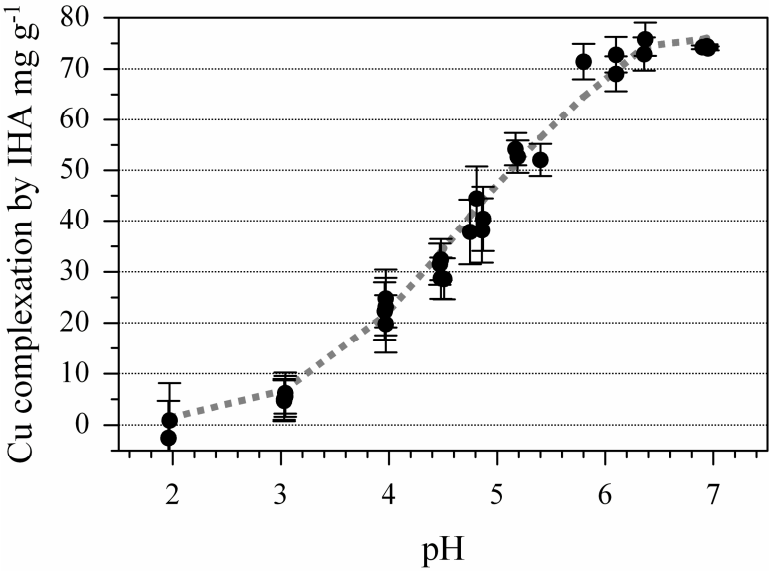

Figure B-1. Cu complexation by IHA as a function of pH. Black dots are measured values, the grey line represents modeled values of the NICA-Donnan model with input parameters from Table B-2 (Saito et al., 2004; Weber et al., 2006a).

4 Results

Copper complexation by the IHA ranged from approximately 0.9 to 74 mg g^{-1} Cu between pH 2.0 and 6.9, which means that 1 to 95% of total Cu was bound by the IHA (Tab. B1, Fig. B-1&B-3). To estimate fractionation between IHA and Cu in solution, the δ^{65}Cu values of two samples were excluded as outliers (grey marked in Tab. B1). The outliers might be caused by irreversible nonequilibrium binding to IHA causing Rayleigh-type fractionation with fractionation factors similar to that of equilibrium fractionation (Fig. B-2). In our graphical assessment, the remaining values showed a good correlation (R^2= 0.8625, p= 0.000, Fig. B-2). The slope of this correlation line indicates a $\Delta^{65}Cu_{IHA\text{-}solution}$ of 0.27 ‰. An implication of the linear fractionation line is a similar fractionation factor over the whole observed pH range. This suggests that there

are no differences in isotope fractionation between LAS and HAS of the IHA which we can resolve with our analytical method.

As an alternative to the graphical evaluation (Fig. B-2), $\Delta^{65}Cu_{IHA\text{-}solution}$ can be assessed by calculation according to Equations B-2 and B-3.

$$\Delta^{65}Cu_{\,final\ solution-starting\ solution} = \delta^{65}Cu_{\,final\ solution} - \delta^{65}Cu_{starting\ solution} \quad \text{(B-2)}$$

$$\Delta^{65}Cu_{IHA-\,final\ solution} = \frac{-\Delta^{65}Cu_{\,final\ solution-starting\ solution}}{\%\,Cu_{IHA}} \times 100 \quad \text{(B-3)}$$

where $\delta^{65}Cu_{starting\ solution}$ is the measured isotope composition of the starting solution, $\delta^{65}Cu_{final\ solution}$ is the measured isotope composition of the solution at the end of the sorption experiment and $\%Cu_{IHA}$ is the percentage of Cu complexed by IHA. The Cu isotope fractionation in solution (i.e. the difference in $\delta^{65}Cu$ between the initial and final solutions) reached up to -0.32‰. After excluding the two outliers (Tab. B1, grey marked) and the samples at pH 3 we calculated a mean fractionation $\Delta^{65}Cu_{IHA\text{-}solution}$ of 0.26 ± 0.11‰ (2SD; n = 14). The samples at pH 3 are not included in our calculation, because the observed fractionation in solution and adsorbed amount of Cu were small compared to the precision of isotope measurement (0.06‰) and error of concentration measurement (0.04). However, Figure B-2 shows that these values also fitted well the fractionation line within the analytical error.

Modeling of Cu speciation at the different pH values during the experiments showed that at low pH, HAS complexed only 11% (pH 2.0) of the total IHA-bound Cu. With increasing pH, the Cu fraction complexed by HAS, increased to 35% of the total IHA-bound Cu. However, at all pH ranges LAS contained the largest part (65-89%) of the IHA-bound Cu. Electrostatically adsorbed Cu only contributed a minor part of 0.1-1% to total IHA-bound Cu. The major part of Cu in the solution was Cu^{2+} (83-90% of the total dissolved Cu) and approximately 10% was $Cu(NO_3)_x^x$. The concentration of the $Cu(OH)_x^x$ species increased with increasing pH and contributed up to 7% to total dissolved Cu (Fig. B-3).

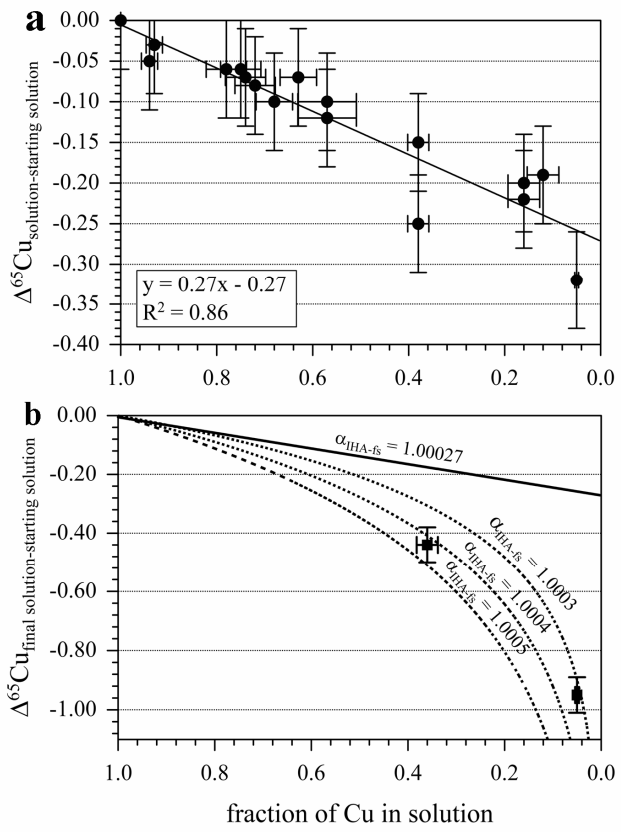

Figure B-2. $\delta^{65}Cu$ values of the final solution as a function of Cu in solution. Error bars on the y axis refer to the 0.06‰ (2SD) long-time reproducibility of our method. Error bars on the x axis refer to reproducibility of complexation of samples with the same initial pH. a) The graphical estimation gives a $\Delta^{65}Cu_{IHA\text{-}solution}$ = 0.27‰ for the samples which follow the equilibrium fractionation line (black dots, solid line). b) The two outliers (black squares) seem to be caused by Rayleigh-type fractionation as can be seen from their position on modeled Rayleigh fractionation curves (dotted lines, $\alpha_{IHA\text{-}fs}$ means $\alpha_{IHA\text{-}final\ solution}$).

Table B-1. pH, complexed Cu, δ^{65}Cu values, and fractionation of Cu isotopes

pH	Cu complexed by IHA	Cu fraction complexed by IHA	δ^{65}Cu solution	2 SD[a]	$\Delta^{65}Cu_{(final\ solution\text{-}starting\ solution)}$	modeled $\Delta^{65}Cu_{(final\ solution\text{-}starting\ solution)}$[b]	$\Delta^{65}Cu_{(IHA\text{-}final\ solution)}$[c]
	mg g^{-1}	%	‰	‰	‰	‰	‰
			Starting solution				
-[d]	-	-	0.63	0.02	-	-	-
			Sorption experiment				
1.97	0.9	1	-	-	-	-	-
1.96	-2.5	-3	-	-	-	-	-
3.03	4.7	6	-	-	-	-	-
3.04	5.6	7	-	-	-	-	-
3.04	6.2	7	0.60	0.02	-0.03	-0.02	-
3.03	5.0	6	0.58	0.01	-0.05	-0.02	-
3.96	22.3	25	0.57	0.03	-0.06	-0.06	0.24
3.97	23.2	26	0.56	0.04	-0.07	-0.06	0.26
3.97	19.8	22	0.57	0.01	-0.06	-0.06	0.26
3.97	24.8	28	0.55	0.02	-0.08	-0.06	0.29
4.47	31.5	36	-	-	-	-	-
4.48	32.4	37	0.56	0.04	-0.07	-0.10	0.19
4.48	28.7	33	-	-	-	-	-
4.51	28.6	32	0.53	0.04	-0.10	-0.10	0.30
4.75	37.8	43	0.51	0.03	-0.12	-0.12	0.27
4.87	40.4	46	-	-	-	-	-
4.86	38.1	43	0.53	0.01	-0.10	-0.13	0.23
4.81	44.4	50	-	-	-	-	-
5.40	54.2	62	0.48	0.05	-0.15	-0.16	0.24
5.17	52.7	64	0.19	0.02	-0.44	-	-
5.19	52.0	62	0.38	0.01	-0.25	-0.18	0.40
5.80	71.5	85	-	-	-	-	-
6.10	69.1	82	-	-	-	-	-
6.10	72.8	87	-	-	-	-	-
6.37	75.8	88	0.44	0.07	-0.19	-0.23	0.21
6.36	72.9	84	0.43	0.03	-0.20	-0.23	0.24
6.36	72.9	84	0.41	0.06	-0.22	-0.23	0.26
6.90	74.3	95	-	-	-	-	-
6.94	74.5	95	0.31	0.04	-0.32	-0.26	0.34
6.95	74.1	95	-0.32	0.02	-0.95	-	-

[a]2SD of 2-4 measurements of one sample. [b]According to Equation B-4 with $\Delta^{65}Cu_{LAS\text{-}final\ solution}$ = 0.267 and $\Delta^{65}Cu_{HAS\text{-}final\ solution}$ = 0.265. [c] According to Equation B-3.

5 Discussion

The knowledge about extent and direction of isotope fractionation during complexation with IHA as a model for natural organic matter (OM) is important for investigating processes in which mobility or toxicity of Cu depend on its speciation. In soils, high amounts of Cu can be bound to mobile but also to immobile OM. Thus, mobility of Cu in soils is highly dependent on occurrence and characteristics of OM (Dube et al., 2001) and the knowledge about Cu isotope fractionation during binding to organic acids might help to reconstruct speciation of Cu during transport in soils from bulk δ^{65}Cu values of soil horizons. These transport processes take place over long time scales and are difficult to assess with other analytical methods (Bigalke et al., 2010).

In natural waters, toxicity of Cu depends on its speciation and complexation with OM decreases toxic effects (Erikson et al., 1996). Stable Cu isotope measurements of natural waters might thus help to assess toxicity of Cu and to improve understanding of chemical speciation and transformation of Cu in natural waters.

Vance et al. (2008) reported large differences in δ^{65}Cu values of dissolved and particulate-bound Cu in river waters. This fractionation is assumed to be caused by equilibrium fractionation between dissolved Cu complexed by strong organic ligands and particulate-bound Cu with $\Delta^{65}Cu_{dissolved\text{-}particulate}$ of up to 1.6‰. This fractionation is much stronger than the equilibrium fractionation between Cu complexed by insolubilized humic acid and dissolved Cu species observed in our study. The strong fractionation between dissolved and particulate-bound Cu in rivers is assumed to be attributable to the binding strength of organic ligands preferentially complexing the heavy ^{65}Cu isotope with log K up to 16 for Cu (Vance et al., 2008). This assumption is not confirmed in our study where Δ^{65}Cu did not show clear differences between functional groups with different stability constants (log K of 2.26 for carboxylic-type groups and log K of 6.96, for phenolic-type groups). Possible explanations for the differences between our observations and those of Vance et al. (2008) include the higher complexity of natural systems with more than one available complexing organic compound, the presence of competing ions, and a different and variable ionic strength affecting complexation reactions.

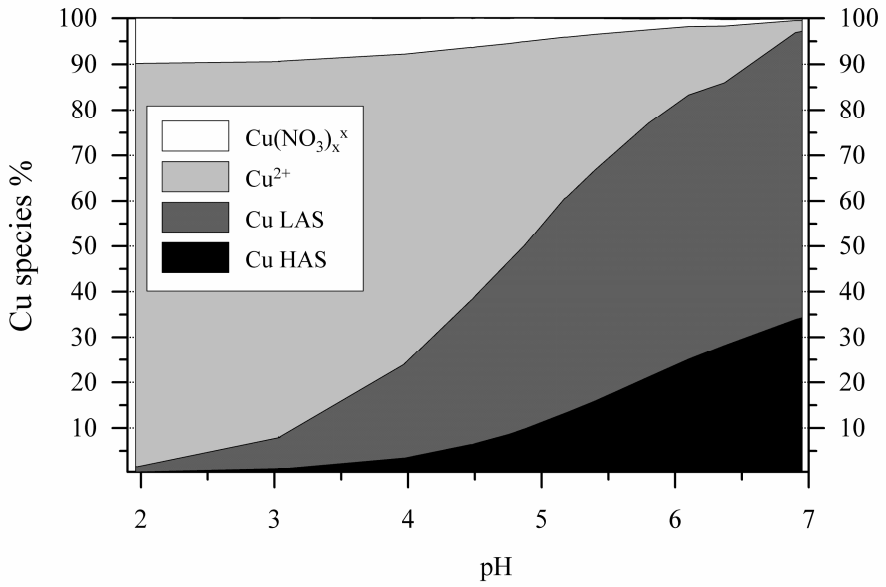

Figure B-3. Copper speciation during the experiment as a function of pH. Cu complexation by IHA was simulated using the NICA-Donnan model. The contribution of electrostatically bound Cu and $Cu(OH)_x^x$ complexes was very low (max. 0.04 % and 0.27 % of the total Cu) and is not shown in the figure.

5.1 Copper binding to humic acid

X-ray absorption spectroscopy (XAS) studies of the coordination of the Cu^{2+} ion in chemical complexes reveal Cu^{2+} as the centre of a Jahn-Teller distorted octahedron (Karlsson et al., 2006). In water, Cu^{2+} occurs as the $Cu(H_2O)_6^{+2}$ aquo complex. In this case, Cu^{2+} is surrounded by six oxygen atoms in the first coordination shell (Korshin et al., 1998). However, also fivefold coordination of Cu^{2+} in water was proposed resulting in fast changing square pyramidal and trigonal bipyramidal forms (Pasquarello et al. 2001). The first coordination shell of the Cu^{2+} ion in natural OM consists of four O or N atoms in the equatorial plane of a Jahn-Teller distorted octahedron and two O atoms in the axial positions. In the second shell, 2-4 C atoms are located corresponding to one- to two five-membered chelate rings involved in Cu binding (Karlsson et al., 2006; Xia et al., 1997). The contribution of the two axial coordinated O atoms to Cu binding to OM is small (Karlsson et al., 2006; Sheals et al. 2001). Because O and N can not be distinguished in XAS studies (Xia et al., 1997), the identification of the functional groups involved in Cu binding is difficult. But it is assumed that especially at low Cu/C ratios N-containing functional groups may play an important role (Frenkel et al., 2000).

In contrast, S-containing functional groups do not seem to substantially contribute to Cu^{2+} binding in OM (Karlsson et al., 2006), even if these bonds are possible (Smith et al., 2002). However, O-containing functional groups like COOH, phenolic OH and C=O are dominating the metal complexing ability of organic matter (Stevenson, 1982). The kind of functional groups involved in Cu binding is of special interest for our study because the complexation of Cu by different functional groups may cause different Cu isotope fractionations, as shown for Zn (Jouvin et al., 2009).

5.2 Copper isotope fractionation by complexation on IHA

The isotope fractionation between complexed Cu and Cu in solution is attributable to the differences in vibrational frequencies and zero point energies of the different isotopes. The heavier isotope has lower vibrational frequencies and forms stronger molecular bonds (O´Neil, 1986). Thus, when Cu complexed by IHA and Cu in solution are in equilibrium, ^{65}Cu will be enriched in the species in which Cu is more strongly bound. Usually bond strength is related to bond length, whereby stronger bonds are shorter (Huggins, 1953), although there may be exceptions (Kaupp et al., 2000). Korshin et al. (1998) reported shorter bonding distances for Cu^{2+} complexed by humic substances compared to Cu^{2+} in the aquo complex. These findings fit well to the observed heavier isotope composition of complexed Cu in our study. Bond length of equatorial Cu-O/N bonds reached from 1.92 to 1.96 Å in organic materials (Korshin et al., 1998; Xia et al., 1997; Sheals et al., 2001). Axial lengths of Cu bonding for these compounds was reported to range from 2.10 to 2.14 Å. In the aquo complex, bond length was 1.97 Å for equatorial and 2.24 Å for the axial coordinated atoms at pH 4 (Korshin et al., 1998; Harding, 1999). Besides bond length and strength also coordination might be a critical control of isotope fractionation (Schauble et al., 2009).

Because the exact composition of functional groups in organic materials is not known, it is not possible to estimate the contribution of different functional groups to differences in bond length analyzed by XAS. Some authors reported bond length for Cu complexation with well defined compounds and found 1.95 Å for sorption on carboxyl resin (Karlsson et al., 2006), 1.93 Å on phenolic groups (O´Neil, 1986), and 1.94 Å (2.20 Å axial) on salicylic acid (at pH 12; Korshin et al., 1998). Different functional groups may share Cu bonding depending on the OM properties, pH, and Cu/OM ratio. Jouvin et al. (2009) observed a pH-dependent isotope fractionation of Zn during

complexation with humic acid and attributed this to the increasing importance of high affinity sites (phenolic groups) as binding sites with increasing pH. Zinc is the only element which is chemically similar to Cu for which stable isotope fractionation was investigated during sorption to HA and for which the different binding sites were considered. In contrast to the findings of Jouvin et al. (2009) for Zn, no indications of pH-dependent differences in fractionation factors of Cu were obvious in our study (Fig. B-2). To estimate the fractionation factors of the different binding sites, δ^{65}Cu values in the solution can be modeled with Equation B-4:

$$Modeled\ \Delta^{65}Cu_{\ final\ solution-starting\ solution} = \frac{-\left[\%\ Cu_{LAS}\ /100\times\Delta^{65}Cu_{LAS-final\ solution} + \%\ Cu_{HAS}\ /100\times\Delta^{65}Cu_{HAS-final\ solution}\right]}{100}\times\%\ Cu_{IHA} \quad \text{(B-4)}$$

with modeled $\Delta^{65}Cu_{\text{final solution-starting solution}}$ (modeled Cu isotope fractionation between the solution at the end and at the beginning of the sorption experiment), $\%Cu_{LAS}$ (the contribution of Cu bound to LAS to the total IHA-bound Cu), $\Delta^{65}Cu_{\text{LAS-solution}}$ (the fractionation Δ^{65}Cu between LAS and the final equilibrium solution), $\%Cu_{HAS}$ (the contribution of Cu bound to HAS to the total IHA-bound Cu), $\Delta^{65}Cu_{\text{HAS-solution}}$ (the fractionation Δ^{65}Cu between HAS and the final equilibrium solution), and $\%Cu_{\text{IHA}}$ (the contribution of Cu bound to IHA to total Cu in the IHA-solution system). We modeled δ^{65}Cu values for every measured δ^{65}Cu value in solution according to Equation B-4. The model was optimized by minimizing the sum of squared differences using the Microsoft EXCEL add-in "Solver" and varying fractionation factors for LAS and HAS by setting constraints on slope and Y-intercept. The result of this optimization was $\Delta^{65}Cu_{\text{binding site-solution}}$ of 0.27 both for LAS and HAS. Additionally, the parameters were fitted manually and results were nondistinguishable (Tab. B3, Fig. B-6). The absence of differences in Cu isotope fractionation between functional groups is further supported by reported results of XAS measurements in the literature. No significant influence of pH in a range between 4 and 6 on bond length and structure of organo-Cu complexes in OM was reported (Karlsson et al., 2006). While bond length of Cu-O bonds for complexes by carboxyl resin, phenolic groups, and salicylic acid (which has both a carboxylic and a phenolic OH group; at pH 12; Karlsson et al., 2006; Harding, 1999)

did not differ much, larger differences in Zn-O bond lengths were observed between carboxylic- (2.00 Å) and phenolic-bound Zn (1.91 Å; Harding, 1999; Karlsson and Skyllberg, 2007). Similar to the findings of Jouvin et al. (2009), the amount of adsorbed Zn and Zn isotope fractionation by sorption to marine diatoms were different for different diatom species (Gelabert et al., 2006). Furthermore, a relationship of sorption constants with extent of isotope fractionation was suggested (Gelabert et al., 2006). The logK for Zn binding was 0.11 for carboxylic and 2.39 for phenolic binding sites of humic acid (Milne et al., 2003) and 4.25 for surface sorption on AMIN (*Achnanthidium minutissimum*) and 5 for NMIN (*Navicula minima*) diatom species (Gelabert et al., 2006) and the measured isotope fractionations were $\Delta^{66}Zn_{solid\text{-}solution}$ = 0.00‰ and 0.24‰ for humic acid (Jouvin et al., 2009) and 0.27‰ and 0.43‰ for diatom species (Gelabert et al., 2006).

However, there are different findings concerning the relationship between bonding strength and isotope fractionation reported for Cu and Zn. While these relationships were confirmed for Zn binding to humic acid (Jouvin et al., 2009) and diatom species (Gelabert et al., 2006) and for Cu binding on oxy(hydr)oxides and bacteria (Pokrovsky et al., 2008), no relationship was found between bonding strength and extent of fractionation for Zn binding on oxy(hydr)oxides (Pokrovsky et al., 2005) and IHA (this study). A possible explanation of the different findings is related to the differential experimental designs, the kind and concentration of element of interest and background electrolyte, and pH which all influence the type of binding to the sorbent (Schauble et al., 2009).

The different findings in isotope behavior of Cu and Zn during binding on organic substances like diatoms, bacteria, and dissolved and immobilized HA may furthermore be explained by a number of reasons:

I. The NICA-Donnan model used in the study of Jouvin et al. (2009) for Zn and in our study for Cu assumes only two types of binding sites for metals in humic acid, which is a simplification of the reality. More specific binding sites for individual metals might contribute to metal binding to HA. Copper, for example, seems to bind to N-containing functional groups (Frenkel et al., 2000). For Zn the occurrence of S in the first coordination shell is reported indicating the contribution of thiol groups to inner-sphere complexes of Zn (Karlsson and

Skyllberg, 2007; Xia et al., 1997) while the contribution of thiol groups in Cu binding to HA is negligible (Karlsson et al., 2006). Thus differences in isotope behavior might be attributable to contributions of different binding sites which are not accounted for in the NICA-Donnan model. While Zn-OM complexes show only one C atom in the second coordination shell (Xia et al., 1997; Julliot et al., 2003), Cu-OM complexes show 2-4 C atoms in the second coordination shell (Karlsson et al., 2006; Xia et al., 1997) in XAS analysis. This may indicate the simultaneous contribution of different functional groups in the inner-sphere complexation of a Cu atom and a higher contribution of chelate complexes.

II. Cu and Zn may have different coordination numbers in aqueous solution and at binding sites of humic substances (HS). For Cu in aqueous solution a sixfold coordination is proposed (Korshin et al., 1998; Frenkel et al., 2000) while in another study only a fivefold coordination is assumed (Pasquarello et al., 2001). Copper bound to OM seem to occur in sixfold coordination only (Karlsson et al., 2006; Pasquarello et al., 2001). Zinc occurs in sixfold coordination in aqueous complexes (Sarret et al., 1997), but for binding to OM, fourfold coordination is observed (Sarret et al., 1997) in addition to the dominating sixfold coordination (Juillot et al., 2003). Harding (1999) extracted results from the Cambridge structural database and reported coordination numbers from 4-6 for Cu in aqueous complexes, carboxylic complexes and phenolic complexes. For Zn, coordination numbers of 4-6 were reported in aqueous complexes and carboxylic complexes and of 4-5 in phenolic complexes (Harding et al., 1999). As the coordination environment of the atom has a critical effect on isotope fractionations (Schauble et al., 2009), also differences in complex structures may explain different isotope fractionations by organo-complexation of Cu and Zn.

III. The cupric ion, Cu^{2+} and Cu bound to IHA were not the only species which occurred during the experiment. In addition, $Cu(OH)_x^x$ and $Cu(NO_3)_x^x$ species contributed up to 0.27 % and 0.5- 10%, respectively, to the total Cu and ca. 0-7% and ca. 10% to dissolved Cu species over the investigated pH range. Also these inorganic complexes might have effect on observed fractionation factor between dissolved and bound species. The influence of $Cu(NO3)_x^x$ seems, however, to be small because the fractionation factor did not change over the

studied pH range although the contribution of $Cu(NO3)_x^x$ to the total dissolved Cu strongly decreased with increasing pH (Fig. B-3). The hydroxo-complex $Cu(OH)_x^x$ is only a minor species and therefore likely has a negligible influence on the fractionation factor.

IV. Differences between observed isotope fractionation between Cu and Zn might also be attributed to the different humic acids used and the different dominance of binding groups and the insolubilization of the humic acid in our study. The insolubilization of the aldrich humic acid seems to significantly decrease the number of phenolic-type groups (Seki and Suzuki, 1995) but not to alter generally the complexing properties of the functional groups of the IHA. This can be seen from the fact that NICA-Donnan parameters (Tab. B2) used by Saito et al. (2004) for describing Cu binding to normal Aldrich humic acid also show a good match for Cu binding on IHA. However, IHA is an artificially modified material used as a model substance for HA because of experimental advantages and thus it is not clear if findings can directly be transferred to natural HA.

V. There is the possibility that changes in Cu isotope fractionation because of different bond strengths of functional groups are too small to be detected with our method. Considering the given precision of our isotope measurements and the fact that differences between LAS and HAS are diluted because at the given Cu concentration even at pH 6.9 only 35% of adsorbed Cu was bound to HAS, it is still possible that LAS and HAS have different fractionation factors even if there is no indication for that in our study.

The differences in isotope behavior of Cu and Zn during binding to organic and oxy(hydr)oxide surfaces indicate further need of research to improve our knowledge of trace metal binding to OM and of mechanisms driving isotope fractionation during sorption.

6 Acknowledgments

Prescribed by the regulations of the internet publisher (ArchiMed) this section had to be deleted for data protection reasons. I want to thank all people listed in the printetd version.

7 References

Artiola, J. F. 2005. Speciation of copper in the environment. In Handbook of elemental speciation 2 - species in the environment, food, medicine an occupational health, Cornelis, R., Ed. John Wiley & Sons: Chinchester.

Balistrieri, L. S.; Borrok, D. M.; Wanty, R. B.; Ridley, W. I. 2008. Fractionation of Cu and Zn isotopes during adsorption onto amorphous Fe(III) oxyhydroxide: Experimental mixing of acid rock drainage and ambient river water. Geochim. Cosmochim. Acta 72, (2), 311-328.

Benedetti, M. F.; Milne, C. J.; Kinniburgh, D. G.; Vanriemsdijk, W. H.; Koopal, L. K. 1995. Metal-ion binding to humic substances - application of the nonideal competitive adsorption model. Environ. Sci. Technol. 29, (2), 446-457.

Bigalke, M.; Weyer, S.; Wilcke, W. 2010. Stable copper isotopes: A novel tool to trace copper behavior in hydromorphic soils. Soil Sci. Soc. Am. J. 74, (1), 60-73.

Borrok, D. M.; Ridley, W. I.; Wanty, R. B. 2008. Isotopic fractionation of Cu and Zn during adsorption onto bacterial surfaces. Geochim. Cosmochim. Acta 72, (12), A99-a99.

Buck, K. N.; Ross, J. R. M.; Flegal, A. R.; Bruland, K. W. 2007. A review of total dissolved copper and its chemical speciation in San Francisco Bay, California. Environ. Res. 105, (1), 5-19.

Clayton, R. E.; Hudson-Edwards, K. A.; Houghton, S. L. 2005. Isotopic effects during Cu sorption onto goethite. Geochim. Cosmochim. Acta 69, (10), A216-a216.

Dideriksen, K.; Baker, J. A.; Stipp, S. L. S. 2008. Equilibrium Fe isotope fractionation between inorganic aqueous Fe(III) and the siderophore complex, Fe(III)-desferrioxamine B. Earth Planet. Sci. Lett. 269, (1-2), 280-290.

Dube, A.; Zbytniewski, R.; Kowalkowski, T.; Cukrowska, E.; Buszewski, B. 2001. Adsorption and migration of heavy metals in soil. Pol. J. Environ. Stud. 10, (1), 1-10.

Erickson, R. J.; Benoit, D. A.; Mattson, V. R.; Nelson, H. P.; Leonard, E. N. 1996. The effects of water chemistry on the toxicity of copper to fathead minnows. Environ. Toxicol. Chem. 15, (2), 181-193.

Frenkel, A. I.; Korshin, G. V.; Ankudinov, A. L. 2000. XANES study of Cu2+-binding sites in aquatic humic substances. Environ. Sci. Technol. 34, (11), 2138-2142.

Gelabert, A.; Pokrovsky, O. S.; Viers, J.; Schott, J.; Boudou, A.; Feurtet-Mazel, A. 2006. Interaction between zinc and freshwater and marine diatom species: Surface complexation and Zn isotope fractionation. Geochim. Cosmochim. Acta 70, (4), 839-857.

Harding, M. M. 1999. The geometry of metal-ligand interactions relevant to proteins. Acta Crystallogr. D 55, 1432-1443.

Hoffmann, S. R.; Shafer, M. M.; Armstrong, D. E. 2007. Strong colloidal and dissolved organic ligands binding copper and zinc in rivers. Environ. Sci. Technol. 41, (20), 6996-7002.

Huggins, M. L. 1953. Atomic Radii. 4. Dependence of Interatomic Distance on Bond Energy. J. Am. Chem. Soc. 75, (17), 4126-4133.

Juillot, F.; Morin, G.; Ildefonse, P.; Trainor, T. P.; Benedetti, M.; Galoisy, L.; Calas, G.; Brown, G. E. 2003. Occurrence of Zn/Al hydrotalcite in smelter-impacted soils from northern France: Evidence from EXAFS spectroscopy and chemical extractions. Am. Mineral. 88, (4), 509-526.

Jouvin, D.; Louvat, P.; Juillot, F.; Marechal, C. N.; Benedetti, M. F. 2009. Zinc Isotopic Fractionation: Why Organic Matters. Environ. Sci. Technol. 43, (15), 5747-5754.

Karlsson, T.; Persson, P.; Skyllberg, U. 2006. Complexation of copper(II) in organic soils and in dissolved organic matter - EXAFS evidence for chelate ring structures. Environ. Sci. Technol. 40, (8), 2623-2628.

Karlsson, T.; Skyllberg, U. 2007. Complexation of zinc in organic soils - EXAFS evidence for sulfur associations. Environ. Sci. Technol. 41, (1), 119-124.

Kaupp, M.; Metz, B.; Stoll, H. 2000. Breakdown of bond length-bond strength correlation: A case study. Angew. Chem.-Int. Edit. 39, (24), 4607-+.

Kinniburgh, D. G.; Milne, C. J.; Benedetti, M. F.; Pinheiro, J. P.; Filius, J.; Koopal, L. K.; VanRiemsdijk, W. H. 1996. Metal ion binding by humic acid: Application of the NICA-Donnan model. Environ. Sci. Technol. 30, (5), 1687-1698.

Korshin, G. V.; Frenkel, A. I.; Stern, E. A. 1998. EXAFS study of the inner shell structure in copper(II) complexes with humic substances. Environ. Sci. Technol. 32, (18), 2699-2705.

Kudeyarova, A. Y. 2007. Application of basic chemical concepts to understanding the formation and transformation mechanisms of humic substances: A revue of publications and own experimental data. Eurasian Soil Sci. 40, (9), 934-948.

Kunito, T.; Saeki, K.; Oyaizu, H.; Matsumoto, S. 1999. Influences of copper forms on the toxicity to microorganisms in soils. Ecotox. Environ. Safe. 44, (2), 174-181.

Marechal, C. N.; Telouk, P.; Albarede, F. 1999. Precise analysis of copper and zinc isotopic compositions by plasma-source mass spectrometry. Chem. Geol. 156, (1-4), 251-273.

Marechal, C.; Albarede, F. 2002. Ion-exchange fractionation of copper and zinc isotopes. Geochim. Cosmochim. Acta 66, (9), 1499-1509.

Mathur, R.; Ruiz, J.; Titley, S.; Liermann, L.; Buss, H.; Brantley, S. 2005. Cu isotopic fractionation in the supergene environment with and without bacteria. Geochim. Cosmochim. Acta 69, (22), 5233-5246.

Milne, C. J.; Kinniburgh, D. G.; Van Riemsdijk, W. H.; Tipping, E. 2003. Generic NICA-Donnan model parameters for metal-ion binding by humic substances. Environ. Sci. Technol. 37, (5), 958-971.

O´Neil, J. R. 1986. Theoretical and experimental aspects of isotopic fractionation. In Stable isotopes in high temperature geological processes, Valley, J. W.; Taylor, H. P.; J.R., O. N., Eds. Mineralogical Society of America: Michigan, Vol. 16, pp 1-40.

Pasquarello, A.; Petri, I.; Salmon, P. S.; Parisel, O.; Car, R.; Toth, E.; Powell, D. H.; Fischer, H. E.; Helm, L.; Merbach, A. E. 2001. First solvation shell of the Cu(II) aqua ion: Evidence for fivefold coordination. Science 291, (5505), 856-859.

Pokrovsky, O. S.; Viers, J.; Freydier, R. 2005. Zinc stable isotope fractionation during its adsorption on oxides and hydroxides. J. Colloid Interf. Sci. 291, (1), 192-200.

Pokrovsky, O. S.; Viers, J.; Emnova, E. E.; Kompantseva, E. I.; Freydier, R. 2008. Copper isotope fractionation during its interaction with soil and aquatic microorganisms and metal oxy(hydr) oxides: Possible structural control. Geochim. Cosmochim. Acta 72, (7), 1742-1757.

Saito, T.; Nagasaki, S.; Tanaka, S.; Koopal, L. K. 2004. Application of the NICA-Donnan model for proton, copper and uranyl binding to humic acid. Radiochim. Acta 92, (9-11), 567-574.

Sarret, G.; Manceau, A.; Hazemann, J. L.; Gomez, A.; Mench, M. 1997. EXAFS study of the nature of zinc complexation sites in humic substances as a function of Zn concentration. J. Phys. IV 7, (C2), 799-802.

Schauble, E. A.; Meheut, M.; Hill, P. S. 2009. Combining metal stable isotope fractionation theory with experiments. Elements 5, (6), 369-374.

Seki, H.; Suzuki, A. 1995. Adsorption of Heavy-Metal Ions onto Insolubilized Humic-Acid. J. Colloid Interf. Sci. 171, (2), 490-494.

Sheals, J.; Persson, P.; Hedman, B. 2001. IR and EXAFS spectroscopic studies of glyphosate protonation and copper(II) complexes of glyphosate in aqueous solution. Inorg. Chem. 40, (17), 4302-4309.

Smith, D. S.; Bell, R. A.; Kramer, J. R. 2002. Metal speciation in natural waters with emphasis on reduced sulfur groups as strong metal binding sites. Comp. Biochem. Phys. C 133, (1-2), 65-74.

Stevenson, F. J. 1982. Humus chemistry: Genesis, composition, reactions. Wiley: New York, p XIII, 443 S.

Vance, D.; Archer, C.; Bermin, J.; Perkins, J.; Statham, P. J.; Lohan, M. C.; Ellwood, M. J.; Mills, R. A. 2008. The copper isotope geochemistry of rivers and the oceans. Earth Planet. Sci. Lett. 274, (1-2), 204-213.

Villaverde, P.; Gondar, D.; Antelo, J.; Lopez, R.; Fiol, S. 2009. Arce, F., Influence of pH on copper, lead and cadmium binding by an ombrotrophic peat. Europ. J. Soil Sci. 60, (3), 377-385.

Weber, T.; Allard, T.; Tipping, E.; Benedetti, M. F. 2006. Modeling iron binding to organic matter. Environ. Sci. Technol. 40, (24), 7488-7493.

Weber, T.; Allard, T.; Benedetti, M. F. 2006. Iron speciation in interaction with organic matter: Modelling and experimental approach. J. Geochem. Explor. 88, (1-3), 166-171.

Xia, K.; Bleam, W.; Helmke, P. A. 1997. Studies of the nature of Cu2+ and Pb2+ binding sites in soil humic substances using X-ray absorption spectroscopy. Geochim. Cosmochim. Acta 61, (11), 2211-2221.

Xia, K.; Bleam, W.; Helmke, P. A. 1997. Studies of the nature of binding sites of first row transition elements bound to aquatic and soil humic substances using X-ray absorption spectroscopy. Geochim. Cosmochim. Acta 61, (11), 2223-2235.

8 Supporting material Section B

8.1 Complement to materials and methods.

8.1.1 Characterization of IHA and pH measurements

Elemental composition of the IHA was determined by dry combustion with a CHNS analyzer (Vario EL, Elementar Analysensysteme, Hanau, Germany). Iron, Al and Ca contents of the IHA were measured after digestion with concentrated HNO_3 in a microwave oven (MARS5Xpress, CEM Corp., Matthews, NC) with a flame AAS (AA 240 FS, Varian, Palo Alto, CA). The IHA contained 618 mg g^{-1} C, 253 mg g^{-1} N, 3.5 mg g^{-1} S, 428 µg g^{-1}Fe, 111 µg g^{-1} Al, and 228 µg g^{-1} Ca. The pH was measured with an InoLab® pH720 pH-meter and a SenTix® 41 Plus electrode (WTW, Weilheim-Schongau, Germany) which was calibrated directly before measurement. As solutions were not buffered, pH changes occurred during equilibration. We only used the pH after equilibration for our interpretations (Tab. B-1).

8.1.2 Materials

All reagents used for the preparation of the isotope samples were of Rotipuran® supra (Carl Roth, Karlsruhe, Germany) or trace select® (Fluka, Seelze, Germany) quality, A Na salt of humic acid was obtained in technical quality (Aldrich, Steinheim, Germany) and purified as described above, $NaNO_3$ was of trace select® (Fluka, Seelze, Germany) quality, $Cu(NO_3)_2$ hemipentahydrate was of 99.99+% metal basis quality (Aldrich, Steinheim, Germany). Water was taken from a TKA GenPure UV (TKA, Niederelbert, Germany) water purification system and was of ≥18 MΩ cm quality. Purifications were performed under clean air conditions in a clean bench and evaporation was done in boxes supplied with hepa filtered air.

8.1.3 Additional information about Cu isotope measurements

Copper isotope ratios were measured with a Finnigan-Neptune (ThermoFisher) multiple collector inductively-coupled plasma mass spectrometer (MC-ICP-MS) similar to the method described in Bigalke et al. (2010). The samples were introduced with a combination of a cyclonic and a Scott double pass-type spray chamber. Aluminum cones were used to avoid influence of Ni cones on the spike. A Ni spike (NIST 986)

was used for mass bias correction (Markl et al., 2006; Li et al., 2009). Masses 60 (Ni), 61 (Ni), 62 (Ni), 63 (Cu), 64 (Zn+Ni), 65 (Cu), and 66 (Zn) were detected simultaneously. The correction was performed according to the certified $^{62}Ni/^{60}Ni$ ratio (0.138600) of NIST 986 that was added to all samples and the Cu standard prior to measurement and by applying the exponential law. A standard (NIST 976) was measured between every three samples (Bigalke et al., 2010). Samples and standards were introduced in 2% HNO_3 at concentrations of 300 ng g^{-1} Cu and 1000 ng g^{-1} Ni. The $\delta^{65}Cu$ value of the samples was calculated as the deviation of the isotope ratio of the mass bias corrected samples from the average isotope ratio of the mass bias corrected bracketing standards (Li et al., 2009).

8.1.4 Speciation modeling

Values for NICA-Donnan parameters were taken from the literature and are summerized in Tab. B-2. The details about the NICA-Donnan model and describtion of the imput parameters can be found in the literature (Benedetti et al., 1995; Kinniburgh et al., 1996).

Table B-2. NICA-Donnan parameters to describe Cu binding on IHA

	Q_{max} [a]	log K_H [b]	n_H [b]	p [b]	log K_{Cu} [b]	n_{Cu} [b]
Carboxylic-type groups	1.98	3.53	0.659	0.894	2.26	0.421
Phenolic-type groups	0.98	7.95	0.66	0.375	6.96	0.471

[a] Data from Weber et al. (2006); [b] Data from Saito et al. (2004)

8.2 Kinetics of Cu sorption to IHA

To examine equilibrium time in the experimental setup, sorption of Cu to IHA was measured at eight time steps between 2 hours and 7 days. For every time step, three replicates were set up according to the procedures described in the material and methods part. The samples were shaken, centrifuged, and solution and IHA were separated at the given time. Copper concentrations were measured in solution. Equilibrium was reached after 24 to 48 hours (Figure B-4).

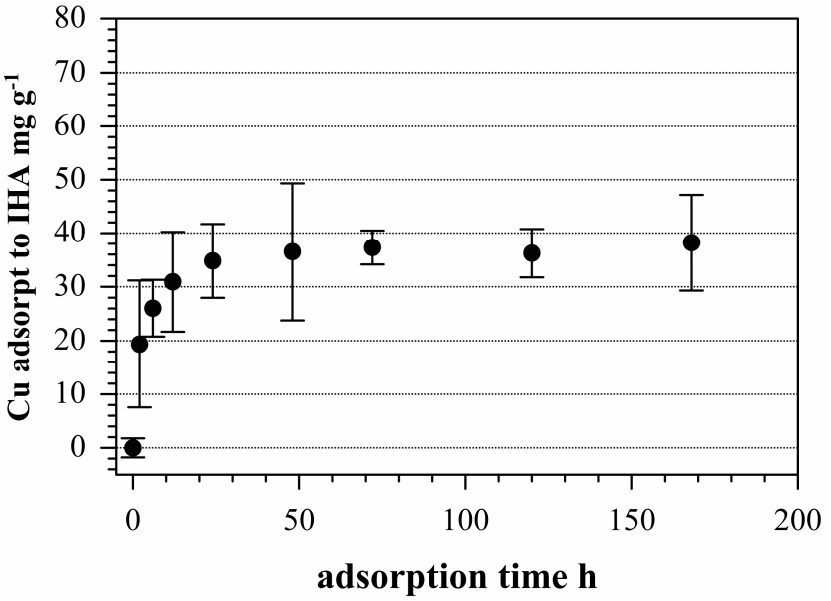

Figure B-4. Kinetics of Cu sorption on IHA. The pH at the end of the experiment was 4.7. Error bars represent 2SD of the three individual replicates.

8.3 Reversibility of Cu sorption to IHA

To check for reversibility of Cu sorption to IHA, sorption-desorption experiments were performed on eleven samples. Sorption-desorption experiments were performed after a method modified from Fowl and Fein (2000). Sorption experiments were done as described above at pH values between 6 and 9 to realize complete sorption of Cu. Samples were shaken for three days to achieve equilibrium. After three days, diluted HNO_3 was added to lower pH values and initiate desorption. Samples were again left three days on a shaker to reach equilibrium. After this period, IHA was separated from solution and Cu concentrations and pH were measured in solution. Measured concentrations and calculated Cu sorption fit well the sorption curve predicted by the NICA-Donnan model (Figure B-5), indicating reversibility of Cu sorption to IHA.

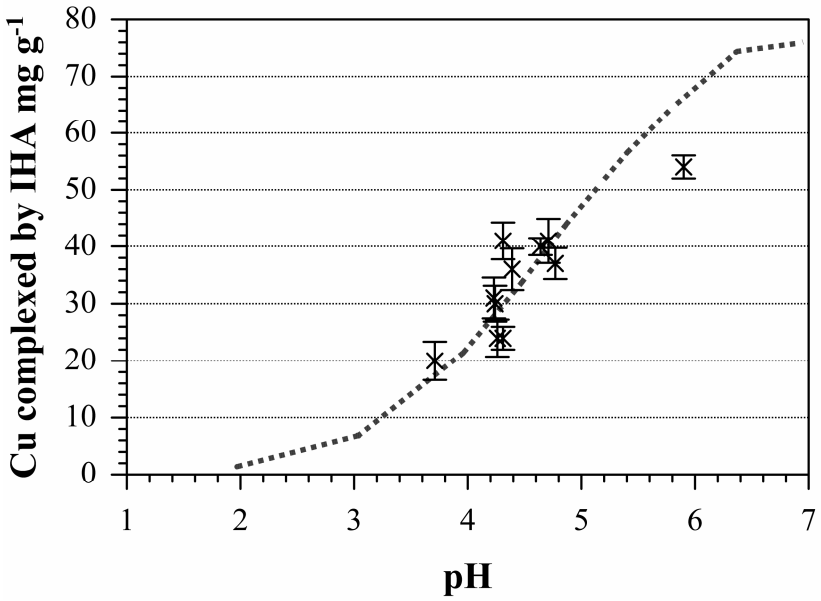

Figure B-5. Reversibility of Cu sorption to IHA. Black crosses represent measured values after desorption, the grey line represents modeled values of the NICA-Donnan model with input parameters from Table B-2. Error bars represent 2SD of measurement error.

8.4 Solubilisation of IHA

To proof that IHA was not solubilized during the experiment and that IHA was completely separated from solution by centrifugation, the sorption experiment was at pH between 3.1 and 5.7. After separation of IHA from solution, DOC was measured in solution. No measurable DOC (0.26 ± 0.74 mg l^{-1} DOC, n = 8) and no significant difference from blank samples (0.84 ± 0.74 mg l^{-1} DOC, n = 2) which were shaken for the same time without IHA was found. The fact that DOC in samples even tended to be lower compared to blank values may be caused by sorption of DOC originating from water and leaching of polypropylene vessels to IHA

8.5 Estimation of specific fractionation for low affinity sites (LAS) and high affinity sites (HAS)

Data from Equation B-4 were fitted manually in addition to the fitting using Excel-Solver. The manual fitting was done by varying $\Delta^{65}Cu_{(LAS\text{-}solution)}$ and $\Delta^{65}Cu_{(HAS\text{-}solution)}$

to obtain a slope of unity and a Y axis intersect of zero in a measured $\delta^{65}Cu_{solution}$ vs. modeled $\delta^{65}Cu_{solution}$ plot (Figure B-6 and Tab. B-3). The best fit was identified by starting with a coarse scan of $\Delta^{65}Cu$ of 0.1‰ steps to identify regions were the Y axis intersect was minimized and continuing with a fine and very fine scan in this regions (grey marked in Tab. B-3). At low $\Delta^{65}Cu_{(LAS\text{-}solution)}$ the Y axis intersect was negative when the slope was ≈ 1 and became more positive with increasing $\Delta^{65}Cu_{(LAS\text{-}solution)}$. The values where the Y axis intersect reached ≈ 0 and slope was ≈ 1 were identified at $\Delta^{65}Cu_{(LAS\text{-}solution)}$ = 0.265 and $\Delta^{65}Cu_{(HAS\text{-}solution)}$ = 0.267.

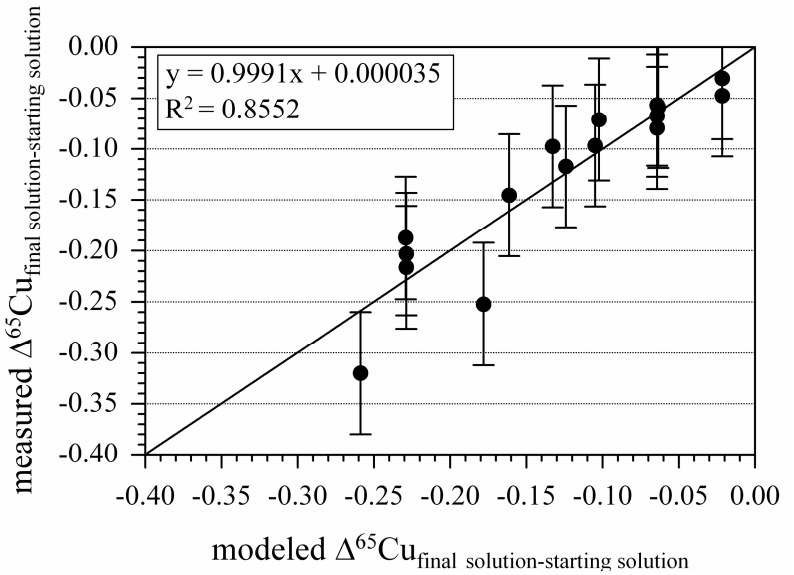

Figure B-6. Plot of measured Δ^{65}Cufinal solution-starting solution values versus modeled Δ^{65}Cufinal solution-starting solution (according to equation B-4). Δ^{65}CuLAS-solution and Δ^{65}CuHAS-solution values were optimized to approach a slope of unity and a Y axis intersect of 0. Figure shows optimal fit with Δ^{65}CuLAS-solution = 0.267 and Δ^{65}CuHAS-solution = 0.265. Error bars on the Y axis refer to the 0.06‰ (2SD) long-time reproducibility of the measurement.

Table B-3. Manual fit of $\Delta^{65}Cu_{(LAS\text{-}solution)}$ and $\Delta^{65}Cu_{(HAS\text{-}solution)}$ to obtain a slope of unity and a Y axis intersect of 0.

$\Delta^{65}Cu_{(LAS\text{-}solution)}$ ‰	$\Delta^{65}Cu_{(HAS\text{-}solution)}$ ‰	Slope	Intersection	R^2
		coarse		
0.200	0.200	1.330	0.000	0.855
0.200	0.300	1.123	-0.006	0.859
0.200	0.400	0.969	-0.011	0.861
0.200	0.500	0.852	-0.015	0.861
0.300	0.100	1.166	0.012	0.839
0.300	0.200	1.009	0.005	0.850
0.300	0.300	0.887	0.000	0.855
0.300	0.400	0.790	-0.004	0.858
0.400	0.000	1.028	0.020	0.819
0.400	0.100	0.909	0.014	0.835
0.400	0.200	0.812	0.008	0.845
		fine		
0.260	0.260	1.023	0.000	0.855
0.260	0.270	1.009	-0.001	0.856
0.260	0.280	0.995	-0.001	0.856
0.260	0.290	0.982	-0.002	0.857
0.270	0.240	1.027	0.002	0.854
0.270	0.250	1.013	0.001	0.854
0.270	0.260	0.999	0.000	0.855
0.270	0.270	0.985	0.000	0.855
0.280	0.230	1.016	0.003	0.853
0.280	0.240	1.002	0.002	0.853
0.280	0.250	0.989	0.002	0.854
0.280	0.260	0.976	0.001	0.854
		very fine		
0.266	0.265	1.0015	0.0000	0.8553
0.266	0.266	1.0001	-0.0001	0.8554
0.266	0.267	0.9987	-0.0001	0.8554
0.266	0.268	0.9974	-0.0002	0.8555
0.267	0.263	1.0019	0.0001	0.85520
0.267	0.264	1.0005	0.0001	0.8552
0.267	0.265	0.9991	0.0000	0.8553
0.267	0.266	0.9977	0.0000	0.8553
0.268	0.261	1.0022	0.0003	0.8551
0.268	0.262	1.0008	0.0003	0.8551
0.268	0.263	0.9995	0.0002	0.8552
0.268	0.264	0.9981	0.0001	0.8552

8.6 References supporting material

Benedetti, M. F.; Milne, C. J.; Kinniburgh, D. G.; Vanriemsdijk, W. H.; Koopal, L. K. 1995. Metal-ion binding to humic substances - application of the nonideal competitive adsorption model. Environ. Sci. Technol. 29, (2), 446-457.

Bigalke, M.; Weyer, S.; Wilcke, W. 2010. Stable copper isotopes: A novel tool to trace copper behavior in hydromorphic soils. Soil Sci. Soc. Am. J. 74, (1), 60-73.

Fowle, D. A.; Fein, J. B. 2000. Experimental measurements of the reversibility of metal-bacteria adsorption reactions. Chem. Geol. 168, (1-2), 27-36.

Kinniburgh, D. G.; Milne, C. J.; Benedetti, M. F.; Pinheiro, J. P.; Filius, J.; Koopal, L. K.; VanRiemsdijk, W. H. 1996. Metal ion binding by humic acid: Application of the NICA-Donnan model. Environ. Sci. Technol. 30, (5), 1687-1698.

Markl, G.; Lahaye, Y.; Schwinn, G. 2006. Copper isotopes as monitors of redox processes in hydrothermal mineralization. Geochim. Cosmochim. Acta 70, (16), 4215-4228.

Li, W. Q.; Jackson, S. E.; Pearson, N. J.; Alard, O.; Chappell, B. W. 2009. The Cu isotopic signature of granites from the Lachlan Fold Belt, SE Australia. Chem. Geol. 258, (1-2), 38-49.

Saito, T.; Nagasaki, S.; Tanaka, S.; Koopal, L. K. 2004. Application of the NICA-Donnan model for proton, copper and uranyl binding to humic acid. Radiochim. Acta 92, (9-11), 567-574.

Weber, T.; Allard, T.; Benedetti, M. F. 2006. Iron speciation in interaction with organic matter: Modelling and experimental approach. J. Geochem. Explor. 88, (1-3), 166-171.

C Stable Cu isotopes: a novel tool to trace Cu behavior in hydromorphic soils

Moritz Bigalke[1,3], Stefan Weyer[2+], Wolfgang Wilcke[3]

[1]Johannes Gutenberg University Mainz, Earth System Science Research Center, Geographic Institute, Professorship of Soil Science/Soil Geography, Johann-Joachim-Becher-Weg 21, 55128 Mainz, Germany.

[2]University of Frankfurt, Institute of Geoscience, Altenhöferallee 1, 60438 Frankfurt am Main, Germany.

[3]Geographic Institute, University of Berne, Hallerstrasse 12, 3012 Berne, Switzerland.

[+]Current address: Institute of Geology and Mineralogy, University of Cologne, Zülpicher Str. 49b, 50674 Köln

Soil Science Society of America Journal 74, 60-73.

1 Abstract

Copper is an essential micronutrient for all organisms but may also be a pollutant. We studied the natural abundance of stable Cu isotope ratios in four soils to test whether δ^{65}Cu values can be used as a tracer for biogeochemical processes in hydromorphic soils. Two of the soils were affected by stagnant water and the other two by groundwater. We determined standard soil properties and Cu partitioning into seven fractions of a sequential extraction. Copper stable isotope ratios were measured in total soil digests with multicollector inductively-coupled plasma mass spectrometry. Copper concentrations in the study soils were low to average (5–34 mg kg^{-1}). The variation in Cu isotope ratios was up to 0.6‰ in an individual soil. The organic layers of two of the profiles had lighter δ^{65}Cu values than the mineral soil, indicating isotope fractionation of Cu during soil–plant–soil transfer. In the mineral soil, Cu isotope ratios showed distinguishable variations of up to 0.45‰. The vertical distribution of the

δ^{65}Cu values, which paralleled that of the poorly crystalline to crystalline Fe oxide ratios, offers the first hints that Cu isotope ratios in soils may be influenced by alternating redox conditions. We conclude that variations in δ^{65}Cu in soils are large enough to be distinguished and may be indicative of biogeochemical cycling and geochemical processes. In particular, Cu isotope ratios might be helpful to trace long-term processes such as element transport and redox conditions, which are difficult to assess otherwise.

2 Introduction

Copper is an essential micronutrient for plants, animals, and humans; however, it may also be a pollutant if it occurs at high concentrations in the soil (Alloway, 1995). Therefore, knowledge of Cu cycling in soils is required both for guaranteeing proper nutrition and to control possible risks arising from Cu pollution.

Copper is a redox-sensitive transition metal and is found as a trace element in most soils at an average concentration of 30 mg kg^{-1} and in a range of 2 to 100 mg kg^{-1}. It occurs predominantly as Cu^{2+} while also Cu^{+} species and elemental Cu may be present (Artiola, 2005; Grybos et al., 2007; Weber et al., 2009). In soils, Cu is mostly complexed by organic matter, incorporated in and adsorbed to Fe oxides and primary or secondary silicates. Only small parts are found in weakly bound exchangeable forms. The particular Cu speciation differs, however, among soils with different physicochemical properties (Dube et al., 2001; Wilcke et al., 2005). Organic substances can adsorb or complex Cu with different stabilities reaching from relatively weakly bound complexes at surface sites to inert complexes at intraparticle binding sites (Senesi et al., 1986; Osterberg et al., 1999). Metal oxy(hydr)oxides may adsorb or occlude Cu either as a free ion or as an organo–metal complex (Alcacio et al., 2001). At low redox potentials in hydromorphic soils, Fe oxides are reduced and release associated metals including Cu; however, frequently changing redox conditions may also cause the enhanced fixation of Cu in Fe oxy(hydr)oxides (Contin et al., 2007). In the presence of Fe^{2+}, Cu^{2+} can be transformed to Cu^{+} in reducing environments (Matocha et al., 2005), which may also alter its binding type and its mobility. One possible effect of Cu reduction may also be precipitation as Cu(s) (Grybos et al., 2007). The increase in pH during chemical reduction reactions may cause the release of dissolved organic matter, which also enhances metal mobility (Grybos et al., 2007). Weber et al. (2009) reported formation of elemental Cu and Cu_xS nanoparticles in flooded soils, which can enhance Cu mobility. But in unflooded soils, Cu^{2+} might also be reduced to elemental Cu nanoparticles by plants. The formation of Cu nanoparticles by plants is thought to be a defense mechanism against Cu toxicity and may only occur in polluted soils (Manceau et al., 2008).

Many attempts have been made to improve our understanding of trace metal behavior in soil. For Cu, the most common tools to assess its fate are sequential extractions to study the binding of metals to various soil constituents (Bacon and Davidson, 2008). Other approaches to assess Cu speciation in soil include infrared and electron spin resonance spectroscopy (Senesi et al., 1986), extended X-ray absorption fine structure spectroscopy (Alcacio et al., 2001), exchange with added isotopically labeled Cu (Ma et al., 2006), and voltammetry to measure dissolved Cu in soil solution (Pelfrene et al., 2008). But there are still several open questions in our understanding of Cu behavior in the highly complex soil system. This is particularly true for the long-term effects of transport and redox processes in soil at time scales up to hundreds or thousands of years, which are experimentally not directly accessible. Investigation of stable isotope ratios, which integrate the effects of such long-term processes, might therefore be a useful tool to further the understanding of the biogeochemical cycling of Cu in the environment.

The measurement of "traditional" stable isotope systems (C, H, N, O, and S) has become a well established analytical tool for ecological investigations over many years (Fry, 2006; Tiunov, 2007). After early measurements by thermal ionization mass spectrometry (TIMS; Shields et al., 1965), with the first introduction of multicollector inductively-oupled plasma mass spectrometry (MC-ICPMS) around 1992 (Walder and Freedman, 1992) the exploration of "non-traditional" heavier isotope systems (Fe, Cu, Zn, etc.) developed rapidly, providing new tools in geologic, environmental, and many other fields of research (Douthitt, 2008). Variations in stable isotope compositions are usually expressed as per mil (‰) difference relative to a standard reference material. For Cu, this difference is expressed relative to the reference material NIST 976 (National Institute of Standards and Technology, Gaithersburg, MD) as δ^{65}Cu values (see below for exact definition).

Up to now, most studies of Cu isotope ratios have addressed geochemical questions (Albarede, 2004). Li et al. (2009) reported that δ^{65}Cu values of granites clustered mostly between −0.4 and 0.4‰ but can reach values as high as 1.5‰ in rare cases, while Othman et al. (2003, 2004) found that terrestrial basalts and other mantle rocks cluster tightly around 0‰. These rocks are common bedrocks for soil development and may reflect the starting point of the development of δ^{65}Cu in soils. Another important parent

material for soils is loess, which is frequently admixed to surficial layers from which soils develop. Chinese loesses had $\delta^{65}Cu$ values of 0.01 and −0.02‰ (Li et al., 2009). Thus, the parent rocks of soil formation may display some Cu isotope variations, but they mostly cluster around 0‰ (Fig. C-1).

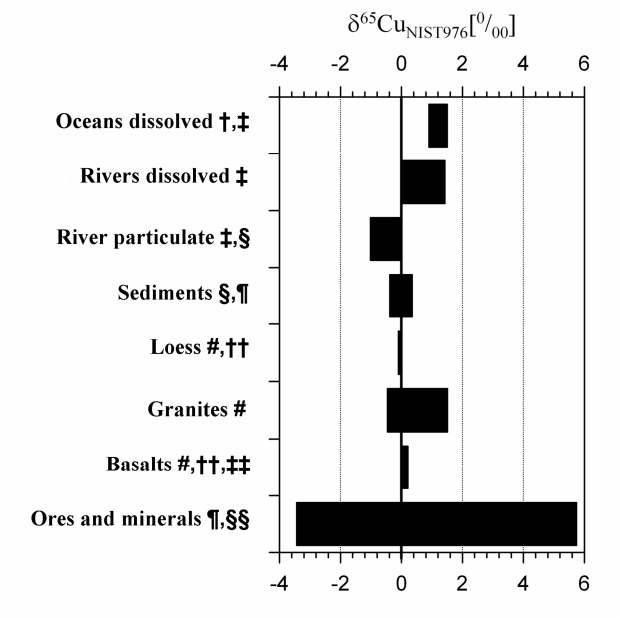

Figure C-1. The $\delta^{65}Cu$ values of natural materials. For some materials, only a few measurements have been previously published (e.g., three values for loess). Therefore, the real variation in nature might be larger than shown in this figure. † Bermin et al. (2006); ‡ Vance et al. (2008); § Petit et al. (2008); ¶ Marechal et al. (1999); # Li et al. (2009); †† this study; ‡‡ Archer and Vance (2004); §§ Asael et al. (2007).

Although the Cu isotope fractionation in soils has not yet been studied, it is known that several processes that take place in soils cause Cu isotope fractionations (Fig. C-2). Variations of up to 5.4‰ were found in hydrothermal fields after partial oxidation of primary Cu(I) to secondary Cu(II) minerals. Fractionations of up to 3‰ were reported during mineral precipitation in ore-forming environments (Markl et al., 2006; Maher and Larson, 2007). These findings were confirmed in laboratory experiments. Zhu et al. (2002) observed fractionations with $\Delta^{65}Cu_{(Cu(II)-Cu(I))}$ of 4‰ (i.e., a difference in the $\delta^{65}Cu$ value between the educt Cu(II) and the product Cu(I) of 4‰) after Cu^{2+} reduction with iodine. Ehrlich et al. (2004) reported a fractionation of $\Delta^{65}Cu_{(Cu(II)-CuS)}$ of 3‰ after formation of covellite from aqueous Cu(II). In general, the extent of equilibrium isotope

fractionation is inversely correlated with the temperature at which the reaction takes place (Marechal and Sheppard, 2002; Ehrlich et al., 2004).

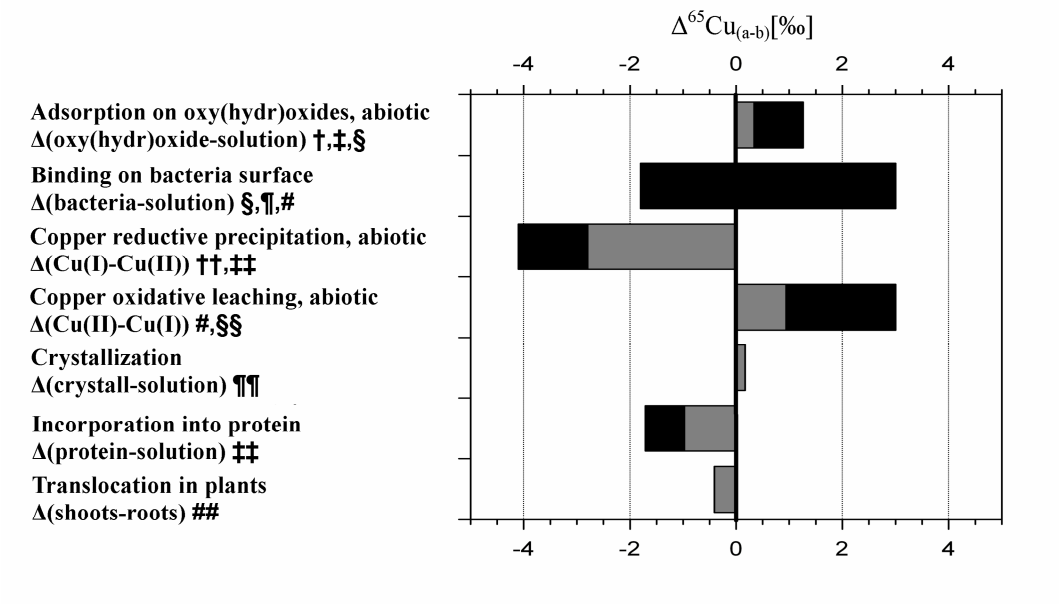

Figure C-2. Fractionation of Cu isotopes by different processes. Gray bars show the minimum fractionation observed, black areas show the interval of observed fractionation. † Balistrieri et al. (2008); ‡ Clayton et al. (2005); § Pokrovsky et al. (2008); ¶ Borrok et al. (2008); # Mathur et al. (2005); †† Ehrlich et al. (2004); ‡‡ Zhu et al. (2002); §§ Asael et al. (2005); ¶¶ Li et al. (2008); ## Jouvin et al. (2008).

Furthermore, biological transformation may fractionate Cu. For instance, it was shown that the uptake of Cu into proteins causes fractionations of up to $\Delta^{65}Cu_{(protein-solution)}$ of 2‰ (Zhu et al., 2002), while the fractionation by surface adsorption of Cu to different microorganisms was pH dependent (Pokrovsky et al., 2008). There was only weak fractionation at pH 4 to 8, but differences of −0.6 to −1.8‰ in the $\delta^{65}Cu$ values ($\Delta 65Cu_{(bacteria-solution)}$) occurred between the bacteria and solution in acidic solutions of pH 1.8 to 3.3. Mathur et al. (2005) reported that Fe-oxidizing bacteria may deplete ^{65}Cu of their environment because of preferential sorption of isotopically heavy Cu ($\Delta^{65}Cu_{(solid-solution)}$ ~ 3‰) to Fe oxides formed at their surfaces. The preferential sorption of ^{65}Cu on Fe and Al oxy(hydr)oxides was confirmed in other studies with $\Delta^{65}Cu_{(solid-solution)}$ between 0.35 and 1.3‰ (Clayton et al., 2005; Balistrieri et al., 2008; Pokrovsky et al., 2008). The effect of organo complexation - one important process to which Cu is subject in soil - on $\delta^{65}Cu$ is unknown but organo

complexation of Zn and Fe resulted in isotope fractionations with the heavier isotopes enriched in the organically complexed form by 0.24 (Zn on humic acid, only at pH > 6) and 0.60‰ (Fe on siderophores), respectively, under equilibrium conditions (Dideriksen et al., 2008; Jouvin et al., 2009).

The initial studies of Jouvin et al. (2008) indicated isotope fractionation of Cu isotopes between plant roots and shoots, with a depletion of the heavy isotope of $\Delta 65Cu_{(roots-shoots)}$ of 0.41‰. More detailed information is available for Fe and Zn isotopes. Guelke and von Blanckenburg (2007) reported that different uptake strategies of plants may cause opposite directions in Fe isotope fractionation. In a tropical watershed, the $\delta^{66}Zn$ of deeper soil horizons differed by 0.5‰ from the topsoil. In the same watershed, isotope fractionation up to ±0.5‰ between the soil and plant (depending on the plant part) was found (Viers et al., 2007). A plant-induced fractionation of stable Zn isotope ratios was also shown in laboratory experiments resulting in isotope differentiation between distinct plant parts, with heavier isotope composition in roots than in shoots (Weiss et al., 2005), in seeds than in leaves, and in roots than in leaves (Moynier et al., 2009). But there is a need for further studies to test if similar fractionations occur for Cu.

Our overall objective was to explore the potential of Cu isotope ratios to trace the behavior of Cu in soils and to answer the questions (i) if there is a measurable isotope fractionation of Cu among different soil horizons, (ii) if the $\delta^{65}Cu$ in organic soil horizons is lighter than in the mineral soil because of plant-induced isotope fractionation, and (iii) if changing redox conditions affect the $\delta^{65}Cu$ values of redoximorphic soils because of changing Cu speciation and mobility, which may also fractionate Cu isotopes.

The potential Cu fractionation cannot be interpreted without detailed knowledge of soil properties and chemical Cu forms in soil. We characterized the study soils physically and chemically (by determining texture, pH, cation-exchange capacity, base saturation, and C, N, and Fe concentrations) and partitioned soil Cu into seven operationally defined fractions with a sequential extraction procedure. The fractions of the sequential extraction procedure were not analyzed for Cu isotopes because artificial fractionation of isotope ratios by the extraction is probable.

3 Materials and methods

3.1 Sampling sites and soils

Soil samples were taken from two soils affected by stagnant water and two soils affected by groundwater (Table C-1). All four soils showed hydromorphic properties (i.e., bleached zones and Fe oxide mottles). The soils classify as a Skeleti-Stagnic Luvisol (IUSS Working Group, 2006) or Aeric Epiaqualf (Soil Survey Staff, 2006), a Stagnic Cambisol or Aeric Epiaquept, a Calcari-Humic Gleysol or Fluvaquentic Humaquept, and a Dystric Gleysol or Humic Endoaquept. The soil morphology was described according to FAO (2006).

The Skeleti-Stagnic Luvisol, Stagnic Cambisol, and Dystric Gleysol were located in the Variscan mountain area in slope positions. Like most central European soils, three of the four studied soils (the Skeleti-Stagnic Luvisol, Stagnic Cambisol, and Dystric Gleysol) developed from periglacial cover beds consisting of up to three solifluctional layers. The fourth soil (the Calcari-Humic Gleysol) developed from fluvic material.

The Skeleti-Stagnic Luvisol was located in Idstein, near Wiesbaden in Germany. The organic layer had a depth of 5 cm and consisted of two horizons. The mineral soil consisted of six horizons that are characterized by the formation of brown-colored Fe oxy(hydr)oxides in the upper soil horizons and the influence of stagnant water and clay illuvation in the lower soil horizons, as demonstrated by the presence of clay cutans on ped surfaces. The deepest two horizons were impermeable to water. The soil had developed from three different layers, with the lowest layer consisting mainly of weathered bedrock (slate), while the two upper layers contained varying contents of loess and tephra from the volcanic eruption of Lake Maria Laach (Laacher See tephra). These substrates had initially variable clay contents, which might explain why the lessivation was not reflected in large textural contrasts between elluviated and illuviated horizons (Table C-2). To account for different $\delta^{65}Cu$ values among parent materials and to identify changes in the $\delta^{65}Cu$ values caused by pedogenesis, pure slate, loess, and Laacher See tephra were sampled from outcrops and deposits near the studied soil. The slate and loess were sampled in Idstein, the Laacher See tephra was sampled at Hohe Wurzel near Wiesbaden (Stuckrad et al., 2008).

The Stagnic Cambisol was located approximately 1 km northeast of Chata Slana Voda, near Oravska in Slovakia. The organic layer had a depth of 7.5 cm and consisted of three horizons; the mineral soil had four horizons (Table C-2). The Ah horizon was characterized by humus accumulation; the Ahg, Bg1, and II Bg2 horizons showed stagnic properties (mottling); the II Bg2 horizon was impermeable and had developed from a different geologic layer.

Table C-1. Soil type, location, altitude, slope, bedrock, climate, and vegetation of the study sites

Soil type FAO	**Location**	**Altitude** m above sea level	**Slope**	**Bedrock**	**Age**	**Rainfall** mm yr^{-1}	**Temp-erature** January/ July [°C]	**Vegetat-ion**
Skeleti-Stagnic Luvisol	Germany 50°13'N, 8°16'E	400	6°	slate	early Devonian	700-800	0 - 18	beech
Stagnic Cambisol	Slovakia 49°56'N, 19°26'E	800	2°	sandstone with muscovite mudstone	Eocene flysch with mudstone	1000-1200	-7 - 16	spruce, horsetail, and moss
Calcari-Humic Gleysol	Germany 49°56'N, 8°04'E	88	0°	fluvic materials	Pleistocene	500- 600	0 - 18	alder, and grass
Dystric Gleysol	Slovakia 49°22'N, 19°37'E	630	2°	granite and sandstone	Pliocene	700-800	-7- 18	spruce, blueberry, and moss

The Calcari-Humic Gleysol was sampled in Groß-Winternheim, near Mainz in Germany, next to a small creek. The organic layer had a depth of 3 cm consisting of weakly decomposed leaves. There was an irregular vertical distribution of organic C concentrations in the upper mineral soil, indicating that the soil developed from fluvic sediments. The lower horizons showed the influence of fluctuating groundwater (mottling), with the lowest horizon indicating permanent reducing conditions (gray color).

The Dystric Gleysol was sampled approximately 4 km northeast of Trstena in Slovakia. The organic layer had a depth of 14.5 cm and consisted of three horizons (Table C-2). The great depth of the organic layer and the high organic C concentrations in the Ah horizon were probably attributable to frequent waterlogging and low pH. The

deeper two soil horizons showed the influence of mostly oxic groundwater (i.e., mottling even in the permanently wet horizon). The II Bl2 horizon had developed from a different geogenic layer.

The Stagnic Cambisol and the Dystric Gleysol were already described in Lobe et al. (1998) and the Skeleti-Stagnic Luvisol was described by S. Stückrad (personal communication, 2008). Tables C-1 and C-2 summarize site conditions and soil properties.

3.2 Sampling and sample preparation

The soil profiles were macroscopically characterized in the field and each horizon was sampled in a representative way. The samples were air dried and sieved to <2 mm. For Cu isotope analyses and to determine total Cu and Fe concentrations, the samples were ground in a planetary mill.

Texture was determined with the pipet method after the destruction of organic matter with H_2O_2, dispersion with $Na_6P_6O_{18}\cdot 6H_2O$, and wet sieving of the sand fractions (Schlichting et al., 1995). The pH was measured in 0.1 mol l^{-1} $CaCl_2$ at a soil/solution ratio of 1:2.5 after equilibration for 2 h with a glass electrode; the C, N, and S concentrations were determined by dry combustion with a CHNS analyzer (Vario EL, Elementar Analysensysteme, Hanau, Germany). The S concentrations were detected with a sensitive infrared detector. The effective cation-exchange capacity (ECEC) was determined as the sum of the charge equivalents of Ca, K, Mg, Na, Mn, and Al extracted with 1 mol l^{-1} NH_4NO_3; base saturation (BS) was calculated as the sum of the charge equivalents of Ca, Mg, Na, and K divided by the ECEC and expressed as a percentage.

Copper was sequentially extracted using the method of Zeien and Brümmer (1989) to assess operationally defined Cu fractions in the soil. Briefly, for the sequential extraction 2 g of air-dried soil was extracted with 50 ml each of: 1 mol l^{-1} NH_4NO_3 for 24 h (Fraction 1, readily soluble and exchangeable), 1 mol l^{-1} NH_4OAc at pH 6.0 for 24 h (Fraction 2, specifically absorbed and other weakly bound species), 0.1 mol l^{-1} $NH_2OH\cdot HCl$ + 1 mol l^{-1} NH_4OAc at pH 6.0 for 0.5 h (Fraction 3, bound to Mn oxides), 0.025 mol l^{-1} NH_4 ethylenediaminetetraacetic acid at pH 4.6 for 1.5 h (Fraction 4, bound to organic matter), 0.2 mol l^{-1} ammonium oxalate at pH 3.25 for 4 h in the dark

(Fraction 5, bound to poorly crystalline Fe oxides), 0.1 mol l^{-1} ascorbic acid in 0.2 mol l^{-1} ammonium oxalate at pH 3.25 for 0.5 h in hot water (Fraction 6, bound to crystalline Fe oxides), and 67% HNO_3 + 50% HF (3:1) (Fraction 7, residual). Fractions 1 to 5 were extracted at room temperature, Fraction 6 was extracted at 96°C, and Fraction 7 was digested at 200°C under pressure in a microwave oven. All fractions except Fraction 7 were centrifuged at 2500 rpm for 15 min and filtered with blue ribbon (Whatman Schleicher and Schuell, Kent, UK, 2-µm retention) filter paper after extraction. After every extraction step except for Fractions 1 and 7, the sample was rinsed once (Fractions 2, 4, 5, and 6) or twice (Fraction 3) with 25 ml of 1 mol l^{-1} NH_4NO_3 (Fraction 2), 1 mol l^{-1} NH_4OAc (pH 6, Fraction 3), 1 mol l^{-1} NH_4OAc (pH 4.6, Fraction 4), and 0.25 mol l^{-1} ammonium oxalate (pH 3.25, in the dark, Fraction 5 and 6) for 10 min. The extracts and rinses were combined.

Total Fe concentrations were measured in total digests with concentrated HF/concentrated HNO_3 (1:3). Poorly crystalline and crystalline Fe fractions were measured in Fractions 5 and 6 of the sequential extraction. The ratio of poorly crystalline to crystalline Fe concentrations is referred to as $Fe_{poorly\ crystalline}/Fe_{crystalline}$. This ratio is different than the frequently used oxalate-extractable Fe/dithionite-extractable Fe (Fe_o/Fe_d), which would approximately correspond to the ratio of the sum of Fe extracted with Fractions 1 to 5 divided by the sum of Fe extracted with Fractions 1 to 6 of the sequential extraction procedure. The precision of a triplicate measurement of the $Fe_{poorly\ crystalline}/Fe_{crystalline}$ ratio (Δy) was 15.2% (2 RSD) and was calculated using the error propagation law:

$$\Delta y = \left|\frac{1}{x_2}\right|\Delta x_1 + \left|-\frac{x_1}{x_2^2}\right|\Delta x_2 \qquad \text{(C-1)}$$

where x_1 represents the $Fe_{poorly\ crystalline}$ concentration and x_2 the $Fe_{crystalline}$ concentration, $\Delta x1$ is the relative standard deviation of the triplicate measurement of the $Fe_{poorly\ crystalline}$ concentration, and Δx_2 is the relative standard deviation of the triplicate measurement of the $Fe_{crystalline}$ concentration.

Copper concentrations were determined by electrothermal atomic absorption spectrometry (ETAAS; Unicam Solaar 989, Thermo Scientific, Waltham, MA) and the concentrations of Fe, Ca, K, Mg, Na, Mn, Al were measured by flame atomic absorption spectrometry (AAS 240 FS, Varian, Palo Alto, CA).

The accuracy of the Cu concentration measurements was controlled by measuring the total digests of the certified reference material (CRM) 7003 (a silty clay loam) from the Czech Meteorology Institute (Brno, Czech Republic) and basalt of the Columbia River (BCR-2) and granodiorite silver plume (GSP-2) reference materials from the United States Geological Survey. We determined a concentration of 27 ± 2.5 mg kg^{-1} Cu (2 standard deviations [SD], $n = 3$) for CRM 7003 (certified value, 29.1 ± 0.8 mg kg^{-1} Cu), 16.8 ± 1.2 mg kg^{-1} Cu (2 SD, $n = 8$) for BCR-2 (certified value, 19 ± 2 mg kg^{-1} Cu), and 38.8 ± 3.9 mg kg^{-1} Cu (2 SD, $n = 5$) for GSP-2 (certified value, 42 ± 4 mg kg^{-1} Cu). The reproducibility of replicate digestions and measurements of the reference materials was always ≤10% (2 RSD). The accuracy of the sequential extraction procedure could not be controlled with a CRM because of the lack of such a material. Therefore we processed CRM 7003 three times. The precision of the sum of fractions was 13% (2 RSD), with all sums of concentrations of the seven fractions falling in the range of ±10% of the certified value. For each sample, we checked whether the concentrations of all seven fractions deviated >20% from the concentrations measured in the total digests. If so, the results were discarded and the sample was processed once more.

For isotope analysis, 200 to 500 mg of ground soil was weighed in a ceramic crucible and ashed at 450°C overnight. The sample was transferred to a microwave digestion vessel and digested at 200°C under pressure in a mixture of concentrated HF/concentrated HNO_3 (1:3) in a microwave oven (MARS5Xpress, CEM Corp., Matthews, NC). The acid was evaporated to dryness; 1 ml of HNO_3 was added to drive out the remaining HF and again evaporated to dryness. The sample was redigested in 10 mol l^{-1} HCl with some drops of H_2O_2 at 200°C under pressure to remove any remaining fluorides and then transferred to Savillex (Minnetonka, MN) vials, evaporated again, and redissolved in 7 mol l^{-1} HCl and 0.001% H_2O_2 for purification on the anion exchange resin. The total digests were purified on AG MP-1 Biorad resin after a protocol modified from Marechal et al. (1999). The resin was cleaned before purification by leaching sequentially with 10 ml of H_2O, 10 ml of 7 mol l^{-1} HCl, 10 ml

Table C-2. Selected properties of the study soils from Germany and Slovakia

Soil	Horizon	Depth	Color	Sand	Silt	Clay	Gravel	ECEC	BS	OC	N	S	$CaCO_3$	pH	Fe
		cm		---------- g kg^{-1} -- ----------				mmol kg^{-1}	%	%	%	mg kg^{-1}	%	($CaCl_2$)	g kg^{-1}
Skeleti-Stagnic Luvisol	Ah	3	10YR 2/2	53	242	115	590	90	45	7.8	0.6	252	0	3.7	28
	Bw	20	2.5YR 5/4	99	302	120	480	50	24	0.9	0.1	56	0	4.0	32
	Bwg	50	2.5YR 6/4	97	229	114	560	50	9	0.5	0.1	61	0	3.8	43
	II Bgt1	75	2.5YR 6/4	76	256	92	580	30	53	0.3	0.1	34	0	4.0	27
	II Bgt2	115	10YR 6/5	150	229	62	560	40	23	0.3	0.1	38	0	3.9	47
	III Bgt3	>115	10YR 6/5	96	148	46	710	40	67	0.2	0.1	34	0	4.3	28
Stagnic Cambisol	Ah	5	5Y 2/1	100	610	290	0	130	17	6.6	0.4	224	0	3.2	9
	Ahg	8	2.5Y 4/2	100	640	260	0	80	22	2.6	0.2	114	0	3.6	25
	Bg1	29	2.5Y 5/3	170	580	260	0	60	41	0.7	0.1	48	0	3.8	15
	II Bg2	>29	10YR 5/6	135	522	243	100	70	61	0.4	0.1	53	0	4.0	37
Calcari-Humic Gleysol	Ah	7	2.5Y 3/2	260	610	120	0	-	100	5.2	0.2	252	26	6.9	20
	Bh	35	2.5Y 4/3	70	680	250	0	-	100	4.0	0.2	187	22	7.0	24
	Bl1	60	10YR 5/3	120	660	220	0	-	100	3.1	0.0	110	22	7.0	19
	Bl2	80	2.5Y 4/4	140	670	180	0	-	100	2.5	0.1	115	17	7.1	18
	Br	>80	2.5YR 5/2	70	690	240	0	-	100	3.6	0.1	439	21	7.1	19
Dystric Gleysol	Ah	15	5YR 1,7/1	203	245	252	300	160	12	9.9	0.6	424	0	3.2	9
	Bl1	20	2.5Y 4/4	217	266	217	300	110	13	2.0	0.1	75	0	3.6	12
	II Bl2	>20	2.5YR 5/4	105	295	105	500	50	28	0.3	0.0	37	0	3.8	22

of H_2O, 10 ml of 0.5 mol l^{-1} HNO_3, and 10 ml of H_2O. Because of the low Cu to high matrix ratio, one single purification run was not sufficient to achieve good matrix separation. The whole purification procedure was therefore repeated for each sample. After the second purification, the sample was dried and the residue treated with 200 µl of concentrated HNO_3 and 200 µl of 30% H_2O_2 to destroy organic compounds released from the resin and drive out any remaining HCl. After some reaction time, the sample was evaporated and redissolved in 2% HNO_3 for isotope ratio measurement.

Recovery was checked for every sample to rule out isotope fractionation on the resin (Marechal and Albarede, 2002). Recoveries were checked with ETAAS and samples that did not show recovery of 100 ± 5% were discarded. All reagents used for the preparation of the isotope samples were double subboiled, of suprapure (Merck, Darmstadt, Germany) or trace select (Fluka, Seelze, Germany) quality. Water was taken from a TKA GenPure UV (TKA, Niederelbert, Germany) water purification system and was of ≥18 MΩ cm quality. All critical steps were performed under clean air conditions in a clean bench, evaporations were done in boxes supplied with high-efficiency particulate filtered air. Copper blanks for the whole procedure were 6.6 ± 9.9 (2 SD) ng compared with at least 500 ng of Cu in the sample. The range of the Cu isotope signature observed in nature reaches from −3.44 to 5.74‰ (Asael et al., 2007; Marechal et al., 1999, Fig. C-1). As our samples cluster around 0‰, contamination in the sample may deviate by a maximum of ~ 6‰. Thus a contamination of 6.6 ng Cu would affect the Cu isotope ratio with a maximum of 0.075‰, which is half of the measurement uncertainty we give.

3.3 Copper isotope measurements

Copper isotope ratios were measured with a Finnigan-Neptune (Thermo Scientific, Waltham, MA) MC-ICPMS with high mass resolution capabilities (Weyer and Schwieters, 2003). All Cu isotope ratios were expressed as δ^{65}Cu values relative to NIST 976 isotope reference material according to Equation C-2.

$$\delta^{65}Cu[‰] = \left(\frac{\left({}^{65}Cu/{}^{63}Cu\right)_{sample}}{\left({}^{65}Cu/{}^{63}Cu\right)_{NIST\,976}} - 1 \right) * 1000 \qquad \text{(C-2)}$$

Masses 60 (Ni), 61 (Ni), 62 (Ni), 63 (Cu), 64 (Zn + Ni), 65 (Cu), and 66 (Zn) were detected simultaneously. Nickel was used for instrumental mass-bias correction of the measured $^{65}Cu/^{63}Cu$ ratio (Ehrlich et al., 2004; Li et al., 2009; Markl et al., 2006). The correction was performed according to the certified $^{62}Ni/^{60}Ni$ ratio (0.138600) of a natural Ni standard (NIST 986) that was added to all samples and the Cu standard before measurement and by applying the exponential law. Additionally, after every third sample, the NIST 976 was measured as a kind of sample standard bracketing. The $\delta^{65}Cu$ values were calculated as the deviation of the isotope ratio of the mass-bias corrected samples from the isotope ratio of the mass-bias corrected bracketing standards (Li et al., 2009). The samples and standards were measured in 2% HNO_3 with concentrations of 300 µg kg^{-1} Cu and 1000 µg kg^{-1} Ni in low resolution and 600 µg kg^{-1} Cu and 2000 µg kg^{-1} Ni in high resolution.

The samples were introduced with a combination of a cyclonic and a Scott double pass-type spray chamber. Membrane desolvating nebulizer introduction systems were avoided because of previously described problems with mass-bias instabilities (Archer and Vance, 2004). Aluminum cones were used for the measurements to avoid any potential effect of Ni cones on the spike. Samples were measured in both low- and high-resolution modes. The high-resolution mode was necessary for some initial samples where interfering Ti was not completely separated from Cu. Where Ti separation was not sufficiently good, mass interferences such as $^{48}Ti^{14}N$, $^{46}Ti^{16}O$, $^{47}Ti^{16}O$, and $^{49}Ti^{16}O$ may occur on ^{62}Ni, ^{63}Cu, and ^{65}Cu, respectively. These interferences shift the measured isotope ratio to more negative values because of the Ti interference on ^{62}Ni and the absence of such an interference on mass ^{60}Ni, which cause an overcorrection of measured values. The Finnigan- Neptune high-resolution mode, with a mass resolution power of ~10,000 M/ΔM (Weyer and Schwieters, 2003), was sufficient to resolve these interferences. Some samples with sufficient Ti separation were measured with both high- and low-resolution modes and the respective results were indistinguishable (Table C-3). The sample purification procedure was adjusted more carefully by rinsing eight times with altogether 10 ml of 7 mol l^{-1} HCL + 0.001% H_2O_2 after sample application

on the resin. After adjustment of the purification procedure, the mean Ti/Cu ratio was reduced from 289 in the not purified samples to 0.02 (n = 18) after the two column purifications.

All samples were measured at least twice. For samples that showed abnormal values or large differences between the two measurements, sample preparation and measurement were repeated. A Cu inductively-coupled plasma standard (Merck, Darmstadt, Germany) was used as an in-house standard to check for intra-day and long-term reproducibility. The long-term reproducibility of this standard was 0.07‰ (2 SD, n = 20). To check for reproducibility of the samples, three CRMs (BCR-2, GSP-2, and CRM 7003) and selected samples were repeatedly digested and purified two to five times and each extract was measured independently (Table C-3). Reproducibility was determined as two times the standard deviation of all measured values and was always better than 0.15‰ (2 SD). To test for accuracy of the measurement, the BCR-2 basalt was independently digested, purified, and measured five times and the GSP-2 granodiorite twice (Table C-3). We measured a δ^{65}Cu value of 0.22 ± 0.06‰ (2 SD, n = 5) for BCR-2, which differs from the 0.07 ± 0.08 ‰ reported by Archer and Vance (2004) for BCR-1. We assume that this difference might be attributable to isotope inequality of BCR-1 and BCR-2. For the GSP-2 granodiorite, no δ^{65}Cu values have been published to date, but the measured value of 0.25 ± 0.03‰ (n = 2) fits well in the range of −0.4 to 0.4‰ reported for granites from the Lachlan Fold Belt (Li et al., 2009). The loess sample measured as bedrock for the Skeleti-Stagnic Luvisol had δ^{65}Cu values of −0.10 ± 0.04‰, which is similar to the 0.03 and −0.02‰ reported for Chinese loess (Li et al., 2009). The silty clay loam CRM 7003 had a δ^{65}Cu value of 0.21 ± 0.11‰ (2 SD, n = 4).

Table C-3. Copper concentrations, $\delta^{65}Cu$ values of the soil samples and reference materials, standard deviation of replicate measurement, and resolution mode of the Multicollector-ICP-MS device

Soil	Horizon	Cu concentration mg kg^{-1}	$\delta^{65}Cu_{NIST976}$[‰]	2SD	Resolution mode
Skeleti-Stagnic Luvisol	Oi	12.9	-0.10	0.03	LR
	Oe	16.4	-0.10	0.01	LR
	Ah	16.7	-0.15	0.06	HR
	Bw	13.8	-0.17	0.10	HR
	Bwg	20.2	-0.10	0.01	HR
	II Bgt1	12.3	0.04	0.09	HR/LR
	II Bgt2	14.7	0.02	0.07	HR
	III Bgt3	12.1	0.16	0.21	HR/LR
Parent materials	Laacher Lake Tephra	5.8	-0.03	0.05	LR
	Loess	17.8	-0.10	0.04	LR
	Slate	16.4	-0.15	0.16	LR
Stagnic Cambisol	Oi	12.2	-0.34	0.18	LR
	Oe	16.7	-0.23	0.11	LR
	Oa	13.8	0.08	0-19	HR
	Ah	9.5	-0.13	0.16	LR
	Ahg	7.8	-0.06	0.10	LR
	Bg1	8.2	0.02	0.07	HR
	II Bg2	19.8	-0.09	0.09	HR
Calcari-Humic Gleysol	Oi	16.1	0.13	0.09	HR
	Ah	34.2	-0.08	0.04	HR
	Bh	31.8	0.03	0.01	HR
	Bl1	14.0	-0.08	0.12	HR
	Bl2	9.0	0.12	0.06	HR
	Br	15.1	0.13	0.04	HR
Dystric Gleysol	Oi	7.3	-0.26	0.15	LR
	Oe	11.7	-0.21	0.13	LR
	Oa	9.1	0.20	0.21	LR
	Ah	6.2	0.10	0.02	LR
	Bl1	5.7	0.33	0.08	LR
	Bl2	5.4	-0.12	0.08	LR/HR
Silty Clay Loam (CRM 7003, Czech Meteorology Institute)	7003	26.2	0.18	0.13	HR
	7003	26.5	0.29	0.00	HR
	7003	28.5	0.20	0.12	HR
	7003	25.9	0.16	0.06	LR
Cu ICP	Cu ICP	-	0.84	0.07	LR/HR
BCR-2 (CRM, USGS)	BCR-2 1	16.2	0.21	0.08	LR
	BCR-2 2	15.9	0.22	0.03	LR
	BCR-2 3	17.4	0.18	0.11	LR
	BCR-2 4	16.9	0.24	0.00	LR
	BCR-2 5	17.3	0.25	0.04	LR
GSP-2 (CRM, USGS)	GSP-2 1	38.7	0.24	0.00	LR
	GSP-2 2	37.4	0.26	0.04	LR

4 Results

Copper concentrations in the soil samples ranged between 5 and 34 mg kg^{-1} (Fig. C-3; Table C-3) and therefore in the lower range of natural Cu concentrations in soil. The organic layers always had concentrations similar to the mineral soil, with the highest concentrations in the Oe horizon if it was present. The Cu concentrations in the Skeleti-Stagnic Luvisol were similar in all horizons except for the Bwg horizon, where an elevated Cu concentration occurred (Fig. C-3; Table C-3). In the Stagnic Cambisol, the Cu concentrations did not vary much among the various soil horizons except for a twofold higher Cu concentration in the II Bg2 horizon, which developed from a geologically different solifluctional layer. In the Calcari-Humic Gleysol, Cu concentrations showed the highest variation, with higher concentrations in the Ah and Bh horizons than the horizons affected by groundwater. The Dystric Gleysol had slightly higher concentrations in the organic layer than in the mineral soil, but Cu concentrations were similar in all mineral horizons.

The sequential extraction of Cu in the mineral soil revealed that Fraction 7 (residual) was the main pool in most horizons, comprising 20 to 80% of total soil Cu. Fractions 5 and 6 (bound to Fe oxides) contained 10 to 50% of the soil Cu, while Fraction 4 (organically bound) varied from 3 to 60%, and Fractions 1 to 3 exchangeable, specifically absorbed, and bound to Mn oxides) always contained only a minor part of the soil Cu (2–17%, Fig. C-4). The two Slovak soils (the Stagnic Cambisol and Dystric Gleysol) always had >50% of their total Cu in Fraction 7, while the Skeleti-Stagnic Luvisol showed elevated Cu concentrations in Fractions 5 and 6. The Calcari-Humic Gleysol had its highest Cu concentrations in Fraction 4.

The $Fe_{poorly\ crystalline}/Fe_{crystalline}$ ratios might be indicative of crystallization conditions and thus of the frequency of waterlogging. The more frequently the soil is waterlogged, the less crystalline is the Fe oxide pool and the higher is the $Fe_{poorly\ crystalline}/Fe_{crystalline}$ ratio. In the Skeleti-Stagnic Luvisol, the $Fe_{poorly\ crystalline}/ Fe_{crystalline}$ ratios were higher in the Bwg and II Bgt horizons than in the Ah and Bw horizons and decreased sharply in the II Bgt2 and III Bgt3 horizons because of a threefold increase in crystalline Fe concentration and a simultaneous halving of poorly crystalline Fe concentrations. In the Stagnic Cambisol, the highest $Fe_{poorly\ crystalline}/Fe_{crystalline}$ ratio occurred in the Bg1 horizon

(Fig. C-5). The Calcari-Humic Gleysol showed little variation in $Fe_{poorly\ crystalline}/Fe_{crystalline}$ ratios. The $Fe_{poorly\ crystalline}/\ Fe_{crystalline}$ ratios in the Dystric Gleysol shifted from low values in the Ah to high values in the Bl1 horizon, and an intermediate value in the II Bl2 horizon.

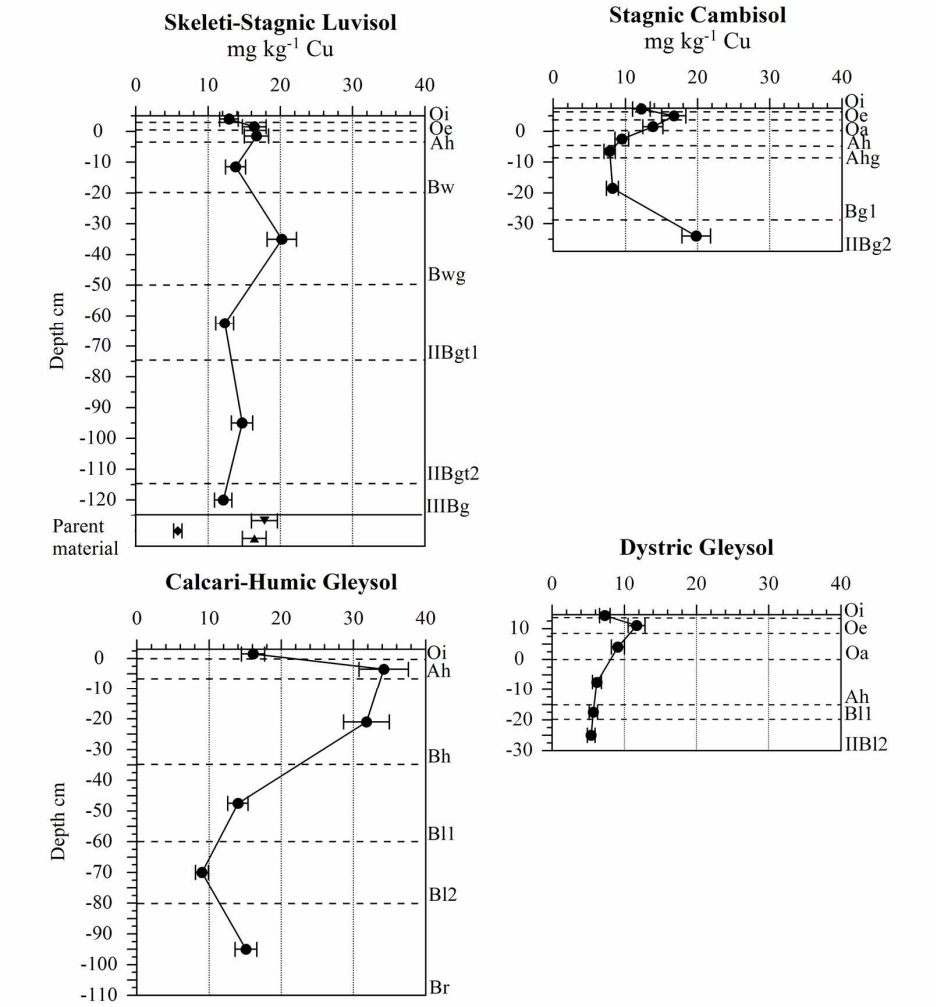

Figure C-3. Copper concentrations in the soil horizons (Cu concentrations for ▲ slate, ▼ loess, and ♦ tephra of the volcanic eruption of Lake Maria Laach, representing the mixed parent materials in the periglacial cover beds from which the Skeleti-Stagnic Luvisol developed). Error bars represent 10% of the mean, i.e., two times the relative standard deviation, which is the precision of the analytical method used.

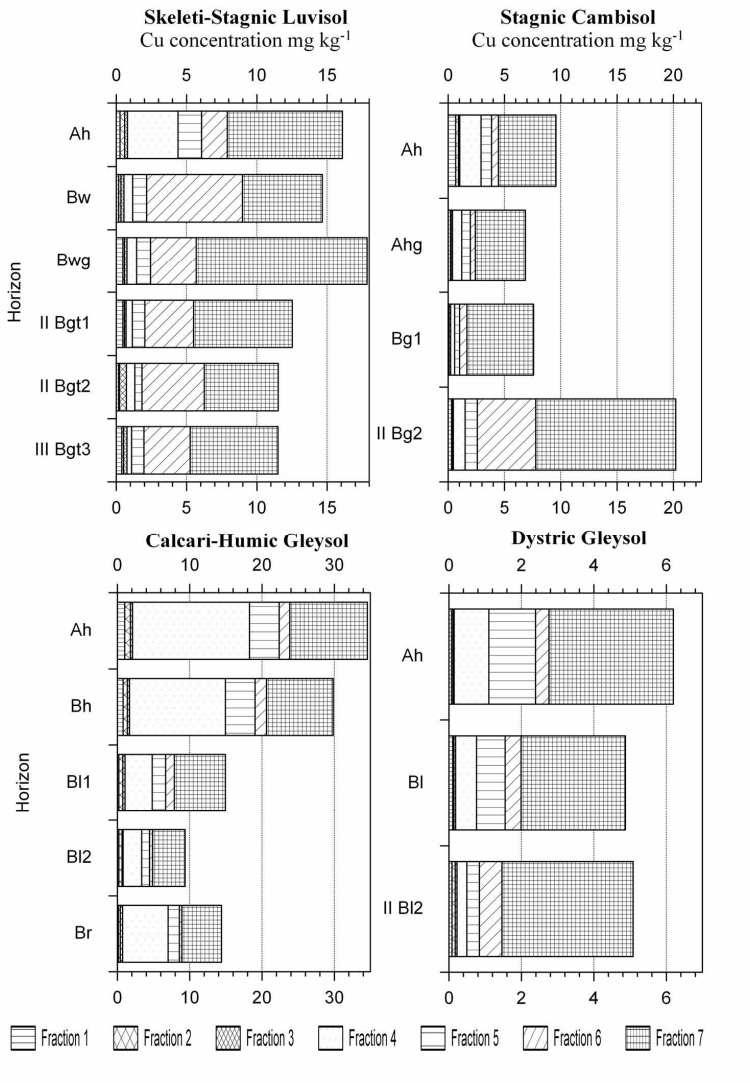

Figure C-4. Copper concentrations in the seven fractions of the sequential extraction of Zeien and Brümmer (1989). Fractions are thought to represent (1) readily soluble and exchangeable, (2) specifically absorbed and other weakly bound species, (3) bound to Mn oxides, (4) bound to organic matter, (5) bound to poorly crystalline Fe oxides, (6) bound to crystalline Fe oxides, and (7) residual fractions.

The δ^{65}Cu values in all horizons ranged between −0.34 and 0.33‰. The highest variation in δ^{65}Cu in an individual soil was 0.59‰ in the Dystric Gleysol (Table C-3; Fig. C-5). The heavy ^{65}Cu isotope was depleted in the organic layers of the Dystric Gleysol and the Stagnic Cambisol compared with the mineral soil. The Oi and Oe horizons had δ^{65}Cu values between −0.34 and −0.21‰. Only the Oi horizon of the Calcari-Humic Gleysol had a positive δ^{65}Cu value of 0.13‰. The δ^{65}Cu values of the

Oa horizons were more similar to the mineral soil than to the Oi and Oe horizons. The Stagnic Cambisol and the Calcari-Humic Gleysol showed little variation in δ^{65}Cu values in the mineral soil. The Skeleti-Stagnic Luvisol revealed a trend to heavier δ^{65}Cu values in the temporally waterlogged subsoil. This cannot be explained by the δ^{65}Cu values of the parent rock (slate) or admixed components like loess or Laacher See tephra because these materials were isotopically lighter than the deeper soil horizons (Fig. C-5). The Dystric Gleysol showed a marked shift in δ^{65}Cu values between the Bl1 and II Bl2 horizons.

5 Discussion

5.1 Variation in Cu isotope ratios in the soil system

The maximum Cu isotope variation in an individual soil profile was 0.59‰ in the Dystric Gleysol, with a maximum Cu isotope variation of 0.45‰ in the mineral soil and 0.46‰ between the Oi and Oa horizons in the organic layers. These differences were in a range that can be distinguished with the precision of 0.15‰ (2 SD) reached by our method. Copper isotope variations in soils show a similar range as observed for Fe and Zn isotopes. The δ^{57}Fe values varied by 0.3‰ in total digests of samples from redoximorphic soils and by ~1.15‰ in samples from Podzols (Wiederhold et al., 2007a,b). Other researchers reported δ^{56}Fe variations between 0.3 and 0.9‰ among the various horizons of different soils (Fantle and DePaolo, 2004; Emmanuel et al., 2005; Thompson et al., 2007). The maximum isotope variations in δ^{66}Zn in deeply weathered tropical soils were ~0.7‰ (Viers et al., 2007).

Sequential extraction is an established procedure to gain information about the partitioning of soil Cu among differently reactive Cu pools (Bacon and Davidson, 2008) and may offer valuable information if coupled with Cu isotope investigations. Isotope effects may be much bigger in the labile Cu pools where chemical reactions and transport of Cu occur, while the residual Cu pool representing the isotope ratios of parent rock, which vary comparatively little, may dilute these effects. For Fe, sequential extraction procedures were used to investigate the isotope composition of different soil Fe pools. In these studies, an isotope variation of up to >3‰ (δ^{57}Fe) between different fractions was reported (Wiederhold et al., 2007a, b).

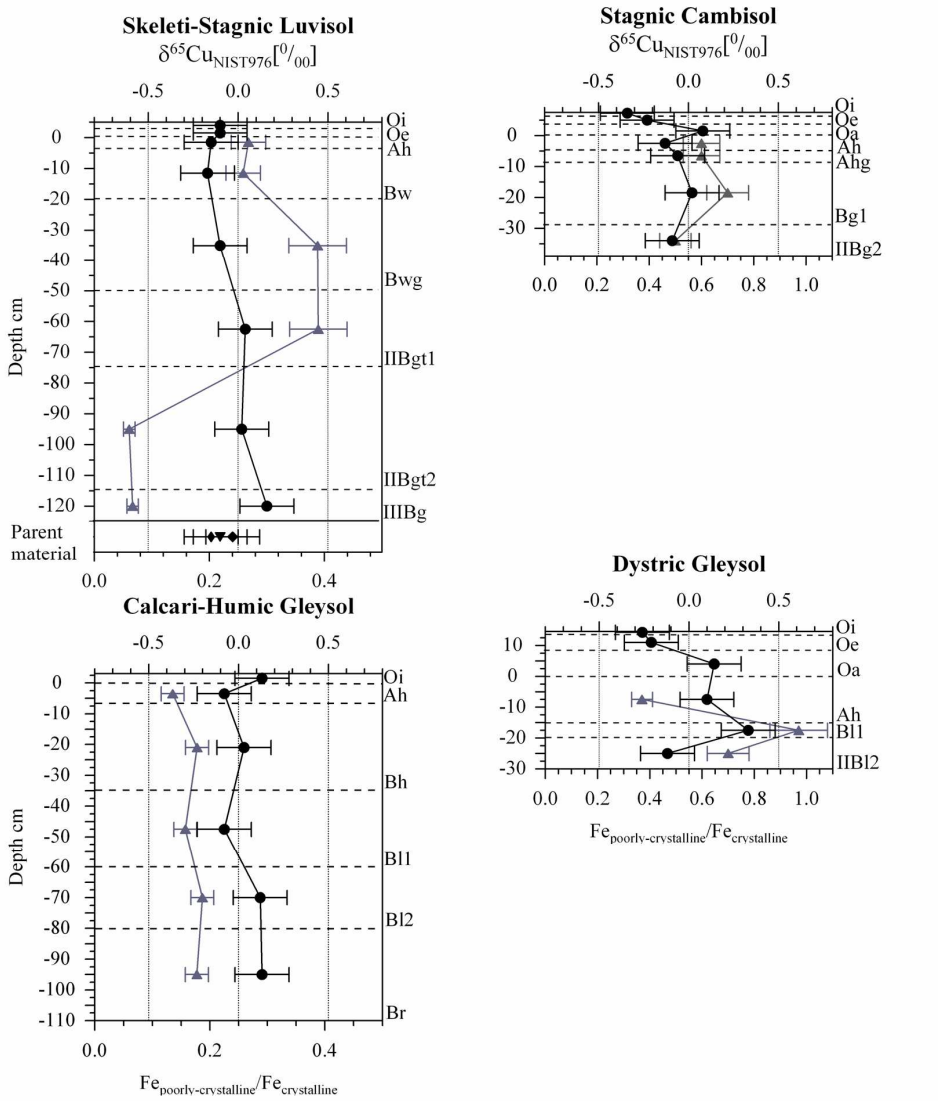

Figure C-5. Copper isotope composition ($\delta^{65}Cu$ values) and poorly crystalline/crystalline Fe ($Fe_{poorly\ crystalline}/Fe_{crystalline}$) ratios in the soil horizons (● $\delta^{65}Cu$ values, ▲ $Fe_{poorly\ crystalline}/Fe_{crystalline}$ ratios; $\delta^{65}Cu$ for ▲ slate,▼ loess, and ♦ tephra from the volcanic eruption of Lake Maria Laach, representing the mixed parent materials in the periglacial cover beds from which the Skeleti-Stagnic Luvisol developed). Error bars represent 0.15‰, i.e., two times the standard deviation, which is the precision of the analytical method used. Please note that the $Fe_{poorly\ crystalline}/Fe_{crystalline}$ ratios are scaled differently. Error bars of $Fe_{poorly\ crystalline}/Fe_{crystallin}$. ratios represent 15.2% (two relative standard deviations).

Fantle and DePaolo (2004) reported differences of 0.9‰ (δ^{56}Fe) between bulk and leached fractions (0.5 mol l^{-1} HCl). These fractionations are far larger than those observed in total digests. Sequential extraction procedures have to be developed carefully, however. Extraction steps may artificially fractionate isotopes because of kinetic and equilibrium effects, as described for Fe (Wiederhold et al., 2006). No reliable procedure has yet been developed that has been proven to be sufficiently specific for defined Cu pools and that does not result in artificial isotope fractionation. Therefore, no Cu isotope measurements were done on sequential extracts in our study. The development of such an extraction procedure should be a future step to deepen our understanding of Cu biogeochemistry in the soil system.

5.2 Copper isotope ratios in the organic layer

As Cu isotope ratios differ between roots and shoots, with the shoots depleted in ^{65}Cu (Jouvin et al., 2008), fractionation during transport in plants seems probable. For Zn, a similar shift in stable isotope ratios was reported from roots to shoot. Zinc fractionation between roots and shoots seems to depend on Zn speciation in the solution from which plants take up their nutrients, usually the soil solution (Weiss et al., 2005; Moynier et al., 2009). Similarly, the Fe stable isotope ratios in plant compartments depend on uptake mechanisms and hence speciation of assimilated Fe (Guelke and von Blanckenburg, 2007). Fractionation during translocation is explained by diffusion and cross-cell membrane transport for Zn (Moynier et al., 2009) and redox reactions and fractionation during incorporation into organic molecules for Fe (Guelke and von Blanckenburg, 2007). In the light of these considerations, we expected a lighter isotope composition of the organic soil layers compared with the mineral soil because organic horizons result from plant litter. The organic layer of two of the four studied soils was depleted in ^{65}Cu compared with the Ah horizons (Fig. C-5). We suggest two explanations for this finding: (i) plants take up Cu from the soil solution, and if this plant-available Cu pool was isotopically different from the Cu in the total soil digests, plants would recycle Cu to the organic layer via litter fall, which would isotopically differ from the total Cu of the solid mineral soil; and (ii) Cu isotopes are fractionated during translocation in plants as shown by Jouvin et al. (2008) and also fractionation might occur during uptake such as has been observed for Fe and Zn isotopes (Guelke and von Blanckenburg, 2007; Weiss et al., 2005). Pokrovsky et al. (2008) furthermore

reported that light Cu can accumulate at the surface of microorganisms at acidic pH, which might also contribute to the retention of light Cu in the organic horizons during organic matter turnover. In our study, organic horizons under coniferous vegetation showed lighter isotope signatures than organic horizons under deciduous trees (Table C-1), which had similar or even more positive δ^{65}Cu values compared with the underlying Ah horizons (Fig. C- 5). These differences might have been caused by different tissue structures responsible for water and nutrient transport in coniferous and deciduous trees and these different plant anatomic properties might influence Cu isotope fractionation. While most coniferous trees have a more primitive xylem consisting of tracheids only, the xylem of most deciduous trees consists of tracheids and trachea. Trachea have larger diameters than tracheids, and cell walls hindering horizontal transport of water and nutrients are reduced or even absent. These vessel systems often have lengths in the range of several centimeters up to 1 m and can reach up to 10 m. In contrast, tracheids are small and each cell is bordered by cell walls, which have pits through which transport takes place. We speculate that water and Cu transport is faster and contact to surfaces reduced in tracheas compared with tracheids, which may reduce the interaction of Cu with the cell surfaces during transport, resulting in less fractionation of Cu isotopes. Copper deposition from the atmosphere might also have an impact on Cu isotope patterns in organic layers. Wilcke and Dohler (1995) estimated the mean atmospheric Cu deposition in Germany at 5.3 mg m^{-2} yr^{-1} (range: 1.2–17 mg m−2 yr^{-1}). The isotope pattern of Cu deposition seems to depend on the source and varies without a particular trend (Gale et al., 1999; Matielli et al., 2006). Therefore, the direction of the expected shift in δ^{65}Cu values of soils affected by Cu deposition from the atmosphere cannot be generally predicted. The influence of deposition on metal concentrations in soils is usually indicated by elevated metal concentrations in the organic layer compared with the mineral soil (Filipinski and Grupe, 1990; Lobe et al., 1998; Wilcke et al., 1999). This is the case for the two Slovakian soils, which showed also comparatively light δ^{65}Cu values in the organic layer. Thus, the input of atmospheric Cu with a sufficiently different isotope ratio from that of the soils might have an influence on the δ^{65}Cu values of soil organic layers. Copper concentrations in the organic layers were low (in the range of normal background concentrations; Artiola, 2005), however, and comparable to those in the mineral soil (Fig. C-3).

Especially near industrial emitters and in agricultural areas, Cu contamination because of anthropogenic input is possible. While industrial emitters release Cu as a byproduct, a broad range of intentionally applied compounds including pesticides and slurries may include substantial amounts of Cu (L'Herroux et al., 1997; Epstein and Bassein, 2001).

Where an Oa horizon was present, its isotope composition was more similar to the mineral than to the organic horizons; the Oa horizons even tended to be isotopically heavier than the underlying Ah horizons (Fig. C-5). Based on the assumption that Oi horizons show a similar Cu isotope signature to plants, diverse processes might explain isotope differentiation between Oi and Oa: (i) during different stages of decomposition, plant components with different stabilities will sequentially decompose and release Cu that corresponds to the isotope signature of the decomposed part; (ii) soil organisms might transport metabolized Cu between different horizons; (iii) kinetic and equilibrium effects may occur because of sorption effects during transport between horizons under non-steady-state conditions (Mikutta et al., 2009); and (iv) the Oa horizon consists of organic matter that has been disintegrated, metabolized, and condensed to a broad mixture of compounds offering diverse sites for metal complexation. In the latter case, the findings of Dideriksen et al. (2008) and Jouvin et al. (2009) for Zn and Fe isotopes suggest an enrichment of heavy isotopes in the organo-complexed form due to stronger bonding under equilibrium conditions.

5.3 Copper isotope gradients in individual soils

The Skeleti-Stagnic Luvisol showed a shift in δ^{65}Cu values to more heavy isotopes with increasing soil depth (Fig. C-5). Because the Skeleti-Stagnic Luvisol developed from different geologic layers (periglacial cover beds), this shift might be related to different δ^{65}Cu values in the various parent materials (slate, loess, and Laacher See tephra), which are mixed to different degrees in the periglacial cover beds. Therefore, we determined the Cu isotope composition of all the parent substrates. The δ^{65}Cu values of the three parent substrates ranged between −0.03 and −0.15‰, all being isotopically lighter than the B horizons of the geogenic layers II and III. Thus, the difference in δ^{65}Cu values between the lower and upper mineral horizons cannot be explained by the mixture of parent materials. This was particularly the case for the lowest horizon (III

Bgt3) of the Skeleti-Stagnic Luvisol with a δ^{65}Cu value of 0.16‰ although this horizon was developed exclusively from slate with a δ^{65}Cu value of −0.15‰ (Fig. C-5). Thus, our results demonstrate that pedogenetic Cu isotope fractionation occurs in soils. Surprisingly, the higher Cu concentration in the Bwg horizon of the Skeleti-Stagnic Luvisol was not associated with a marked change in δ^{65}Cu. Because mixing of the periglacial cover beds did not always result in a homogeneous distribution of Cu in solifluctional layers, the initial Cu concentrations of soil horizons may vary. The Cu

partitioning in the Bwg horizon of the Skeleti-Stagnic Luvisol (Fig. C-4) shows that the concentration peak in total Cu concentrations is caused by elevated Cu concentrations in the residual fraction and can therefore be explained by a locally increased Cu concentration as a consequence of inhomogeneous mixing of the three different parent substrates of this horizon (slate, loess, and Laacher See tephra). The Stagnic Cambisol did not show distinguishable Cu isotope signatures among the mineral horizons. Even the deepest horizon, which developed from a different geogenic layer, as illustrated by the much higher Cu concentration and the differences in Cu partitioning among the seven fractions of the sequential extraction (Fig. C-2 and 3) had a similar δ^{65}Cu value as the other mineral horizons (Fig. C-5). The lack of isotope fractionation might be attributed to little vertical and lateral Cu transport in this soil.

The Cu isotope ratios in the mineral soil of the Calcari-Humic Gleysol showed only small isotope variations around 0‰, which again suggests that little vertical redistribution of fractionated Cu took place. In contrast to that, large shifts in Cu concentrations are observed in this profile, which might point to the fact that either the Cu concentrations reflect different Cu concentrations of the various deposited fluvic materials or transport of Cu in the profile was not associated with isotope fractionation. Only in the Bl2 and the Br horizons, which are the most strongly water-affected horizons, can a slight shift to heavier Cu isotope signatures be seen (Fig. C-5). The Dystric Gleysol is influenced by oxic groundwater and did not develop a permanently reduced horizon characterized by gray color like the Br of the Calcari-Humic Gleysol. With respect to the Cu isotope signature, especially the shift between the Bl1 and II Bl2 horizons is striking because both horizons seem to have developed under similar conditions. As the Bl1 and II Bl2 of the Dystric Gleysol developed from different

geologic layers, a difference in the initial Cu isotope composition is a possible reason for this shift.

5.4 Copper geochemistry and isotope fractionation in the mineral soil

As total digests of soil horizons were analyzed for Cu isotopes, only differences in isotope signatures of the parent material and processes that cause redistribution of Cu among horizons can be traced. Thus, the only biogeochemical processes that can be detected with stable Cu isotope ratios are those causing mobilization and translocation of fractionated Cu. Although the vertical distribution of Cu does not indicate the transport of large quantities of Cu in all the studied soils, such transport may still have occurred and vertical or lateral illuvation might have compensated eluviation of Cu. Furthermore, the transported species usually resulting from the less strongly bound Cu fractions in soil might show distinctly different Cu isotope ratios than the less reactive but quantitatively dominating Cu.

In the studied soils, large portions (10–50%) of Cu are bound to oxy(hydr)oxides, as indicated by Fraction 5 and 6 of the sequential extraction (Fig. C-2). As the soils are influenced by stagnanic water or groundwater, redox condition fluctuate as indicated by the redoximorphic features that were visible in all four profiles (Vepraskas, 1992).

Under reducing conditions, (i) reductive dissolution of metal oxy(hydr)oxides and (ii) release of organic matter during waterlogging as a consequence of the associated increase in pH affect Cu speciation (Grybos et al., 2007). This change in Cu speciation may, on the one hand, fractionate Cu isotopes due to changes of redox state, ad- and desorption processes, and organo complexation of Cu (Pokrovsky et al., 2008; Zhu et al., 2002). On the other hand, it may also influence Cu mobility by precipitation of Cu^{2+} and Cu^{+} compounds and elemental Cu of low solubility, ad- and desorption processes, or complexation with organic ligands (Grybos et al., 2007). Additionally, redox-induced concentration gradients are possible driving forces for metal transport in the saturated zone. The mobility of Cu under reducing conditions has been intensively studied, mostly in sediments. In general, pore water concentrations of Cu, and thus mobility, decrease at low Eh values in the presence of available S because of the formation of CuS and Cu_2S and coprecipitation and adsorption on Fe sulfides (Simpson et al., 2000; Billon et al., 2001; Du Laing et al., 2007). Apart from the sulfide-bound Cu fractions, a considerable part remains bound to organic matter (Yu et al., 2001). The formation of

sulfide compounds seems to follow distinct cycles, with primary reduction of available (poorly crystalline) Fe, followed by reduction of SO_4^{2-} only after Fe reduction is complete, because of competition among the respective microbial communities (Lovley and Phillips, 1987). If redox conditions change to oxic, pH decreases, metal sulfides are oxidized, and metals are released, causing increasing pore water concentrations (Du Laing et al., 2007; Grybos et al., 2007). But contrasting results were found by Miao et al. (2006), who reported increased mobility of Cu in sediments under reducing conditions and a decrease of mobility when conditions changed to oxic. Weber et al. (2009) reported formation of elemental Cu colloids shortly after flooding of soil. Colloids of elemental Cu were successively replaced by Cu_xS colloids with continuing time under flooded conditions. These colloids keep Cu in the soil solution and therefore relatively mobile. The question remains, however, to what extent these findings are transferable to natural soil. Even if few researchers give Cu concentration data for the solid phase of sediments, we have the impression that the sediments and soils studied to date have shown higher Cu concentrations than our study soils. The sediments studied by Yu et al. (2001) had concentrations of up to 1238 mg kg^{-1} and the sediment-derived soil used by Du Laing et al. (2007) in a lab experiment had 109 mg kg^{-1} Cu; furthermore, the S concentrations and the amount of organic matter might be higher in sediments than in soils. Delaune and Smith (1985) reported total S concentrations of 1.8 g kg^{-1} for freshwater and 3.6 g kg^{-1} S for saline sediments, while Du Laing et al. (2007) reported total organic C values of 10.5%, both of which are substantially higher than in the redox-influenced horizons of our study soils (Table C-2). Besides S concentrations, S speciation and redox dynamics also may be substantially different in soil than in sediment. In soils, redox conditions often change at short intervals and on a small scale. Redoximorphic features become visible if reducing conditions are prolonged or repeated because of the redistribution of Fe and Mn in the soil. The reduced Fe and Mn ions are redistributed among depletion and accumulation zones at soil pore surfaces and in soil peds because of small-scale redox gradients or may be leached from the horizon where reduction took place to deeper horizons (Vepraskas, 1992). Nodules that form in redoximorphic soil as a result of metal accumulation also show enrichment of Cu compared with the surrounding soil matrix, which is probably attributable to the incorporation and adsorption of Cu to Mn and Fe oxy(hydr)oxides (Dowding and Fey,

2007; Timofeeva and Golov, 2007). If oxy(hydr)oxides are dissolved under reducing conditions, associated Cu is released as Cu^{2+}. Isotope fractionation of Cu can result from subsequent redox reactions of Cu^{2+} (1) or by indirect effects of lowered redox potential (2): 1. If Cu^{2+} is not reduced to Cu^{+} or elemental Cu, it may react with organic matter and any remaining oxy(hydr)oxides, leaving the Cu in solution relatively depleted in ^{65}Cu (Pokrovsky et al., 2008), or it may form Cu_xS. In the case that Cu^{2+} is reduced to Cu^{+}, it may be further reduced to elemental Cu, stabilized by complexing agents such as those observed in seawater (Moffett and Zika, 1983) or bound in sulfides (Cu_2S; Simpson et al., 2000). If reduced Cu forms insoluble Cu compounds or elemental Cu, these immobile fractions would be isotopically lighter than the oxidized species (Zhu et al., 2002). If Cu^{+} was stable under reducing conditions, it would be isotopically lighter (Zhu et al., 2002). If the release of organic matter during waterlogging as a consequence of the associated increase in pH controls Cu mobility in soil (Grybos et al., 2007), complexed mobile fractions would probably be heavier because of the stronger binding environment, as shown for Fe and Zn (Dideriksen et al., 2008; Jouvin et al., 2009).

One motivation of our study was to find out if changing soil redox conditions cause detectable variations in the $\delta^{65}Cu$ values of water-influenced soils. Considering all four profiles, no consistent trend was visible that supports this idea. The Skeleti-Stagnic Luvisol and the Calcari-Humic Gleysol showed a slight shift to heavier $\delta^{65}Cu$ values in the lower water-influenced horizons, which would be consistent with the findings for Fe isotopes in soil showing an enrichment of heavy isotopes under anoxic weathering conditions (Fantle and DePaolo, 2004; Thompson et al., 2007). In the Stagnic Cambisol and the Dystric Gleysol, a shift to slightly heavier $\delta^{65}Cu$ values in the water-affected horizons is visible, which is interrupted in the deepest horizons (Fig. C-5) and could also be a result of the different geologic layers from which the horizons developed. If we interpret our data such that Cu isotopes tend to shift to more heavy $\delta^{65}Cu$ values in redoximorphic soils, this would probably point at the presence of more mobile reduced Cu forms in the redoximorphic soil sometime during redox cycles. This idea is supported by a recent study of Weber et al. (2009), who found mobile reduced Cu colloids in flooded soil. This interpretation, however, has to be confirmed by further studies.

5.5 Crystallinity of Fe oxy(hydr)oxides and Cu isotope ratios

Iron oxy(hydr)oxide crystallinity in soils is influenced by time and the conditions of soil development. Furthermore, the presence of organic compounds that hinder crystallization and redox alternations influence crystallinity (Cornell and Schwertmann, 1996). Because the most pronounced changes in a single soil profile were found in the water-influenced horizons and the $Fe_{poorly\ crystalline}$/ $Fe_{crystalline}$ ratios did not follow the typical gradient of higher ratios in the upper horizons (Cornell and Schwertmann, 1996), we suggest that redox changes governed crystallinity of the Fe oxy(hydr)oxide pool in our study soils. There are different views about how redox processes affect the crystallinity of soil Fe oxy(hydr)oxides. Fiedler and Sommer (2004) assumed inhibition of Fe oxy(hydr) oxide crystallization under reducing conditions, while recently Thompson et al. (2006) found evidence for increasing crystallization because of redox oscillations. We observed the highest $Fe_{poorly\ crystalline}/Fe_{crystalline}$ ratios in horizons in which the changes in redox conditions were most frequent, mainly in horizons above water-saturated or impermeable horizons (i.e., II Bgt1 in the Skeleti-Stagnic Luvisol, Bg1 in the Stagnic Cambisol, Bl2 in the Calcari-Humic Gleysol, and Bl1 in the Dystric Gleysol, Fig. C-5). In contrast, the permanently water-saturated or impermeable horizons showed decreased $Fe_{poorly\ crystalline}/Fe_{crystalline}$ ratios in three of the four soils, probably linked to prolonged reducing conditions. The vertical distribution of the $Fe_{poorly\ crystalline}/Fe_{crystalline}$ ratios paralleled that of the $\delta^{65}Cu$ values (Fig. C-5). Exceptions, however, were the deeper horizons of the Skeleti-Stagnic Luvisol where the gradient of the $Fe_{poorly\ crystalline}/Fe_{crystalline}$ ratio showed contrasting behavior. The mostly similar gradients for Fe crystallinity and $\delta^{65}Cu$ values suggest that these parameters are controlled by similar processes (e.g., redox processes) or that Fe oxy(hydr)oxides affect the Cu isotope ratio, for example by adsorption. Because these findings were not consistent, however, they need to be confirmed by further studies.

6 Conclusions

1. The Cu isotope ratios in the four studied soils ranged around 0‰ relative to NIST 976 and showed detectable variations of up to 0.6‰, which cannot be explained as a mixture of the isotope composition of the parent materials and thus demonstrate biogeochemical Cu fractionation in bulk soils. These variations had a similar size as observed for Fe or Zn isotopes in the literature.

2. Organic horizons tended to have lighter δ^{65}Cu values than mineral soils because either the Cu in the soil solution that is taken up by plants is isotopically lighter than in the bulk soil or because of plant-induced fractionation during uptake and translocation within the plant. Copper deposition from the atmosphere might also influence the Cu isotope signature, although none of our study sites showed indications of strong Cu contamination by deposition from the atmosphere.

3. There were first hints at a relationship between redox conditions and Cu isotope ratios; however, further efforts are necessary before Cu stable isotope ratios can potentially be used as a predictor of long-term redox conditions. Our pilot study of stable Cu isotopes in soils demonstrates that Cu isotope fractionation occurs in the soil–plant–water system. Our findings indicate that Cu isotopes may provide a new proxy for elucidating biogeochemical processes and may initiate further investigation of Cu isotope variations in soils. Stable Cu isotopes are promising for studying the cycling of Cu between soils and plants, assessing the fate of Cu in polluted soil, and further improving our knowledge about Cu behavior during long-term pedogenic processes.

Especially helpful might be the development of an adequate sequential extraction procedure that avoids artificial isotope fractionations, the study of nodules in hydromorphic horizons, and the analysis of soil solution to further elucidate the fate of Cu under changing redox conditions in field studies. Laboratory experiments focusing on Cu isotope fractionation during complexation by organic matter, adsorption on clay minerals, chemical reduction and reoxidation of soil samples, and plant-induced

fractionation could be helpful to interpret the observed Cu isotope variations in the soil and to reveal the potential of Cu isotope ratios as a new biogeochemical tracer.

7 Acknowledgments

Prescribed by the regulations of the internet publisher (ArchiMed) this section had to be deleted for data protection reasons. I want to thank all people listed in the printetd version.

8 References

Albarede, F. 2004. The stable isotope geochemistry of copper and zinc. Rev. Mineral. Geochem. 54, 409–427.

Alcacio, T.E., Hesterberg D., Chou J.W., Martin J.D., Beauchemin S., and Sayers D.E., 2001. Molecular scale characteristics of Cu(II) bonding in goethite–humate complexes. Geochim. Cosmochim. Acta 65, 1355–1366.

Alloway, B.J., 1995. Heavy metals in soils. 2nd ed. Chapman and Hall, London.

Archer, C., and Vance D., 2004. Mass discrimination correction in multiplecollector plasma source mass spectrometry: an example using Cu and Zn isotopes. J. Anal. At. Spectrom. 19, 656–665.

Artiola, J.F. 2005. Speciation of copper in the environment. In: Cornelis, R. (Ed.) Handbook of elemental speciation II: species in the environment, food, medicine and occupational health. John Wiley & Sons, Chichester, UK.

Asael, D., Matthews A., Bar-Matthews M., and Halicz L., 2007. Copper isotope fractionation in sedimentary copper mineralization (Tinma Valley, Israel). Chem. Geol. 243,238–254.

Asael, D., Matthews A., Bar-Matthews M., Halicz L., Ehrlich S., and Teplyakov, N., 2005. Redox fractionation of copper isotopes in sedimentary conditions. Geochim. Cosmochim. Acta 69:A216.

Bacon, J.R., and Davidson, C.M., 2008. Is there a future for sequential chemical extraction? Analyst 133,25–46.

Balistrieri, L.S., Borrok D.M., Wanty R.B., and Ridley W.I., 2008. Fractionation of Cu and Zn isotopes during adsorption onto amorphous Fe(III) oxyhydroxide: experimental mixing

of acid rock drainage and ambient river water. Geochim. Cosmochim. Acta 72,311–328.

Bermin, J., Vance, D., Archer, C., and Statham, P.J., 2006. The determination of the isotopic composition of Cu and Zn in seawater. Chem. Geol. 226,280–297.

Billon, G., Ouddane B., Laureyns J., and Boughriet A., 2001. Chemistry of metal sulfides in anoxic sediments. Phys. Chem. Chem. Phys. 3,3586–3592.

Borrok, D.M., Ridley, W.I., and Wanty, R.B., 2008. Isotopic fractionation of Cu and Zn during adsorption onto bacterial surfaces. Geochim. Cosmochim. Acta 72,A99.

Clayton, R.E., Hudson-Edwards K.A., and Houghton, S.L., 2005. Isotopic effects during Cu sorption onto goethite. Geochim. Cosmochim. Acta 69,A216.

Contin, M., Mondini, C., Leita, L. and De Nobili, M., 2007. Enhanced soil toxic metal fixation in iron (hydr)oxides by redox cycles. Geoderma 140,164–175.

Cornell, R.M., and Schwertmann, U., 1996. The iron oxides: structure, properties, reactions, occurrence, and uses. VCH Verlag, Weinheim, Germany.

Delaune, R.D., and Smith, C.J., 1985. Release of nutrients and metals following oxidation of fresh-water and saline sediment. J. Environ. Qual. 14,164–168.

Dideriksen, K., Baker, J.A., and Stipp, S.L.S., 2008. Equilibrium Fe isotope fractionation between inorganic aqueous Fe(III) and the siderophore complex, Fe(III)–desferrioxamine B. Earth Planet. Sci. Lett. 269,280–290. Douthitt, C.B. 2008. The evolution and applications of multicollector ICPMS (MC-ICPMS). Anal. Bioanal. Chem. 390, 437–440.

Dowding, C.E., and Fey M.V., 2007. Morphological, chemical and mineralogical properties of some manganese-rich Oxisols derived from dolomite in Mpumalanga Province, South Africa. Geoderma 141,23–33.

Dube, A., Zbytniewski, R., Kowalkowski, T., Cukrowska, E., and Buszewski, B., 2001. Adsorption and migration of heavy metals in soil. Pol. J. Environ. Stud. 10,1–10.

Du Laing, G., Vanthuyne, D.R.J., Vandecasteele, B., Tack, F.M.G., and Verloo, M.G., 2007. Influence of hydrological regime on pore water metal concentrations in a contaminated sediment-derived soil. Environ. Pollut. 147,615–625.

Ehrlich, S., Butler, I., Halicz, L., Rickard, D., Oldroyd, A., and Matthews, A., 2004. Experimental study of the copper isotope fractionation between aqueous Cu(II) and covellite, CuS. Chem. Geol. 209,259–269.

Emmanuel, S., Erel, Y., Matthews, A., and Teutsch, N., 2005. A preliminary mixing model for Fe isotopes in soils. Chem. Geol. 222, 23–34.

Epstein, L., and Bassein, S., 2001. Pesticide applications of copper on perennial crops in California, 1993 to 1998. J. Environ. Qual. 30,1844–1847.

Fantle, M.S., and DePaolo, D.J., 2004. Iron isotopic fractionation during continental weathering. Earth Planet. Sci. Lett. 228, 547–562.

FAO. 2006. Guidelines for soil description. 4th ed. FAO, Rome.

Fiedler, S., and Sommer, M., 2004. Water and redox conditions in wetland soils: their influence on pedogenic oxides and morphology. Soil Sci. Soc. Am. J. 68, 326–335.

Filipinski, M., and Grupe, M., 1990. Distribution of lithogenic, pedogenic and anthropogenic heavy metals in soils. Z. Pflanzenernaehr. Bodenkd. 153, 69–73.

Fry, B. 2006. Stable isotope ecology. Springer, New York.

Gale, N.H., Woodhead, A.P., Stos-Gale, Z.A., Walder, A. and Bowen, I., 1999. Natural variations detected in the isotopic composition of copper: possible applications to archaeology and geochemistry. Int. J. Mass Spectrom. 184, 1–9.

Grybos, M., Davranche, M., Gruau, G. and Petitjean, P., 2007. Is trace metal release in wetland soils controlled by organic matter mobility or Fe oxyhydroxides reduction? J. Colloid Interface Sci. 314, 490–501.

Guelke, M., and von Blanckenburg, F., 2007. Fractionation of stable iron isotopes in higher plants. Environ. Sci. Technol. 41, 1896–1901.

IUSS Working Group. 2006. World reference base for soil resources. World Soil Resour. Rep. 103. FAO, Rome.

Jouvin, D., Louvat, P., Juillot, F., Marechal, C., and Benedetti, M., 2009. Zn isotopic fractionation: why organic matters. Geochim. Cosmochim. Acta 73, A606.

Jouvin, D., Louvat, P., Marechal, C. and Benedetti, M.F., 2008. Fractionation of copper isotopes in plants. Geochim. Cosmochim. Acta 72,A441.

L'Herroux, L., LeRoux, S., Appriou, P. and Martinez, J., 1997. Behaviour of metals following intensive pig slurry applications to a natural field treatment process in Brittany (France). Environ. Pollut. 97, 119–130.

Li, J., Zhu, X.K. and Tang, S.H., 2008. Experimental study on Cu isotope fractionation during crystallization and reduction at low temperatures. Geochim. Cosmochim. Acta 72, A540.

Li, W.Q., Jackson, S.E., Pearson, N.J., Alard, O. and Chappell, B.W., 2009. The Cu isotopic signature of granites from the Lachlan Fold Belt, SE Australia. Chem. Geol. 258, 38–49.

Lobe, I., Wilcke, W., Kobza, J. and Zech, W., 1998. Heavy metal contamination of soils in northern Slovakia. Z. Pflanzenernaehr. Bodenkd. 161, 541–546.

Lovley, D.R., and Phillips, E.J.P., 1987. Competitive mechanisms for inhibition of sulfate reduction and methane production in the zone of ferric iron reduction in sediments. Appl. Environ. Microbiol. 53, 2636–2641.

Ma, Y.B., Lombi, E., Nolan, A.L. and McLaughlin, M.J., 2006. Determination of labile Cu in soils and isotopic exchangeability of colloidal Cu complexes. Eur. J. Soil Sci. 57,147–153.

Maher, K.C., and Larson, P.B., 2007. Variation in copper isotope ratios and controls on fractionation in hypogene skarn mineralization at Coroccohuayco and Tintaya, Peru. Econ. Geol. 102, 225–237.

Manceau, A., Nagy, K.L., Marcus, M.A., Lanson, M., Geoffroy, N., Jacquet, T. and Kirpichtchikova, T., 2008. Formation of metallic copper nanoparticles at the soil–root interface. Environ. Sci. Technol. 42, 1766–1772.

Marechal, C., and Albarede, F., 2002. Ion-exchange fractionation of copper and zinc isotopes. Geochim. Cosmochim. Acta 66,1499–1509.

Marechal, C.N., and Sheppard, S.M.F., 2002. Isotopic fractionation of Cu and Zn between chloride and nitrate solutions and malachite or smithsonite at 30 degrees and 50 degrees C. Geochim. Cosmochim. Acta 66, A484.

Marechal, C.N., Telouk, P and Albarede, F., 1999. Precise analysis of copper and zinc isotopic compositions by plasma-source mass spectrometry. Chem. Geol. 156, 251–273.

Markl, G., Lahaye, Y. and Schwinn, G., 2006. Copper isotopes as monitors of redox processes in hydrothermal mineralization. Geochim. Cosmochim. Acta 70,4215–4228.

Mathur, R., Ruiz, J., Titley, S., Liermann, L., Buss, H. and Brantley, S., 2005. Cu isotopic fractionation in the supergene environment with and without bacteria. Geochim. Cosmochim. Acta 69,5233–5246.

Matielli, N., Rimetz, J., Petit, J., Perdrix, E., Deboudt, K., Flament, P. and Weis, D., 2006. Zn–Cu isotopic study and speciation of airborne metal particles within a 5-km zone of a lead/zinc smelter. Geochim. Cosmochim. Acta 70, A401.

Matocha, C.J., Karathanasis, A.D., Rakshit, S. and Wagner, K.M., 2005. Reduction of copper(II) by iron(II). J. Environ. Qual. 34,1539–1546.

Miao, S.Y., DeLaune, R.D. and Jugsujinda, A., 2006. Influence of sediment redox conditions on release/solubility of metals and nutrients in a Louisiana Mississippi River deltaic plain freshwater lake. Sci. Total Environ. 371, 334–343.

Mikutta, C., Wiederhold, J.G., Cirpka, O.A., Hofstetter, T.B., Bourdon, B., and von Gunten, U., 2009. Iron isotope fractionation and atom exchange during sorption of ferrous iron to mineral surfaces. Geochim. Cosmochim. Acta 73, 1795–1812.

Moffett, J.W., and Zika, R.G., 1983. Oxidation kinetics of Cu(I) in seawater: implications for its existence in the marine environment. Mar. Chem. 13, 239–251.

Moynier, F., Pichat, S., Pons, M.-L., Finke, D., Balter, V. and Albarede, F., 2009. Isotopic fractionation and transport mechanisms of Zn in plants. Chem. Geol. 267, 125–130.

Osterberg, R., Wei, S.Q., and Shirshova, L., 1999. Inert copper ion complexes formed by humic acids. Acta Chem. Scand. 53,172–180.

Othman, D.B., Luck, J.M. and Albarede, F., 2004. Cu–Zn isotope fractionation in recent mantle (MORB, OIB, peridotites, lherzolites), and comparison with the early Archean. Geochim. Cosmochim. Acta 68,A750.

Othman, D.B., Luck, J.M., Tchalikian, A. and Albarede, F., 2003. Cu–Zn isotope systematics in terrestrial basalts. Abstr. 9669. In Geophys. Res. Abstracts 5, EGS-AGU-EUG Joint Assembly, Nice, France. 6–11 Apr. 2003. Eur. Geophys. Union, Strasbourg, France.

Pelfrene, A., Gassama, N. and Grimaud, D., 2008. Dissolved Cu(II) speciation in unpolluted soil solutions of a planosolic horizon. Electroanalysis 20,841–850.

Petit, J.C.J., de Jong, J., Chou, L. and Mattielli, N., 2008. Development of Cu and Zn isotope MC-ICP-MS measurements: application to suspended particulate matter and sediments from the Scheldt estuary. Geostandard. Geoanal. Res. 32, 149–166.

Pokrovsky, O.S., Viers, J., Emnova, E.E., Kompantseva, E.I., and Freydier, R., 2008. Copper isotope fractionation during its interaction with soil and aquatic microorganisms and metal oxy(hydr)oxides: possible structural control. Geochim. Cosmochim. Acta 72, 1742–1757.

Schlichting, E., Blume, H.P. and Stahr, K., 1995. Practical course in soil science. (In German.) 2nd ed. Enke, Stuttgart, Germany.

Senesi, N., Sposito, G., and Martin, J.P., 1986. Copper(II) and iron(III) complexation by soil humic acids: an Ir and electron-spin-resonance study. Sci. Total Environ. 55, 351–362.

Shields, W.R., Goldich, S.S., Garner, E.L. and Murphy, T.J., 1965. Natural variations in abundance ratio and atomic weight of copper. J. Geophys. Res. 70, 479–491.

Simpson, S.L., Rosner, J. and Ellis, J., 2000. Competitive displacement reactions of cadmium, copper, and zinc added to a polluted, sulfidic estuarine sediment. Environ. Toxicol. Chem. 19, 1992–1999.

Soil Survey Staff. 2006. Keys to Soil Taxonomy. 10th ed. NRCS, Washington, DC.

Stuckrad, S., Sabel, K.-J. and Wilcke, W., 2008. Periglacial transport distance of Pb derived from small-scale ore veins in the Rhenish Slate Mountains. Geoderma 148, 232–239.

Thompson, A., Chadwick, O.A., Rancourt, D.G. and Chorover, J., 2006. Iron oxide crystallinity increases during soil redox oscillations. Geochim. Cosmochim. Acta 70, 1710–1727.

Thompson, A., Ruiz, J., Chadwick, O.A., Titus, M. and Chorover, J., 2007. Rayleigh fractionation of iron isotopes during pedogenesis along a climate sequence of Hawaiian basalt. Chem. Geol. 238, 72–83.

Timofeeva, Y.O., and Golov, V.I., 2007. Sorption of heavy metals by iron-manganic nodules in soils of Primorskii region. Eurasian Soil Sci. 40,1308–1315.

Tiunov, A.V. 2007. Stable isotopes of carbon and nitrogen in soil ecological studies. Biol. Bull. 34, 395–407.

Vance, D., Archer, C., Bermin, J., Perkins, J., Statham, P.J., Lohan, M.C., Ellwood, M.J. and Mills, R.A., 2008. The copper isotope geochemistry of rivers and the oceans. Earth Planet. Sci. Lett. 274, 204–213.

Vepraskas, M.J. 1992. Redoximorphic features for identifying aquatic conditions. North Carolina Agric. Res. Serv., Raleigh, USA.

Viers, J., Oliva, P., Nonell, A., Gelabert, A., Sonke, J.E., Freydier, R., Gainville, R. and Dupre, B., 2007. Evidence of Zn isotopic fractionation in a soil–plant system of a pristine tropical watershed (Nsimi, Cameroon). Chem. Geol. 239, 124–137.

Walder, A.J., and Freedman, P.A., 1992. Isotopic ratio measurement using a double focusing magnetic-sector mass analyzer with an inductively coupled plasma as an ion source. J. Anal. At. Spectrom. 7, 571–575.

Weber, F.-A., Voegelin, A., Kaegi, R. and Kretzschmar, R., 2009. Contaminant mobilization by metallic copper and metal sulphide colloids in flooded soils. Nature Geosci. 2, 267–271.

Weiss, D.J., Mason, T.F.D., Zhao, F.J., Kirk, G.J.D., Coles, B.J. and Horstwood, M.S.A., 2005. Isotopic discrimination of zinc in higher plants. New Phytol. 165, 703–710.

Weyer, S., and Schwieters, J., 2003. High precision Fe isotope measurements with high mass resolution MC-ICPMS. Int. J. Mass Spectrom. 226, 355–368.

Wiederhold, J.G., Kraemer, S.M., Teutsch, N., Borer, P.M., Halliday, A.N. and Kretzschmar, R., 2006. Iron isotope fractionation during proton-promoted, ligand-controlled, and reductive dissolution of goethite. Environ. Sci. Technol. 40, 3787–3793.

Wiederhold, J.G., Teutsch, N, Kraemer, S.M., Halliday, A.N. and Kretzschmar, R., 2007a. Iron isotope fractionation during pedogenesis in redoximorphic soils. Soil Sci. Soc. Am. J. 71, 1840–1850.

Wiederhold, J.G., Teutsch, N., Kraemer, S.M., Halliday, A.N. and Kretzschmar, R., 2007b. Iron isotope fractionation in oxic soils by mineral weathering and podzolization. Geochim. Cosmochim. Acta 71, 5821–5833.

Wilcke, W., and Dohler, H., 1995. Heavy metals in agriculture. (In German.) KTBL-Arbeitspap. 217. Kuratorium fur Technik und Bauwesen in der Landwirtschaft, Darmstadt, Germany.

Wilcke, W., Guschker, C., Kobza, J. and Zech, W., 1999. Heavy metal concentrations, partitioning, and storage in Slovak forest and arable soils along a deposition gradient. J. Plant Nutr. Soil Sci. 162, 223–229.

Wilcke, W., Krauss, M, and Kobza, J., 2005. Concentrations and forms of heavy metals in Slovak soils. J. Plant Nutr. Soil Sci. 168, 676–686.

Yu, K.C., Tsai, L.J., Chen, S.H.and Ho, S.T., 2001. Chemical binding of heavy metals in anoxic river sediments. Water Res. 35, 4086–4094.

Zeien, H., and Brummer, G.W., 1989. Chemical extraction to determine the chemical forms of heavy metals in soils. (In German.) Mitteilu. Dtsch. Bodenkundl. Gesellsch. 59, 505–510.

Zhu, X.K., Guo, Y., Williams, R.J.P., O'Nions, R.K., Matthews, A., Belshaw, N.S., Canters, G.W., de Waal, E.C., Weser, U., Burgess, B.K. and Salvato, B., 2002. Mass fractionation processes of transition metal isotopes. Earth Planet. Sci. Lett. 200, 47–62.

D Stable Cu isotope fractionation in soils during oxic weathering and podzolation

Moritz Bigalke[1,3], Stefan Weyer[2+], Wolfgang Wilcke[3]

[1]Johannes Gutenberg University Mainz, Earth System Science Research Center, Geographic Institute, Professorship of Soil Science/Soil Geography, Johann-Joachim-Becher-Weg 21, 55128 Mainz, Germany.

[2]University of Frankfurt, Institute of Geoscience, Altenhöferallee 1, 60438 Frankfurt am Main, Germany.

[3]Geographic Institute, University of Berne, Hallerstrasse 12, 3012 Berne, Switzerland.

[+]Current address: Institute of Geology and Mineralogy, University of Cologne, Zülpicher Str. 49b, 50674 Köln

Submitted to Geochimica et Cosmochimica Acta

1 Abstract

Copper stable isotope ratios show fractionation at various biogeochemical processes and may trace the fate of Cu during long-term pedogenetic processes. We assessed the effects of oxic weathering (formation of Cambisols) and podzolization on Cu isotope ratios (δ^{65}Cu). Two Cambisols (oxic weathered soils without strong vertical translocations of soil constituents) and two Podzols (soils showing vertical translocation of organic matter, Fe and Al) were analyzed for Cu concentrations, partitioning of Cu in seven fractions of a sequential extraction and δ^{65}Cu values in bulk soil. Cu concentrations in the studied soils were low (1.4-27.6 µg g^{-1}) and mainly associated with strongly bound Fe oxide- and silicate-associated forms. Bulk δ^{65}Cu values varied between -0.57 and 0.44 ‰ in all studied horizons. The O horizons had on average significantly lighter Cu isotope ratios (-0.21‰) than the A horizons (0.13‰) which can either be explained by Cu isotope fractionation during cycling through the plants or deposition of isotopically lighter Cu from the atmosphere. Oxic weathering without pronounced podzolization in both Cambisols and a weakly developed Podzol (Haplic Podzol 2) caused no significant fractionation in the single profiles, while a slight trend to lighter δ^{65}Cu with depth was visible in all four profiles. This is the opposite depth trend of δ^{65}Cu values to that we observed in hydromorphic soils (soils which show indication of redox changes because of the influence of water) in a previous study. In a more pronounced Podzol (Haplic Podzol 1), δ^{65}Cu values and Cu concentrations decreased from Ah to E horizons and increased again deeper in the soil. Humus-rich sections of the Bhs horizon had higher Cu concentrations (2.8 µg g^{-1}) and a heavier δ^{65}Cu value (-0.18‰) than oxide-rich sections (1.9 µg g^{-1}, -0.35‰) suggesting Cu translocation between E and B horizons as organo-Cu complexes. The different depth distributions in oxic weathered and hydromorphic soils and the pronounced vertical differences in δ^{65}Cu values in Haplic Podzol 1 indicate a promising potential of δ^{65}Cu values to improve our knowledge oft the fate of Cu during long-term pedogenetic processes.

2 Introduction

Copper in soil deserves scientific attention because it is an essential micronutrient but can also be a potentially toxic pollutant at high concentrations (Alloway, 1990). Copper occurs in unpolluted soils in concentrations of approx. 30 µg g^{-1} and varies in a range of 2-100 µg g^{-1} (Artiola, 2005). Copper may be present in soil as elemental Cu, Cu^{+} and Cu^{2+} but Cu^{2+} is the dominating form (Artiola, 2005; Weber et al., 2009). The Cu^{2+} ion may adsorb on negatively charged surfaces of clay minerals and organic matter (OM), be incorporated in the crystal structure of clay minerals, or may be bound at the surface or on inner binding sites of oxy(hydr)oxides, while a part remains in mostly silicatic unweathered minerals derived from the bedrock (Ildefonse et al. 1986; Alcacio et al., 2001; Artiola, 2005; Contin et al., 2007). The speciation of dissolved Cu in soil solution depends on pH and availability of interacting substances. The dominating species are Cu^{2+} ions, hydroxo-, carbonato- and sulphato-complexes and in the presence of organic acids chelates of Cu (i.e. polydentate organo-complexes, Artiola, 2005). Dissolved and colloidial species can be transported in the soil and cause a redistribution of Cu in the profile (Keller and Domergue, 1996). Elemental Cu and Cu^{+} mainly form under reducing conditions when oxygen supply in soil is suppressed, i.e. by waterlogging (Artiola, 2005; Grybos, 2007; Weber et al., 2009). During prolonged waterlogging, Cu_xS may form (Weber et al., 2009). Reduction of Cu^{2+}, however, can also occur in oxic environments by plants as previously described for contaminated soils (Manceau et al., 2008).

Cambisols are one of the most widespread soil types of the world. They form under oxic weathering conditions and cover approx. 1.5 billion hectares with a dominance in the temperate regions (IUSS Working Group WRB, 2006). These soils are comparatively young and developed in regions which were under influence of glaciations during the Pleistocene, or in mountain regions as a consequence of continuous erosion. Cambisols are characterized by the beginning of horizontal differentiation in the subsoil as indicated by changes in color or clay and carbonate concentrations (IUSS Working Group WRB, 2006). Podzols show zonal distribution in some boreal and temperate regions but also occur in the tropics on sandy parent

materials (IUSS Working Group WRB, 2006). Podzols are characterized by acid bleaching of an upper subsurface horizon because of leaching of Fe oxy(hydr)oxides and OM. This bleached horizon overlies a dark accumulation horizon characterized by the input of the leached humus and Fe compounds followed by a reddish horizon in which mainly oxides of Al, Fe, and Mn (the sesquioxides) accumulated (IUSS Working Group WRB, 2006). Also Cu and other trace metals are translocated to a smaller extent from the leached horizon to the accumulation horizon during podzolization (Schwertmann et al., 1982; Wilcke et al., 1996; Jersak et al., 1997; Nikonov et al., 1997; Kotowski, 1998).

The natural abundance of Cu isotope ratios may be a new tool to increase our knowledge about Cu cycling in soil. Copper isotopes in hydromorphic soils (soils which show indication of alternating reduction and oxidation processes because of the influence of water) show variations in δ^{65}Cu values of up to 0.6‰ and cluster around 0‰ (Bigalke et al., 2010a). Common rocks like basalts (-0.02 to -0.21‰; Archer and Vance, 2004; Li et al., 2009) and loess (-0.1 to -0.01‰; Li et al., 2009; Bigalke et al., 2010a) cluster around 0‰. While most granites also generally cluster close to 0‰ in a relatively narrow range between –0.4 and +0.4‰, a larger total variability was found (-0.46 to 1.51‰, Li et al., 2009) and is assumed to be caused by secondary processes. Thus, these parent materials for soil formation seem to show limited variations in Cu isotope ratios. In contrast, large variations in δ^{65}Cu values are found for ores and minerals ranging between -3.44 and 7.74‰ (Asael et al., 2007; Gale et al., 1999; Marechal et al., 1999). However, the number of analyses of common parent materials for soil development is still limited and the above mentioned ranges of δ^{65}Cu values may therefore not be representative for the entire range in nature.

The effects of some biogeochemical processes on Cu isotope ratios have been investigated in laboratory experiments. Adsorption of Cu on Fe and Al oxy(hydr)oxides causes fractionation of $\Delta^{65}Cu_{(oxy(hydr)oxide\text{-}solution)}$ from 0.34 to 1.26‰ (Balistrieri et al., 2008; Clayton et al., 2005; Pokrovsky et al., 2008). A study of Cu isotope fractionation during complexation with insolubilized humic acid revealed preferential complexation of heavy Cu ($\Delta^{65}Cu_{IHA\text{-}solution}$ 0.26 ± 0.11 ‰; Bigalke et al., 2010b). Binding on bacteria surfaces can cause different fractionations of $\Delta^{65}Cu_{(bacteria\text{-}solution)}$ ranging between -1.8 and 0.6‰ depending on pH, bacterium species, and environmental conditions (Borrok

et al., 2008; Pokrovsky et al., 2008). Mathur et al. (2005) even found $\delta^{65}Cu$ enriched by up to 3‰ in metal precipitates on bacteria surfaces compared to the aqueous medium. The most pronounced isotope fractionation was observed during reduction of Cu^{2+} to Cu^{+} ($\Delta^{65}Cu_{(CuI-CuII)}$ = -4.1 to -2.8‰; Ehrlich et al., 2004; Zhu et al., 2002) or oxidation of reduced Cu^{+} minerals to Cu^{2+} ($\Delta^{65}Cu_{(CuII-CuI)}$ = 0.94 to 3‰; Asael et al., 2005; Mathur et al., 2005). But also plants fractionate Cu isotopes during internal translocation ($\Delta^{65}Cu_{(root-shoot)}$ = 0.41‰, Jouvin et al., 2008) and uptake from the soil (Zhu et al., 2010), which may influence the Cu isotope composition of organic surface horizons of soils.

While in a previous study we assessed the influence of redox variations because of waterlogging in hydromorphic soils and assumed that waterlogging shifts $\delta^{65}Cu$ values towards heavier Cu isotope compositions (Bigalke et al., 2010a), nothing is known of Cu isotope fractionation in well aerated soils like the widespread Cambisols and Podzols. The only other transition metals for which natural abundance stable isotope ratios in oxic soils were studied up to now are Fe and Zn. Wiederhold et al. (2007) investigated one Cambisol and two Podzols for Fe isotope fractionation in total digests and using a sequential extraction procedure. The $\delta^{57}Fe$ values in total digests varied by approx. 1.15‰ with the lightest isotope ratios in the Bh horizons. The sequential extraction procedure was used to determine the Fe isotope composition of different soil Fe pools finding variations of up to >3‰ ($\delta^{57}Fe$) among different fractions (Wiederhold et al., 2007). Other authors reported $\delta^{56}Fe$ variations between 0.3‰ and 0.9‰ among the various horizons of different soils (Fantle and DePaolo, 2004; Emmanuel et al., 2005; Thompson et al., 2007). The maximum variation in stable Zn isotope ratios ($\delta^{66}Zn$) in deeply weathered tropical soils was ca. 0.7‰ (Viers et al., 2007).

The objectives of our study are (I) to investigate the influence of vegetation and atmospheric input on the $\delta^{65}Cu$ values of organic horizons, (II) to gain insights into $\delta^{65}Cu$ behavior during oxic weathering of soils, (III) to improve the understanding of the fate of Cu during podzolization and (IV) to compare Cu isotope variations in oxic weathered soils to those in hydromorphic soils taken from the literature (Bigalke et al., 2010a). We hypothesize that the natural abundance of stable Cu isotopes can be used to draw conclusions on long-term biogeochemical processes during soil genesis.

As the interpretation of δ^{65}Cu values in soils also require knowledge of general soil properties and of Cu forms in soil, we combined our Cu isotope analyses with the determination of selected soil properties related to the fate of Cu and partitioned soil Cu into seven operationally defined fractions with a sequential extraction procedure. Because an artificial fractionation of isotope ratios by the sequential extraction is likely, only concentrations and no isotope ratios were determined in the extracts.

3 Materials and methods

3.1 Study soils

Four soil profiles were sampled according to their pedomorphic horizons. The soils are a Skeletic Cambisol (Cambisol with ≥40 vol.% gravel up to a depth of 1m) and a Dystric Cambisol (Cambisol with a base saturation, i.e. a coverage of the effective cation-exchange capacity by the charge equivalents of Na, K, Mg, and Ca, <50 % between 0.2 and1.0 m depth) and two of the soils are Haplic Podzols (Podzol with no other specific characteristics; IUSS Working Group WRB, 2006). The Skeletic Cambisol and the Haplic Podzol 1 were sampled in Germany, while the Dystric Cambisol and the Haplic Podzol 2 were sampled in Slovakia (Table D-1). All four soils are located in the Variscan mountain area in slope positions and developed from periglacial cover beds consisting of up to three solifluctional layers (produced by slow soil movement downslope during the periglacial period). The soil morphology was described according to FAO (2006).

The Skeletic Cambisol is located in Idstein near Wiesbaden. The organic layer has a depth of 3 cm and consists of one horizon only. The mineral soil consists of three horizons with high gravel content. While the two upper mineral horizons (Ah and Bw) developed from a solifluctional layer in which bedrock (slate) is mixed with loess and Laacher See tephra, the lowest horizon (IICR) developed from bedrock alone. The Dystric Cambisol is located approx. 3 km south of Namestovo. The organic layer has a depth of 7 cm and consists of three horizons. The mineral soil has four horizons. Haplic Podzol 1 is located near Affolterbach, ca. 35 km northeast of Mannheim. The organic layer has a depth of 10 cm and consists of two horizons. The mineral soil consists of six horizons which show the typical Podzol characteristics of a strongly bleached E horizon

above a well developed Bhs horizon. The IIBhs horizon has a strong brown color and patchy accumulations of humic substances. Besides the bulk IIBhs horizon, spots with dark black color and spots with strong red color were sampled. It was assumed that spots with dark color represent accumulations of humic matter, while spots with strong red color are enriched in Fe oxy(hydr)oxides, which was confirmed by the measured C and Fe concentrations (Tab. D-2). The spots are further on referred to as IIBhs humic and IIBhs oxidic, respectively. The soil developed from three solifluctional layers (I-III). While the main component of all three layers is weathered bedrock (sandstone) different amounts of loess might be mixed in the two upper layers (I, II). The uppermost soil layer (I) shows depletion of fine particles (clay; Table D-2). The Haplic Podzol 2 is located in the Rohácska valley in the Zapadné Tatry. The organic layer has a depth of 7.5 cm and consists of three horizons. The mineral soil has three horizons, revealing the consequences of leaching in the AEh and accumulation in the Bhs horizons (Tab. D-2). Macroscopic observations imply that podzolization was less advanced in the Haplic Podzol 2 than in the Haplic Podzol 1. The Haplic Podzol 2 and the Dystric Cambisol were already described in Lobe et al. (1998) and the Haplic Podzol 1 was part of an excursion of the German Soil Science Society meeting 2005. Tables D-1 and D-2 summarize site and soil properties.

Table D-1. Soil type, location, altitude, slope, parent rock, climate, and vegetation of the study sites

Soil type	Location	Altitude	Slope	Bedrock	Age	Rainfall	Temper-ature	Vegetation
FAO		m above sea level				mm yr^{-1}	January / July [°C]	
Skeletic Cambisol	Germany 50°13´N 8°16´E	400	12°	slate	early Devonian	700-800	0/18	beech
Dystric Cambisol	Slovakia 49°23´ N 19°29´ E	1100	13°	sandstone	Eocene Flysch	1000-1200	-7/16	spruce, blueberry, and fern
Haplic Podzol 1	Germany 49°35´ N 8°50´ E	424	10°	sandstone	early Triassic	1000-1300	0/18	pine
Haplic Podzol 2	Slovakia 49°13´ N 19°45´ E	1400	23°	granodiorite	age unknown	1200-1400	-10/8	spruce, blueberry, and fern

3.2 Sampling and sample preparation

The soil profiles were macroscopically characterized in the field and each horizon was sampled in a representative way. The samples were air-dried and sieved to <2 mm (fine earth). The fraction >2mm is gravel. For Cu isotope analyses and to determine total Cu and Fe (Fe_{tot}) concentrations, samples were ground in a planetary mill with agate sample beakers. The texture was determined with the "pipet method" after destruction of organic matter with H_2O_2, dispersion with $Na_6P_6O_{18} \cdot 6H_2O$ (Schlichting et al., 1995). This method separates clay (<0.002 mm) and silt (0.002-0.063 mm) by their sedimentation time in water, while the sand (0.063 - 2 mm) fraction is determined by wet sieving (Table D-2). Mass fractions of the various texture classes were determined gravimetrically by weighing the whole fraction (sand) or aliquots extracted with a pipet after different sedimentation times in Atterberg cylinder (silt, clay). The pH was measured in 0.1 mol l^{-1} $CaCl_2$ at a soil:solution ratio of 1:2.5 after equilibration for two hours with a glass electrode. Total C and N concentrations were determined by dry combustion with a CHNS analyzer (Vario EL, Elementar Analysensysteme, Hanau, Germany). The effective cation-exchange capacity (ECEC) was determined as the sum of the charge equivalents of Ca, K, Mg, Na, Mn, Al and H extracted with 1 M

NH_4NO_3. Base saturation (BS) was calculated as the sum of the charge equivalents of Ca, Mg, Na and K divided by ECEC and expressed in percent.

Copper was sequentially extracted with the method of Zeien and Brümmer (1989) to assess operationally defined Cu fractions in soil. Briefly, for the sequential extraction 2 g of air-dried soil were extracted with 50 ml of each:1 M NH_4NO_3, 24 h (fraction 1, readily soluble and exchangeable), 1 M NH_4O-acetate, pH 6.0, 24 h (fraction 2, specifically absorbed and other weakly bound species), 0.1 M $NH_2OH \cdot HCl$ + 1 M NH_4O-acetate, pH 6.0, 0.5 h (fraction 3, bound to Mn oxides), 0.025 M NH_4EDTA, pH 4.6, 1.5 h (fraction 4, bound to organic matter), 0.2 M NH_4-oxalate, pH 3.25, 4 h in the dark (fraction 5, bound to poorly crystalline Fe oxides), 0.1 M ascorbic acid in 0.2 M NH_4-oxalate, pH 3.25, 0.5 h in the hot water bath (fraction 6 bound to crystalline Fe oxides) and 67% HNO_3 + 50% HF (3:1) (fraction 7, residual). Fractions 1-5 were extracted at room temperature, fraction 6 was extracted at 96°C, and fraction 7 was digested at 200°C under pressure in a microwave oven. All fractions except fraction 7 were centrifuged at 2500 rpm for 15 minutes and filtered with blue ribbon filter paper (Whatman Schleicher and Schuell, Kent, England, 2µm retention) after extraction. After every extraction step except for fractions 1 and 7, the sample was rinsed once (fractions 2, 4, 5, and 6) or twice (fraction 3) with 25 ml of 1 M NH_4NO_3 (fraction 2), 1 M NH_4O-acetate (pH 6, fraction 3), 1 M NH_4O-acetate (pH 4.6, fraction 4) and 0.25 M NH_4-oxalate (pH 3.25, in the dark, fraction 5 and 6) for 10 minutes. Extracts and the rinses were combined. This method is an optimization of a number of previous methods (Zeien, 1995).

Total Cu and Fe concentrations were measured in total digests with concentrated HF: concentrated HNO_3 (1:3). Fe concentrations were also measured in the fractions 5 and 6 of the sequential extraction, which are thought to represent poorly-crystalline (fraction 5, similar to the traditional oxalate extract but without the easily extractable Fe pools) and crystalline oxy(hydr)oxides (fraction 6, similar to the traditional,dithionite extract but without the easily and oxalate-extractable Fe pools). Analogously to the conventionally used oxalate-extractable Fe/dithionite-extractable Fe (Fe_o/Fe_d) ratio (Cornell and Schwertmann 1996) as measure of the crystallinity of pedogenic Fe oxides we calculated the ratio of fraction 5/(fraction 5 + fraction 6) further referred to as $Fe_{f5/f5+f6}$ (Table D-2). Copper concentrations were determined by electrothermal atomic

absorption spectrometry (ETAAS, Unicam Solaar 989, Thermo Scientific, Waltham, USA) and the concentrations of Fe, Ca, K, Mg, Na, Mn, Al were measured by flame atomic absorption spectrometry (FAAS, AA 240 FS, Varian, Palo Alto, USA). The accuracy of the Cu concentration measurements was controlled by measuring total digests of the certified reference material (CRM) 7003 (Silty Clay Loam) of the Czech Meteorology Institute (Brno, Czech Republic) and BCR-2 reference material from the United States Geological Survey (USGS, Reston, USA). We determined values of 28.6 ± 2.9 µg g^{-1} Cu (two standard deviations, 2SD, n=2) for CRM 7003 (certified value, 29.1 ± 0.8 µg g^{-1} Cu) and 16.8 ± 1.7 µg g^{-1} Cu (2SD, n = 2) for BCR-2 (certified value, 19 ± 2 µg g^{-1} Cu). The accuracy of the sequential extraction procedure could not be controlled with a certified reference material because of the lack of such a material. Therefore we processed CRM 7003 three times. Precision of the sum of fractions was 13% (2RSD). If the sum of the concentrations of all seven fractions of a sample (Fig. D-2) deviated by >20 % from that of the total digestion (Table D-3), the results were discarded and the sample was processed once more.

The digestion and purification procedure for Cu isotope analysis is described in detail in Bigalke et al. (2010a). Briefly, the samples were ashed at 450°C overnight and thereafter totally digested in a microwave oven (MARS5Xpress, CEM, Matthews, USA) using HF and HNO_3. The extracts were purified according to a method modified from Marechal et al. (1999). Because of the low Cu to matrix ratio, one single purification run was not sufficient to achieve good matrix separation. The whole purification procedure was therefore repeated for each sample. Recovery was checked for every sample to rule out isotope fractionation on the resin (Marechal and Albarede, 2002). Recoveries were checked with ETAAS and samples which did not show a recovery of 100 ± 5% were discarded. All reagents used for the preparation of the isotope samples were double subboiled, of suprapur (Merck, Darmstadt, Germany), Rotipuran® supra (Carl Roth, Karlsruhe, Germany), or trace select (Fluka, Seelze, Germany) quality. Water was taken from a TKA GenPure UV (TKA, Niederelbert, Germany) water purification system and was of ≥ 8 MΩ cm quality. All critical steps were performed under clean air conditions in a clean bench, evaporations were realized in boxes supplied with hepa filtered air.

3.3 Calculations and statistical evaluation

Soil Cu storages were calculated for O horizons and the 0-50 cm layer of the mineral soil, which is assumed to be the main rooting zone. Pools were calculated by multiplying Cu concentrations of the single horizons with volume (depth of horizon times m^2), soil density and fraction of soil fine material (<2mm) and are expressed as kg ha^{-1}.

Data from this study were compared with data from Bigalke et al. (2010) to assess the potentially different Cu isotope fractionation during oxic and water-influenced weathering regime. To check for significant differences of mean δ^{65}Cu values among soil horizons t tests were performed with SPSS 15 (SPSS inc., Chicago, Illinois, USA). For the t test, differences between A and the subsurface horizons of every profile were calculated. The mean of the differences between A and subsurface horizons in the oxic weathered soils were tested against the mean of the differences between the A and the subsurface horizons in the hydromorphic soils and against 0. Differences between horizons and not δ^{65}Cu values of the horizons were used for calculation because inherited Cu isotope variations from the substrates the soils developed from could mask Cu isotope fractionation by biogeochemical processes. The Kolmogorov-Smirnov test was used to check for normal distribution of the datasets as a precondition for the t test. Significance was set at $P<0.05$.

Table D-2. Selected properties of the four study soils

Soil	Horizon	Depth	Sand	Silt	Clay	Gravel	ECEC	Base-saturation	C_{org}	N	pH	Fe_{f5}	Fe_{f5+f6}	$Fe_{f5/f5+f6}$	Fe_{tot}
		cm	--------- g kg^{-1}----------				mmol kg^{-1}	%	- g kg^{-1}-		$CaCl_2$	---g kg^{-1}---			g kg^{-1}
Skeletic Cambisol	Ah[a]	-3	76	167	78	679	136.8	68.5	123	4	4.1	1.5	16.0	0.09	20.5
	Bw[b]	-45	141	102	74	682	66.8	14.5	19	1	3.7	3.6	22.4	0.16	31.3
	II R[c]	>45	59	20	8	913	25.4	45.1	1	0	3.6	1.4	16.2	0.08	26.7
Dystric Cambisol	Ah[a]	-5	556	239	205	0	95.3	6.5	39	2	3.1	2.4	6.5	0.36	12.9
	Bw1[b]	-25	510	226	164	100	49.6	7.4	17	1	3.8	4.8	9.1	0.52	14.6
	Bw2[b]	-43	504	225	172	100	36.9	8.4	12	1	4.0	4.2	9.5	0.44	16.7
	C[d]	>43	229	106	65	600	35.6	7.7	11	1	4.0	3.9	9.4	0.41	15.9
Haplic Podzol 1	Ah[a]	-8	768	167	4	62	91.6	97.4	83	3	3.9	0.1	1.3	0.09	2.7
	AEh[ae]	-15	835	97	3	65	18.3	44.4	27	1	3.2	0.0	1.1	0.03	2.2
	E[e]	-50	831	93	2	74	3.9	25.8	3	0	3.7	0.0	1.2	0.01	2.0
	II Bhs[f]	-75	743	136	106	15	43.8	2.8	19	1	3.9	4.1	9.0	0.46	9.9
	II BCs[gd]	-90	687	94	64	155	5.8	1.0	4	0	4.2	0.3	1.9	0.18	2.7
	III CR[dc]	>100	625	88	122	165	4.5	2.3	2	0	4.5	0.2	2.1	0.10	3.0
	II Bhs[f] oxid	50-75	-	-	-	-	-	-	10	0	-	-	-	-	13.0
	II Bhs[f] humic	50-75	-	-	-	-	-	-	32	1	-	-	-	-	10.0
Haplic Podzol 2	AhE[ae]	-4	437	293	170	100	101.6	5.8	67	4	3.0	0.7	1.4	0.52	8.0
	Bhs[f]	-18	330	215	154	300	100.7	3.8	65	3	3.6	9.2	12.0	0.77	17.9
	Bs[g]	-38	419	189	92	300	56.2	5.9	42	19	3.9	15.8	18.8	0.84	26.1

(a) Ah, mineral surface horizon with accumulation of organic matter; (b) Bw, mineral subsurface horizon with development of color or structure; (c) R, bedrock; (d) C, horizon relatively unaffected by pedogenetic processes; (e) E, eluvial horizon, loss of silicate clay, iron and aluminum; (f) Bhs, mineral subsurface horizon with accumulation of sesquioxides and organic matter; (g) Bs, mineral subsurface horizon with accumulation of sesquioxides.

3.4 Copper isotope measurements

Copper isotope ratios were measured with a Finnigan-Neptune (ThermoFisher) multiple collector inductively-coupled plasma mass spectrometer (MC-ICP-MS) with high mass resolution capabilities (Weyer and Schwieters, 2003). All Cu isotope ratios were expressed as δ^{65}Cu values relative to NIST 976 reference material according to Equation D-1.

$$\delta^{65}Cu[‰] = \left(\frac{\left(^{65}Cu/^{63}Cu\right)_{sample}}{\left(^{65}Cu/^{63}Cu\right)_{NIST\,976}} - 1 \right) * 1000 \qquad \text{(D-1)}$$

The method is described in detail in Bigalke et al. (2010a). Briefly, a Ni standard (NIST 986) was used for instrumental mass bias correction (Ehrlich et al., 2004; Li et al., 2009; Markl et al., 2006). The correction was performed according to the certified ^{62}Ni/^{60}Ni ratio (0.138600) of a natural Ni standard (NIST 986) and by applying the exponential law. Additionally, standard sample bracketing was applied, by measuring NIST 976 after every third sample. The δ^{65}Cu values were calculated as the deviation of the isotope ratio of the mass bias-corrected samples from the isotope ratio of the mass bias-corrected bracketing standards (Li et al., 2009). The high mass resolution mode was necessary for some initial sample analyses where interfering Ti was not completely separated from Cu. Titanium in the sample may cause mass interferences such as ^{48}Ti^{14}N, ^{46}Ti^{16}O, ^{47}Ti^{16}O, and ^{49}Ti^{16}O on ^{62}Ni, ^{63}Cu and ^{65}Cu, respectively. These interferences shifted the measured isotope ratio to more negative values, because of the Ti interference on ^{62}Ni and the absence of such interference on mass ^{60}Ni, which cause an overcorrection of measured values and the two interferences of ^{47}Ti^{16}O and ^{49}Ti^{16}O on ^{63}Cu and ^{65}Cu. To test the influence of Ti on Cu isotope ratio measurements, mixtures of Cu (NIST 976), Ni (NIST 986) and Ti were measured with different Cu/Ti ratios and corrected δ^{65}Cu values are displayed in Table D-4. The Finnigan-Neptune high resolution mode, with a mass resolution power of ≈ 10,000 M/ΔM (Weyer and Schwieters, 2003), was sufficient to resolve these interferences. Some samples with sufficient Ti separation were measured with both high and low resolution mode and reproducibility was not substantially different from that of samples measured either in the high or low resolution modes (Tab. D-3). The sample purification procedure was adjusted after the Ti interferences were noticed. After adjustment of the purification

procedure the mean Ti/Cu ratio was reduced from 727 in the not purified samples to 0.02 (n = 11) after the two-step purification

A Cu ICP standard (Merck, Darmstadt, Germany) was used as an in-house standard to check for intra-day and long-term reproducibility. The long-term reproducibility of this standard was 0.06‰ (2SD, n = 49). Every δ^{65}Cu value given in Table D-3 and Figure D-3 is the mean of at least two replicate measurements. The BCR-2 and the SCL 7003 reference materials were digested, purified and measured two times to test for accuracy of the measurement. We measured BCR-2 with 0.18 ± 0.09 ‰ (2SD / n = 2) and SCL 7003 with 0.14 ± 0.02‰ (2SD / n = 2), which is comparable to the values reported in Bigalke et al. (2010a).

Copper blanks for the whole procedure were 4.9 ± 9.1 (2SD) ng compared to at least 250 ng of Cu in the sample. Because some samples were only digested and purified one time, error bars in Figure D-3, D-4 and D-5 show 0.09‰, which is the mean 2SD of the samples and reference materials and is similar to the reproducibility of our in-house standard. If measured 2SD were bigger than 0.09‰, the measured 2SD was given.

Table D-3. Copper concentrations, $\delta^{65}Cu$ values of the soil and reference samples, and resolution of the Cu isotope measurements with MC-ICP-MS

Soil	Horizon	Cu µg g^{-1}	$\delta^{65}Cu_{(NIST\ 976)}$ ‰	2SD ‰	n[a]	Resolution
Skeletic Cambisol	Oi[b]/Oe[c]	9.5	-0.19	0.09	1	HR
	Ah	12.9	-0.02	0.09	1	HR
	Bw	9.8	-0.07	0.09	1	HR
	II R	7.4	-0.32	0.09	1	HR
Dystric Cambisol	Oi[b]	10.8	-0.12	0.09	1	LR
	Oe[c]	27.6	-0.29	0.09	2	LR
	Oa[d]	12.6	-0.11	0.09	1	HR
	Ah	4.3	0.08	0.09	1	HR
	Bw1	4.5	0.05	0.09	3	LR/HR
	Bw2	6.4	-0.02	0.16	3	LR/HR
	C	4.8	-0.05	0.09	1	HR
Haplic Podzol 1	Oi[b]	5.2	-0.45	0.09	1	LR
	Oe[c]	8.5	-0.01	0.09	1	LR
	Ah	5.8	0.44	0.09	1	LR
	AEh	3.5	0.18	0.09	1	LR
	E	1.4	-0.57	0.09	2	LR
	II Bhs	1.8	-0.29	0.09	1	LR
	II BCs	1.8	-0.42	0.09	2	LR
	III CR	3.5	-0.39	0.13	2	LR
	II Bhs oxidic	1.9	-0.35	0.18	2	LR
	II Bhs humic	2.8	-0.18	0.09	1	LR
Haplic Podzol 2	Oi[b]	10.6	-0.20	0.14	2	HR/LR
	Oe[c]	16.0	-0.23	0.09	1	LR
	Oa[d]	22.5	-0.21	0.09	1	LR
	AEh	2.7	-0.04	0.09	2	LR
	Bhs	3.2	-0.07	0.09	2	LR
	Bs	1.9	-0.13	0.09	2	LR
CRM	BCR-2	16.8	0.18	0.09	2	LR
CRM	SCL 7003	28.6	0.14	0.09	2	LR

(a) n is the number of independent digestions and purifications, every purified sample was measured twice; (b) Oi, slightly decomposed organic matter; (c) Oe, moderately decomposed organic matter; (d) Oa, highly decomposed organic matter.

Table D-4. Influence of Ti/Cu ratio in the sample on measured $\delta^{65}Cu$

Ti/Cu ratio	$\delta^{65}Cu_{(NIST976)}$ ‰	2 SD ‰[a]
0.00	0.00	0.01
0.10	-0.12	0.03
0.50	-0.50	0.10
1.00	-0.92	0.08

(a) based on two to four measurements.

4 Results

The Cu concentrations in the studied soils ranged between 1.4 and 27.6 µg g^{-1} and were thus at the low end of natural background concentrations (Fig. D-1, Tab. D-3, Artiola, 2005). The Cu concentrations in the organic layers were higher than in the mineral soil except in the Skeletic Cambisol. In the mineral soil, Cu concentrations ranged between 1.4 and 12.9 µg g^{-1}, while in the organic horizons concentrations ranged between 5.2 and 27.6 µg g^{-1}. In the Skeletic Cambisol, Cu concentrations were the highest in the Ah horizon (surface mineral horizon with organic matter). In the mineral soil, Cu concentrations decreased with increasing depth. The Dystric Cambisol had its highest Cu concentration in the O (organic) horizons while Cu concentrations in the mineral soil varied little. In the Haplic Podzol 1, Cu concentrations were the highest in the Oe (moderately decomposed organic) horizon (Fig. D-1, Table D-3), decreased strongly in the E horizon (mineral horizon from which Fe, Al and organic matter was leached), increased again in the IIBhs (mineral horizon with accumulation of organic matter and oxy(hydr)oxides, roman numbering indicates lithological layering with I assigned to the uppermost layer), and finally increased slightly in the IIIRC horizon (weathered bedrock). Fractions of the IIBhs horizon enriched in oxy(hydr)oxides had Cu concentrations similar to bulk IIBhs horizons, while fractions enriched in organic matter had higher Cu concentrations (Table D-3). The Haplic Podzol 2 had comparable high concentrations in the O horizons as the Haplic Podzol 1. In the mineral soil of Haplic Podzol 2, Cu concentrations increased from AEh (surface mineral horizon with organic matter showing beginning leaching of Fe, Al and organic matter) to Bhs and

decreased again in the Bs horizon (mineral horizons with accumulation of oxy(hydr)oxides).

In the sequential extraction, the largest part of soil Cu appears in fraction 7 (residual) which contained between 26% of total Cu in weathered slate (IICR, Skeletic Cambisol) and 94% of total Cu in weathered sandstone (IIIRC, Haplic Podzol 1; Fig. D-2). Fractions 5 & 6 (bound to pedogenic Fe oxides) together contained the second largest part with between 3 % (IIIRC, Haplic Podzol 1) and 70% (IICR, Sleletic Cambisol) of total Cu. Fraction 4 (organically bound, 0- 29%) had the largest contribution to total Cu in A horizons and decreasing contributions with increasing depth down to 0% in weathered bedrock (IIIRC, Haplic Podzol 1). Fractions 1, 2, and 3 (exchangeable, specifically absorbed, bound to Mn oxides, respectively) together only contributed 0-11% to total Cu in mineral horizons, with largest contributions to total Cu usually in the A horizons, but also e.g., in the E horizon of the Haplic Podzol 1

The δ^{65}Cu values in the studied soil horizons ranged between -0.57 and 0.44‰ (Tab. D-3, Fig. D-3). The most pronounced variation of 1.01‰ occurred in the Haplic Podzol 1. In the other soils, total variations in δ^{65}Cu values were between 0.30‰ in the Skeletic Cambisol and 0.37‰ in the Dystric Cambisol. The Haplic Podzol 2 showed a variation of 0.19‰. In all four soils, organic layers had a lighter Cu isotope composition than the underlying mineral topsoils. In the mineral soil horizons of the Skeletic Cambisol, the Dystric Cambisol and the Haplic Podzol 2, the δ^{65}Cu values decreased consistently with depth. In the Haplic Podzol 1, δ^{65}Cu values increased from the Oi to the A horizon and strongly decreased in the E horizon. In the II Bhs, Cu was isotopically heavier than in the E horizon but deeper in the soil the Cu became again isotopically lighter (Tab. D-3, Fig. D-3). The δ^{65}Cu value of the mineral horizons and the organic- and oxide-rich spots of the IIBhs horizon of the Haplic Podzol 1 correlated significantly with the organic C and Cu concentrations (Fig. D-4). There was an overall trend of increasingly lighter δ^{65}Cu values with increasing depth (Figs. D-3 and D-5). The mean δ^{65}Cu value of the A horizons was significantly heavier than of the subsoil horizons ($p = 0.006$, Fig. D-6).

To assess the influence of biogeochemical cycling on δ^{65}Cu values in soil samples, Cu storage in the main rooting zone in mineral soil (0-50 cm depth) and organic layers were calculated and Cu storage in biomass was estimated from the literature. If an

aboveground dry biomass of 300 Mg $ha^{-1}$of standing vegetation was assumed based on a study of (Heinrichs and Mayer, 1980) , who found 311 and 324 Mg ha^{-1} in beech and

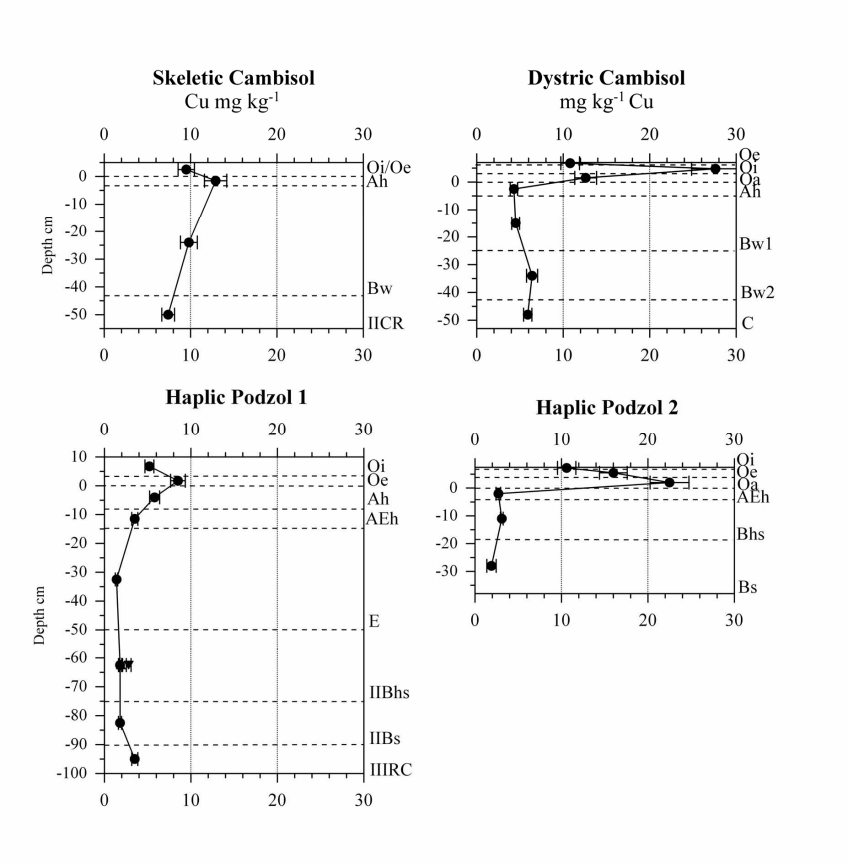

Figure D-1. Total Cu concentrations of the soil horizons (black dots). Up and down pointing triangles represent spots enriched in oxy(hydr)oxides and humic substance, respectively. Error bars represent two times the relative standard deviation, which is the precision of the used analytical method.

spruce forest respectively in a middle mountain area in Germany, which is climatically and pedologically similar to our study region. Copper concentrations in plants were estimated from Cu concentrations in Oi horizons which originate from relatively unaltered plant litter (Table D-5).

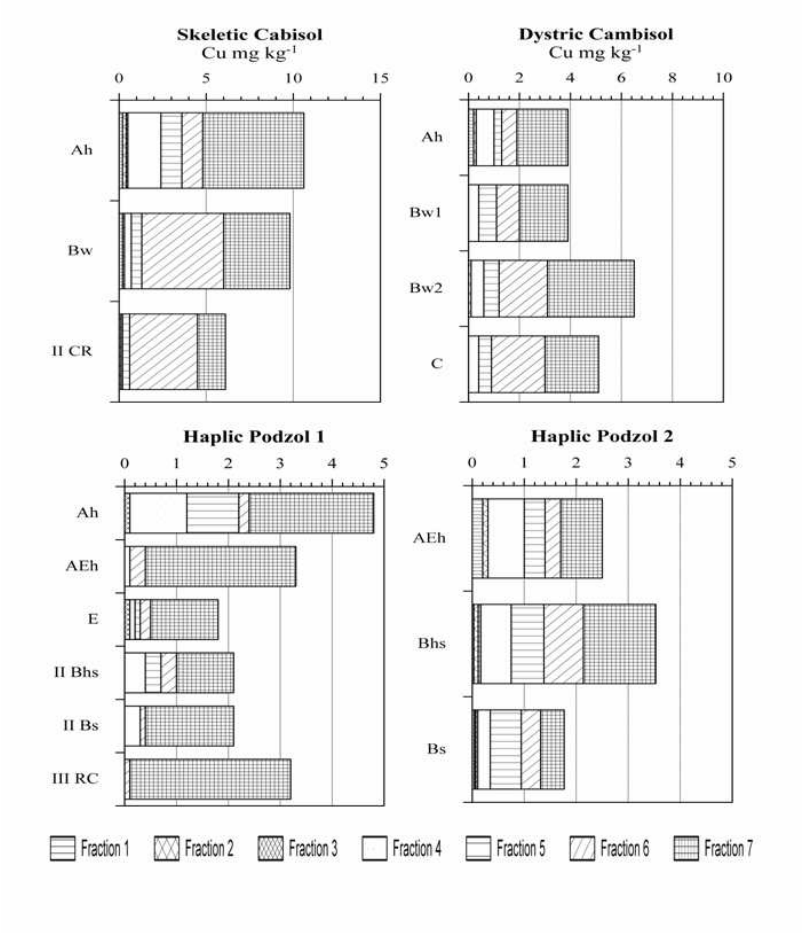

Figure D-2. Copper concentrations in the seven fractions of the sequential extraction of Zeien and Brümmer (1989). Fractions are supposed to represent (1) readily soluble and exchangeable, (2) specifically adsorbed and other weakly bound species, (3) bound to Mn oxides, (4) bound to organic matter, (5) bound to poorly crystalline Fe oxides, (6) bound to crystalline Fe oxides and (7) residual fractions. Please note the different scalings of the X axes.

5 Discussion

As we analyzed total digests of soil horizons for Cu isotope ratios, only inherited differences in Cu isotope signatures of the parent material and processes which cause redistribution of Cu among horizons can be traced because horizon-internal processes do not change the overall Cu isotope signal of the whole horizon. Sequential extractions may be a useful tool to get further information about Cu isotope variation in soil, but may artificially fractionate Cu isotopes because of kinetic or equilibrium effects during extraction. Artificial isotope fractionations might result from the failure of an extraction

step to selectively extract all Cu in the addressed fraction. Consequently, the used extraction procedure must be carefully checked and adjusted in terms of selectivity, extraction yield and effect on Cu isotope ratios. Currently, no such method is available for Cu. We therefore did not determine Cu isotope ratios in the sequential soil extracts.

We selected Cambisols representing a wide-spread group of soils showing oxic weathering without pronounced vertical translocation of metals and Podzols, in which in contrast, a pronounced vertical translocation of metals occurs within the soil profile. The studied Haplic Podzol 1 and the Haplic Podzol 2 showed different degrees of differentiation.

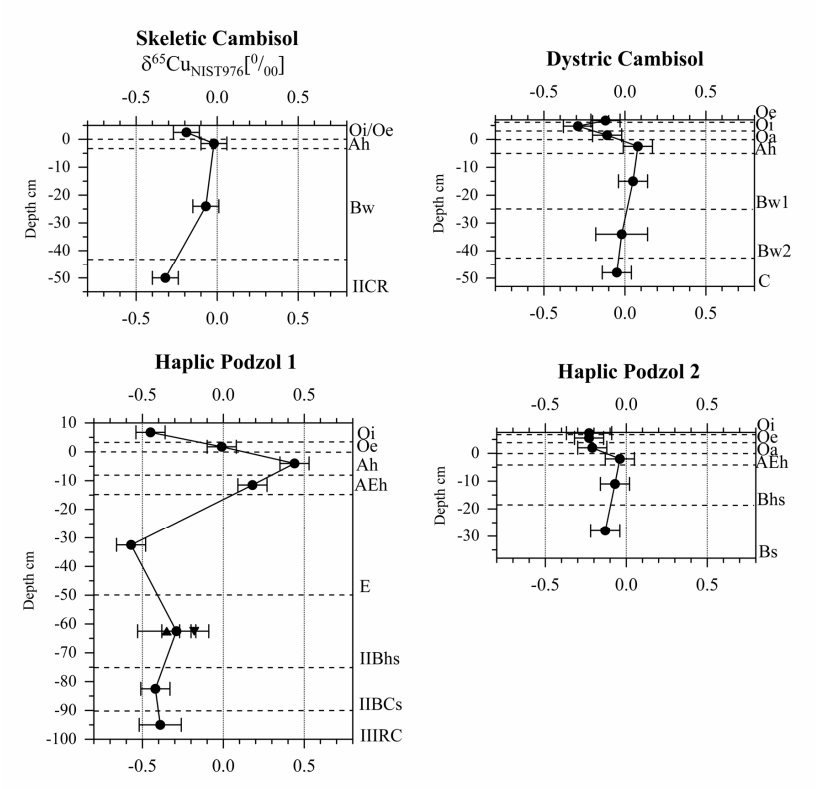

Figure D-3. Copper isotope composition ($\delta^{65}Cu$ values) in the soil horizons. Filled black circles show $\delta^{65}Cu$ values, up and down pointing triangles represent spots enriched in oxy(hydr)oxides and humic substance, respectively.

5.1 Copper isotope ratios in the organic layer

In all studied soils, O horizons contained isotopically lighter Cu associated with usually higher Cu concentrations than the underlying A horizons (Fig. D-3, Tab D-3). We assume that these differences are either caused by fractionation during biogeochemical cycling of Cu in the plant-soil system and/or by deposition of Cu from the atmosphere.

O horizons consist of differently decomposed organic matter originating mainly from leaf litter. First studies about Cu fractionation during uptake and transport in plants showed that light Cu is taken up preferentially by the plant and that the extent of fractionation depends on soil properties (Zhu et al., 2010). During transport in the plant, Cu was found to be fractionated between roots and shoots with shoots beeing isotopically lighter ($\Delta^{65}Cu_{(root\text{-}shoot)}$ of 0.41‰; Jouvin et al., 2008) while leaves are enriched in the heavy isotopes compared to stem by ca. 0.3 ‰ (Zhu et al., 2010). Thus, uptake of Cu in the mineral soil, cycling in the plant and accumulation in the organic layers might be one reason for Cu isotope differentiation in soil. Biogeochemical cycling might also be responsible for elevated Cu concentration in the organic layers, as plants are able to concentrate metals in organic horizons (Goldschmidt, 1937).

One the other hand, Cu concentrations in the organic layers were strongly elevated (Fig. D-3) and might also be caused by anthropogenic Cu inputs, which are accumulated in the organic layers as a consequence of the high affinity of Cu to organic matter (Filipinski and Grupe, 1990; Wilcke et al., 1999). As all study soils were located in remote areas far from direct Cu inputs most probable Cu sources are diffuse inputs from the atmosphere (Nriagu and Pacyna, 1988).

Copper enrichment factors in the organic layer calculated as the depth-weighted mean Cu concentration of all O horizons divided by the Cu concentration of the C horizons (as no C horizon was available for Haplic Podzol 2, the Bs horizon of this soil was used to calculate enrichment factors) in the study soils were 3.5 and 10.5 for the two Slovakian soils (Dystric Cambisol and Haplic Podzol 2) and 1.3 and 2.1 for the two German soils (Skeletic Cambisol, Haplic Podsol 1) respectively. If we compare these factors to those reported by Reimann et al. (2009) of 2.4 in uncontaminated soils which were attributable to plant cycling alone, we can assume that the two German soils are relatively unpolluted, while the two Slovak soils may be affected by metal deposition

from the atmosphere possibly originating from industrial regions in Poland, Czech Republic, and local industrial sources (Lobe et al., 1998). As the δ^{65}Cu value of deposition from the atmosphere is unknown, we are not able to assess the influence of these inputs on the δ^{65}Cu values of the organic layers.

The two Slovak soils and the German Skeletic Cambisol showed similar differences in δ^{65}Cu values between O and A horizons, while the differences between O and A horizons of the Haplic Podzol 1 were stronger and dominated by the heavy Cu isotope signal in the A horizons. However, the Haplic Podzol 1 generally showed a different Cu isotope pattern from the other soils which might be a consequence of the pronounced podzolization.

Table D-5. Copper storages in aboveground bioamss, O- and mineral horizons.

	Aboveground biomass (estimated, kg ha^{-1})	O horizons (kg ha^{-1})	Mineral soil (0-50 cm, kg ha^{-1})	Contribution to total storage
Skeletic Cambisol	2.8	0.4	18.3	15.0
Dystrsic Cambisol	3.2	1.5	27.6	14.7
Haplic Podzol 1	1.6	0.8	13.2	15.4
Haplic Podzol 2	3.2	2.3	10.3	34.8

5.2 Copper concentrations and isotope ratios in the Cambisols

Two Cambisol profiles were investigated for Cu concentrations, Cu partitioning in seven operationally defined fractions, and Cu isotope ratios. The Skeletic Cambisol showed a gradient in Cu concentrations between the Ah and IICr horizons (Table D-3, Fig. D-1). The Cu concentrations in fractions 1-4 decreased with increasing depth because of decreasing organic matter concentrations and weathering intensity. The Dystric Cambisol had similar Cu concentrations in all horizons (Fig. D-1). The Cu

partitioning between the seven sequential extraction steps revealed the typical pattern of decreasing Cu concentrations in fractions 1-4 and increasing Cu concentrations in fractions 5-7 with increasing depth (Fig. D-2). This can be attributed to input of organic matter and increased weathering in the upper horizons. In the Haplic Podzol 2, the podzolization process was less pronounced than in the Haplic Podzol 1 and the depth distribution of the δ^{65}Cu values was more similar to the two Cambisol profiles. Although the vertical distribution of Fe concentrations indicated podzolization in the Haplic Podzol 2 and also Cu translocation can be assumed from Cu concentrations (Table D-2), this process did not seem to affect the δ^{65}Cu values strongly, as the vertical distribution of δ^{65}Cu values was similar to that of the Cambisols.

The individual δ^{65}Cu values of all mineral soil samples of the Cambisols and the Haplic Podzol 2 overlap within uncertainties. The only horizon with a markedly different δ^{65}Cu value beyond the mean±2SD ranges was the IICR horizon of the Skeletic Cambisol. However, this horizon developed from another periglacial cover bed than the overlying horizons (see above) and thus the difference in the δ^{65}Cu value of between this and the other mineral soil horizons might be inherited from the parent materials and is no evidence for biogeochemical Cu isotope fractionation in the soil. Even if no clear differences in δ^{65}Cu values can be seen in the individual Cambisol profiles and the Haplic Podzol 2 (Fig. D-3), an overall trend of increasingly lighter δ^{65}Cu values with increasing depth exists (Figs. D-3 and D-5). The subsoil horizons were, on average, significantly Cu isotopically lighter than the A horizons ($p = 0.006$; Fig. D-6). This depth trend might indicate small isotope fractionation during weathering and biogeochemical cycling. Possible explanations for this trend include:

1. During weathering of primary minerals, the released Cu is partly incorporated into pedogenic minerals such as clay minerals and oxides (Contin et al., 2007) and partly bound to cation-exchange sites (Alcacio et al., 2001; Artiola, 2005), which fractionates the bound Cu towards a heavier Cu isotope composition (Li et al., 2008; Pokrovsky et al., 2008) leaving light Cu mobile and possibly leached.
2. Biogeochemical cycling might change the Cu isotope composition of mineral horizons by removing light Cu isotopes in the main rooting area and transfer

them to the organic horizons because it is known, that Cu isotopes are fractionated during plant cycling (Jouvin et al, 2008; Zhu et al., 2010).

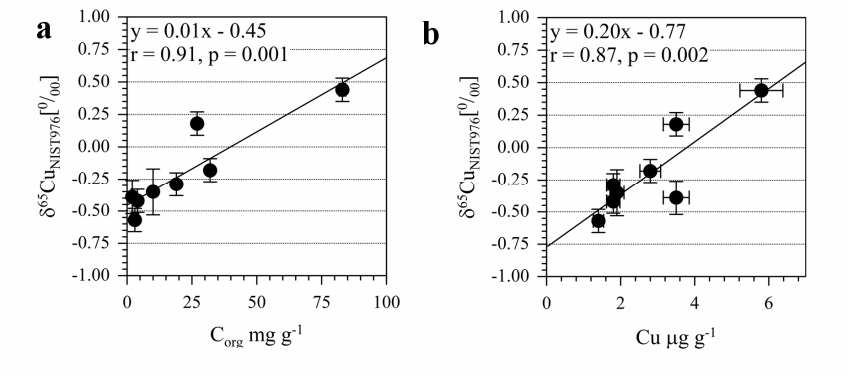

Figure D-4. Relationship between (a) C concentrations and (b) Cu concentrations and δ^{65}Cu values

To assess the influence of plant-induced Cu isotope fractionation on Cu isotope ratios in the mineral soil, we estimated the various Cu storages in aboveground biomass, organic layer, and mineral soil. Because (i) aboveground biomasses for forests reported in the literature vary much (Finer et al., 2003; Heinrichs and Mayer, 1980; Weis et al., 2009), (ii) Cu concentrations in the plants depend on soil properties and Cu concentrations (Kabata-Pendias and Pendias, 2001), and (iii) Cu concentrations in the different plant parts may differ (Heinrichs and Mayer, 1980) our estimate of the Cu storage in aboveground biomass is a rough approximation (Table D-5). The comparison of Cu in plants and organic horizons and Cu pool in mineral soil (main rooting zone of 0-50 cm depth) revealed that between 15 and 34% of total Cu in this pool was stored in plants and organic horizons (Table D-5). Considering the fact that the organic Cu pools have a limited lifespan and that organic layers are turned over several times during soil development (Gaudinski et al., 2000) it is likely that biogeochemical cycling affects δ^{65}Cu values in the mineral soil. Especially the surface horizons, which are most strongly rooted may display influence of biogeochemical cycling.

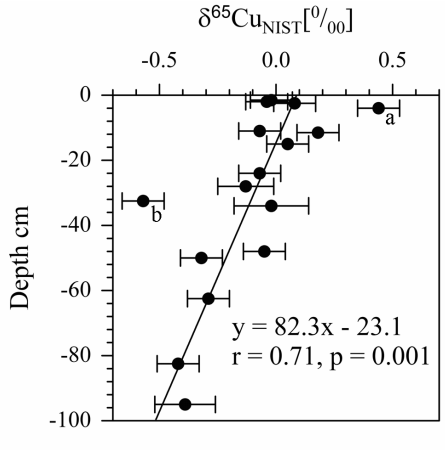

Figure D-5. Depth distribution of δ^{65}Cu values of all four soils. Samples in which δ^{65}Cu values deviate markedly from the regression line include the Ah (a) and E (b) horizons of the Haplic Podsol 1.

5.3 Copper concentrations and isotope ratios in the Podzols

The investigated Podzols showed the typical features of the podzolization process with a translocation of Fe, organic C, and increasing pH from the E to the Bhs horizon (Tab. D-2). There are numerous explanations for the mobilization and immobilization of Al, Fe, Si and organic substances, which are extensively discussed in the literature (Farmer, 1982; Lundström et al., 2000; Sauer et al., 2007). Because the vertical distribution of δ^{65}Cu values in Haplic Podzol 2 was more similar to that of the Cambisols than to that of Haplic Podzol 1 we discussed the Cu isotope ratios in Section 4.2 above together with the Cambisols.

While soil description is based on Fe, Al, and organic matter transport, to a smaller extent also transport of trace metals like Cu takes place from E to B(h)s horizons (Keller and Domergue, 1996; Wilcke et al., 1996; Jersak et al., 1997; Nikonov et al., 1997; Tyler, 2004). For Cu, organic complexation is assumed as the dominating mobilization mechanism. Therefore, mobilization of Cu depends on dissolved organic matter concentrations in soil solution (Berggren, 1992, Kotowski, 1998). A transport of Cu from the E to the Bhs horizon in the Haplic Podzol 1 seems likely because the E horizon had the lowest Cu concentration (1.4 µg g^{-1}, compared to 3.5 µg g^{-1} in the AEh and 1.8 µg g^{-1}in the Bhs) in the whole profile and organic-rich spots in Bhs horizons showed

higher Cu concentrations (2.8 µg g^{-1}) than the bulk Bhs horizon (1.8 µg g^{-1}), which might point on illuvation of Cu complexed with organic acids. The sequential extraction showed that in the Bhs horizons, Cu was to a larger extent associated with fractions 4-6 which represent organically and oxy(hydr)oxide-bound Cu than in the over- and underlying horizons further supporting our assumption of vertical Cu transport during podzolization.

The Haplic Podzol 1 showed a strong variation in $\delta^{65}Cu$ values among O, A, E, and B horizons (Fig. D-3). This variation might be partly caused by differences in isotope compositions of the three solifluctional layers from which this soil developed. The first layer (Ah, AEh and E horizon), developed from sandstone and loess and is depleted in fine material, the second layer (Bhs, Bs horizon) also developed from sandstone and loess potentially with a different sandstone/loess ratio than in the uppermost layer, while the third layer developed from sandstone bedrock only. However, the main component of all layers was the sandstone and strongest variations occurred between Ah and E horizons which developed from the same lithological layer strongly suggesting that the observed variation in $\delta^{65}Cu$ values is attributable to biogeochemical processes in soil. The E horizon had the most negative $\delta^{65}Cu$ value of the whole soil which might indicate preferential leaching of isotopically heavy Cu. This assumption is supported by the fact that the IIBhs horizon showed a heavier isotope composition than the E and the IIBCs horizons (which developed from the same layer as the IIBhs horizon), indicating preferential illuviation of the heavy Cu isotope . As complexation of Cu with organic acids causes a Cu isotope fractionation ($\Delta^{65}Cu_{\text{insolubilized humic acid-solution}}$) of 0.27‰ (Bigalke et al., 2010b) direction and extent of variation in Cu isotope ratios between eluvial E and illuvial B horizons might indicate complexation of heavy Cu in the E horizon and leaching of the complexes to the Bhs horizons. The assumption of Cu transport as organic complex is further supported by the finding that the organic-rich spot of IIBhs horizon had a heavier $\delta^{65}Cu$ value and a higher Cu concentration than the bulk of the IIBhs horizon in line with the literature (Berggren, 1992, Kotowski, 1998). Finally, the close correlation of the organic C and Cu concentrations with the $\delta^{65}Cu$ values of the mineral horizons and the organic- and oxide-rich spots of the IIBhs horizon of the Haplic Podzol 1 (Fig. D-4) again suggests that Cu fractionation is attributable to organo-complexation.

In contrast to the differences in Cu isotope composition of E and B horizons, we do not have a definite explanation for the strong difference in Cu isotope composition of the A (i.e. Ah, AEh) and the other mineral horizons in the Haplic Podzol 1. In principle, biogeochemical fractionations, differences in the substrates and contamination might be possible fractionating processes. As the Haplic Podzol 1 was located directly under a tree, plant-induced fractionation of Cu isotopes (Jouvin et al., 2008; Zhu et al., 2010) is one possible explanation for pronounced differences in δ^{65}Cu values of the A and the other mineral soil horizons. Copper storage in plants and organic layers comprised approx. 15% of the total Cu in the ecosystem down to 50 cm mineral soil depth (Table D-5). The Cu pool in aboveground biomass and organic layers is periodically turned over at much shorter temporal scales than pedogenesis (i.e., year-decades vs. centuries to millennia). Consequently, large proportions of plant-available Cu will be cycled through the plants. Given the low Cu concentrations in the study soils and the small plant-available percentage of total Cu (fractions 1-4, Fig. D-2), a strong influence of Cu cycling through plants on the δ^{65}Cu values of the A horizons of the Haplic Podzol 1 seems possible.

Another explanation for the heavy δ^{65}Cu values in the A horizons of might be an a priori heavier δ^{65}Cu value of the substrates from which this horizon developed. However, as Ah and E horizons developed from the same substrate, this would imply an even more pronouncesd Cu isotope fractionation in the E horizon. Furthermore, the main component of all substrates the soil developed from was sandstone, which is assumed to be relatively homogeneous.

Finally, the Haplic Podzol 1 shows a base saturation of nearly 100% in the Ah horizon. This high base saturation is caused by high exchangeable Ca and Mg concentrations, which is uncommon at the low pH (the “base metals” should already have been leached) and might indicate that the soil was affected by liming in the past. If this lime contained Cu with a heavy δ^{65}Cu value, its application might also have contributed to the observed Cu isotopical composition of the A horizon.

5.4 Comparison of Cu isotope pattern in Cambisols, Podzols, and hydromorphic soils

Bigalke et al. (2010a) determined Cu concentrations, δ^{65}Cu values and Cu partitioning in seven fractions of a sequential extraction in a set of four hydromorphic soils with the same methods as in this study. They found a significant variation of δ^{65}Cu values of up to 0.6‰ in whole soils (including organic layer and mineral soil), while the maximum variation in mineral soil was 0.45‰. Variations in organic layers were attributed to biogeochemical cycling of Cu, while atmospheric contamination could not be excluded as possible source. Variations in δ^{65}Cu values of the mineral soil horizons were assumed to be affected by alternating redox conditions in the soils. Comparing the findings of Bigalke et al. (2010a) to those of this study it can be summarized that:

1. O horizons of the Slovak soils investigated by Bigalke et al. (2010a, i.e. a Stagnic Cambisol and a Dystric Gleysol) had a lighter Cu isotope signal in line with the four soils investigated in this study. In contrast, two hydromorphic German soils did not have lighter δ^{65}Cu in the O horizons. Bigalke et al. (2010a) suggested physiological differences between deciduous and coniferous trees as possible reason for different δ^{65}Cu values in O horizons of the soils. This assumption is not confirmed by the present study were O horizon originating from litter of both deciduous and coniferous trees (Tab. D-1) showed lighter δ^{65}Cu values than the A horizons (Tab. D-3). Considering all eight soil profiles in the light of the first studies of Cu isotope fractionation in plants (Jouvin et al. 2008, Zhu et al., 2010) it might be assumed that biogeochemical cycling is the main factor determining δ^{65}Cu values of O horizons. However, the elevated Cu concentrations in some of the O horizons imply that atmospheric Cu contamination is present in some of the soils and might affect the δ^{65}Cu values of O horizons to different degrees.
2. The depth trend of δ^{65}Cu values in the oxic weathered soils was different to that previously observed in hydromorphic soils by Bigalke et al. (2010a). The significantly heavier mean δ^{65}Cu value of the A horizons than in the subsoil horizons of the oxic weathered soils ($p = 0.006$) was opposite to previous observations for the hydromorphic soils, in which δ^{65}Cu values of A horizons were significantly lighter than of subsoil horizons ($p = 0.011$, Fig. D-6). This

supports the assumption of Bigalke et al. (2010a) who assumed that redox induced processes like changes in pH, release of organic matter, reduction of Fe oxy(hydr)oxides and changes in Cu redox state in the subsoils during waterlogging significantly affect δ^{65}Cu values. The differences in the vertical distribution of δ^{65}Cu values in the mineral soils among oxic weathered soils, the Haplic Podzol 1, and the hydromorphic soils of Bigalke et al. (2010a) suggest that δ^{65}Cu measurements are capable of differentiating among different soil genetic processes. However, more detailed knowledge of the individual effects of all contributing biogeochemical processes is needed before our δ^{65}Cu values can be safely used as tracers of soil genetic processes.

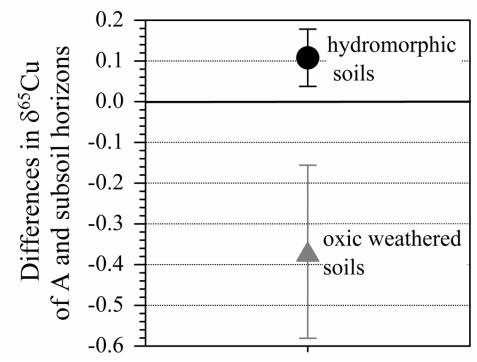

Figure D-6. Mean differences in δ^{65}Cu values between A and subsoil horizons of hydromorphic and oxic weathered soils. Error bars represent 95% confidence intervals. Data for hydromorphic soils were taken from Bigalke et al. (2010a). Please mind that the means refer to differences between one A and various subsoil horizons of four of each of hydromorphic and oxic weathered soils.

6 Conclusion

I. Organic horizons show a lighter Cu isotope signal than the A horizons in all four profiles. One possible reason is plant-induced isotope fractionation of Cu and recycling to the soil but the δ^{65}Cu values might also be affected by deposition of Cu from the atmosphere.

II. In the Cambisols, and Haplic Podzol 2 differences in δ^{65}Cu values among the mineral soil horizons of individual soils were within measurement

uncertainty. However, there was an overall significant trend of increasingly lighter δ^{65}Cu values with increasing mineral soil depth, which we assume to be caused by isotope fractionations during weathering and/or biogeochemical transformations.

III. The Cu isotope fractionation, concentration and distribution in the Haplic Podzol 1 indicates that Cu was transported vertically in the soil. Furthermore, it is suggested that Cu transport during podzolization occurs predominantly in form of Cu complexed by organic acids.

IV. The depth distribution of δ^{65}Cu values in the Cambisols and the Haplic Podzol 2 differed from that in the Haplic Podzol 1. This is probably attributable to different soil genetic processes, i.e. oxic weathering without pronounced vertical Cu transport vs. podzolization with pronounced vertical Cu transport. Furthermore, the depth distributions of δ^{65}Cu values differed between oxic weathered hydromorphic soils in the literature. Thus, δ^{65}Cu might be a promising tracer to detect different soil genetic processes.

Overall the results of our study indicate the potential of Cu stable isotope investigations to gain new insights in the fate of Cu in the environment. However, information about Cu isotope fractionation during many environmental processes like weathering of minerals, transport and biogeochemical cycling are still limited, rendering interpretation of δ^{65}Cu values in the complex soil-plant system difficult. Therefore, there is a future need for elucidating Cu isotope fractionation by the involved biogeochemical and transport processes. This also involves the development of new tools like a suitable sequential extraction technique for isotope investigations and the analysis of soil solutions which reflect the reactive portion of Cu in soil and faster responds to change of physico-chemical soil conditions than the solid phase.

7 Acknowledgements

Prescribed by the regulations of the internet publisher (ArchiMed) this section had to be deleted for data protection reasons. I want to thank all people listed in the printetd version.

8 References

Alcacio, T. E., Hesterberg, D., Chou, J. W., Martin, J. D., Beauchemin, S., and Sayers, D. E., 2001. Molecular scale characteristics of Cu(II) bonding in goethite-humate complexes. *Geochim. Cosmochim. Acta* **65**, 1355-1366.

Alloway, B. J., 1990. Heavy metals in soils. Blackie ; Halsted Press, Glasgow, New York.

Archer, C. and Vance, D., 2004. Mass discrimination correction in multiple-collector plasma source mass spectrometry: an example using Cu and Zn isotopes. *J. Anal. Atom. Spectrom.* **19**, 656-665.

Artiola, J. F., 2005. Speciation of copper in the environment. In: Cornelis, R. (Ed.), *Handbook of elemental speciation 2 - species in the environment, food, medicine and occupational health*, John wiley & Sons, Chinchester.

Asael, D., Matthews, A., Bar-Matthews, M., and Halicz, L., 2007. Copper isotope fractionation in sedimentary copper mineralization (Tinma Valley, Israel). *Chem. Geol.* **243**, 238-254.

Asael, D., Matthews, A., Bar-Matthews, M., Halicz, L., Ehrlich, S., and Teplyakov, N., 2005. Redox fractionation of copper isotopes in sedimentary conditions. *Geochim. Cosmochim. Acta* **69**, A216-a216.

Balistrieri, L. S., Borrok, D. M., Wanty, R. B., and Ridley, W. I., 2008. Fractionation of Cu and Zn isotopes during adsorption onto amorphous Fe(III) oxyhydroxide: Experimental mixing of acid rock drainage and ambient river water. *Geochim. Cosmochim. Acta* **72**, 311-328.

Berggren, D., 1992. Speciation of Copper in Soil Solutions from Podzols and Cambisols of S Sweden. *Water Air Soil Poll.* **62**, 111-123.

Bigalke, M., Weyer, S., and Wilcke, W., 2010a. Stable copper isotopes: A novel tool to trace copper behavior in hydromorphic soils. *Soil Sci. Soc. Am. J.* **74**, 60-73.

Bigalke, M., Weyer, S., and Wilcke, W., 2010b. Isotopic fractionation of Cu during complexation with humic acid. *Environ. Sci. Techn.* **44**, 5496-5502.

Borrok, D. M., Ridley, W. I., and Wanty, R. B., 2008. Isotopic fractionation of Cu and Zn during adsorption onto bacterial surfaces. *Geochim. Cosmochim. Acta* **72**, A99-a99.

Clayton, R. E., Hudson-Edwards, K. A., and Houghton, S. L., 2005. Isotopic effects during Cu sorption onto goethite. *Geochim. Cosmochim. Acta* **69**, A216-a216.

Contin, M., Mondini, C., Leita, L., and De Nobili, M., 2007. Enhanced soil toxic metal fixation in iron (hydr)oxides by redox cycles. *Geoderma* **140**, 164-175.

Cornell, R. M. and Schwertmann, U., 1996. The iron oxides : Structure, properties, reactions, occurrence, and uses. VCH, Weinheim ; New York.

Ehrlich, S., Butler, I., Halicz, L., Rickard, D., Oldroyd, A., and Matthews, A., 2004. Experimental study of the copper isotope fractionation between aqueous Cu(II) and covellite, CuS. *Chem. Geol.* **209**, 259-269.

Emmanuel, S., Erel, Y., Matthews, A., and Teutsch, N., 2005. A preliminary mixing model for Fe isotopes in soils. *Chem. Geol*. **222**, 23-34.

Fantle, M. S. and DePaolo, D. J., 2004. Iron isotopic fractionation during continental weathering. *Earth Planet. Sci. Lett.* **228**, 547-562.

FAO. 2006. Guidelines for soil description. Food and Agriculture Organization of the United Nations, Rome.

Farmer, V. C., 1982. Significance of the presence of allophane and imogolite in podzop Bs horizons for podzolization mechanisms: A review. *Soil Sci. Plant Nutr.* **24**, 571-578.

Filipinski, M. and Grupe, M., 1990. Distribution of Lithogenous, Pedogenous and Anthropogenous Heavy-Metals in Soils (in German). *Z. Pflanz. Bodenkunde* **153**, 69-73.

Finer, L., Mannerkoski, H., Piirainen, S., and Starr, M., 2003. Carbon and nitrogen pools in an old-growth, Norway spruce mixed forest in eastern Finland and changes associated with clear-cutting. *Forest. Manag.* **174**, 51-63.

Gale, N. H., Woodhead, A. P., Stos-Gale, Z. A., Walder, A., and Bowen, I., 1999. Natural variations detected in the isotopic composition of copper: possible applications to archaeology and geochemistry. *Int. J. Mass Spectrom.* **184**, 1-9.#

Gaudinski, J. B., Trumbore, S. E., Davidson, E. A., and Zheng, S. H., 2000. Soil carbon cycling in a temperate forest: radiocarbon-based estimates of residence times, sequestration rates and partitioning of fluxes. *Biogeochemistry* **51**, 33-69.

Goldschmidt, V. M., 1937. The principles of distribution of chemical elements in minerals and rocks. *J. Chem. Soc. London*, 655-673.

Grybos, M., Davranche, M., Gruau, G., and Petitjean, P., 2007. Is trace metal release in wetland soils controlled by organic matter mobility or Fe-oxyhydroxides reduction? *J. Colloid Interf. Sci.* **314**, 490-501.

Heinrichs, H. and Mayer, R., 1980. The Role of forest vegetation in the biogeochemical cycle of heavy metals. *J. Environ. Qual.* **9**, 111-118.

Ildefonse, P., Manceau, A., Prost, D., and Groke, M. C. T., 1986. Hydroxy-Cu-Vermiculite Formed by the Weathering of Fe-Biotites at Salobo, Carajas, Brazil. *Clay. Clay Miner.* **34**, 338-345.

IUSS Working Group WRB, 2006. *World Soil Resource Reports No. 103*. FAO, Rome.

Jersak, J., Amundson, R., and Brimhall, G., 1997. Trace metal geochemistry in spodosols of the northeastern United States. *J. Environ. Qual.* **26**, 511-521.

Jouvin, D., Louvat, P., Marechal, C., and Benedetti, M. F., 2008. Fractionation of copper isotopes in plants. *Geochim. Cosmochim. Acta* **72**, A441-a441.

Kabata-Pendias, A. and Pendias, H., 2001. *Trace elements in soils and plants*. CRC Press, Boca Raton, Fla.

Keller, C. and Domergue, F. L., 1996. Soluble and particulate transfers of Cu, Cd, Al, Fe and some major elements in gravitational waters of a Podzol. *Geoderma* **71**, 263-274.

Kotowski, M., 1998. The role of organic matter and aluminum in zinc and copper transport through forest podsol soil profiles. In: Pawlowski, L., Gonzales, M. A., Dudzinska, M. R., and Lacy, W. J. Eds.), *Chemistry for the Protection of the Environment 3*. Plenum Press Div Plenum Publishing Corp, New York.

Li, J., Zhu, X. K., and Tang, S. H., 2008. Experimental study on Cu isotope fractionation during crystallization and reduction at low temperatures. *Geochim. Cosmochim. Acta* **72**, A540-a540.

Li, W. Q., Jackson, S. E., Pearson, N. J., Alard, O., and Chappell, B. W., 2009. The Cu isotopic signature of granites from the Lachlan Fold Belt, SE Australia. *Chem. Geol.* **258**, 38-49.

Lobe, I., Wilcke, W., Kobza, J., and Zech, W., 1998. Heavy metal contamination of soils in Northern Slovakia. *Z. Pflanz. Bodenkunde* **161**, 541-546.

Lundstrom, U. S., van Breemen, N., and Bain, D., 2000. The podzolization process. A review. *Geoderma* **94**, 91-107.

Manceau, A., Nagy, K. L., Marcus, M. A., Lanson, M., Geoffroy, N., Jacquet, T., and Kirpichtchikova, T., 2008. Formation of metallic copper nanoparticles at the soil-root interface. *Environ. Sci. Technol.* **42**, 1766-1772.

Marechal, C. N., Telouk, P., and Albarede, F., 1999. Precise analysis of copper and zinc isotopic compositions by plasma-source mass spectrometry. *Chem. Geol.* **156**, 251-273.

Marechal, C. and Albarede, F., 2002. Ion-exchange fractionation of copper and zinc isotopes. *Geochim. Cosmochim. Acta* **66**, 1499-1509.

Markl, G., Lahaye, Y., and Schwinn, G., 2006. Copper isotopes as monitors of redox processes in hydrothermal mineralization. *Geochim. Cosmochim. Acta* **70**, 4215-4228.

Mathur, R., Ruiz, J., Titley, S., Liermann, L., Buss, H., and Brantley, S., 2005. Cu isotopic fractionation in the supergene environment with and without bacteria. *Geochim. Cosmochim. Acta* **69**, 5233-5246.

Nikonov, V. V., Lukina, N. V., and Frontaseva, M. V., 1997. Trace elements in the Al-Fe-humus podzolization process. *Euras. Soil Sci.* **30**, 1181-1192.

Nriagu, J. O. and Pacyna, J. M., 1988. Quantitative Assessment of Worldwide Contamination of Air, Water and Soils by Trace-Metals. *Nature* **333**, 134-139.

Pokrovsky, O. S., Viers, J., Emnova, E. E., Kompantseva, E. I., and Freydier, R., 2008. Copper isotope fractionation during its interaction with soil and aquatic microorganisms and metal oxy(hydr) oxides: Possible structural control. *Geochim. Cosmochim. Acta* **72**, 1742-1757.

Reimann, C., Englmaier, P., Flem, B., Gough, L., Lamothe, P., Nordgulen, O., and Smith, D., 2009. Geochemical gradients in soil O-horizon samples from southern Norway: Natural or anthropogenic? *Appl. Geochem.* **24**, 62-76.

Sauer, D., Sponagel, H., Sommer, M., Giani, L., Jahn, R., and Stahr, K., 2007. Review Article Podzol: Soil of the Year 2007 A review on its genesis, occurrence, and functions. *J Plant. Nutr. Soil Sc.* **170**, 581-597.

Schlichting, E., Blume, H. P., and Stahr, K., 1995. *Practical course in soil science* (in German). Enke, Stuttgart.

Schwertmann, U., Fischer, W. R., and Fechter, H., 1982. Trace-Elements in Pedosequences .1. 2 Braunerde-Podsol-Sequences on Slate (in German). *Z. Pflanz. Bodenkunde.* **145**, 161-180.

Thompson, A., Ruiz, J., Chadwick, O. A., Titus, M., and Chorover, J., 2007. Rayleigh fractionation of iron isotopes during pedogenesis along a climate sequence of Hawaiian basalt. *Chem. Geol.* **238**, 72-83.

Tyler, G., 2004. Vertical distribution of major, minor, and rare elements in a Haplic Podzol. *Geoderma* 119, 277-290.

Viers, J., Oliva, P., Nonell, A., Gelabert, A., Sonke, J. E., Freydier, R., Gainville, R., and Dupre, B., 2007. Evidence of Zn isotopic fractionation in a soil-plant system of a pristine tropical watershed (Nsimi, Cameroon). *Chem. Geol.* **239**, 124-137.

Weber, F. A., Voegelin, A., Kaegi, R., and Kretzschmar, R., 2009. Contaminant mobilization by metallic copper and metal sulphide colloids in flooded soil. *Nature Geosc.* **2**, 267-271.

Weis, W., Gruber, A., Huber, C., and Gottlein, A., 2009. Element concentrations and storage in the aboveground biomass of limed and unlimed Norway spruce trees at Hoglwald. *Eur. J. Forest Res.* **128**, 437-445.

Weyer, S. and Schwieters, J., 2003. High precision Fe isotope measurements with high mass resolution MC-ICPMS. *Int. J. Mass Spectrom.* **226**, 355-368.

Wiederhold, J. G., Teutsch, N., Kraemer, S. M., Halliday, A. N., and Kretzschmar, R., 2007. Iron isotope fractionation in oxic soils by mineral weathering and podzolization. *Geochim. Cosmochim. Acta* **71**, 5821-5833.

Wilcke, W., Baumler, R., Deschauer, H., Kaupenjohann, M., and Zech, W., 1996. Small scale distribution of Al, heavy metals, and PAHs in an aggregated Alpine Podzol. *Geoderma* **71**, 19-30.

Wilcke, W., Guschker, C., Kobza, J., and Zech, W., 1999. Heavy metal concentrations, partitioning, and storage in Slovak forest and arable soils along a deposition gradient. *J. Plant. Nutr. Soil. Sc.* **162**, 223-229.

Zeien, H., 1995. Chemische Extraktionen zur Bestimmung der Bindungsformen von Schwermetallen in Böden. *Bonner Bodenkundliche Abhandlungen* **17**, Rheinische Friedrich-Wilhelms-Universität Bonn, Germany, 284 p.

Zeien, H. and Brümmer, G. W., 1989. Chemical extraction to determine the chemical forms of heavy metals in soil (in German). *Mitt. Deutsch. Bodenkund. G.* **59**, 505-510.

Zhu, X. K., Guo, Y., Williams, R. J. P., O'Nions, R. K., Matthews, A., Belshaw, N. S., Canters, G. W., de Waal, E. C., Weser, U., Burgess, B. K., and Salvato, B., 2002. Mass fractionation processes of transition metal isotopes. *Earth. Planet. Sc. Lett.* **200**, 47-62.

Zhu, X. K., Li, S. Z., Luo, Y. M., and Wu, L. H., 2010. Copper isotope fractionation by higher plants. Geochim. Cosmochim. Acta 74, A1234.

E Stable Cu and Zn isotope ratios as tracers of sources and transport of Cu and Zn in contaminated soil

Moritz Bigalke[1,4*], Stefan Weyer[2+], Jozef Kobza[3], Wolfgang Wilcke[4]

[1]Johannes Gutenberg University Mainz, Earth System Science Research Center, Geographic Institute, Professorship of Soil Science/Soil Geography, Johann-Joachim-Becher-Weg 21, 55128 Mainz, Germany,

[2]University of Frankfurt, Institute of Geoscience, Altenhöferallee 1, 60438 Frankfurt am Main, Germany,

[3]Soil Science and Conservation Research Institute, Mládežnícka 36, 974 04 Banská Bystrica, Slovakia,

[4]Geographic Institute, University of Berne, Hallerstrasse 12, 3012 Berne, Switzerland

[+]Current address: Institute of Geology and Mineralogy, University of Cologne, Zülpicher Str. 49b, 50674 Köln

Geochimica et Cosmochimica Acta, DOI : 10.1016/j.gca.2010.08.044

1 Abstract

Copper and Zn metals are produced in large quantities for different applications. During Cu production, large amounts of Cu and Zn are released to the environment. Therefore, the surroundings of Cu smelters are frequently metal-polluted. We determined Cu and Zn concentrations and Cu and Zn stable isotope ratios (δ^{65}Cu, δ^{66}Zn) in three soils at distances of 1.1, 3.8, and 5.3 km from a Slovak Cu smelter and in smelter wastes (slag, sludge, ash) to trace sources and transport of Cu and Zn in soils. Stable isotope ratios were measured by multicollector inductively coupled plasma mass spectrometry (MC-ICP-MS) in total digests. Soils were heavily contaminated with concentrations up to 8087 µg g^{-1} Cu and 2084 µg g^{-1} Zn in the organic horizons. The δ^{65}Cu values varied little (-0.12 to 0.36‰) in soils and most wastes and therefore no source identification was possible. In soils, Cu became isotopically lighter with increasing depth down to 0.4 m, likely because of equilibrium reactions between dissolved and adsorbed Cu species during transport of smelter-derived Cu through the soil. The $\delta^{66}Zn_{IRMM}$ values were isotopically lighter in ash (-0.41‰) and organic horizons (-0.85 to -0.47‰) than in bedrock (-0.28‰) and slag (0.18‰) likely because of kinetic fractionation during evaporation and thus allowed for separation of smelter-Zn from native Zn in soil. In particular in the organic horizons large variations in δ^{66}Zn values occur, probably caused by biogeochemical fractionation in the soil-plant system. In the mineral horizons, Zn isotopes showed only minor shifts to heavier δ^{66}Zn values with depth mainly because of the mixing of smelter-derived Zn and native Zn in the soils. In contrast to Cu, Zn isotope fractionation between dissolved and adsorbed species was probably only a minor driver in producing the observed variations in δ^{66}Zn values. Our results demonstrate that metal stable isotope ratios may serve as tracer of sources, vertical dislocation, and biogeochemical behavior in contaminated soil.

2 Introduction

Toxic metals can be released into the environment by anthropogenic processes. Copper and Zn emissions from metal processing are the major sources of these metals in the atmosphere (Pacyna and Pacyna, 2001; Nriagu and Pacyna, 1988). In the direct surroundings of Cu smelters, the environment is frequently heavily contaminated (McMartin et al., 1999; Wilcke et al., 1999). Metals are emitted in gaseous or particulate form and may be deposited to the surface, contaminating waters and soils (Dudka and Adriano, 1997). However, they can also be transported in soils, and finally contaminate groundwater (Alloway, 1990).

Copper and Zn in dust was reported to be associated with S and O depending on the ore and processing step from which it was emitted (Barcan, 2002b). Williamson et al. (2004) observed chalcopyrite ($CuFeS_2$), Zn_2SnO_4, gunningite ($[Zn, Mn]SO_4 \cdot H_2O$), zincite (ZnO), and sphalerite (ZnS) as the main Cu and Zn minerals in dust and snow samples near a Cu smelter in Karabash (Russia), while Barcan (2002b) observed chalcopyrite ($CuFeS_2$), chalcocite (Cu_2S), covellite (CuS), cuprite (Cu_2O), tenorite (CuO), and metallic Cu(0) as the main Cu species in dust from a Cu-Ni smelter in Monchegorsk (Russia). During the smelting process, dust is emitted to the atmosphere and may reach the soil by dry or wet deposition. If soil is under forest, dust particles may adsorb onto plant surfaces, be washed to the soil by rain events or reach the soil with litterfall (Nieminen et al., 2004). Barcan (2002a) percolated organic layer material contaminated with dust from a Ni-Cu smelter and estimated that Cu would need 100-200 years to leach from organic layers into the mineral soil. McMartin et al. (1999) reported that most of the metals emitted from a smelter were fixed in the organic layers and only reach the mineral soil at strongly polluted sites. Zinc oxide (ZnO) from filter dust experimentally amended to field soils was dissolved completely within nine months. Half of the Zn re-precipitated as Zn-layered double hydroxide or Zn phyllosilicate, while the other half was adsorbed to relatively little mobile organic and inorganic soil particles (Voegelin et al., 2005).

Transport of Cu and Zn in soil occurs in dissolved or colloidal form (de Jonge et al., 2004; Keller and Domergue, 1996). In soil solutions, Cu and Zn mostly exist as Cu^{2+} and Zn^{2+}. Depending on pH and interacting substances, hydroxo-, (hydrogen)carbonato-

, sulfato-, and organo-complexes may also be present in various mixtures (Artiola, 2005; de Jonge et al., 2004; Günther and Kastenholz, 2005). Dissolved Cu and Zn species may adsorb on negatively charged surfaces of clay minerals and organic matter, and may be strongly bound at the surface of oxy(hydr)oxides as outer- or inner-spheric complexes or occluded in the oxides (Alcacio et al., 2001; Artiola, 2005; Contin et al., 2007; Dube et al., 2001, Ildefonse et al., 1986). Under reducing conditions, sulfides of Cu and Zn may form (Artiola, 2005; Günther and Kastenholz, 2005).

A recent review suggested Cd, Cu, and Zn isotopes as new tools to trace the sources of metals in the environment (Weiss et al., 2008). Similarly, Fe isotopes have been used for this purpose (Borrok et al., 2009; Majestic et al., 2009). Copper does not fractionate during the smelting process, probably because of its high boiling temperature, so that smelting products reflect the mineralogical differences of the processed ores (Gale et al., 1999; Mattielli et al., 2006). However, because Cu ores and minerals show a wide range of isotope ratios, with δ^{65}Cu of -17 to +10‰ (Mathur et al. 2009), which is far larger than the isotope fractionation in natural soils (ca.1‰ with clustering around 0‰, Bigalke et al., 2009), it is possible that Cu stable isotope ratios of anthropogenic emissions are different from those of natural soils.

Zinc isotope ratios have already been successfully used to distinguish between anthropogenic and natural metal sources (Chen et al., 2009; Cloquet et al., 2006; Sivry et al., 2008; Sonke et al., 2008). There are indications that the boiling point of Zn in Zn minerals is below the temperatures used in metal production with a blast furnace. Consequently, Zn is evaporated and the Zn vapor phase is enriched in light Zn isotopes, while the residues of the smelting process are enriched in heavy Zn isotopes (Mattielli et al., 2009). Because of the isotopic fractionation in the vapor phase, Zn emitted to the atmosphere is isotopically light and different from Zn in soils and rocks (Mattielli et al., 2009), while Zn released from waste dumps is isotopically heavy and can be distinguished from native Zn in sediment cores (Sivry et al., 2008). One first study reported that the isotope ratio of Zn pollution around a metal smelter also depends on distance from the smelter. They assumed that near the smelter heavy Zn blown out from waste dumps and ores contaminates the surroundings in addition to isotopically light Zn originating from the emissions of the smelting process, while at greater distances only the latter light Zn is deposited (Mattielli et al., 2009). As smelter-emitted Cu and Zn

enter soils from the surface, a separation of anthropogenic from native Cu and Zn with the help of the natural abundance of stable metal isotopes might help to better understand transport of these metals in soil.

The objectives of our study are (I) to trace sources of Cu and Zn emissions with the help of their stable isotope ratios and (II) to use Cu and Zn stable isotopes to assess the vertical transport of smelter-derived Cu and Zn in soil.

3 Materials and methods

3.1 Sampling site

Copper production in Krompachy (Slovakia) started in 1937 and is still on-going. Mainly sulfidic Cu ore concentrates, but also scrap, was processed in the smelter. The process of metal production from ore starts with a concentration melting step, followed by converting, fire refining, anode casting, and electrolytic refining, with at least 99.9% electrolytic Cu as the product. Since the year 2000, only scrap has been used for Cu production and parts of the production line were abandoned. During the lifetime of the smelter, different kinds of filters were used to prevent environmental pollution with fly ashes and SO_2 emissions (Turčan, 2006). Nevertheless, the surroundings of the smelter are heavily polluted with various metals including Cu and Zn (Wilcke et al., 1999). In the fly ash emitted during the various smelting processes, elements with low boiling points like Cd, Zn, Pb, and As are enriched compared to the ore because they are volatilized during the smelting process (Barcan, 2002b; Williamson et al., 2004). In Krompachy, fly ash from the shaft furnaces contained 50-60% Zn, 5-7%Pb, and 2-3% Sn in the 1950s before new filters were installed (Turčan, 2006). Besides emissions from furnaces and chimneys, dust originating from open-air ore storage and waste dumps may also contaminate the surroundings of smelters (Dudka and Adriano, 1997). During the lifetime of the smelter mainly local ore from Slovinky, Slovakia, and to a smaller extent also ore from other smaller Slovak and Romanian mines was processed (Turčan, 2006).

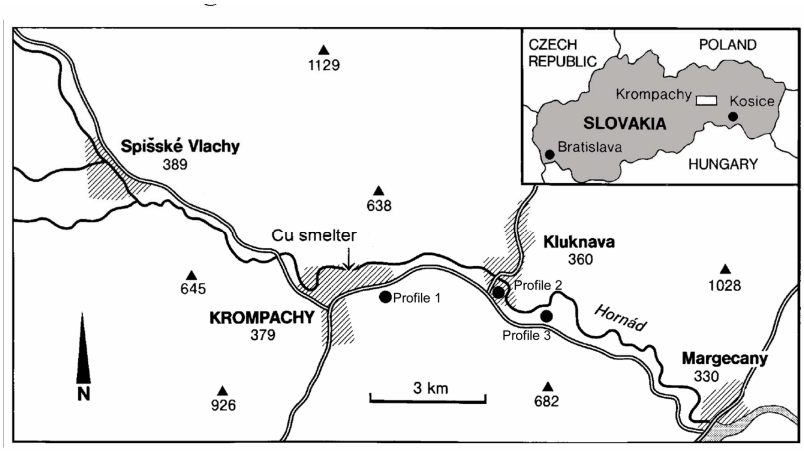

Figure E-1. Map of the Krompachy area in Slovakia (small map) and detailed map of Krompachy area with location of the smelter and sampled soil profiles. Hatched areas indicate settlements, black triangles indicate mountain tops, black line indicates river, white lines bordered by black lines indicate the main streets and all numbers indicate height above sea level.

3.2 Study soils

Three soils at different distances from the Cu smelter in Krompachy were sampled according to their pedogenetic horizons. Additionally, bedrock was sampled from an outcrop in the city of Krompachy and smelter wastes from a waste dump. All three soils were located in forests in the southeast (in main wind direction) of the smelter (Fig. E-1). The first soil was a Dystric Cambisol (IUSS Working Group WRB, 2006) at a distance of 1.1 km (Dystric Cambisol 1.1), the second soil was a Dystric Cambisol at a distance of 3.8 km (Dystric Cambisol 3.8) and the third soil was a Stagni-Eutric Cambisol at a distance of 5.3 km from the smelter. Each of the three soils had an organic layer on top of the mineral soil, each consisting of three organic horizons with total depths of 0.15, 0.13, and 0.04 m, respectively. The mineral soil of the Dystric Cambisol 1.1 and the Dystric Cambisol 3.8 consisted of A, B, and C horizons. The Stagni-Eutric Cambisol was influenced by stagnic water in the two mineral subsoil horizons (Bwg and Bg). All three soils developed from Permian tuffite at current mean annual temperatures of 7°C and mean annual rainfall of 700 mm. Vegetation was dominated by pine (*Pinus sylvestris* L., Dystric Cambisol 1.1) or spruce (*Picea abies* (L.) Karst., Dystric Cambisol 3.8, Stagni-Eutric Cambisol) and mixed with hornbeam (*Carpinus betulus* L.) and linden (*Tilia cordata* L.). The waste dump was located to the

west of the smelter. From the waste dump, we collected a grained slag and a hyaline tube furnace slag, two different sludges, and a rocklike heavy solid material. Additionally, an ash sample was supplied by the staff of the Cu smelter.

3.3 Sampling and sample preparation

The soil profiles were macroscopically characterized in the field according to FAO (2006) and each horizon was sampled in a representative way from the front of a hand-dug profile pit. The samples were air-dried and sieved to <2 mm. The pH was measured in 0.1 mol l^{-1} KCl at a soil:solution ratio of 1:2.5 after equilibration for two hours with a glass electrode. Total C, N, and S concentrations were determined by dry combustion with a CHNS analyzer (Vario EL, Elementar Analysensysteme, Hanau, Germany). The effective cation-exchange capacity (ECEC) was determined as the sum of the charge equivalents of Ca, K, Mg, Na, Mn, and Al extracted with 1 mol l^{-1} NH_4NO_3. Base saturation (BS) was calculated as the sum of the charge equivalents of Ca, Mg, Na, and K divided by ECEC and expressed in percent. In the 1 mol l^{-1} NH_4NO_3 extracts, concentrations of Ca, K, Mg, Na, Mn, and Al were measured by flame atomic absorption spectroscopy (FAAS, AA 400, Varian, Palo Alto, USA). Soil properties are summarized in Table E-1.

For Cu and Zn isotope analyses, and to determine total Cu and Zn concentrations, samples were ground in a ball mill. For isotope analysis of Cu and Zn, 100-400 mg of ground sample was weighed in a ceramic crucible and ashed at 450°C overnight. The samples were transferred to a microwave digestion vessel and digested at 200°C under pressure in a mixture of concentrated HF and concentrated HNO_3 (1:3) in a microwave oven (MARS5Xpress, CEM, Matthews, USA). Some samples of the organic horizons contained many hardly soluble organic compounds that were neither ashed nor dissolved with this method. Therefore, the procedure was modified for these samples. After ashing overnight the sample was digested first in 9 ml HNO_3 and 2 ml H_2O_2 with a maximum temperature of 225°C for 1 h, after cooling 3 ml of HF were added and the microwave program was repeated twice. This procedure resulted in clear digests. The samples were transferred to ®Savillex vials and evaporated to dryness on a hot plate, 1 ml of HNO_3 was added to drive off remaining HF and again evaporated to dryness. The sample was redigested in 10 mol l^{-1} HCl (with a few drops of H_2O_2) until all solids were

dissolved, evaporated to dryness again and redissolved in 7 mol l^{-1} HCl and 0.001% H_2O_2 for purification on anion-exchange resin.

Table E-1. Selected soil properties of the three study soils

Soil / Distance	Horizon	Depth cm	pH KCl	ECEC[a] mmol kg^{-1}	BS[b] %	C	N	S
						----------g kg^{-1}----------		
Dystric Cambisol 1.1 km	Oi[c]	15	4.0	221	89	454	20.6	3.3
	Oe[d]	10	4.0	168	81	357	19.5	3.5
	Oa[e]	4	4.6	117	71	279	11.1	2.8
	Ah[f]	0	3.9	111	81	47.8	3.4	0.6
	Bw[g]	-10	3.5	77	44	16.8	1.3	0.3
	C[h]	<-18	3.4	70	35	8.9	9.1	0.3
Dystric Cambisol 3.8 km	Oi[c]	17	4.1	200	91	465	16.2	2.6
	Oe[d]	13	3.8	181	74	385	16.5	3.0
	Oa[e]	3	4.1	161	40	240	10.8	2.2
	Ah[f]	0	3.2	103	27	31.9	1.6	0.4
	Bw[g]	-10	3.1	103	29	19.2	1.2	0.4
	C[h]	<-25	3.4	99	27	14.2	1.2	0.4
Stagnic-Eutric Cambisol 5.3 km	Oi[c]	4	4.9	391	97	452	18.6	2.7
	Oe[d]	3	4.5	433	96	361	19.8	3.0
	Oa[e]	1	4.6	349	93	226	14.2	2.3
	Ah[f]	0	5.2	173	99	29.3	2.1	0.4
	Bwg[i]	-15	4.9	124	94	8.9	0.8	0.2
	Bg[j]	<-30	4.9	86	95	6.0	0.7	0.2

(a) ECEC, effective cation exchange capacity; (b) BS, base saturation; (c) Oi, slightly decomposed organic matter; (d) Oe, moderately decomposed organic matter; (e) Oa, highly decomposed organic matter; (f) Ah, mineral surface horizon with accumulation of organic matter; (g) Bw, mineral subsurface horizon with development of color or structure; (h) C, horizon relatively unaffected by pedogenetic processes; (i) Bwg, mineral subsurface horizon with development of color or structure and influenced by stagnic water; (j) Bg, mineral subsurface horizon influenced by stagnic water.

Copper and Zn were separated from the matrix of the total digests by exchange chromatography using AG MP-1 ®Biorad resin after a protocol modified from Marechal et al. (1999). The resin was cleaned before purification (Bigalke et al., 2010a). Because of the low Cu to matrix ratio, one single purification run was not sufficient to achieve good matrix separation for Cu as some Ti remained in the sample. The Cu purification procedure was therefore repeated for each sample, which reduced Ti to irrelevant levels (Bigalke et al. 2010a). For Zn, a single purification step was sufficient. Purity of

extracts was checked for some selected samples, without finding relevant concentrations of interfering elements. After purification, the sample was dried and the residue treated with 200 µl of concentrated HNO_3 and 200 µl of 30% H_2O_2 to destroy organics released from the resin and drive off remaining HCl. After at least 3 h reaction time on a hot plate, the solution was evaporated and samples were redissolved in 2% HNO_3 for isotope ratio measurement. Recovery was checked for every Cu and Zn sample to rule out isotope fractionation on the resin (Marechal and Albarede, 2002). Recoveries were checked with electrothermal atomic absorption spectroscopy (Cu, ETAAS Unicam Solaar 989, Thermo Scientific, Waltham, USA) or flame atomic absorption spectroscopy (Zn, FAAS, AA 240 FS, Varian, Palo Alto, USA) and samples which did not show recovery of 100 ± 6% were discarded. Copper and Zn concentrations were measured in total digests by ETAAS and FAAS. The reproducibility of Cu and Zn concentration measurements was ca. 10% (2RSD) which is indicated by the size of the error bars in respective figures. Accuracy of concentration measurements was checked by repeated analysis of different reference materials and results were always within 10% of the certified values. The used reference materials with measured and certified values are listed in Table E-2.

All reagents used for the preparation of the isotope samples were of suprapur (Merck, Darmstadt, Germany), Rotipuran® supra (Carl Roth, Karlsruhe, Germany), or trace select (Fluka, Seelze, Germany) quality. Water was taken from a TKA GenPure UV (TKA, Niederelbert, Germany) water purification system and was of >18 MΩ cm quality. All critical steps were performed under clean-air conditions in a clean bench, evaporations were conducted in boxes supplied with hepa filtered air. Copper blanks for the whole procedure were 5.1 ± 5.4 (2SD) ng compared to at least 410 ng of Cu in the bedrock sample. For all other samples the mean Cu blank was less than 0.5% of the amount of Cu in the sample. Zinc blanks were 42.5 ± 63.5 (2SD) ng compared to at least 2408 ng of Zn in the tube furnace slag and 2743 ng of Zn in the bedrock sample. For all other samples, the mean Zn blank was less than 0.7% of the amount in the sample.

3.4 Copper and Zn isotope measurements

Copper and Zn isotope ratios were measured with a Finnigan-Neptune (Thermo Scientific, Waltham, MA, USA) multiple collector inductively-coupled plasma mass

spectrometer (MC-ICP-MS). The samples were introduced with a dual quartz glass spray chamber (Thermo Scientific). Aluminum cones were used to avoid contamination from the Ni cones. Copper isotope ratios were measured similarly to the method described in Bigalke et al. (2010a). A Ni standard (NIST 986) was added to all samples and the Cu standards prior to measurement and was used for instrumental mass bias correction (Li et al., 2009; Markl et al., 2006). Masses 60 (Ni), 61 (Ni), 62 (Ni), 63 (Cu), 64 (Zn+Ni), 65 (Cu), and 66 (Zn) were detected simultaneously. Mass bias was corrected according to the certified $^{62}Ni/^{60}Ni$ ratio (0.138600) of NIST 986 by applying the exponential law. The use of Ni for mass bias correction of Cu has been used in other studies before (Ehrlich et al. 2004, Li et al. 2009, Markl et al. 2006) because the mass bias of Cu and Ni is more similar than that of Cu and Zn, which is commonly used (eg. Marechal et al., 1999). This is probably attributable to more similar ionisation temperatures and result in ln ($^{65}Cu/^{63}Cu$) vs. ln ($^{62}Ni/^{60}Ni$) slopes very close to 1 (Fig. E-2).

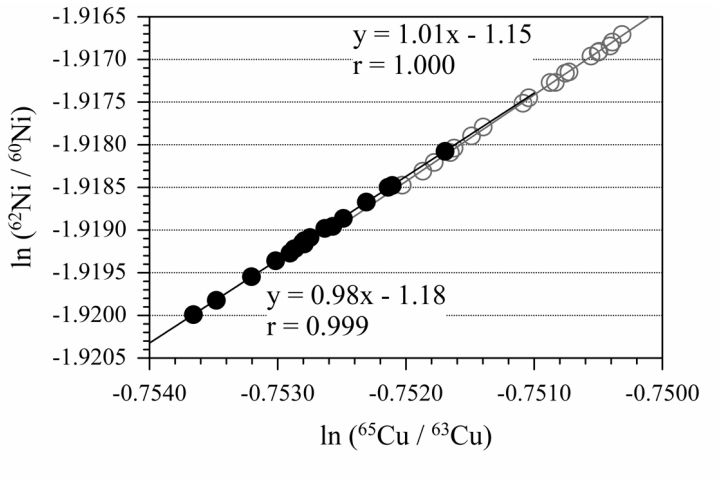

Figure E-2. ln $^{62}Ni/^{60}Ni$ vs ln $^{65}Cu/^{63}Cu$ plot of Nist 976 spiked with NIST 986 during two analytical sessions (filled and open dots).

After every third sample, the Cu standard (NIST 976) was measured. The $\delta^{65}Cu$ values of the samples were calculated as the deviation of the mass bias-corrected Cu isotope ratio of the samples from the mean of the mass bias-corrected Cu isotope ratios of the bracketing standards (Bigalke et al., 2010a; Li et al., 2009). Samples and standards were introduced in 2% HNO_3 at concentrations of 300 ng g^{-1} Cu and 1000 ng g^{-1} Ni. A Cu-ICP standard (Merck, Darmstadt, Germany) was used as an in-house

standard to check for intra-day and long-term reproducibility. The long-term reproducibility of this standard was 0.06‰ (2 SD, n = 49). Every purified sample was analyzed twice and the mean reported. The average reproducibility of different aliquots of samples that were separately digested, purified and measured was 0.08‰ (2SD), which is also displayed in the error bars in the figures. Where 2SD of individual samples was larger than 0.08‰, the larger value is displayed. All Cu isotope ratios were expressed as δ^{65}Cu values relative to the NIST 976 isotope reference material according to Equation D-1.

$$\delta^{65}Cu[‰] = \left(\frac{\left(^{65}Cu/^{63}Cu\right)_{sample}}{\left(^{65}Cu/^{63}Cu\right)_{NIST\,976}} - 1 \right) * 1000 \qquad \text{(E-1)}$$

A Cu in-house standard was used to correct the mass bias of Zn isotope measurements. The Cu standard was 0.84 ± 0.06‰ (2SD, n = 49) different from NIST 976 and the Zn isotope ratios were mass bias-corrected by applying the exponential law. After every third sample, the Zn standard (IRMM 3702) was measured. The δ^{66}Zn values of the samples were calculated as the deviation of the mass bias-corrected Zn isotope ratio of the samples from the mean of the mass bias-corrected Zn isotope ratios of the bracketing standards. Samples and standards were introduced in 2% HNO_3 at concentrations of 1000 ng g^{-1} Zn and 300 ng g^{-1} Cu. The Zn isotope ratios were measured relative to the Zn isotope reference material IRMM 3702 according to Equation D-2.

$$\delta^{66}Zn_{IRMM}[‰] = \left(\frac{(^{66}Zn/^{64}Zn)_{sample}}{(^{66}Zn/^{64}Zn)_{IRMM\,3702}} - 1 \right) * 1000 \qquad \text{(E-2)}$$

The long-term reproducibility of a Zn in-house standard was 0.08‰ (2SD, n=10). Every sample was measured twice and the mean reported. The average reproducibility of two to five aliquots of a samples that were separately digested, purified and measured was 0.07‰ (2SD). The long time reproducibility of 0.08‰ is indicated by the respective error bars in the figures. Where 2SD of individual samples was larger than 0.08‰ (2SD) the larger value is displayed. To check for mass dependency and absence of interferences δ^{66}Zn was plotted against δ^{67}Zn and δ^{68}Zn (Fig. E-3) and samples which did not show a proper fit were rejected.

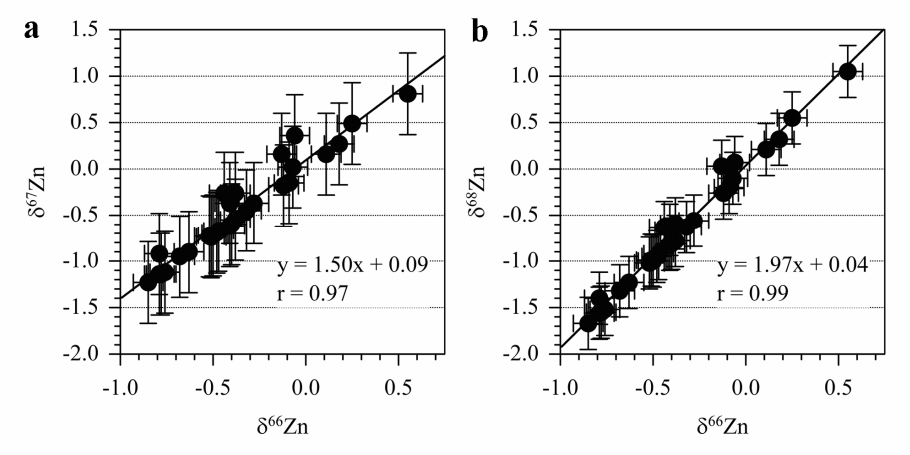

Figure E-3. Plot of (a) $\delta^{66}Zn$ vs. $\delta^{67}Zn$ and (b) of $\delta^{66}Zn$ vs. $\delta^{68}Zn$ of all investigated samples.

Because Zn isotope data are frequently reported relative to a Johnson Matthey (JMC) standard solution (batch 3-0749L), Zn isotope ratios measured relative to IRMM 3702 were converted by adding 0.32‰, which is the $\delta^{66}Zn_{JMC}$ value of the IRMM 3702 standard (Cloquet et al., 2006; John et al., 2007). The value of 0.32‰ may slightly change when more authors report their results. These changes are small compared to the total variation found in our samples (1.10‰). To generate values which can be compared to other studies which report $\delta^{66}Zn$ values relative to JMC Zn, $\delta^{66}Zn_{JMC}$ can be estimated with Equation D-3.

$$\delta^{66}Zn_{JMC\ Zn}[‰] \approx 0.32 + \left(\frac{(^{66}Zn/^{64}Zn)_{sample}}{(^{66}Zn/^{64}Zn)_{IRMM\,3702}} - 1 \right) * 1000 \qquad \text{(E-3)}$$

Use of this simplified equation induces an error. But this error is by far smaller than the analytical error and can be neglected for real world Zn isotope variations. The calculated $\delta^{66}Zn_{JMC}$ values are presented as an extra column in Table E-2, while all figures and the discussion are based on $\delta^{66}Zn_{IRMM}$ values.

Accuracy of isotope measurements was assessed by measuring reference materials from the United States Geological Survey (USGS): BCR-2, GSP-2 and NOD-P-1. $\delta^{65}Cu$ values measured for BCR-2 and GSP-2 reference material were 0.19 ± 0.06‰ and 0.35 ± 0.10‰ and thus similar to those reported in Bigalke et al (2010a; BCR-2 = 0.22 ± 0.06‰; GSP-2 = 0.25 ± 0.03‰). While BCR-2 seems to be slightly different from BCR-1 in respect to Cu isotopes (Bigalke et al, 2010a), the estimated $\delta^{66}Zn_{JMC}$ value of 0.22 ± 0.08‰ fits quite well the 0.20 ± 0.09‰ reported by Archer and Vance (2004) for

BCR-1. The $\delta^{65}Cu$ and estimated $\delta^{66}Zn_{JMC}$ values of NOD-P-1were 0.35 ± 0.11‰ and 0.84 ‰ respectively, and are thus not significantly different from values reported by Chapman et al. (2006; 0.46 ± 0.08‰; 0.78 ± 0.09‰).

4 Results and discussion

Natural systems are complex and the main challenge in discussing Cu and Zn isotope variation in these systems is the overlap of various possible fractionation processes. In our study, two generally different kinds of processes affect Cu and Zn isotope variations in the analyzed samples. The first group of processes is related to smelting and electroplating, which control metal isotope ratios in wastes of the processed ores and determine the isotope ratios of metal emissions and depositions to the soils. The second group of processes controlling isotope ratios are natural and include plant cycling, adsorption, precipitation, and mixing of different metal sources which occur in the soil and might help to understand the fate of metals after entering the soil.

4.1 Wastes

The technical products sampled from the waste dump of the smelter and the ash sample supplied by the smelter staff varied considerably in Cu and Zn concentrations and Cu and Zn isotope composition (Fig. E-4, Table E-2). The grained slag and fly ash had high Cu and Zn concentrations and $\delta^{65}Cu$ values close to zero. Similar $\delta^{65}Cu$ values in slag and ash of Cu smelting were also reported by Gale et al. (1999) and Mattielli et al. (2006), who attributed this finding to a lack of Cu isotope fractionation during smelting. The $\delta^{66}Zn$ value of the grained slag was positive and heavier by 0.49‰ and 1.03‰ than those of the slag and uppermost soil organic layers, respectively (Table E-2). The reason is Zn isotope fractionation during phase change in the smelting process, resulting in Zn isotopically light emissions and isotopically heavy Zn residues (Mattielli et al., 2009; Sonke et al., 2008).

Table E-2. Copper and Zn concentrations and $\delta^{65}Cu$ and $\delta^{66}Zn$ values

Profile / Distance	Horizont	Depth	Zn µg g^{-1}	$\delta^{66}Zn_{(IRMM\ Zn)}$ ‰[a]	*$\delta^{66}Zn_{(JMC\ Zn)}$ ‰[b]*	Cu µg g^{-1}	$\delta^{65}Cu_{(NIST\ 976)}$ ‰[a]
Dystric Cambisol 1.1 km	Oi	0 to -5	1081	-0.79	*-0.47*	4367	0.33
	Oe	-11	2084	-0.68	*-0.36*	8087	0.20
	Oa	-15	1715	-0.48[c]	*-0.16*	2636	0.19[c]
	Ah	-25	153	-0.44	*-0.12*	128	0.11
	Bw	-33	265	-0.50[c]	*-0.18*	12	0.17
	C	<-33	97	-0.40	*-0.08*	23	-0.12
Dystric Cambisol 3.8 km	Oi	0 to -4	1173	-0.79	*-0.47*	3335	0.34
	Oe	-14	1324	-0.78	*-0.46*	4605	0.19
	Oa	-17	1889	-0.52[c]	*-0.20*	3056	0.16[c]
	Ah	-27	99	-0.51	*-0.19*	72	0.09
	Bw	-42	79	-0.38	*-0.06*	26	-0.05
	C	<-42	52	-0.32	*0.00*	16	0.18
Stagni-Eutric Cambisol 5.3 km	Oi	0 to -1	1071	-0.85	*-0.53*	1168	0.36
	Oe	-3	925	-0.63	*-0.31*	2164	0.19
	Oa	-4	666	-0.47	*-0.15*	2016	0.16
	Ah	-19	233	-0.38	*-0.06*	162	0.1
	Bwg	-34	88	-	-	38	0.01
	Bg	<-34	57	-	-	17	0.00
Bedrock	Tuffite		28	-0.28	*0.04*	5	0.14[c]
Waste products	Grained slag		24044	0.18	*0.5*	14607	0.05
	Tube furnance slag		41	-0.41	*-0.09*	26	-
	Sludge 1		910	0.11	*0.43*	16989	1.81
	Sludge 2		29982	-0.76	*-0.44*	14961	0.81
	solid waste		18738	0.25	*0.57*	25110	0.16
	fly ash		437550	-0.41[c]	*-0.09*	9325	0.11[c]
Reference Materials	BCR-2[e]		140.3 (127±9)[d]	-0.09[c]	*0.23 (0.20±0.09)[e]*	17.6 (19±2)[d]	0.19[c] (0.22±0.06)[e]
	GSP-2[f]		119.3 (120±10)[d]	-	-	39.4 (43±4)[d]	0.35[c] (0.25±0.03)[f]
	SCL-7003[g]		76.7 (81±7.6)[d]	-	-	27.3 (29.1±0.8)[d]	-
	NOD-P-1[h]		1467.5 (1600±6)[d]	0.55	*0.87 (0.78±0.09)[h]*	11386.5 (11500±50)[d]	0.35[c] (0.46±0.08)[h]

(a) reproducibility of $\delta^{66}Zn$ and $\delta^{65}Cu$ values is 0.08‰; (b) $\delta^{66}Zn_{JMC}$ values as estimated from Equation E-3 (c) indicate samples which were independently digested, purified and analyzed 2-5 times; (d) values certified by USGS are given in brackets; (e) published isotope values: $\delta^{66}Zn$ 0.20 ± 0.09‰ (for BCR-1; Archer and Vance, 2004), $\delta^{65}Cu$ 0.22 ± 0.06‰ (Bigalke et al., 2010a), (f) published isotope values: $\delta^{65}Cu$ 0.25 ± 0.03‰ (Bigalke et al., 2010a); (h) approximated according to Equation E-3, published values: $\delta^{66}Zn_{JMC}$ 0.78 ± 0.09‰, $\delta^{65}Cu$ 0.46 ± 0.08‰ (Chapman et al., 2006).

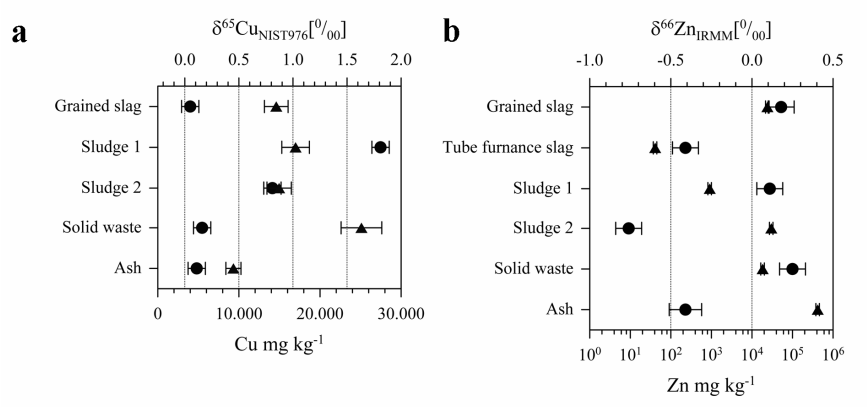

Figure E-4. (a) Cu concentrations (up-pointing triangles) and δ^{65}Cu values (dots) in the waste samples. (b) Zn concentrations (up-pointing triangles) and δ^{66}Zn values (dots) in the waste samples. Please mind the logarithmic scaling of Zn concentration axis.

The tube furnace slag showed markedly lower Cu and Zn concentration than the other technical materials (Table E-2). The δ^{66}Zn value of the tube furnace slag was similar to that of the ash sample. As slag is supposed to have a heavier δ^{66}Zn compared to ash, this would suggest that δ^{66}Zn in the ash from this production step would be even lighter compared with our ash sample. The resulting isotopically light Zn emissions (even lighter δ^{66}Zn value than -0.41‰ measured in the ash) would be in line with the low δ^{66}Zn values of the Oi horizons of the soils, where the deposition first arrives.

The two sludge samples possibly originate from electrolysis, acid leaching of minerals, or precipitation in neutralized waste waters. The two sludge samples had similarly high Cu concentrations and their δ^{65}Cu values were by far the highest in our study. The large isotope fractionation might be attributable to electrolytic refining. Electroplating, i.e. chemical reduction, of Fe and Zn results in the deposition of isotopically light metal leaving the dissolved metal isotopically heavy (Kavner et al., 2005; Kavner et al., 2008). Chemical reduction is also known to strongly fractionate Cu (Zhu et al., 2002). The δ^{66}Zn values of the two sludge samples differed by 0.86‰. Sludge 1 had a lower Zn concentration and a higher δ^{66}Zn value than Sludge 2. The positive δ^{66}Zn value of Sludge 1 is in accordance with the δ^{65}Cu values in both sludges and probably attributable to chemical reduction during electrolytic refining. We do not have an explanation for the negative δ^{66}Zn of Sludge 2.

The rock-like solid waste had high Cu and Zn concentrations. The δ^{65}Cu value was in the middle of the range observed in our study, while the δ^{66}Zn value was the most positive. Unfortunately, the production process from which the rock-like solid waste originated is unknown. The Cu concentration in the ash was 0.93% and the δ^{65}Cu value was similar to that of slag which further supports the assumption that Cu isotopes were not fractionated during smelting (Gale et al., 1999). The ash had a Zn concentration of 44% and a negative δ^{66}Zn value, which is in line with the assumption of Zn isotope fractionation during evaporation. The Cu and Zn stable isotope ratios in the studied waste materials seem to be mainly influenced by redox processes during electrolytic refining and in the case of Zn additionally by fractionation during evaporation.

4.2 Source tracing of Cu and Zn

Strong Cu and Zn accumulations in the soil organic layers indicate strong contamination of the investigated soils, and the decreasing Cu and Zn concentrations with increasing distance from the smelter reveal the smelter as the point source (Figs. E-5 & E-6, Table E-2). The fact that Cu concentrations in the organic layers were higher than Zn concentrations, although Zn is enriched in fly ash because of its low boiling point (e.g., in our ash sample, Table E-2), indicate that large proportions of Cu in organic layers originate from emissions of open-air storage of ores, waste, and working units and not from the smelting process itself. On the other hand, Zn is likely mainly distributed via emissions from the chimney, as can be seen from light δ^{66}Zn. In contrast to the concentrations, δ^{65}Cu and δ^{66}Zn values were not related to distance from the smelter (Table E-2).

In the absence of a Cu isotope fractionation by smelting (Gale et al., 1999), Cu emissions mainly reflect the Cu isotope composition of the processed ores (Mattielly et al., 2006). Although δ^{65}Cu values in ores and minerals cover a wide range (-17 to +10‰, Mathur et al. 2009), the δ^{65}Cu values in most primary magmatic sulfides – mainly used in the studied smelter – display only a limited spread (Graham et al., 2004; Larson et al., 2003; Markl et al., 2006; Mason et al., 2005). Stronger fractionations seem to be coupled to secondary processes like oxidation, reduction, and remineralization taking place in ore deposits (Asael et al., 2007).

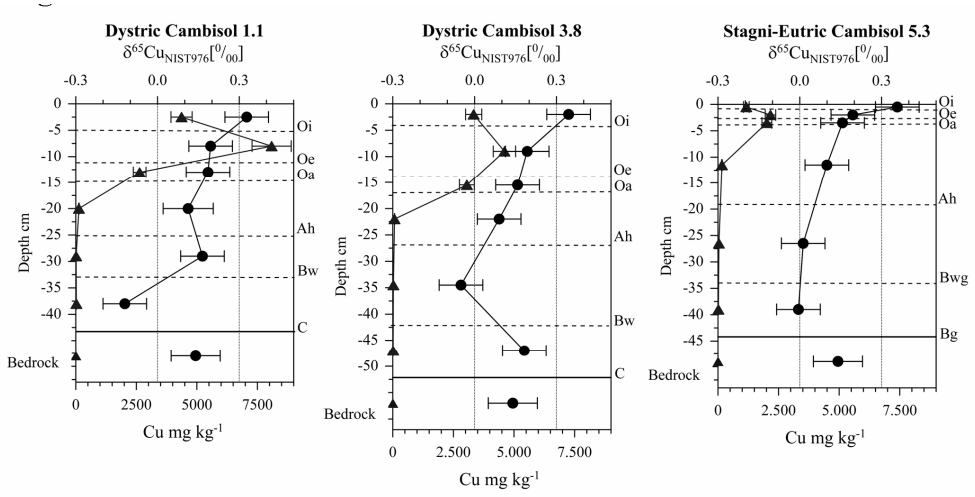

Figure E-5. Depth distribution of Cu concentrations (up-pointing triangles) and δ^{65}Cu values (dots) in the three soil profiles and bedrock.

As Zn isotope variations in natural materials on Earth are small, but large during high-temperature combustion, Zn isotopes are particularly useful for the identification of smelter-induced contamination. In soils in the surroundings of a Pb-Zn refinery, Matielli et al. (2009) observed variations in δ^{66}Zn values of up to 0.7‰. Near the smelter, coarse particles from slag heaps and working units were interpreted to cause a heavier Zn isotope signal, while emissions from the main chimney had δ^{66}Zn values down to -0.67‰ and caused negative δ^{66}Zn values in depositions at greater distance (1720-4560 m). Zinc isotope ratios have furthermore already been used for source identification of anthropogenic Zn in the atmosphere (Cloquet et al., 2006; Dolgopolova, 2006; Mattielli et al., 2009), rain water (Luck and Ben Othman, 1998), rivers (Borrok et al., 2009; Chen et al., 2008; Chen et al., 2009), sediments (Sivry et al., 2008; Sonke et al., 2008), and peat (Weiss et al., 2007).

The Oi horizons had heavier δ^{65}Cu and lighter δ^{66}Zn values than deeper horizons (Figs. E-5 & E-6, Table E-2). The uppermost organic soil horizon (Oi) is thought to be closest to the isotope signature of emitted dust because it is directly impacted by smelter dust. The Cu and Zn isotope composition of Oi horizons can therefore be considered as a mixture of Cu and Zn originating from smelter and tailing dusts and native Cu and Zn in soil. The Cu and Zn isotope signature of this mixture is modified by biogeochemical and physical processes in the soil-plant system.

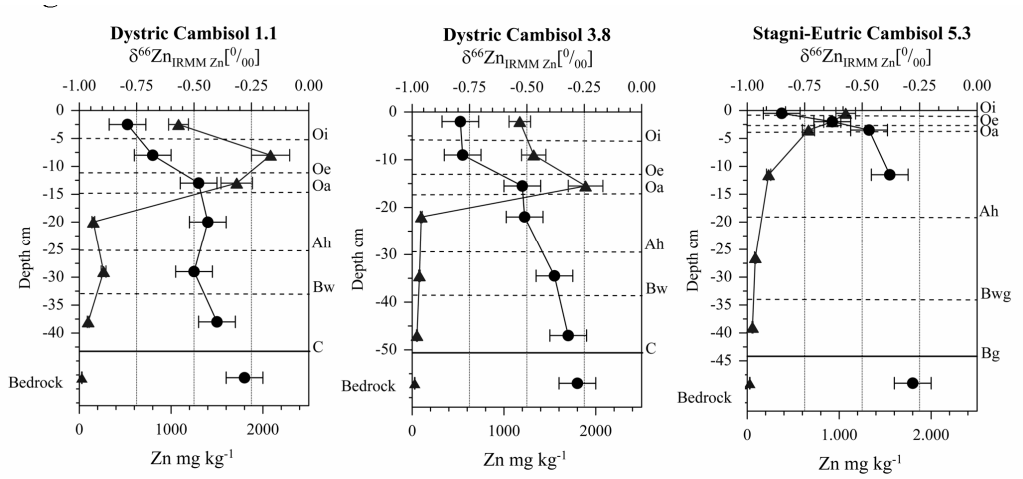

Figure E-6. Depth distribution of Zn concentrations (up-pointing triangles) and δ^{66}Zn values (dots) in the three soil profiles and bedrock.

The heavier δ^{65}Cu values in Oi horizons than in deeper soil horizons (Fig. E-5, Table E-2) are in contrast to some initial δ^{65}Cu values reported for unpolluted soils in which organic horizons are enriched in the light ^{63}Cu isotope (Bigalke et al. 2009), which is assumed to be caused by plant-induced fractionation (Jouvin et al., 2008). However, given the large contribution of smelter-derived Cu to total Cu concentrations in the Oi horizons, the effect of plant-induced fractionation may be small compared to the Cu isotope signal introduced by the smelter.

The lighter δ^{66}Zn values of the Oi horizons than the deeper soil horizons in our study area (Fig. E-6, Table E-2) further support the assumption that Zn in soils originated mainly from the emission of the smelting process and not from resuspension of Zn from slag dumps, ore storages, and working units. The fact that δ^{66}Zn values in organic layers were even lighter than in the ash (Table E-2) might be attributable to mixing of different emissions from different processing steps (Mattielli et al., 2009) and further biogeochemical fractionation in the soil-plant system (see below).

Because of the small total variation of Cu and the similar δ^{65}Cu values in bedrock, organic layers, ash, and slags, Cu does not seem to be suitable for source tracing in our study area while the significantly lighter δ^{66}Zn values of the smelter emissions render the isotope ratios of Zn a suitable tracer of smelter-derived Zn in soil. This assumption is supported by the mixing plots of δ^{65}Cu and δ^{66}Zn values versus their reverse

concentrations which only supported two-end-member mixing for Zn in the mineral soil (Fig. E-7).

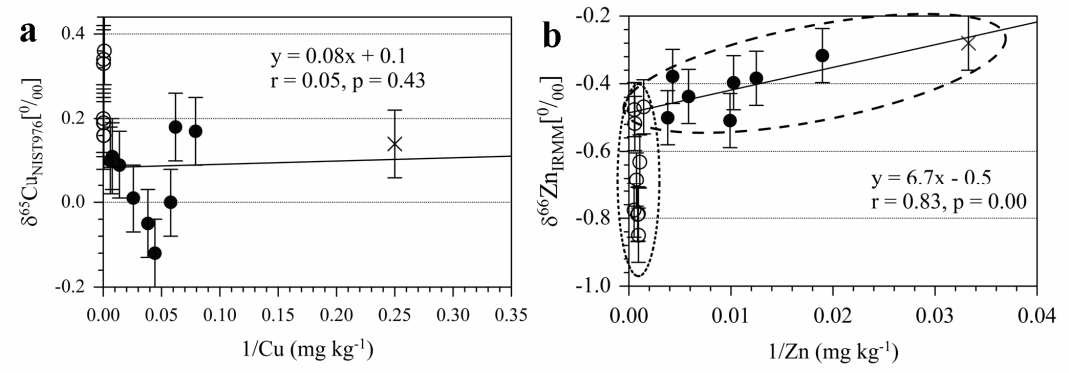

Figure E-7. Mixing plots of (a) δ^{65}Cu values vs. 1/Cu concentrations and (b) δ^{66}Zn values vs. 1/Zn concentrations. Values for organic horizons (open circles), mineral horizons (dots) and bedrock (X) are given. Straight lines show correlations for lowermost organic horizons (Oa), mineral horizons and bedrock, numbers for y, r and p refer to these correlations. Dotted ovals in plot b should help to visualize the two overlapping groups of organic and mineral horizons in which variation of δ^{66}Zn is probably driven by different mechanisms. High variation in organic horizons is thought to be mainly caused by biogeochemical cycling in the soil plant system, while variation in subsoil is possibly due to mixing of Zn leached from the organic horizons and Zn originating from the weathering of bedrock.

4.3 Variations in Cu isotope ratios in soil

The variations in δ^{65}Cu values of Cu in the studied soils cannot just be explained by mixing of natural and anthropogenic Cu because of similar δ^{65}Cu values in deposition, soil, and bedrock. Therefore, biogeochemical Cu fractionation in soil needs to be considered to explain the observed patterns. If the data of all studied soils is combined, the decreasing δ^{65}Cu values in soil down to 0.4 m depth (Fig. E-8) might be explained by fractionation of Cu during transport through the soil. The deposited smelter-derived Cu is first dissolved in the soil solution and then interacts with soil-internal surfaces causing Cu isotope fractionations. During sorption on oxy(hydr)oxides (Balistrieri et al., 2008; Clayton et al., 2005; Pokrovsky et al., 2008), organic matter (Bigalke et al. 2010b) and possibly also on other adsorption sites in soil, heavy Cu is preferentially bound leaving the solution enriched in isotopically light Cu. Consequently, the isotopically light Cu is preferentially leached to deeper soil horizons explaining decreasing δ^{65}Cu values down the profile (Fig. E-8). In principle, this effect is similar to

isotope fractionation observed on ion exchange columns (Marechal and Albarede, 2002), albeit opposite in direction.

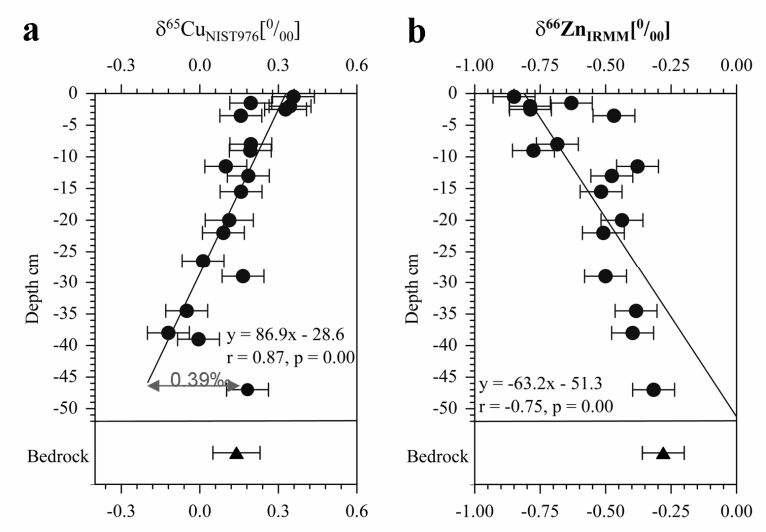

Figure E-8. (a) Relationship between soil depth and δ^{65}Cu values in all three soils (dots) and bedrock (up-pointing triangle). (b) Relationship between soil depth and δ^{66}Zn values in all three soils (dots) and bedrock (up-pointing triangle).

The deepest soil horizon at 0.47 m (C horizon of the Dystric Cambisol 3.8) showed a δ^{65}Cu value deviating from this trend by 0.39‰ but is almost identical with the δ^{65}Cu value of the bedrock (Fig. E-8). This might indicate that at a depth of >0.4 m, the soil is not, or only little, affected by the input of anthropogenic Cu, and that anthropogenic Cu has only been transported to a depth of ca. 0.4 m during the 60 years between the start of smelting operations and sampling. This would mean a transport rate of 0.0066 m y^{-1} and seems realistic when compared to Pb which was reported to migrate ca. 0.005 m y^{-1} (Erel et al., 1997). But as this assumption is only based on a single soil sample at this depth, our interpretation must be considered as preliminary.

Another possible reason for Cu isotope fractionation in the soil profile is the fact, that in smelter dust, Cu occurs as chalcopyrite ($CuFeS_2$), calcosite (Cu_2S) covellite (CuS), cuperite (Cu_2O), tenorite (CuO), and metallic Cu (Barcan, 2002b; Williamson et al., 2004) and thus partly in a reduced oxidation state (Cu^+, elemental Cu) and immobile forms. Accordingly, Cu transported in the soil must have undergone changed speciation to mobil and probably oxidized species (Cu^{2+}), which is likely coupled to isotope

fractionation. However, this type of isotope fractionation can hardly explain the observed systematic depth distribution of the δ^{65}Cu values.

4.4 Variations in Zn isotope ratios in soil

Zinc isotope ratios in the soils are clearly influenced by the smelter-derived deposition as can be seen from very light δ^{66}Zn in topsoils. Zinc concentrations decrease with depth while δ^{66}Zn values became heavier until reaching the δ^{66}Zn value of bedrock in C horizons (Figs. E-6 & E-8). The strongest variations in δ^{66}Zn values occurred in the organic horizons and are associated with the highest Zn concentrations in soil (Fig. E-6).

With increasing state of decomposition, organic horizons become heavier from Oi to Oa horizons to a similar extent (0.27-0.38‰) in the three soil profiles (Fig. E-6, Table E-2). Possible explanations for this depth gradient in Zn isotope ratios include biogeochemical fractionation within the soil-plant system, changes in Zn speciation during alteration of Zn dust and Zn transport in soil. A portion of soil Zn is recycled by plants and returned to the Oi horizon via litterfall. In the plant, Zn isotopes are fractionated, with shoots and leaves being isotopically lighter than roots (Moynier et al., 2009, Weiss et al. 2005). Thus, plant-induced Zn isotope fractionation might contribute to the observed depth distribution of δ^{66}Zn values in the study soils by recycling leaves enriched in light isotopes to the soil surface, and may also explain why the organic layers show even lighter δ^{66}Zn value than the ash (Table E-2). Biological fractionation of Zn isotopes was suggested to be a major factor affecting δ^{66}Zn values in biogeochemical systems (Viers et al., 2007; Weiss et al., 2005). Another reason for the increasingly higher δ^{66}Zn values in deeper organic horizons might be the release of light Zn during alteration of deposition Zn dusts (Voegelin et al., 2005) and decomposition of organic layers and subsequent leaching of isotopically light Zn into the mineral soil leaving the more decomposed older Oe and Oa horizons heavier. This is supported by the fact that the studied A horizons still had lighter δ^{66}Zn values than the bedrock. Similar findings were reported by Couder et al. (2009), who observed a 0.41‰ lighter δ^{66}Zn value in litter leachate than in bulk O horizons.

Zinc isotope ratios in the mineral horizons show only little variation and approach that of the bedrock with increasing depth (Fig. E-8b). A mixing plot of Zn (Fig. E-7b)

implies two different fractionation processes in organic layers and in the mineral horizons, respectively. The δ^{66}Zn values of Oa horizons (the organic horizons directly above mineral soil surface), mineral soil and bedrock all fall on the same mixing line (Fig. E-7b), suggesting that variations δ^{66}Zn values of these horizons can mainly be explained by mixing of isotopically light Zn leached from organic layers and native Zn of bedrock. The correlation implies that 69% of the variation in δ^{66}Zn values in the mineral horizons can be explained by mixing of these two end members.

The depth trend of δ^{66}Zn values is in opposite direction than that observed for δ^{65}Cu values in the same profiles. For Cu, we assume isotope fractionation during transport because of interaction with soil sorption sites. Because of the stronger binding of ^{65}Cu to sorption sites, the light Cu is preferentially translocated to deeper soil horizons. The effect of the interaction of Zn with adsorption sites on δ^{66}Zn values seems to be less homogeneous. Zinc adsorption on oxy(hydr)oxides causes Zn isotope fractionations with opposing directions of $\Delta^{66}Zn_{solid\text{-}solution}$ from -0.2 to 0.6‰ depending on the type of mineral and pH (Balistrieri et al., 2008; Pokrovsky et al., 2005) and complexation on purified humic acid causes fractionation of 0.24‰ ($\Delta^{66}Zn_{PHA\text{-}solution}$) only at pH > 6 (Jouvin et al., 2009), which is much higher than the pH in our study soils (Table E-1). Transport through an anion-exchange resin in strong hydrochloric acid media caused a Zn isotope fractionation that was an order of magnitude smaller than that of Cu (Marechal and Albarede, 2002). Thus, we assume that fractionation of δ^{66}Zn values during transport of Zn through the soil was weak compared to Cu and probably only had minor affects on the δ^{66}Zn values in the studied soils. This is in accordance with Pokrovsky et al. (2005), who postulated that adsorption reactions only contribute to a minor degree to Zn isotope fractionation in natural settings, and that co-precipitation and biological uptake are the main fractionating mechanisms.

5 Conclusions

1. At our study site, source identification of Cu with the help of stable Cu isotope ratios was not possible because the smelter-related Cu variation was in the range of that observed in soils. But Cu isotopes may allow for estimation of contaminant transport and are thus valuable for investigation of polluted soils. Zinc was already proven to be a powerful source tracer in several studies and this is confirmed in our study. However, biogeochemical processes in soil modify the δ^{66}Zn values in addition to mixing of smelter-derived with native Zn in soil.
2. Copper isotopes were fractionated during transport in soil, probably because of interactions with sorption sites. Equilibrium fractionation between dissolved and sorbed species is assumed to cause a trend to lighter Cu isotope composition down to a depth of ca. 0.4 m. One horizon sampled at greater depth showed a δ^{65}Cu value similar to the bedrock and is thought not to be affected by smelter-derived Cu. We attribute the trend to lighter δ^{65}Cu values with increasing soil depth to the transport of smelter-derived Cu in soil and suggest that the depth of 0.4 m is the location of the Cu leaching front after 60 years of smelting. The depth distribution of δ^{66}Zn in the organic horizons can be explained by the admixture of smelter-derived Zn and cycling of Zn in the soil-plant system, which both fractionates Zn towards isotopically lighter δ^{66}Zn values. The small variations in the mineral soil can probably attributed to mixing of light Zn leached from the organic layer into the mineral soil with native Zn in soil.

The differences in δ^{66}Zn values and the depth distributions of δ^{65}Cu and δ^{66}Zn values allow for conclusions on source, biogeochemical behavior, and depth transport of Cu and Zn in soil.

6 Acknowledgments

Prescribed by the regulations of the internet publisher (ArchiMed) this section had to be deleted for data protection reasons. I want to thank all people listed in the printetd version.

7 References

Alcacio, T. E., Hesterberg, D., Chou, J. W., Martin, J. D., Beauchemin, S., and Sayers, D. E., 2001. Molecular scale characteristics of Cu(II) bonding in goethite-humate complexes. Geochim. Cosmochim. Acta 65, 1355-1366.

Alloway, B. J., 1990. Heavy metals in soils. Blackie, Halsted Press, Glasgow, New York.

Archer, C. and Vance, D., 2004. Mass discrimination correction in multiple-collector plasma source mass spectrometry: an example using Cu and Zn isotopes. J. Anal. Atom. Spectrom. 19, 656-665.

Artiola, J. F., 2005. Speciation of copper in the environment. In: Cornelis, R. (Ed.), Handbook of elemental speciation 2 - species in the environment, food, medicine an occupational health. John Wiley & Sons, Chinchester.

Asael, D., Matthews, A., Bar-Matthews, M., and Halicz, L., 2007. Copper isotope fractionation in sedimentary copper mineralization (Tinma Valley, Israel). Chem. Geol. 243, 238-254.

Balistrieri, L. S., Borrok, D. M., Wanty, R. B., and Ridley, W. I., 2008. Fractionation of Cu and Zn isotopes during adsorption onto amorphous Fe(III) oxyhydroxide: Experimental mixing of acid rock drainage and ambient river water. Geochim. Cosmochim. Acta 72, 311-328.

Barcan, V., 2002a. Leaching of nickel and copper from soil contaminated by metallurgical dust. Environ. Int. 28, 63-68.

Barcan, V., 2002b. Nature and origin of multicomponent aerial emissions of the copper-nickel smelter complex. Environ. Int. 28, 451-456.

Bigalke, M., Weyer, S., and Wilcke, W., 2009. Isotopic fractionation of copper during soil genesis. Geochim. Cosmochim. Acta 73, A121-A121.

Bigalke, M., Weyer, S., and Wilcke, W., 2010a. Stable copper isotopes: A novel tool to trace copper behavior in hydromorphic soils. Soil Sci. Soc. Am. J. 74, 60-73.

Bigalke, M, Weyer S., Wilcke W., 2010b. Copper isotope fractionation during complexation with insolubilized humic acid. Environ. Sci. Technol. Doi: 10.1021/es1017653

Borrok, D. M., Wanty, R. B., Ridley, W. I., Lamothe, P. J., Kimball, B. A., Verplanck, P. L., and Runkel, R. L., 2009. Application of iron and zinc isotopes to track the

sources and mechanisms of metal loading in a mountain watershed. Appl. Geochem. 24, 1270-1277.

Chapman, J. B., Mason, T. F. D., Weiss, D. J., Coles, B. J., and Wilkinson, J. J., 2006. Chemical separation and isotopic variations of Cu and Zn from five geological reference materials. Geostandard Geoanal. Res. 30, 5-16.

Chen, J. B., Gaillardet, J., and Louvat, P., 2008. Zinc isotopes in the Seine River waters, France: A probe of anthropogenic contamination. Environ. Sci. Technol. 42, 6494-6501.

Chen, J. B., Gaillardet, J., Louvat, P., and Huon, S., 2009. Zn isotopes in the suspended load of the Seine River, France: Isotopic variations and source determination. Geochim. Cosmochim. Acta 73, 4060-4076.

Clayton, R. E., Hudson-Edwards, K. A., and Houghton, S. L., 2005. Isotopic effects during Cu sorption onto goethite. Geochim. Cosmochim. Acta 69, A216-a216.

Cloquet, C., Carignan, J., and Libourel, G., 2006. Isotopic composition of Zn and Pb atmospheric depositions in an urban/periurban area of northeastern France. Environ. Sci. Technol. 40, 6594-6600.

Contin, M., Mondini, C., Leita, L., and De Nobili, M., 2007. Enhanced soil toxic metal fixation in iron (hydr)oxides by redox cycles. Geoderma 140, 164-175.

Couder, E., Delvaux, B., Maerschalk, C., and Mattielli, N., 2009. Delta (66) Zn as a tracer of the zinc biogeochemical cycle. Geochim. Cosmochim. Acta 73, A247-A247.

de Jonge, L. W., Kjaergaard, C., and Moldrup, P., 2004. Colloids and colloid-facilitated transport of contaminants in soils: An introduction. Vadose Zone J. 3, 321-325.

Dolgopolova, A., D.J. Weiss, R. Seltmann, B. Kober, T.F.D. Mason, B. Coles, C.J. Stanley, 2006. Use of isotope ratios to assess sources of Pb and Zn dispersed in the environment during mining and ore processing within the Orlokava-Spokinoe mining site (Russia). Appl. Geochem., 563-579.

Dube, A., Zbytniewski, R., Kowalkowski, T., Cukrowska, E., and Buszewski, B., 2001. Adsorption and migration of heavy metals in soil. Pol. J. Environ. Stud. 10, 1-10.

Dudka, S. and Adriano, D. C., 1997. Environmental impacts of metal ore mining and processing: A review. J. Environ. Qual. 26, 590-602.

Erel, Y., Veron, A. and L. Halicz, L., 1997. Tracing the transport of anthropogenic lead in the atmosphere and in soils using isotope ratios. Geochim. Cosmochim. Acta 61, 4495-4505.

Ehrlich, S., Butler, I., Halicz, L., Rickard, D., Oldroyd, A., and Matthews, A., 2004. Experimental study of the copper isotope fractionation between aqueous Cu(II) and covellite, CuS. Chem Geol 209, 259-269.

FAO, 2006. Guidlines for soil description. Food and Agriculture Organization of the United Nations, Rome.

Gale, N. H., Woodhead, A. P., Stos-Gale, Z. A., Walder, A., and Bowen, I., 1999. Natural variations detected in the isotopic composition of copper: Possible applications to archaeology and geochemistry. Int. J. Mass Spectrom. 184, 1-9.

Graham, S., Pearson, N., Jackson, S., Griffin, W., and O'Reilly, S. Y., 2004. Tracing Cu and Fe from source to porphyry: In situ determination of Cu and Fe isotope ratios in sulfides from the Grasberg Cu-Au deposit. Chem. Geol. 207, 147-169.

Günther, K. and Kastenholz, B., 2005. Speciation of Zinc. In: Cornelis, R., Caruso, J., Crews, H., and Heumann, K. Eds.), Handbook of elemental speciation II - species in the environment, food, medicine and occupational health. John Wiley &Sons Ltd, Chichester.

Ildefonse, P., Manceau, A., Prost, D., and Groke, M. C. T., 1986. Hydroxy-Cu-vermiculite formed by the weathering of Fe-biotites at Salobo, Carajas, Brazil. Clay. Clay Miner. 34, 338-345.

IUSS Working Group WRB, 2006. World Soil Resource Reports No. 103. FAO, Rome.

John, S. G., Geis, R. W., Saito, M. A., and Boyle, E. A., 2007. Zinc isotope fractionation during high-affinity and low-affinity zinc transport by the marine diatom Thalassiosira oceanica. Limnol. Oceanogr. 52, 2710-2714.

Jouvin, D., Louvat, P., Marechal, C., and Benedetti, M. F., 2008. Fractionation of copper isotopes in plants. Geochim. Cosmochim. Acta 72, A441-a441.

Jouvin, D., Louvat, P., Juillot, F., Marechal, C. N., and Benedetti, M. F., 2009. Zinc isotopic fractionation: Why organic matters. Environ. Sci. Technol. 43, 5747-5754.

Kavner, A., Bonet, F., Shahar, A., Simon, J., and Young, E., 2005. The isotopic effects of electron transfer: An explanation for Fe isotope fractionation in nature. Geochim. Cosmochim. Acta 69, 2971-2979.

Kavner, A., John, S. G., Sass, S., and Boyle, E. A., 2008. Redox-driven stable isotope fractionation in transition metals: Application to Zn electroplating. Geochim. Cosmochim. Acta 72, 1731-1741.

Keller, C. and Domergue, F. L., 1996. Soluble and particulate transfers of Cu, Cd, Al, Fe and some major elements in gravitational waters of a Podzol. Geoderma 71, 263-274.

Larson, P. B., Maher, K., Ramos, F. C., Chang, Z. S., Gaspar, M., and Meinert, L. D., 2003. Copper isotope ratios in magmatic and hydrothermal ore-forming environments. Chem. Geol. 201, 337-350.

Li, W. Q., Jackson, S. E., Pearson, N. J., Alard, O., and Chappell, B. W., 2009. The Cu isotopic signature of granites from the Lachlan Fold Belt, SE Australia. Chem. Geol. 258, 38-49.

Luck, J. M. and Ben Othman, D., 1998. Geochemistry and water dynamics II. Trace metals and Pb-Sr isotopes as tracers of water movements and erosion processes. Chem. Geol. 150, 263-282.

Majestic, B. J., Anbar, A. D., and Herckes, P., 2009. Elemental and iron isotopic composition of aerosols collected in a parking structure. Sci. Total Environ. 407, 5104-5109.

Marechal, C. N., Telouk, P., and Albarede, F., 1999. Precise analysis of copper and zinc isotopic compositions by plasma-source mass spectrometry. Chem. Geol. 156, 251-273.

Marechal, C. and Albarede, F., 2002. Ion-exchange fractionation of copper and zinc isotopes. Geochim. Cosmochim. Acta 66, 1499-1509.

Markl, G., Lahaye, Y., and Schwinn, G., 2006. Copper isotopes as monitors of redox processes in hydrothermal mineralization. Geochim. Cosmochim. Acta 70, 4215-4228.

Mason, T. F. D., Weiss, D. J., Chapman, J. B., Wilkinson, J. J., Tessalina, S. G., Spiro, B., Horstwood, M. S. A., Spratt, J., and Coles, B. J., 2005. Zn and Cu isotopic

variability in the Alexandrinka volcanic-hosted massive sulphide (VHMS) ore deposit, Urals, Russia. Chem. Geol. 221, 170-187.

Mattielli, N., Rimetz, J., Petit, J., Perdrix, E., Deboudt, K., Flament, P., and D. Weis, 2006. Zn-Cu isotopic study and speciation of airborne metal particles within a 5-km zone of a lead zinc smelter. Geochim. Cosmochim. Acta 70, A 401.

Mattielli, N., Petit, J. C. J., Deboudt, K., Flament, P., Perdrix, E., Taillez, A., Rimetz-Planchon, J., and Weis, D., 2009. Zn isotope study of atmospheric emissions and dry depositions within a 5 km radius of a Pb-Zn refinery. Atmos. Environ. 43, 1265-1272.

Mathur, R., Titley, S., Barra, F., Brantley, S., Wilson, M., Phillips, A., Munizaga, F., Maksaev, V., Vervoort, J., and Hart, G., 2009. Exploration potential of Cu isotope fractionation in porphyry copper deposits. J. Geochem. Explor. 102, 1-6.

McMartin, I., Henderson, P. J., and Nielsen, E., 1999. Impact of a base metal smelter on the geochemistry of soils of the Flin Flon region, Manitoba and Saskatchewan. Can. J. Earth Sci. 36, 141-160.

Moynier, F., Pichat, S., Pons, M. L., Fike, D., Balter, V., and Albarede, F., 2009. Isotopic fractionation and transport mechanisms of Zn in plants. Chem. Geol. 267, 125-130.

Nieminen, T. M., Derome, J., and Saarsalmi, A., 2004. The applicability of needle chemistry for diagnosing heavy metal toxicity to trees. Water Air Soil Poll. 157, 269-279.

Nriagu, J. O. and Pacyna, J. M., 1988. Quantitative assessment of worldwide contamination of air, water, and soils by trace metals. Nature 333, 134-139.

Pacyna, J.M., Pacyna, E.G., 2001. An assessment of global and regional emissions of trace metals to the atmosphere from anthropogenic sources worldwide, Environ. Rev. 9, 269-298.

Pokrovsky, O. S., Viers, J., and Freydier, R., 2005. Zinc stable isotope fractionation during its adsorption on oxides and hydroxides. J. Colloid Interf. Sci. 291, 192-200.

Pokrovsky, O. S., Viers, J., Emnova, E. E., Kompantseva, E. I., and Freydier, R., 2008. Copper isotope fractionation during its interaction with soil and aquatic

microorganisms and metal oxy(hydr)oxides: Possible structural control. Geochim. Cosmochim. Acta 72, 1742-1757.

Sivry, Y., Riotte, J., Sonke, J. E., Audry, S., Schafer, J., Viers, J., Blanc, G., Freydier, R., and Dupre, B., 2008. Zn isotopes as tracers of anthropogenic pollution from Zn-ore smelters in the Riou Mort-Lot River system. Chem. Geol. 255, 295-304.

Sonke, J. E., Sivry, Y., Viers, J., Freydier, R., Dejonghe, L., Andre, L., Aggarwal, J. K., Fontan, F., and Dupre, B., 2008. Historical variations in the isotopic composition of atmospheric zinc deposition from a zinc smelter. Chem. Geol. 252, 145-157.

Turčan, T., 2006. Dejiny hutníctva na Slovensku = History of metallurgy in Slovakia. Banská agentúra, Košice, Slovakia.

Viers, J., Oliva, P., Nonell, A., Gelabert, A., Sonke, J. E., Freydier, R., Gainville, R., and Dupre, B., 2007. Evidence of Zn isotopic fractionation in a soil-plant system of a pristine tropical watershed (Nsimi, Cameroon). Chem. Geol. 239, 124-137.

Voegelin, A., Pfister, S., Scheinost, A. C., Marcus, M. A., and Kretzschmar, R., 2005. Changes in zinc speciation in field soil after contamination with zinc oxide. Environ. Sci. Technol. 39, 6616-6623.

Weiss, D. J., Mason, T. F. D., Zhao, F. J., Kirk, G. J. D., Coles, B. J., and Horstwood, M. S. A., 2005. Isotopic discrimination of zinc in higher plants. New Phytol. 165, 703-710.

Weiss, D. J., Rausch, N., Mason, T. F. D., Coles, B. J., Wilkinson, J. J., Ukonmaanaho, L., Arnold, T., and Nieminen, T. M., 2007. Atmospheric deposition and isotope biogeochemistry of zinc in ombrotrophic peat. Geochim. Cosmochim. Acta 71, 3498-3517.

Weiss, D. J., Rehkämper, M., Schoenberg, R., McLaughlin, M., Kirby, J., Campbell, P. G. C., Arnold, T., Chapman, J., Peel, K., and Gioia, S., 2008. Application of Nontraditional stable-isotope systems to the study of sources and fate of metals in the environment
Environ. Sci. Technol. 42, 655-664.

Wilcke, W., Guschker, C., Kobza, J., and Zech, W., 1999. Heavy metal concentrations, partitioning, and storage in Slovak forest and arable soils along a deposition gradient. J. Plant. Nutr. Soil. Sc. 162, 223-229.

Williamson, B. J., Udachin, V., Purvis, O. W., Spiro, B., Cressey, G., and Jones, G. C., 2004. Characterisation of airborne particulate pollution in the Cu smelter and former mining town of Karabash, south Ural Mountains of Russia. Environ. Monit. Assess. 98, 235-259.

Zhu, X. K., Guo, Y., Williams, R. J. P., O'Nions, R. K., Matthews, A., Belshaw, N. S., Canters, G. W., de Waal, E. C., Weser, U., Burgess, B. K., and Salvato, B., 2002. Mass fractionation processes of transition metal isotopes. Earth. Planet. Sc. Lett. 200, 47-62.

F Appendix

Table F-1. Masses of Cu and Zn in Blanks

Adsorption experiment on IHA (Section B)	Oxic and hydromorphic soils (Section C-D)	Polluted soils (Section E)	Polluted soils (Section E)
ng Cu	ng Cu	ng Cu	ng Zn
2.3	13.3	3.3	80.5
1.3	2.7	7.1	32.5
3.3	7.1	1.9	71.5
2.8	3.7	8.5	10.8
2.3	2.4	4.8	17.2
1.9	5.6	-	-
-	15.1	-	-
-	2.4	-	-
-	8.8	-	-
-	3.2	-	-
-	2.4	-	-
-	0.8	-	-
-	0.9	-	-
-	0.9	-	-

Table F-2. Measured.δ^{65}Cu and δ^{66}Zn values of the in-house standards

Standard no.	δ^{65}Cu of the Cu-inhouse standard	Standard no.	δ^{65}Cu of the Cu-inhouse standard	Standard no.	δ^{66}Zn of the Zn-inhouse standard
1	0.81	26	0.80	1	0.07
2	0.86	27	0.90	2	0.01
3	0.83	28	0.87	3	0.06
4	0.82	29	0.83	4	0.05
5	0.82	30	0.84	5	0.08
6	0.84	31	0.81	6	0.05
7	0.81	32	0.82	7	0.02
8	0.85	33	0.91	8	0.00
9	0.87	34	0.92	9	-0.04
10	0.82	35	0.83	10	-0.04
11	0.89	36	0.85	11	0.07
12	0.86	37	0.83	-	-
13	0.82	38	0.85	-	-
14	0.89	39	0.85	-	-
15	0.87	40	0.84	-	-
16	0.83	41	0.85	-	-
17	0.83	42	0.86	-	-
18	0.82	43	0.85	-	-
19	0.93	44	0.83	-	-
20	0.79	45	0.84	-	-
21	0.83	46	0.85	-	-
22	0.83	47	0.85	-	-
23	0.81	48	0.82	-	-
24	0.87	49	0.83	-	-
25	0.82	-	-	-	-

Table F-3. Ratio of Ti/Cu of purified and non-purified samples

Soil	Sample	Ti/Cu before purification	Ti/Cu after purification
hydromorphic soils			
Dystric Gleysol	Oa	363	0.02
	Ah	507	0.07
Stagnic Cambisol	Oe	71	0.05
	Ahg	648	0.03
Skeleti-Stagnic Luvisol	Oi	101	0.02
	Oe	58	0.01
	II Bwgt1	404	0.04
	II Bwgt2	333	0.03
	III Bwgt3	-	0.04
	III Bwgt3 (2)	-	0.03
Calcari- Humic Gleysol	Bl1	224	0.00
parent materials	Laacher See tephra	845	0.02
	Loess	303	0.02
	Slate	-	0.02
CRM		188	0.03
	Silty Clay Loam	190	0.00
	Granodiorite silver	102	0.00
	plume 2	96	0.00
aerobically weathered soils			
Dystric Cambisol	Oe	81	0.02
	Bw	893	0.00
Skeletic Cambisol	IIR	508	0.01
	IIR (2)	476	0.00
Haplic Podzol 1	Oi	28	0.00
	IIBhs	1297	0.07
	IIBhs/humic	982	0.01
Haplic Podzol 2	IIBs	665	0.05
	AhE	-	0.00
CRM	Silty Clay Loam	178	0.00

Table F-4. Copper recoveries after purification: adsorption experiment (Section B)

Adsorption experiment IHA		
Experiment	Sample (pH)	Recovery %
IHA adsorption experiment	3.04	98
	3.03	100
	3.96	104
	3.97	104
	3.97	102
	3.97	103
	4.48	103
	4.51	104
	4.75	101
	4.86	105
	5.4	98
	5.17	97
	5.19	99
	6.37	98
	6.36	94
	6.36	101
	6.94	101
	6.95	99

Table F-5. Copper recoveries after purification: hydromorphic soils (Section C)

Hydromorphic soils		
Soil	Horizon	Recovery %
Skeleti-Stagnic Luvisol	Oi	104
	Oe	97
	Ah	96
	Bw	95
	Bwg	105
Parent materials	II Bgt1	99
	II Bgt2	100
	III Bgt3	104
	Laacher See Tephra	104
	Loess	101
	Slate	98
Stagnic Cambisol	Oi	97
	Oe	104
	Oa	103
	Ah	105
	Ahg	96
	Bg1	101
	II Bg2	102
Calcari-Humic Gleysol	Oi	105
	Ah	102
	Bh	97
	Bl1	98
	Bl2	103
	Br	97
Dystric Gleysol	Oi	98
	Oe	99
	Oa	96
	Ah	101
	Bl1	95
	Bl2	102

Table F-6. Copper recoveries after purification: aerobically weathered soils (Section D)

Aerobically weathered soils				
Soil	Horizon	Recovery %	Recovery %	Recovery %
Skeletic Cambisol	Oe	103	-	-
	Ah	104	-	-
	Bw	101	-	-
	II R	104	-	-
Dystric Cambisol	Oi	98	-	-
	Oe	96	97	-
	Oa	98	-	-
	Ah	96	-	-
	Bw1	101	104	98
	Bw2	96	100	100
	C	100	-	-
Haplic Podzol 1	Oi	104	-	-
	Oe	98	-	-
	Ah	98	-	-
	AhE	97	-	-
	E	98	100	-
	II Bhs	101		-
	II BsC	98	100	-
	III CR	96	100	-
	II Bhs oxidic	96	105	-
	II Bhs humic	96	-	-
Haplic Podzol 2	Oi	100	101	-
	Oe	96	-	-
	Oa	104	-	-
	AhE	96	102	-
	Bhs	105	98	-
	Bs	99	98	-

Table F-7. Copper and Zn recoveries after purification: Polluted soils of Krompachy (Section E)

Polluted soils Krompachy					
Soil	Horizon	Cu Recovery %	Cu Recovery %	Zn Recovery %	Zn Recovery %
Dystric Cambisol 1.1 km	Oi	103	-	-	-
	Oe	98	-	100	-
	Oa	103	106	104	106
	Ah	100	-	-	-
	Bw	99	-	-	-
	C	104	-	-	-
Dystric Cambisol 3.8 km	Oi	96	-	99	-
	Oe	106	-	106	-
	Oa	103	106	104	105
	Ah	100	-	-	-
	Bw	99	-	-	-
	C	100	-	-	-
Stagni-Eutric Cambisol 5.3 km	Oi	103	-	98	-
	Oe	101	-	104	-
	Oa	102	-	104	-
	Ah	102	-	105	-
	Bwg	103	-	98	-
	Bg	94	-	94	-
Bedrock	Tuffite	106	94	94	-
Waste products	Grained slag	95	-	101	-
	Tube furnance slag	102	-	99	-
	Sludge 1	100	-	105	-
	Sludge 2	98	-	99	-
	solid waste	98	-	101	-
	fly ash	96	96	100	98

Table F-8. Copper recoveries after purification: reference materials

Reference materials		
Reference materials	Cu Recovery %	Zn Recovery %
SCL-7003	95	99
	96	101
	100	-
	101	-
	99	-
	99	-
BCR-2	100	102
	106	100
	100	106
	101	105
	106	105
	105	-
	100	-
	101	-
	103	-
GSP-2	101	101
	97	95
	97	102
	101	100
NOD-P-1	98	102
	102	-

Table F-9. Measured Cu and Zn concentrations and δ^{65}Cu and δ^{66}Zn values of the reference materials

Reference material	Cu µg l^{-1}	$\delta^{65}Cu_{NIST\ 976}$(‰)	Zn µg l^{-1}	$\delta^{66}Zn_{JMC}$(‰)
SCL-7003	26.5	0.18	76.8	-
SCL-7003	28.5	0.29	76.5	-
SCL-7003	27.4	0.19	-	-
SCL-7003	27.6	0.13	-	-
SCL-7003	29.6	0.14	-	-
SCL-7003	29.9	0.16	-	-
BCR-2	16.8	0.25	138.6	0.20
BCR-2	17.4	0.15	136.6	0.18
BCR-2	16.2	0.21	143.3	0.18
BCR-2	20.5	0.17	140.9	0.26
BCR-2	17.5	0.21	141.9	0.26
BCR-2	17.4	0.22	-	-
BCR-2	16.9	0.18	-	-
BCR-2	17.3	0.24	-	-
BCR-2	18.5	0.19	-	-
GSP-2	38.0	0.39	122.1	-
GSP-2	37.9	0.31	123.9	-
GSP-2	45.4	0.24	114.5	-
GSP-2	44.4	0.26	129.0	-
NOD-P-1	11609	0.39	1468	0.84
NOD-P-1	11164	0.31	-	-

Table F-10. Copper concentrations in the different fractions of the sequential extractions

Soil	Horizon	Fraction 1 mg kg^{-1}	Fraction 2 mg kg^{-1}	Fraction 3 mg kg^{-1}	Fraction 4 mg kg^{-1}	Fraction 5 mg kg^{-1}	Fraction 6 mg kg^{-1}	Fraction 7 mg kg^{-1}
Hydromorphic soils								
Skeleti-Stagnic Luvisol	Ah	0.3	0.3	0.2	3.6	1.7	1.8	8.2
	Bw	0.2	0.2	0.2	0.6	1.0	6.8	5.7
	Bwg	0.5	0.1	0.2	0.7	1.0	3.3	12.2
	II Bgt1	0.5	0.1	0.1	0.5	0.9	3.5	7.0
	II Bgt2	0.2	0.1	0.5	0.6	0.5	4.4	5.3
	III Bgt3	0.4	0.1	0.2	0.3	0.9	3.3	6.2
Stagnic Cambisol	Ah	0.7	0.3	0.1	1.9	0.9	0.6	5.1
	Ahg	0.2	0.1	0.0	0.8	0.8	0.4	4.5
	Bg1	0.0	0.1	0.1	0.4	0.4	0.6	5.9
	II Bg2	0.3	0.1	0.1	1.1	1.1	5.2	12.4
Calcari-Humic Gleysol	Ah	1.0	0.8	0.4	15.8	4.1	1.2	10.8
	Bh	0.8	0.6	0.3	13.3	4.1	1.6	9.2
	Bl1	0.1	0.2	0.3	4.1	2.0	0.9	7.1
	Bl2	0.1	0.2	0.2	2.9	1.2	0.3	4.5
	Br	0.1	0.3	0.3	6.3	1.6	0.3	5.5
Dystric Gleysol	Ah	0.1	0.0	0.0	1.0	1.3	0.4	3.4
	Bl1	0.1	0.0	0.0	0.6	0.8	0.4	2.9
	Bl2	0.1	0.1	0.0	0.3	0.3	0.6	3.6
Aerobically weathered soils								
Skeletic Cambisol	Ah	0.20	0.20	0.10	1.90	1.20	1.20	5.80
	Bw	0.20	0.10	0.00	0.40	0.60	4.70	3.80
	II CR	0.00	0.10	0.00	0.10	0.40	3.90	1.60
Dystric Cambisol	Ah	0.20	0.10	0.00	0.70	0.30	0.60	2.00
	Bw1	0.00	0.00	0.00	0.40	0.70	0.90	1.90
	Bw2	0.00	0.10	0.00	0.50	0.60	1.90	3.40
	C	0.00	0.00	0.00	0.40	0.50	2.10	2.10
Haplic Podzol 1	Ah	0.00	0.00	0.10	1.10	1.00	0.20	2.40
	AEh	0.00	0.00	0.00	0.10	0.00	0.30	2.90
	E	0.00	0.00	0.10	0.10	0.10	0.20	1.30
	II Bhs	0.00	0.00	0.00	0.40	0.30	0.30	1.10
	II Bs	0.00	0.00	0.00	0.30	0.00	0.10	1.70
	III RC	0.00	0.00	0.00	0.00	0.00	0.10	3.10
Haplic Podzol 2	AEh	0.20	0.10	0.00	0.70	0.40	0.30	0.80
	Bhs	0.03	0.09	0.05	0.59	0.63	0.76	1.39
	Bs	0.04	0.03	0.04	0.24	0.60	0.37	0.45

Table F-11. Ratios of $Fe_{poorly\ crystalline}/Fe_{crystalline}$ of the hydromorphic soils

Soil	Horizon	$Fe_{poorly\ crystalline}/Fe_{crystalline}$
Skeleti-Stagnic Luvisol	Ah	0.27
	Bw	0.26
	Bwg	0.39
	II Bgt1	0.39
	II Bgt2	0.06
	III Bgt3	0.07
Stagnic Cambisol	Ah	0.61
	Ahg	0.63
	Bg1	0.71
	II Bg2	0.50
Calcari-Humic Gleysol	Ah	0.14
	Bh	0.18
	Bl1	0.16
	Bl2	0.19
	Br	0.18
Dystric Gleysol	Ah	0.37
	Bl1	0.97
	Bl2	0.70